Title
Immune regulation by the endocannabinoid N-arachidonoyl dopamine (NADA)

Author
Lawton, Samira Khakpour

Publication Date
2017

Peer reviewed|Thesis/dissertation

Immune regulation by the endocannabinoid *N*-arachidonoyl dopamine (NADA)

by

Samira Khakpour Lawton

DISSERTATION

Submitted in partial satisfaction of the requirements for the degree of

DOCTOR OF PHILOSOPHY

in

To Kipp Lawton, my best friend

ACKNOWLEDGEMENTS

First, I would like to thank my graduate advisor, Judith Hellman, for her unconditional support and scientific guidance. Through creativity and determination, we set forth into new frontiers, and I am a better scientist for it. She taught me to follow my heart and never fear the unknown. Judith allowed me to be independent while never feeling alone. I am deeply grateful to have had the chance to experience graduate school with her by my side and will miss her immensely. I also truly appreciate having been able to do science with the rest of the Hellman lab. Fengyun Xu and Erika Wong spent uncountable hours repeating complex experiments, and Alphonso Tran sacrificed endless nights and weekends to help move this project along. I sincerely could not have done this without all of their help and support. Finally, I greatly appreciate my undergraduate research advisor, Will DePaolo, who gave me the foundation in research that has been crucial to my success at UCSF.

I would also like to thank my thesis committee, Matt Springer, Shaun Coughlin, and Mehrdad Matloubian, for their consistent guidance and inspiration. Their perspectives have been critical for helping this project transform from an idea into impactful science.

Thank you to everyone in the Biomedical Sciences program, especially Lisa Magargal, Demian Sainz, and my academic advisor, Mark Ansel. They have always been there for me with open arms when I needed them, and even when I did not. They made the decision to come to UCSF such an easy one, and I thank them for everything that they have done for me.

I would like to thank my classmates and friends who have been my family throughout these five years. You have made moving across the country such a seamless transition, and have been there through all of the good and bad. Thank you Brittany Gianetti, Arshiya Fazal, Olga Karagoz, Anju Goyal, Jeewon Lee, Sarah Moshary, and so many others. Thank you Juliet Goldsmith, who never failed to show up on my doorstep with food and wine, thus creating unrealistic expectations for all future friendships.

Thank you to my family for their unbelievable love and support through all these years, especially my parents, Bagher and Soraya. They have always encouraged my curiosity and pretended to understand what I was talking about. I am who I am because of them. Thank you to my in-laws, Cathy and Patrick, who opened up their hearts to me when I was only twelve years old and have been family ever since. They have done everything in their power to help and support me, even when I hauled their youngest son 2000 miles away. Thank you to my now official siblings, Erin and Brendan. Not everyone is quite as lucky to inherit such a loving and fun family.

And finally, I would like to thank Kipp Lawton, for putting up with me and believing in me through all of this. It is so difficult to find the right way to thank someone who has given me unrelenting and unconditional support for over twelve years. None of this would have been possible without him. While research could be lonely, he showed me that home never had to be. I strive to become the person that he believes me to be.

Contributions to presented work

The work in this dissertation was done under the direct supervision and guidance of Dr. Judith Hellman.

Chapters 1 and 2 contain material previously submitted for publication:

S Khakpour, K Wilhelmsen, and J Hellman. Vascular endothelial cell Toll-like receptor pathways in sepsis. *Innate Immunity*. 2015 Nov;21(8):827-46.

K Wilhelmsen, **S Khakpour**, A Tran, K Sheehan, M Schumacher, F Xu, and J Hellman. The endocannabinoid/endovanilloid *N*-arachidonoyl dopamine (NADA) and synthetic cannabinoid WIN55,212-2 abate the inflammatory activation of human endothelial cells. *Journal of Biological Chemistry*. 2014 May 9;289(19):13079-100. Epub 2014 Mar 18.

Chapter 2 data was collected in collaboration with Kevin Wilhelmsen, who performed qPCR, western blot, neutrophil adhesion, and COMT assays, and helped perform *in vitro* TLR agonist challenge experiments. Alphonso Tran provided assistance with ELISAs. All other experiments were performed by Samira Khakpour Lawton. For data presented in Chapter 3, Fengyun Xu and Alphonso Tran conducted TLR agonist challenge experiments. Erika Wong and Fengyun Xu performed CLP surgeries. Alphonso Tran and Erika Wong helped with the collection and processing of murine plasma samples and assisted with ELISAs. Kevin Wilhelmsen and Arun Prakash helped perform multiplex experiments. All other experiments were performed by Samira Khakpour Lawton. For data presented in Chapter 4, Fengyun Xu performed *in vivo* TLR

agonist challenge experiments. The Roth Laboratory at the University of North Carolina Chapel Hill performed the GPCR-ome screening assay. All other experiments were performed by Samira Khakpour Lawton.

I would like to acknowledge the following funding sources: UCSF Department of Anesthesia and Perioperative Care, UCSF Biomedical Sciences Graduate Program, NSF Graduate Research Fellowship Program (1144247), and the UCSF REAC Program (Huntington Fund).

Immune regulation by the endocannabinoid *N*-arachidonoyl dopamine (NADA)

Samira Khakpour Lawton

ABSTRACT

Arachidonic acid-based lipids, or eicosanoids, are well-known regulators of the inflammatory response. While there are additional classes of eicosanoids that have also been shown to possess immunomodulatory activity, such as the cannabinoids, they remain largely unstudied. We have found that the endocannabinoid *N*-arachidonoyl dopamine (NADA) decreases inflammatory responses *in vitro* in endothelial cells after challenge with TLR agonists, and that this activity is dependent upon the cannabinoid receptors (CB_1R and CB_2R). Furthermore, NADA dramatically reduces systemic inflammation in murine models of bacterial lipopeptide, endotoxemia, and polymicrobial intraabdominal sepsis. Consistent with its classification as a potent endovanilloid, the activity of NADA *in vivo* depends upon the cation channel transient receptor potential vanilloid 1 (TRPV1) expressed in non-hematopoietic cells and may be mediated through neuronal TRPV1. Furthermore, the activity of NADA systemically, in endothelial cells, and in the hematopoietic compartment is dependent upon CB_2R. Finally, we show that the immunomodulatory activity of NADA is mediated in part by its ability to regulate prostanoid production, and its metabolism into the novel lipid prostaglandin D_2-dopamine. These data indicate that NADA can modulate inflammatory activation as

both an endocannabinoid and endovanilloid, and suggests that these pathways may be targeted therapeutically for the treatment of acute inflammatory disorders, such as sepsis.

TABLE OF CONTENTS

LIST OF TABLES

Chapter 2

Chapter 4

LIST OF FIGURES

Chapter 1

Chapter 2

CHAPTER 1

Background

Content in this chapter was modified from the following publication:

S Khakpour, K Wilhelmsen, and J Hellman. Vascular endothelial cell Toll-like receptor pathways in sepsis. *Innate Immunity*. 2015 Nov;21(8):827-46.

Background

Acute inflammatory disorders, such as sepsis, remain a major healthcare problem worldwide, with continued high morbidity and mortality (1). Sepsis remains the primary cause of death from infection, and roughly half of patients who succumb to sepsis die of multiple organ failure (2, 3) . Because the mechanisms underlying sepsis-induced organ failure have yet to be fully unraveled, there remains a barrier to developing sepsis-directed therapies (2, 3). Currently, sepsis is treated with antimicrobial agents, localized control of the source of infection with surgery or drainage, and the supportive care of dysfunctional or failing systems and organs (4). With the recent negative outcomes of several Phase 3 clinical trials, there are currently no approved sepsis-directed adjuvant therapies (1, 5-7). As a result, the need for novel therapies for the treatment of sepsis and other acute inflammatory disorders remains critical.

Endothelial cells are becoming increasingly recognized as being key active participants in the host's immune response to infection and injury, and contributors to patient outcomes during sepsis (8, 9). Endothelial cells line the inner surface of blood vessels and capillary beds, and serve as the interface between circulating blood and surrounding tissues. The average human adult is estimated to contain over 1 trillion endothelial cells, compared to approximately 20-50 billion peripheral blood mononuclear cells (PBMCs) and 1-4 billion circulating monocytes (10-12). Endothelial cells dynamically regulate vascular tone, play central roles in coagulation and hemostasis, and are critically involved in the movement of leukocytes between the bloodstream and extravascular tissues (Figure 1.1). Whereas a great deal is known about the effects of

microorganisms on leukocyte inflammatory pathways, substantially less is known about their effects on endothelial cells, which have not classically been viewed as immune cells. However, similar to leukocytes, endothelial cells express innate immune receptors including Toll-like receptors (TLRs), which promote the expression of specific cytokines, chemokines, and adhesion molecules (13-16). In addition, the activation of coagulation cascades and increased vascular permeability may serve to create a physical barrier that limits the spread of the infection into the bloodstream. Thus, proper functioning of the endothelium is critical for the generation of the initial immune response during an infection, including the activation and recruitment of leukocytes.

In contrast to the beneficial functions of the endothelium, dysregulated activation of endothelial inflammatory pathways leads to pathologic coagulopathy with diffuse microvascular thrombosis, increased leukocyte activation within multiple organs, and capillary leak leading to intravascular hypovolemia and edema (17, 18). These dysfunctional endothelial responses are believed to promote the life-threatening syndromes of septic shock and sepsis-induced multiple organ failure. It is thus important that endothelial inflammatory pathways must be properly regulated during the initial stages of infection to prevent excessive inflammatory activation leading to endothelial dysfunction. Furthermore, it becomes apparent that endothelial inflammatory pathways may serve as important therapeutic targets for the treatment of inflammatory disorders, such as sepsis.

Because sepsis involves the complex activation of numerous inflammatory cascades, it is possible that more effective therapies may be distal and regulate a variety of general outputs, including coagulation, permeability, and inflammation.

Cannabinoids are a structurally diverse group of lipophilic compounds that have been shown to regulate a wide variety of inflammatory outputs throughout the body (19). As a result, the cannabinoid system has been targeted clinically for the treatment of a number of diseases, including diabetes, obesity, multiple sclerosis, allergic asthma, rheumatoid arthritis, pain, colitis, anxiety, depression, and cancer (20-28). A subset of cannabinoids, known as endocannabinoids, is endogenously produced. While endocannabinoids have mostly been studied in leukocytes and neurons, they have been shown to regulate vascular tone and endothelial cell adhesion molecule expression in *in vitro* models of inflammation (29-36). Furthermore, the endocannabinoid system has also been shown to regulate adhesion molecule expression, hypotension, and mortality in *in vivo* endotoxemia models (37, 38). These data suggest that the endocannabinoid system possesses diverse activity in the endothelium. Identifying the role of the endocannabinoid system in the endothelium and during sepsis models may lead to novel therapies for the treatment of sepsis and other acute inflammatory disorders.

Figure 1.1

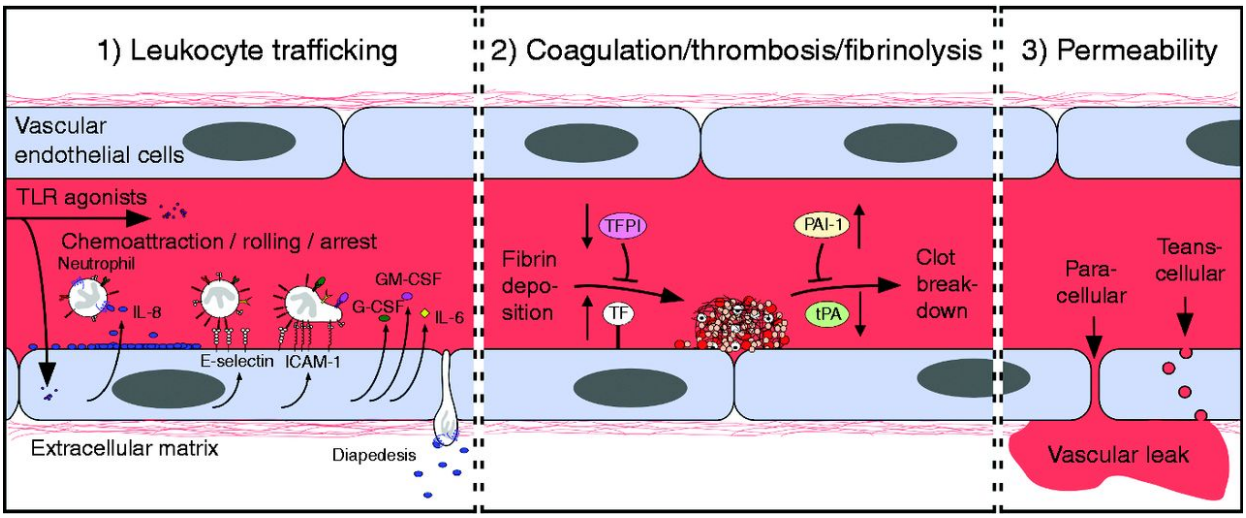
1) Leukocyte trafficking
2) Coagulation/thrombosis/fibrinolysis
3) Permeability
Vascular endothelial cells
TLR agonists
Chemoattraction / rolling / arrest
Neutrophil
IL-8
GM-CSF
G-CSF
IL-6
E-selectin
ICAM-1
Extracellular matrix
Diapedesis
TFPI
TF
Fibrin depo-sition
PAI-1
tPA
Clot break-down
Para-cellular
Teans-cellular
Vascular leak

Figure 1.1. Major outputs after endothelial cell TLR pathway activation.

Endothelial cell TLRs engage microbial- and host-derived factors present within the vascular lumen to initiate inflammation. Activated endothelial cells (1) secrete cytokines and chemokines and express adhesion molecules that facilitate leukocyte movement between the blood and tissues at sites of infection and injury; (2) dysregulate coagulation homeostasis by activating the tissue factor (TF) pathway, causing increased levels of factors that induce thrombosis, and reduced levels of factors involved in clot breakdown (fibrinolysis); and (3) increase permeability of the endothelium which results in the movement of plasma fluid and proteins into tissues.

CHAPTER 2

The endocannabinoid/endovanilloid *N*-arachidonoyl dopamine (NADA) and synthetic cannabinoid WIN55,212-2 abate the inflammatory activation of human endothelial cells

Content in this chapter was modified from the following publication:

K Wilhelmsen, **S Khakpour**, A Tran, K Sheehan, M Schumacher, F Xu, and J Hellman. The endocannabinoid/endovanilloid *N*-arachidonoyl dopamine (NADA) and synthetic cannabinoid WIN55,212-2 abate the inflammatory activation of human endothelial cells. *Journal of Biological Chemistry*. 2014 May 9;289(19):13079-100. Epub 2014 Mar 18.

Abstract

Although cannabinoids, such as Δ^9-tetrahydrocannabinol, have been studied extensively for their psychoactive effects, it has become apparent that certain cannabinoids possess immunomodulatory activity. Endothelial cells (ECs) are centrally involved in the pathogenesis of organ injury in acute inflammatory disorders, such as sepsis, because they express cytokines and chemokines, which facilitate the trafficking of leukocytes to organs, and they modulate vascular barrier function. In this study, we find that primary human ECs from multiple organs express the cannabinoid receptors CB_1R, GPR18, and GPR55, as well as the ion channel transient receptor potential cation channel vanilloid type 1 (TRPV1). CB_2R is only minimally expressed in some EC populations, in contrast to leukocytes. Furthermore, we show that ECs express all of the known endocannabinoid metabolic enzymes. Examining a panel of cannabinoids, we demonstrate that the synthetic cannabinoid WIN55,212-2 and the endocannabinoid *N*-arachidonoyl dopamine (NADA), but neither anandamide nor 2-arachidonoylglycerol, reduce EC inflammatory responses induced by bacterial lipopeptide, LPS, and TNFα. We find that endothelial CB_1R/CB_2R are necessary for the effects of NADA, but not those of WIN55,212-2. Furthermore, while TRPV1 inhibition exacerbates the LPS-induced inflammatory response in ECs in the absence of cannabinoids, it further reduces inflammation in the presence of WIN55,212-2 or NADA. These data indicate that the endocannabinoid system can modulate inflammatory activation of the endothelium and may have important implications for a variety of acute inflammatory disorders that are characterized by EC activation.

Introduction

Cannabinoids are a structurally diverse group of lipophilic compounds that bind the transient receptor potential cation channel vanilloid type 1 (TRPV1) and G protein-coupled receptors, including cannabinoid receptors type 1 and 2 (CB_1R and CB_2R), GPR18, and GPR55 (19). Although some cannabinoids, such as Δ^9-tetrahydrocannabinol, have been studied extensively for their psychoactive effects, cannabinoids are also known to possess medicinal properties. However, support for their use as therapeutic agents did not intensify until the discovery of the endocannabinoid system in the early 1990s (39). The endocannabinoid system is composed of a complex network of metabolic enzymes, arachidonic acid-based lipid messengers (*i.e.* endocannabinoids), and their receptors (20, 40). *N*-arachidonoylethanolamide (AEA; anandamide) and 2-arachidonoylglycerol (2-AG) are the two most thoroughly studied endocannabinoids; however, other endocannabinoids also exist, including 2-arachidonyl glycerol ether (Noladin ether), *O*-arachidonoylethanolamine (virodhamine), *N*-arachidonoylglycine, and *N*-arachidonoyl dopamine (NADA) (19). Although the functions of AEA and 2-AG in neuronal synaptic plasticity have been substantially documented, the functions of these molecules outside the nervous system, and the roles of the other endocannabinoids, are not as well understood (41-44).

Cannabinoid receptors are expressed in immune cells. In particular, CB_2R is expressed at relatively high levels, especially in B-cells, natural killer cells, and monocytes, and its activation can dampen the inflammatory response to infection (21, 45-47). In fact, targeting CB_2R in leukocytes has been suggested as a therapy for

inflammatory disorders such as sepsis (24, 48-50). Although it is clear that several plant-derived (*i.e.* phytocannabinoids) and synthetic cannabinoids possess immunomodulatory activity, prior studies have primarily focused on their effects on leukocytes and microglia without assessing their effects on the endothelium, which is known to be centrally involved in acute inflammatory disorders such as sepsis (18, 51, 52). In sepsis, the persistent, direct, and unresolved engagement of endothelial Toll-like receptors (TLRs) by microbial components, and the sustained secretion of endogenous inflammatory mediators, such as TNFα and IL-1β, lead to endothelial activation and dysfunction (53-57). Ultimately, this contributes to the development of coagulopathy and increased vascular permeability, which subsequently leads to multi-organ failure and death (56). Therefore, therapeutically targeting components of the endothelial endocannabinoid system may represent a novel approach to ameliorating the damaging effects that occur during acute inflammatory disorders.

To this end, we sought to identify cannabinoids that are able to modulate EC inflammation and delineate which components of the endocannabinoid system are expressed by ECs. Using a panel of synthetic cannabinoids, phytocannabinoids, and endocannabinoids, we found that the synthetic cannabinoid WIN55,212-2 and the endocannabinoid NADA have the ability to dampen the activation of primary human lung microvascular ECs (HMVECs) by a variety of inflammatory agonists, including bacterial lipopeptides (TLR2 agonist), lipopolysaccharide (LPS) (TLR4 agonist), and TNFα. Although the anti-inflammatory properties of WIN55,212-2 have previously been described, only a few reports have described the physiological functions of NADA, including its role in inflammation (23, 24, 34, 58-63).

NADA was first described as a putative endocannabinoid in 2000, and was subsequently also identified as an endovanilloid (64, 65). In mice, NADA was shown to induce the following tetrad of physiological paradigms associated with cannabinoids: hypothermia, hypolocomotion, catalepsy, and analgesia (64, 66-68). NADA has been found to play a regulatory role in both the peripheral and central nervous systems and displays antioxidant and neuroprotectant properties (65, 69-72). In addition to its neurological effects, NADA has been implicated in smooth muscle contraction and vasorelaxation in blood vessels (32, 73-75). Additionally, NADA has been observed to suppress inflammatory activation of human Jurkat T-cells and to inhibit the release of prostaglandin E_2 (PGE_2) from LPS-activated astrocytes, microglia, and mouse brain ECs (76-78). NADA also displays inhibitory activity in HIV-1 replication assays (79). Finally, a recent report suggests that NADA can prevent the degranulation and release of TNFα from RBL-2H3 mast cells treated with an IgE-antigen complex (80). Together, these studies show that physiological functions attributed to NADA are multifaceted and include the potential to modulate the immune response.

The binding specificity for the cannabinoid receptors differs between WIN55,212-2 and NADA. Although WIN55,212-2 is a strong agonist of both CB_1R and CB_2R, NADA displays approximately a 40-fold selectivity for CB_1R over CB_2R (19, 64, 81). Moreover, the TRPV1 ion channel is activated by NADA but is inhibited by WIN55,212-2 (65, 82-84). Therefore, we sought to determine the expression repertoire of the four G protein-associated CBRs, and TRPV1, in different human primary endothelial cell niches. We found that primary human ECs from multiple vascular beds all express CB_1R, GPR18, GPR55, and TRPV1 and differentially express CB_2R at relatively low levels.

Additionally, we determined that human ECs express all the endocannabinoid metabolic enzymes identified to date. We find that CB_1R/CB_2R are necessary for the anti-inflammatory properties of NADA but not WIN55,212-2. Furthermore, although TRPV1 inhibition further reduces the LPS-induced inflammatory activation of lung HMVECs in the presence of WIN55,212-2 or NADA, paradoxically, TRPV1 inhibition augments inflammation in the absence of the cannabinoids. Together, these results suggest that human ECs have the machinery to metabolize and respond to NADA and that the endothelial endocannabinoid system represents a novel target for inflammatory disorder therapies.

Results

Endothelial cells from different vascular beds express a similar subset of cannabinoid receptors and endocannabinoid metabolic enzymes

To determine which cannabinoid receptors are expressed in primary human endothelial cells, mRNA expression levels from HUVECs, HCAECs, brain, liver, and lung microvascular ECs (HMVECs) were measured. cDNA derived from human peripheral blood mononuclear cells (PBMCs) was used for comparison. Commercially available assays designed to detect the presence of *CNR1* (CB_1 receptor/CB_1R), *CNR2* (CB_2 receptor/CB_2R), *GPR18*, *GPR55*, and the ion channel *TRPV1* were utilized. Initial results showed that ECs express *CNR1*, *GPR18,* and *TRPV1*, but not *CNR2* nor *GPR55* (Figure 2.1, A–E, and Table 2.1). In contrast, PBMCs expressed *CNR2* and *GPR55* in addition to the other receptors detected in ECs (Figure 2.1F and Table 2.1). Although detectable in all cell lines, endothelial *CNR1* expression was relatively low

and, in fact, was not detected in any of the ECs when an input of 5 ng of cDNA was used (Table 2.1). To confirm the expression profile of *CNR2* and *GPR55* in ECs, qPCR was repeated using different assays (assay 2) containing primers that recognize different exons. Using the assay 2 mixes, *GPR55* was detected in all the ECs tested, and *CNR2* transcripts were detected in HUVECs, brain HMVECs, HCAECs, and PBMCs, although the levels were extremely low (Figure 2.1, G and H). *CNR2* was not detected with assay 2 in any of the ECs or the PBMCs when an input of 5 ng of cDNA was used (Table 2.1). These results suggest that alternative splice variants of *GPR55* and *CNR2* may be expressed in different tissues.

To verify that CB_1R, CB_2R, GPR18, GPR55, and TRPV1 are expressed at the protein level in the aforementioned cell types, immunoblotting was performed using lysates derived from the same primary cells used in qPCR expression analysis. The results appear to corroborate the qPCR expression analysis, although it was difficult to determine the correct protein band in some blots due to excessive background protein staining and to discrepancies between the observed and predicted or described molecular weights (Figure 2.2). Nonetheless, we are confident that CB_1R (protein band 1), GPR18, GPR55, and TRPV1 protein bands were definitively detected in ECs (Figure 2.2). However, in the CB_1R immunoblot, a fainter protein band is detected at ~55 kDa in the PBMC lysates (protein band 2), which is not present in ECs (Figure 2.2A). Because this protein band more closely corresponds to the predicted molecular weight for CB_1R and is consistent with the relatively low expression of *CNR1* in ECs, as observed in the qPCR data, it may represent CB_1R, suggesting this receptor is not detectable by immunoblot in ECs (Figure 2.2A and Table 2.1). Additionally, in Figure 2.2B, if the

protein band observed either at ~25 kDa (protein band 1) or ~52 kDa (*i.e.* the middle band of the triplet found between 50 and 55 kDa; protein band 2) in the PBMC lane is in fact CB_2R, the results indicate that ECs do not express detectable quantities of this G protein-coupled receptor, which would be consistent with our qPCR results using assay 1 (Figures 2.1 and 2.2B, and Table 2.1). Furthermore, several protein bands are in the predicted or previously observed molecular weight ranges for TRPV1; however, in comparison with ECs, some of these are not highly expressed in PBMCs (85, 86). Taken together, the results from our CBR expression studies indicate that ECs express CB_1R, GPR18, GPR55, and TRPV1 and possibly CB_2R at very low levels.

The endocannabinoid system uses a complex network of metabolic enzymes to regulate the synthesis and breakdown of the arachidonic acid-based endocannabinoids (20, 40). Through literature review, we identified 10 enzymes involved in endocannabinoid metabolism. We tested for the presence of these enzymes through qPCR expression profiling in HUVECs and lung HMVECs, again using PBMCs for comparison. Our results show that HUVECs and lung HMVECs express very similar levels of all the endocannabinoid metabolic enzymes tested, including α/β-hydrolase-4, -6, and -12 (*ABHD4, ABHD6,* and *ABHD12*), diacylglycerol lipase α (*DAGLA*), glycerophosphodiesterase (*GDE1*), monoacylglycerol lipase (*MGLL*), *N*-acyl phosphatidylethanolamine phospholipase D (*NAPE-PLD*), and protein-tyrosine phosphatase, nonreceptor type 22 (*PTPN22*) (Figure 2.3, A and B, and Table 2.2). Additionally, fatty acid amide hydrolase 1 and 2 (*FAAH* and *FAAH2*) were expressed in ECs but at relatively low levels. We also found that PBMCs express all the enzymes tested (Figure 2.3C and Table 2.2). These results suggest that ECs and PBMCs are

able to regulate endocannabinoid metabolism.

NADA and WIN55,212-2 negatively regulate EC inflammatory activation

Cannabinoids have been reported to modulate the inflammatory activation of leukocytes, but their effects on endothelial inflammation have not been thoroughly investigated (24, 51). Because the inflammatory activation of ECs also plays a central role in recruiting leukocytes and mounting immune responses, we decided to test a panel of synthetic cannabinoids, phytocannabinoids and endocannabinoids, as well as the TRPV1-activating compound capsaicin, for their ability to regulate the secretion of IL-6 and IL-8 from lung HMVECs activated with the pro-inflammatory agonists FSL-1 (TLR2/6 ligand), LPS (TLR4 ligand), or TNFα. Specific cannabinoids and capsaicin were chosen due to their ability to activate or inhibit the known cannabinoid receptors (Table 2.3). Based on pilot experiments, we chose to pre-incubate lung HMVECs with 10 μM of each cannabinoid or capsaicin for 1 hour and then treat for 6 hours with the inflammatory agonists while in the continuous presence of the compounds. After the 7 hours, we quantified IL-6 and IL-8 levels in culture supernatants. MTT assays were used to ensure that changes in cytokine expression were not due differences in cell viability. In the MTT assays, the ECs were incubated with 10 μM of the different compounds for 7 hours. Figure 2.4 summarizes the combined inflammatory index versus viability index for each cannabinoid tested. A detailed description on how the indices were calculated can be found in the legends of Figure 2.4 and Table 2.4. Of the compounds tested, only the endocannabinoid NADA (IL-6, $p < 0.05$; IL-8, $p < 0.01$) and synthetic cannabinoid WIN55,212-2 (IL-6, $p < 0.001$; IL-8, $p < 0.001$) significantly

reduced IL-6 and IL-8 secretion from ECs after inflammatory agonist treatment without significantly affecting EC viability (MTT, $p < 0.05$) (Figure 2.4 and Table 2.4). We therefore decided to further analyze the anti-inflammatory properties of these two compounds in more detail. Of note, although the CB_2R agonist HU-308 appears to display anti-inflammatory activity without grossly affecting the viability of ECs, we did not follow up on this cannabinoid in this report because its effect on IL-6 and IL-8 secretion was not statistically significant by our criteria ($p < 0.05$) and because of our inconclusive results regarding CB_2R expression in ECs (Figures 2.1, 2.2, and 2.4, and Tables 2.1 and 2.4). Also, although 10 μM CBD strongly inhibited cytokine secretion from all ECs tested, we determined that this reduction was due to a substantial increase in cell death (Figure 2.4 and Table 2.4). Lower concentrations of CBD (<1 μM) did not cause cell death but also did not have a significant effect on cytokine secretion, and therefore, we did not further pursue this phytocannabinoid (data not shown).

WIN55,212-2 inhibits lung HMVEC activation by inflammatory agonists

WIN55,212-2 is a well-studied synthetic compound and has been shown previously to have anti-inflammatory activity in a variety of cells (34, 58-61). We first analyzed the effects of WIN55,212-2 (0.1, 1, and 10 μM) on the FSL-1-, LPS-, and TNFα-induced upregulation of IL-8 in lung HMVECs. We found that 10 μM WIN55,212-2 strongly inhibits the upregulation of IL-8 expression in lung HMVECs treated with all three of the inflammatory agonists (Figure 2.5, A-C). More refined concentration curves of WIN55,212-2 between 1 and 10 μM in FSL-1- and LPS-treated lung HMVECs indicated that the IC_{50} for WIN55,212-2 inhibition of IL-6 and IL-8 secretion is between

2.96 and 3.94 μM (Figure 2.6, A-D). Importantly, we also observed that WIN55,212-2 concentrations of up to 100 μM do not effect cell viability (Figure 2.5D). Additionally, we found that initiating treatment of lung HMVECs with WIN55,212-2 anytime from 2 hours before to 2 hours after the addition of FSL-1 strongly reduced IL-6 and IL-8 secretion (Figure 2.6, E and F). We next used a neutrophil adhesion assay to test the ability of WIN55,212-2 to inhibit the binding of neutrophils to lung HMVECs activated with either FSL-1, LPS, or TNFα. We found that WIN55,212-2 dose-dependently reduces the adhesion of primary human neutrophils to lung HMVEC monolayers activated by all three inflammatory agonists (Figure 2.5E, shown for FSL-1). These results all suggest that WIN55,212-2 robustly inhibits the inflammatory activation of lung HMVECs without affecting cell viability.

As mentioned previously, WIN55,212-2 has high affinity for both CB_1R and CB_2R and is reported to inhibit TRPV1 (19, 81, 83, 84). We first analyzed the effects of the CB_1R antagonist CP945598 and CB_2R inverse agonist SR144528 together (0.1, 1, and 10 μM) on the LPS-induced upregulation of IL-6 and IL-8 in lung HMVECs in the presence and absence of WIN55,212-2. We decided to use these inhibitors in combination to exclude any possibility of compensation by one over the other, given the uncertainty of CB_2R expression in ECs. We found that the effects of WIN55,212-2 on IL-6 secretion are only significantly abrogated in the presence of 0.1 μM CP945598/SR144528 ($p < 0.05$), whereas IL-8 secretion is not significantly affected by the inhibitors, suggesting that CB_1R and CB_2R may have only minimal effects on its anti-inflammatory properties in ECs (Figure 2.5F, shown for IL-8). Note that we used 4 μM WIN55,212-2 in these assays to more closely match its IC_{50} value (Figure 2.6). We

next analyzed the effects of the TRPV1 antagonist AMG9810 (0.1, 1, and 10 μM) on the LPS-induced upregulation of IL-6 and IL-8 in lung HMVECs pretreated with WIN55,212-2. We found that in the presence of 10 μM AMG9810, the WIN55,212-2-dependent decreases in IL-6 and IL-8 secretion were further reduced in LPS-treated lung HMVECs, but surprisingly, in the absence of WIN55,212-2, the LPS-induced inflammatory response was exacerbated in the presence of 10 μM AMG9810 (Figure 2.5G, shown for IL-8). This suggests that TRPV1 promotes inflammation in the presence of WIN55,212-2 but inhibits inflammation in its absence. Importantly, we did not observe significant effects of AMG9810 at concentrations <10 μM, suggesting that these outcomes may be due to the inhibition of another endothelial TRP channel such as TRPA1, -M8, -V3, or -V4 (87, 88).

NADA, and not its chemical constituents arachidonic acid nor dopamine, reduces lung HMVEC activation

We next focused on refining the anti-inflammatory properties of NADA in ECs that were observed in our initial experiments (Figure 2.4). NADA is composed of arachidonic acid (AA) and dopamine moieties covalently linked through an amide bond (Figure 2.7A). Because several endocannabinoid hydrolase enzymes, such as FAAH1/2, MAGL, and ABHD-4, -6, and -12, are expressed in ECs (Figure 2.3), it is possible that either AA or dopamine, or a combination of the two, are responsible for the observed anti-inflammatory properties. To explore this possibility, we compared the effects of AA or dopamine alone, the two compounds in combination, or NADA alone on FSL-1 and TNFα activation of lung HMVECs. Consistent with previous observations, we

found that the presence of AA, either alone or in combination with dopamine, tends to increase the expression of IL-8 by lung HMVECs when treated with either agonist, whereas NADA again decreased cytokine secretion (Figure 2.7B, shown for FSL-1) (89). Polymyxin B was used to show that the additional increase in IL-8 levels after FSL-1 addition in the presence of AA was not due to LPS contamination. These results suggest that NADA itself is directly responsible for the observed anti-inflammatory effects and not its breakdown products AA or dopamine.

Catechol-*O*-methyltransferase (COMT) has been reported to partially inactivate NADA and convert it into *O*-methyl-NADA (OM-NADA) in neurons (65, 90). We found that ECs express COMT (data not shown), and hypothesized that NADA may also have its dopamine moiety inactivated in ECs (Figure 2.8A). We found that COMT inhibition with entacapone, or genetic silencing through COMT siRNA, further decreased LPS-induced IL-6 and IL-8 secretion in the presence of NADA (Figure 2.8, B and C). These results support the fact that NADA, and not its metabolites, is responsible for the anti-inflammatory effects in ECs.

We also tested ethanol preparations of NADA from three different sources (Sigma, Tocris, and Cayman) and found similar decreases in IL-8 secretion in LPS-treated lung HMVECs when pre-incubated with either 10 or 20 μM NADA (Figure 2.9A). Additionally, we found that NADA has no effect on cell viability or cell adherence as measured by MTT and crystal violet (CV) assays, respectively, up to 20 μM *in vitro*, but that higher concentrations did cause significant cell death within 7 hours (Figure 2.7, C and D). It is possible that at higher concentrations NADA may cause EC death via oxidative stress, similar to results reported for hepatic stellate cells (91).

NADA reduces pro-inflammatory cytokine secretion and neutrophil adherence to lung HMVECs activated by inflammatory agonists

Next, we found that NADA dose-dependently inhibits the upregulation of IL-6 and IL-8 expression in lung HMVECs treated with FSL-1, LPS, or TNFα (Figure 2.10, A-F). The IC_{50} values for NADA's inhibitory effects on LPS-induced secretion of IL-6 and IL-8 from lung HMVECs were 12.79 and 18.00 μM, respectively (Figure 2.9, B and C). Additionally, like WIN55,212-2, we found that initiating treatment of lung HMVECs with NADA anytime starting 2 hours before and up to 2 hours after adding FSL-1 strongly reduced the upregulation of both IL-6 and IL-8 (Figure 2.9, D and E). Using flow cytometry, we also determined that NADA reduces the surface expression of E-selectin on HUVECs activated with FSL-1, LPS, or TNFα, suggesting that NADA may reduce the adhesion of leukocytes to the endothelium (Figures 2.11 and 2.12). To test this, we performed a neutrophil adhesion assay (92). We observed that NADA dose-dependently reduces the adhesion of primary human neutrophils to lung HMVEC monolayers activated by any of the inflammatory agonists (Figure 2.13, A-C). These results indicate that NADA can directly dampen the activation of human ECs by both exogenous and endogenous inflammatory mediators.

NADA and WIN55,212-2 do not reduce the permeability of lung HMVEC monolayers

Increased permeability of the vascular endothelium is a hallmark of acute inflammatory disorders such as sepsis, and it is believed to contribute to the

pathogenesis of organ injury and failure (18, 56). We utilized electric cell-substrate impedance sensing (ECIS) to quantify the effects of NADA and WIN55,212-2 on endothelial permeability induced either by FSL-1, LPS, or TNFα. ECIS uses TER to measure electrical current as a surrogate for endothelial permeability. A reduction in TER is consistent with increased permeability. We found that treatment of lung HMVEC monolayers with NADA or WIN55,212-2 did not affect the FSL-1-, LPS-, or TNFα-induced decreases in TER (data not shown). Together, these results suggest that NADA and WIN55,212-2 may not modulate inflammation-induced endothelial permeability.

Effects of CB_1R/CB_2R and TRPV1 inhibition on the anti-inflammatory properties of NADA

NADA is an agonist for CB_1R and CB_2R with differing affinities and can activate the TRPV1 channel (*i.e.* induce cation influx) (64, 65, 82). We analyzed the effects of the CB_1R/CB_2R inhibitors CP945598/SR144528 (0.1, 1, and 10 μM) on the LPS-induced upregulation of IL-6 and IL-8 in lung HMVECs in the presence of NADA. We found that 0.1 and 1 μM CP945598/SR144528 strongly abated the NADA-dependent decrease in IL-6 and IL-8 secretion in LPS-treated lung HMVECs, whereas at the higher concentrations (10 μM) they actually facilitated the NADA-dependent reduction in cytokine secretion in LPS-activated ECs (Figure 2.14, A and B). Because CP945598 and SR144528 display subnanomolar potency in binding and functional assays, the effects at 0.1 and 1 μM may reflect specific inhibition of CB_1 and CB_2 receptors, whereas the outcomes observed at 10 μM may represent off-target effects (93-95).

Therefore, the anti-inflammatory effects of NADA may be at least partially due to agonism at CB_1R and/or CB_2R. We next analyzed the effects of the TRPV1 antagonist AMG9810 (0.1, 1, and 10 μM) on the LPS-induced upregulation of IL-6 and IL-8 in lung HMVECs pretreated with NADA. We found that the presence of 10 μM AMG9810 augmented NADA-dependent decreases in IL-6 and IL-8 by LPS-treated lung HMVECs. Conversely, in the absence of NADA, the LPS-induced inflammatory response was exacerbated in the presence of 10 μM AMG9810 (Figure 2.14, C and D). This suggests that TRPV1 promotes inflammation in the presence of NADA but inhibits inflammation in its absence. Like our studies with WIN55,212-2, we did not observe significant effects of AMG9810 at concentrations <10 μM, again suggesting that these outcomes may be due to the inhibition of another endothelial TRP channel such as TRPA1, -M8, -V3, or -V4 (87, 88). However, we found that NADA dose-dependently induces Ca^{2+} influx into lung HMVECs (Figure 2.14E). Furthermore, this Ca^{2+} influx was observed in NADA-treated wild-type (WT), but not *Trpv1*$^{-/-}$, primary murine lung endothelial cells (Figure 2.14F). In these experiments, 10 μM ATP was used as a positive control (96). These data indicate that NADA is an agonist for endothelial TRPV1.

Human ECs express the dopamine biosynthetic enzyme DDC but endogenous NADA was not detected in lung HMVECs

Two potential biosynthetic routes have been postulated to be responsible for the production of NADA in cells (65, 97, 98). One route requires the direct ligation of dopamine to AA. The other route first requires the ligation of tyrosine to AA to form *N*-arachidonoyl tyrosine. The tyrosine moiety is subsequently converted to L-DOPA by TH

to generate *N*-arachidonoyl-DOPA, and then the L-DOPA moiety is converted to dopamine by DDC to produce NADA (Figure 2.15A). Using qPCR expression analysis, we determined that both HUVECs and lung HMVECs express *DDC*, but not *TH*, although PBMCs express neither and, as expected, adrenal tissue express high levels of both *DDC* and *TH* (Figure 2.15, B and C). These results suggest that in human ECs only the first biosynthetic route for NADA is possible. However, because TH has been detected in murine liver sinusoidal ECs, the mechanisms of NADA synthesis may vary in different EC niches or species (91). We next attempted to quantify endogenous NADA in lysates of lung HMVECs. Using an LC-MS/MS method developed at Cayman Chemical Co., NADA was not detected in lung HMVEC lysates either before or after activation by FSL-1, LPS, or TNFα (data not shown). In the absence of technical issues, such as the inefficient isolation of NADA from lung HMVEC lysates or its degradation prior to LC-MS/MS analysis, this result indicates that lung HMVECs do not endogenously express NADA.

Discussion

We have identified the endocannabinoid/endovanilloid NADA and the synthetic cannabinoid WIN55,212-2 as potent modulators of the inflammatory activation of the endothelium. Other endocannabinoids, including AEA and 2-AG, did not exhibit this immunomodulatory property. Both NADA and WIN55,212-2 reduce the secretion of pro-inflammatory cytokines and the adherence of neutrophils to lung HMVECs activated by bacterial TLR agonists or TNFα. Importantly, our expression profiling data show that primary human ECs express CBRs, TRPV1, and all of the endocannabinoid metabolic

enzymes that have been identified to date. These results strongly support the hypothesis that the endothelial endocannabinoid system represents a novel immune regulatory system that could be exploited therapeutically to ameliorate the deleterious effects of dysregulated inflammation in a variety of disorders, including sepsis and noninfectious inflammatory syndromes.

We transcriptionally detected the expression of *CNR1, GPR18, GPR55,* and *TRPV1* in all five EC types tested. *CNR2*, however, was only detected at low levels in HUVECs, brain HMVECs, and HCAECs by only one of the two primer sets tested (assay 2). However, we were unable to detect CB_2R in ECs by immunoblot, suggesting that if present the CB_2R is expressed at extremely low levels. The expression of CB_1R in ECs is fairly well documented, but the expression of CB_2R in ECs is more controversial (99-104). For example, other investigators have reported the expression of CB_2R in HCAECs and brain HMVECs but not in HUVECs, and interestingly, inflammatory agonists and 2-AG have been observed to induce CB_2R upregulation in brain HMVECs (101, 104-107). Therefore, the detection of CB_2R in EC cultures may depend on several factors, including the EC niche, detection method, and inflammatory state, and on the health, passage number, or growth conditions of the ECs. Nonetheless, the synthetic CB_2R agonists JWH133, HU-308, and O-1966 have been reported to reduce the LPS- and TNFα-induced inflammatory activation of both HCAECs and brain HMVECs and protect barrier function in LPS-treated brain HMVECs (101, 105). Consistent with these results, we observed an anti-inflammatory trend with HU-308 when administered to activated lung HMVECs. Based upon this information, an anti-inflammatory role for CB_2R in ECs cannot be excluded.

We found that the hydrolases FAAH, FAAH2, MAGL, and ABHD4, -6, and -12 are expressed in ECs. Because these enzymes are involved in catabolism of the endocannabinoids AEA and 2-AG, both of which have been reported to reduce inflammation, and NADA has been reported to inhibit both FAAH and MAGL, the observed anti-inflammatory properties of NADA may be indirectly due to increases in either AEA or 2-AG levels (36, 58, 64, 108-113). Furthermore, these hydrolases may catabolize NADA to its constituents AA and dopamine, which themselves could potentially diminish EC activation. However, we did not observe a significant change in IL-6 and IL-8 secretion from ECs treated with inflammatory mediators in the presence of either AEA or 2-AG (Figure 2.4). In fact, 2-AG exhibited a pro-inflammatory trend with IL-8, which is consistent with findings in several published reports (114-116). Additionally, AA also appears to augment inflammation, suggesting that the breakdown of NADA is not a prerequisite for the observed inflammatory reduction. Therefore, it is unlikely that NADA exerts its immunomodulatory effects via the production of AEA and 2-AG or through its catabolism to AA and dopamine, although it is possible that the exogenous application of AA, AEA, or 2-AG to ECs *in vitro* does not replicate their *in vivo* effects on the endothelium.

We observed that NADA concentrations of >1 μM were necessary to elicit its immunomodulatory properties *in vitro*. Although these levels of NADA are unlikely to be present in the circulation, the observed activity of NADA at this concentration may be functionally significant for several reasons. First, many of NADA's targets are intracellular, including its binding site on TRPV1 (70, 117-119). This suggests that NADA must be imported into the cell prior to acting on its receptors when added

exogenously. The anandamide (or endocannabinoid) membrane transporter has been reported to facilitate NADA transport into the cell. Therefore, higher exogenous NADA concentrations may be necessary to efficiently overcome this rate-limiting step or, alternatively, the activity of the anandamide membrane transporter may not be optimal *in vitro* (82, 120-122). Second, the lack of a concurrently activated allosteric pathway (*e.g.* PKC) or allosteric mediators (*e.g.* ATP or low pH), or low expression level of the effectors themselves, may reduce the efficacy of NADA *in vitro* (123-126). These instances indicate that higher concentrations of NADA would be necessary to induce activation of its effectors. Third, relatively high exogenous concentration of NADA may be necessary to overcome its metabolism to a less active form, such as a 3-*O*-methyl derivative (65). Finally, the concentrations of NADA used in our studies are consistent with, or even lower than, those typically used to elicit the effects of histamine on ECs *in vitro*, a compound known to directly activate and induce permeability of the endothelium *in vivo* (3, 127-131).

NADA and WIN55,212-2 have been reported to activate CB_1R and CB_2R on cells (19, 64, 81). Therefore, we determined the contribution of these receptors to the anti-inflammatory properties of NADA and WIN55,212-2 in ECs. The combination of the CB_1R antagonist and CB_2R inverse agonist abrogated the anti-inflammatory properties of NADA, which suggests that CB_1R and/or CB_2R are necessary to elicit the anti-inflammatory properties of NADA in LPS-activated lung HMVECs. In contrast, the inhibitors did not reduce the anti-inflammatory properties of WIN55,212-2, which is unexpected given the high affinity of WIN55,212-2 for both CB_1R and CB_2R (132). Possible explanations are that these inhibitors do not prevent the high affinity binding of

WIN55,212-2 to CB_1R and/or CB_2R or that WIN55,212-2 modulates inflammatory activation of ECs via alternative mechanisms.

To determine the role of TRPV1 in EC inflammation, we utilized AMG9810, a competitive antagonist of TRPV1. Although AMG9810 further reduces the LPS-induced inflammatory activation of ECs in the presence of either WIN55,212-2 or NADA, AMG9810 augments inflammation in their absence. This suggests that cannabinoids may switch the role of TRPV1 from an anti-inflammatory to a pro-inflammatory receptor in ECs, and in conjunction with NADA, TRPV1 may regulate endothelial inflammatory homeostasis. Indeed, we observed that NADA causes a dose-dependent transient increase in calcium levels in ECs, which may promote inflammatory signaling pathways, consistent with its role in activating endothelial TRPV1, the only known ion channel known to be ligand-gated by NADA (65, 82, 133-136). Our results suggest that WIN55,212-2 does not exert its endothelial anti-inflammatory properties via its reported inhibition of TRPV1, as the TRPV1 antagonist augments the anti- inflammatory effects of WIN55,212-2 (83, 84). However, these previous studies were performed primarily in neurons, and the modulation of TRPV1 by WIN55,212-2 may differ between neurons and ECs. It is also possible that our observations were due to the effects of AMG9810 on other TRP channels (87, 88).

Targets other than the endocannabinoid and endovanilloid receptors have also been described for both NADA and WIN55,212-2 (34, 64, 75, 78, 82-84, 113, 132, 137-142). Many of these, including PPAR-α, PPAR-γ, and calcineurin, are expressed in ECs and can themselves modulate endothelial inflammatory outputs (78, 83, 84, 143-145). In fact, WIN55,212-2 has been reported to reduce inflammation in murine brain ECs

through PPAR-γ, independent of CB_1R and C CB_2R, which is consistent with our observations using combined CB_1R antagonist and CB_2R inverse agonist (34, 143, 144). Furthermore, NADA has also been reported to downregulate secretion of the inflammatory mediator PGE_2 from LPS-treated cells, unlike AEA, whose catabolism to AA enhances PGE_2 release (76, 77, 146, 147). Therefore, in addition to CB_1R/CB_2R and TRPV1, NADA and WIN55,212-2 may modulate endothelial inflammation by additional mechanisms.

Studies in neurons have shown that the NADA-dependent activation of CB_1R/CB_2R and TRPV1 can exhibit disparate outcomes within the same cell (118). The canonical pathway activated downstream of CB_1R/CB_2R leads to the inhibition of protein kinase A (PKA) through the $G_{i/o}$ proteins (148). However, the PKA-dependent phosphorylation of TRPV1 augments its sensitization, and correspondingly, a reduction in PKA activity will lead to its inactivation, opposing the agonist activity of NADA at TRPV1 (149). Therefore, NADA may diametrically regulate the influx of cations into the cell by either inducing or reducing cation influx via TRPV1 and CB_1R/CB_2R, respectively, to modulate neuronal homeostasis (118). This dual modulatory effect of NADA has previously been proposed to fine-tune the transmission of glutamate onto dopamine neurons and explain such observations that NADA has both pro- and anti-nociceptive properties (70, 72). Based on our observations that NADA may reduce inflammation through CB_1R/CB_2R, but promote inflammation through TRPV1, a logical conclusion is that NADA may also fine-tune the inflammatory activation of ECs (150). A model based on our observations with NADA in LPS-treated lung HMVECs is shown in Figure 2.16, and a summation can be found in the figure legend.

Recent findings using TRPV1 knockout mice in sepsis models indicate a protective role for TRPV1, which is consistent with our observations that inhibition of TRPV1 in ECs augments the LPS-induced inflammatory response in the absence of cannabinoids (Figures 2.5G, 2.14, C and D, and 2.16) (151, 152). In these published studies, the loss of TRPV1 exacerbates the inflammatory response to infection. This is analogous to the reported effects of deleting the nicotinic acetylcholine receptor α7 subunit (α7nAChR), another cation channel (153). The vagus nerve transmits action potentials via the ganglia to peripheral nerves that terminate in organs, where they stimulate the release of the neurotransmitter acetylcholine (ACh) from T-cells (154). The ACh-induced activation of α7nAChR on leukocytes inhibits pro-inflammatory signaling pathways in these cells (155). Because endogenous NADA has thus far only been detected in various parts of the central and peripheral nervous systems, it is conceivable that it may be a component of the inflammatory reflex arc that regulates EC inflammation, analogous to the role of ACh and α7nAChR in leukocyte inflammatory regulation (65, 70, 156). Interestingly, in the brain there is a close association of ECs and perivascular nerves within the neurovascular unit (157, 158). In such areas, the secretion of NADA from perivascular nerves onto brain microvascular ECs may directly modulate neuroinflammation. We speculate that a similar process may occur within visceral organs, whereby the release of NADA from varicosities on innervating efferent nerve axons directly regulates the inflammatory activation of microvascular ECs. Analogous to neuromuscular junctions on smooth muscle, these putative neuroendothelial junctions would not require specialized structures on the endothelial cells (159). This highly speculative model additionally predicts that localized,

physiologically relevant concentrations of NADA may be achieved at neuroendothelial junctions.

In conclusion, our studies indicate that the endocannabinoid/endovanilloid NADA and the synthetic cannabinoid WIN55,212-2 potently reduce the activation of human ECs in response to endogenous and exogenous inflammatory agonists. Furthermore, our results identify the endothelial endocannabinoid system as a novel regulator of endothelial inflammatory activation. Although further studies are required to thoroughly elucidate the mechanisms of endocannabinoid function in ECs, our observations may have important implications for a variety of acute inflammatory disorders that are characterized by endothelial activation and dysfunction and cause organ injury and failure, such as sepsis and ischemia-reperfusion injury.

Figure 2.1

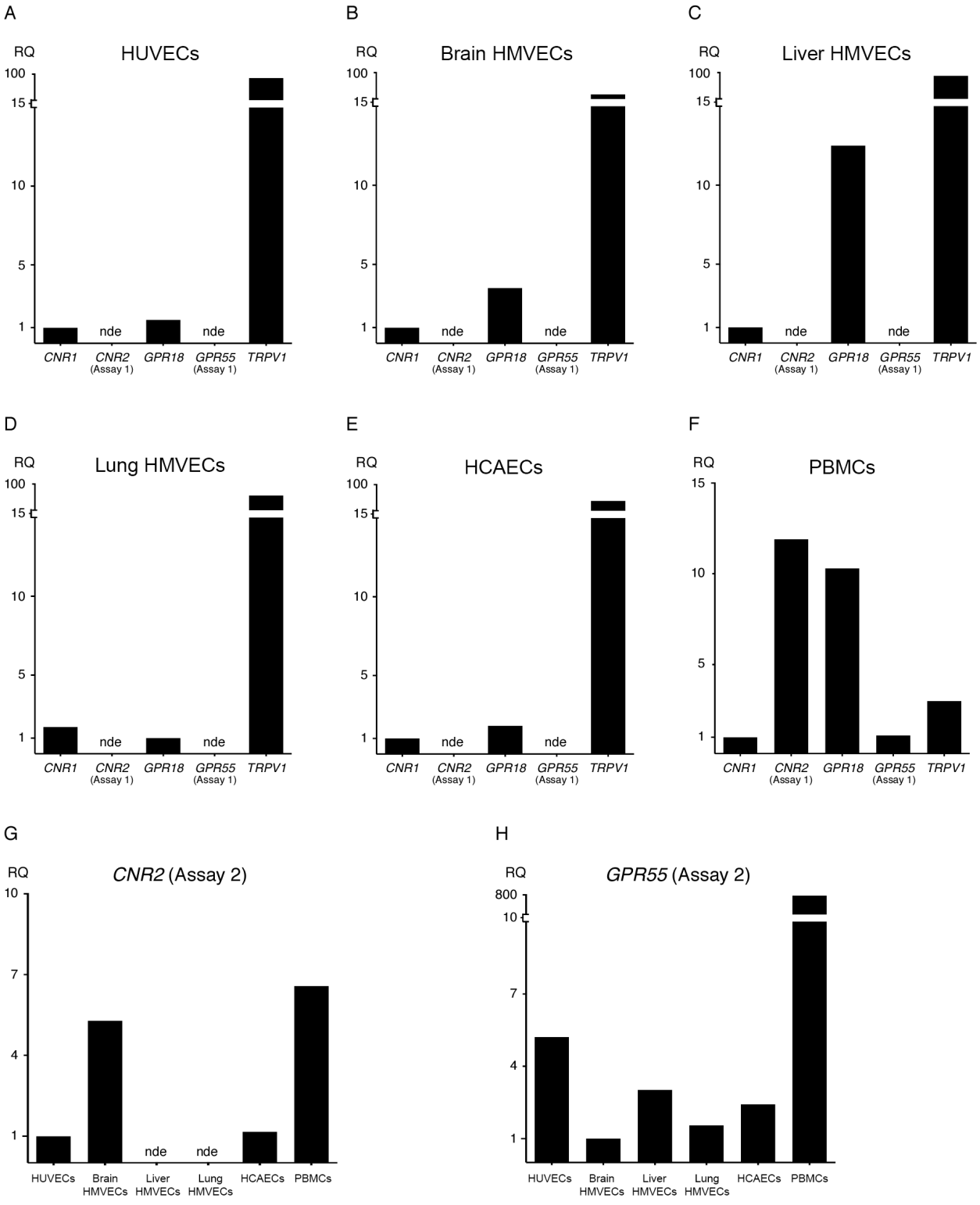
A
HUVECs
RQ
100
15
10
5
1
nde
nde
CNR1
CNR2 (Assay 1)
GPR18
GPR55 (Assay 1)
TRPV1
B
Brain HMVECs
C
Liver HMVECs
D
Lung HMVECs
E
HCAECs
F
PBMCs
G
CNR2 (Assay 2)
HUVECs
Brain HMVECs
Liver HMVECs
Lung HMVECs
HCAECs
PBMCs
H
GPR55 (Assay 2)
800

Figure 2.1. ECs express a similar subset of CBR mRNA transcripts.

HUVECs (multiple donors) (A, G, and H), brain HMVECs (two donors) (B, G, and H), liver HMVECs (one donor) (C, G, and H), lung HMVECs (one donor) (D, G, and H), and HCAECs (one donor) (E, G, and H) were grown in their respective media and lysed with TRIzol upon confluency. PBMCs (three donors) (F, G, and H) were immediately lysed upon isolation. Three biological replicates were analyzed for each donor. The mean C_t value for HPRT1 and GUSB was used as the reference in calculating the ΔC_t values (Table 2.1) for each biological replicate as described in Materials and Methods. 80 ng of cDNA was analyzed for each sample. The relative quantification (RQ) values shown in the *graphs* are relative to lowest detectable expressing CBR gene for each cell type (A-F) or lowest detectable expressing cell type for each gene (G and H). When gene expression was not detected in more than half of the technical replicates, it was defined as not expressed (nde*,* not detectably expressed). Because *CNR1* and *GPR55* were not initially detected using assay 1, a second gene assay (assay 2) was performed using different primers to re-assess expression in the same samples (G and H).

Figure 2.2

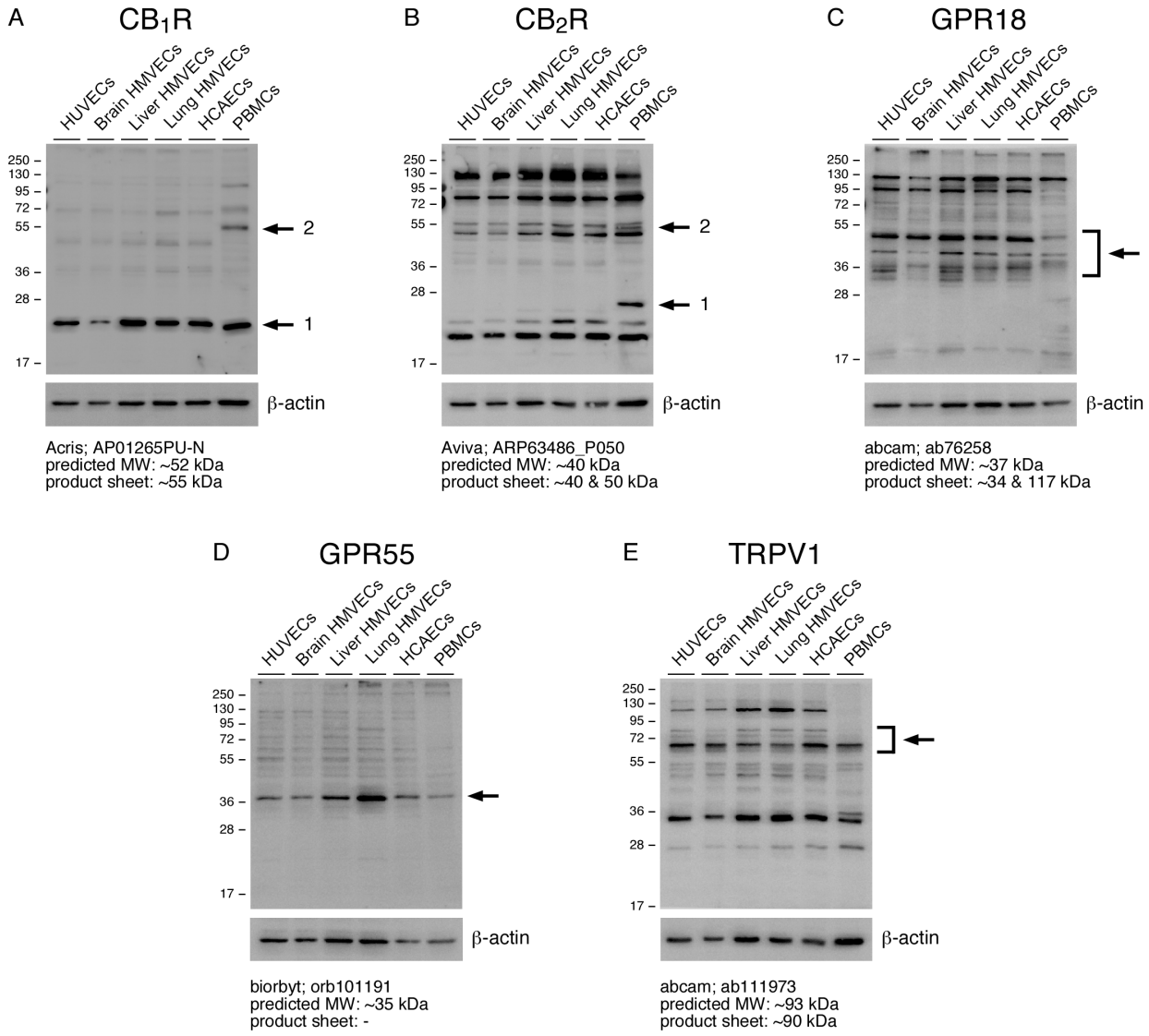
A
CB1R
HUVECs
Brain HMVECs
Liver HMVECs
Lung HMVECs
HCAECs
PBMCs
250
130
95
72
55
36
28
17
2
1
β-actin
Acris; AP01265PU-N
predicted MW: ~52 kDa
product sheet: ~55 kDa
B
CB2R
Aviva; ARP63486_P050
predicted MW: ~40 kDa
product sheet: ~40 & 50 kDa
C
GPR18
abcam; ab76258
predicted MW: ~37 kDa
product sheet: ~34 & 117 kDa
D
GPR55
biorbyt; orb101191
predicted MW: ~35 kDa
product sheet: -
E
TRPV1
abcam; ab111973
predicted MW: ~93 kDa
product sheet: ~90 kDa

Figure 2.2. ECs express CBR and TRPV1 proteins.

HUVECs, brain, liver, and lung HMVECs, and HCAECs were grown to confluency in 6-well plates and lysed with RIPA-LB. CB_1R (A), CB_2R (B), GPR18 (C), GPR55 (D), and TRPV1 (E) protein levels were assessed by immunoblot using the indicated antibodies. PBMCs were immediately lysed in RIPA-LB upon isolation. β-actin levels were assessed as a loading control (bottom panels) (A–E). Arrows indicate candidate CBR or TRPV1 protein bands. For reference, the predicted molecular weight and the molecular weight indicated in the respective products sheets are shown.

Figure 2.3

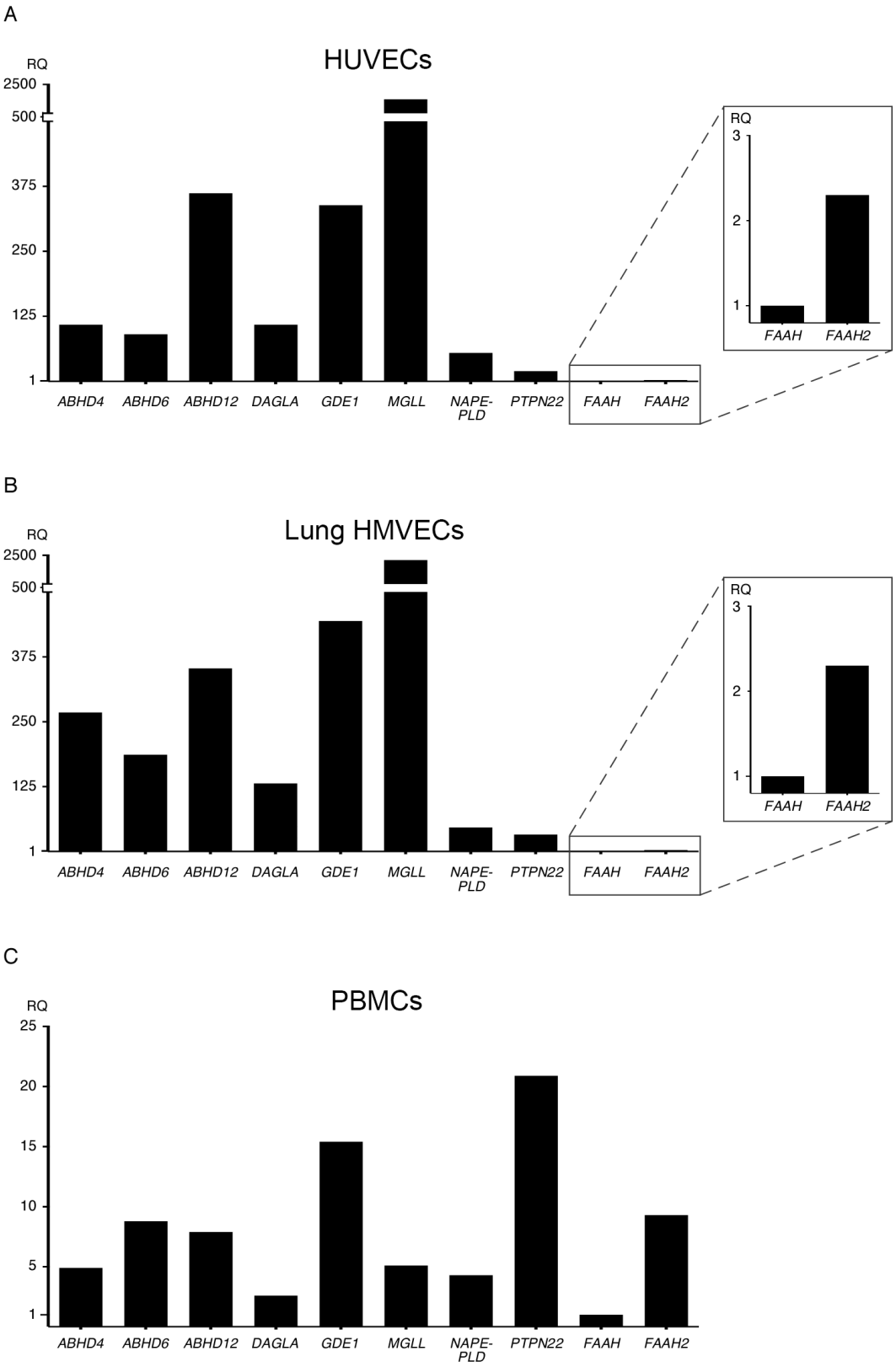
A
HUVECs
RQ
2500
500
375
250
125
1
ABHD4
ABHD6
ABHD12
DAGLA
GDE1
MGLL
NAPE-PLD
PTPN22
FAAH
FAAH2
RQ
3
2
1
FAAH
FAAH2
B
Lung HMVECs
RQ
2500
500
375
250
125
1
ABHD4
ABHD6
ABHD12
DAGLA
GDE1
MGLL
NAPE-PLD
PTPN22
FAAH
FAAH2
RQ
3
2
1
FAAH
FAAH2
C
PBMCs
RQ
25
20
15
10
5
1
ABHD4
ABHD6
ABHD12
DAGLA
GDE1
MGLL
NAPE-PLD
PTPN22
FAAH
FAAH2

Figure 2.3. ECs express the same subset of endocannabinoid metabolic enzymes.

HUVECs (multiple donors) (A) and lung HMVECs (one donor) (B) were grown in their respective media and lysed with TRIzol upon confluency. PBMCs (one donor) (C) were immediately lysed upon isolation. The samples were analyzed as described in Figure 1. RQ, relative quantification.

Figure 2.4

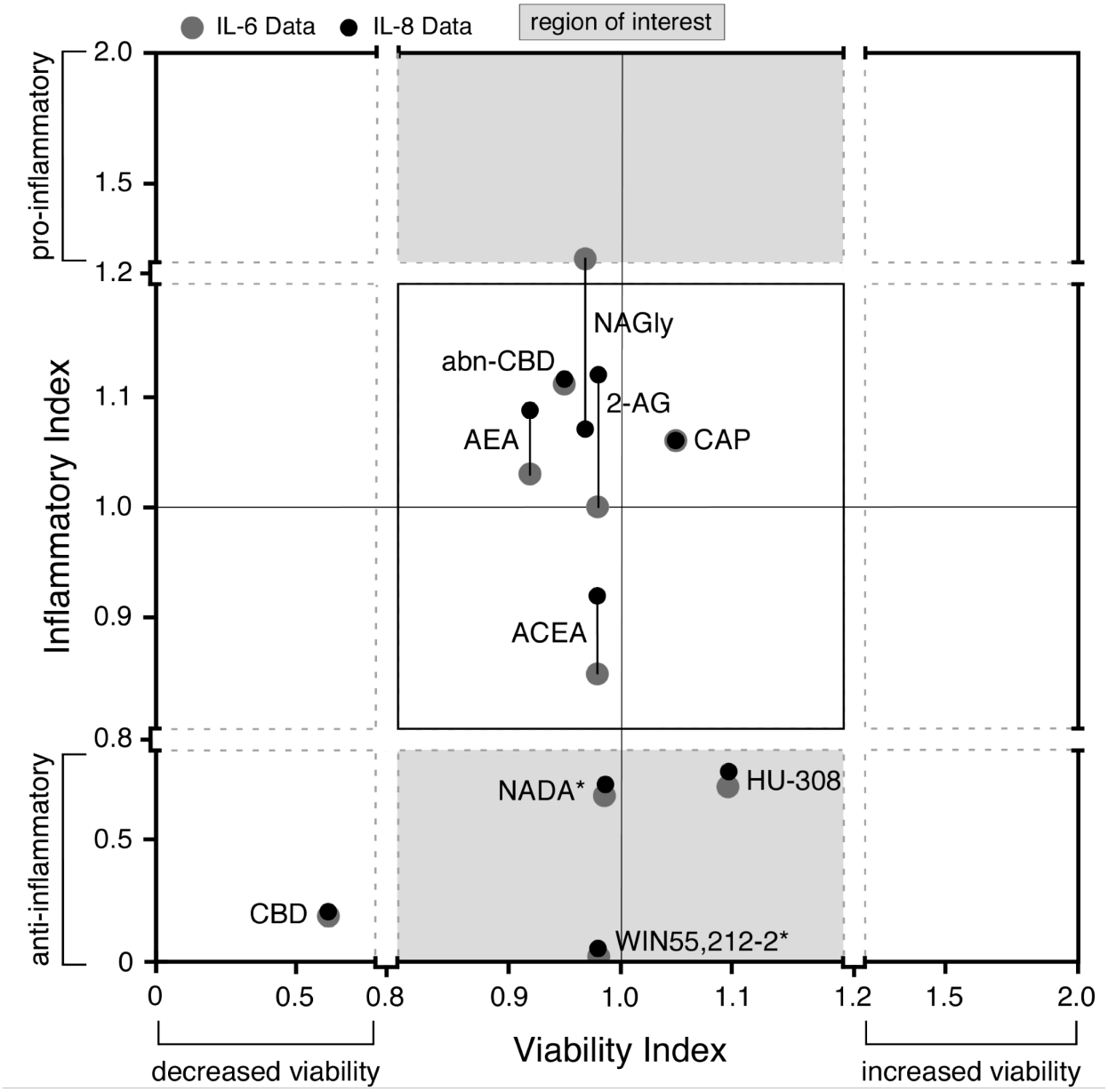
IL-6 Data
IL-8 Data
region of interest
pro-inflammatory
anti-inflammatory
Inflammatory Index
2.0
1.5
1.2
1.1
1.0
0.9
0.8
0.5
0
NAGly
abn-CBD
2-AG
AEA
CAP
ACEA
NADA*
HU-308
CBD
WIN55,212-2*
0
0.5
0.8
0.9
1.0
1.1
1.2
1.5
2.0
decreased viability
Viability Index
increased viability

Figure 2.4. NADA and WIN55,212-2 significantly decrease IL-6 and IL-8 secretion from ECs without affecting cell viability.

Levels of IL-6 and IL-8 were quantified in supernatants of lung HMVECs that were pretreated for 1 hour with 10 μM of the indicated CBR agonist/antagonist and then treated with either 10 μg/mL FSL-1 or LPS or with 100 ng/mL TNFα for an additional 6 hours while in the continuous presence of inhibitor. The relative viability of HUVECs or lung HMVECs was determined by an MTT assay after incubation with 10 μM of the indicated CBR agonist/antagonist, DMSO, or ethanol control for 7 hours. To calculate the inflammatory indices, the relative inflammatory index in each independent experiment for each CBR agonist/antagonist was first calculated (*i.e.* the average cytokine concentration for the samples treated with both the inflammatory agonist (FSL-1, LPS, or TNFα) and CBR agonist/antagonist divided by the average cytokine concentration for the samples treated with inflammatory agonist alone; n=3 minimum). Then, the means of these relative indices for each CBR agonist/antagonist were plotted on the graph (n=4-5; see Table 2.4 for the n value breakdowns for the different inflammatory agonists). The MTT viability indices were calculated in the same manner. The region of interest (shaded gray area) indicates CBR agonists/antagonists that decrease or increase cytokine expression by more than 20% versus control (those compounds with inflammatory indices <0.8 and >1.2, respectively) and do not decrease or increase viability by more than 20% versus control (those compounds with viability indices between 0.8 and 1.2). *, CBR agonists/antagonists that have a significant (p < 0.05) effect on IL-6 and IL-8 secretion, without significantly (p < 0.05) affecting viability (*e.g.* NADA and WIN55,212-2). Note: solutions of AEA in ethanol and Tocrisolve were

tested with similar results. The calculated results, including mean, S.E., and *p* values, are shown in Table 2.3. *abnCBD*, abnormal CBD.

Figure 2.5

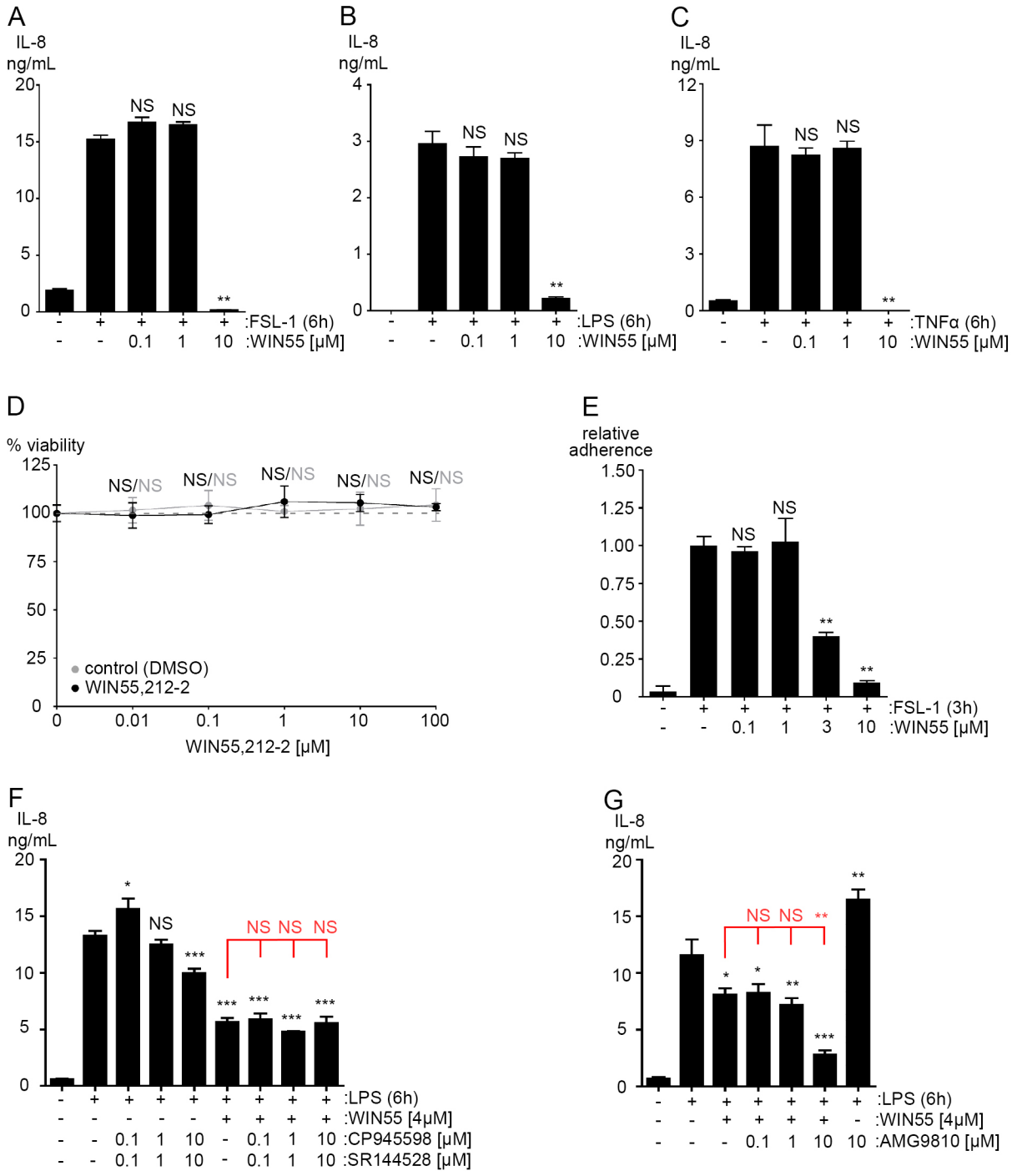
A
IL-8
ng/mL
20
15
10
5
0
NS
NS
**
:FSL-1 (6h)
:WIN55 [μM]
B
IL-8
ng/mL
4
3
2
1
0
NS
NS
**
:LPS (6h)
:WIN55 [μM]
C
IL-8
ng/mL
12
9
6
3
0
NS
NS
**
:TNFα (6h)
:WIN55 [μM]
D
% viability
125
100
75
50
25
0
NS/NS
NS/NS
NS/NS
NS/NS
NS/NS
control (DMSO)
WIN55,212-2
0
0.01
0.1
1
10
100
WIN55,212-2 [μM]
E
relative
adherence
1.50
1.25
1.00
0.75
0.50
0.25
0
NS
NS
**
**
:FSL-1 (3h)
:WIN55 [μM]
F
IL-8
ng/mL
20
15
10
5
0
*
NS
***
NS NS NS
***
***
***
***
:LPS (6h)
:WIN55 [4μM]
:CP945598 [μM]
:SR144528 [μM]
G
IL-8
ng/mL
20
15
10
5
0
**
NS NS **
*
*
**
***
:LPS (6h)
:WIN55 [4μM]
:AMG9810 [μM]

Figure 2.5. WIN55,212-2 reduces the inflammatory activation of lung HMVECs without affecting viability.

(A-C) Levels of IL-8 were quantified in the supernatants of lung HMVECs that were pretreated for 1 hour with the indicated concentrations of WIN55,212-2 and then treated with either 10 μg/mL FSL-1 (A) or LPS (B) or 100 ng/mL TNFα (C) for an additional 6 hours while in the continuous presence of WIN55,212-2 (*n*=3). NS, not significant; **, $p < 0.01$; FSL-1 versus FSL-1 plus WIN55,212-2.

(D) MTT assay was performed on lung HMVECs that were treated for 7 hours at the indicated concentrations of WIN55,212-2. Control samples were incubated with a concentration of DMSO equivalent to that present in the WIN55,212-2-treated samples. NS, not significant

(*E*) Lung HMVECs were pretreated for 1 hour with the indicated concentrations of WIN55,212-2 and then treated with 10 μg/mL FSL-1 for an additional 3 hours while in the continuous presence of WIN55,212-2. The lung HMVECs were then washed and calcein AM-labeled primary human neutrophils were allowed to adhere for 20 minutes. Non-adherent neutrophils were subsequently removed, and the percentage of remaining adherent neutrophils was calculated (*n*=3). **, $p < 0.01$; ANOVA.

(F) Levels of IL-8 were quantified in the supernatants of lung HMVECs that were pretreated for 30 minutes with either 0.1, 1, or 10 μM CP945598/SR144528 and then incubated for another 30 minutes with 4 μM WIN55,212-2 in the presence of CP945598/SR144528. ECs were then treated with 10 μg/mL LPS for an additional 6

hours while in the continuous presence of CP945598/SR144528 and/or WIN55,212-2 (*n*=3). Crystal violet readings between samples were not significantly different

(G) Cells were treated and analyzed similarly as (F), except using the TRPV1 inhibitor AMG9810 (*n*=4). Crystal violet readings for the samples treated with AMG9810 (10 μM) displayed a significant decrease in cell adherence ($p < 0.01$). F and G*, t* tests (black): NS*,* not significant; *, $p < 0.05$; **, $p < 0.01$; ***, $p < 0.001$; LPS versus LPS plus CP945598/SR144528 or AMG9810 and/or WIN55,212-2. ANOVA (red): NS*,* not significant; **, $p < 0.01$, LPS plus WIN55,212-2 versus LPS plus WIN55,212-2 and CP945598/SR144528 or AMG9810. WIN55,212-2 ELISAs were performed three times, and the MTT and neutrophil adhesion assays were performed two times.

Figure 2.6

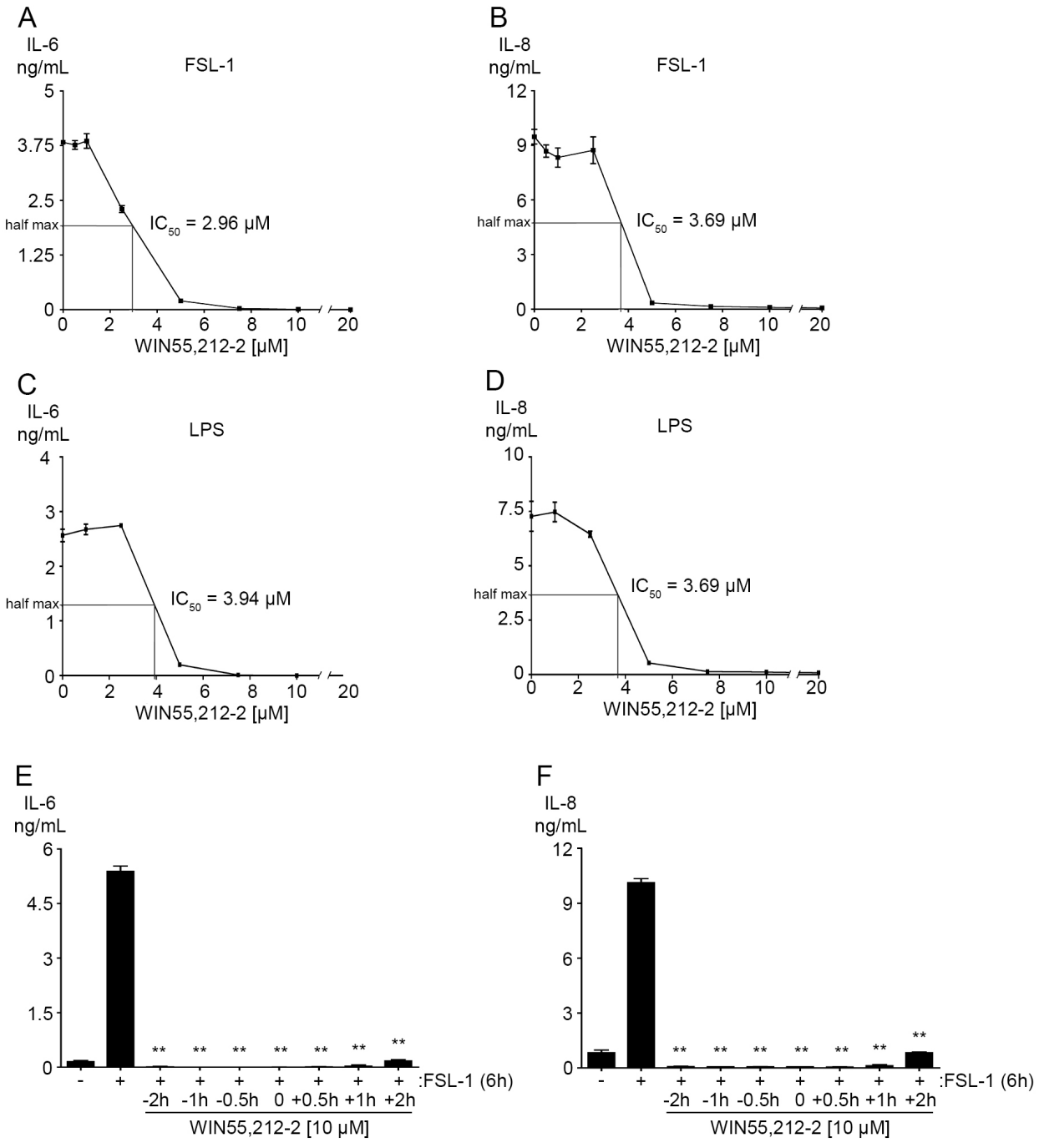
A
IL-6
ng/mL
FSL-1
5
3.75
2.5
half max
1.25
0
IC50 = 2.96 μM
0 2 4 6 8 10 20
WIN55,212-2 [μM]
B
IL-8
ng/mL
FSL-1
12
9
6
half max
3
0
IC50 = 3.69 μM
0 2 4 6 8 10 20
WIN55,212-2 [μM]
C
IL-6
ng/mL
LPS
4
3
2
half max
1
0
IC50 = 3.94 μM
0 2 4 6 8 10 20
WIN55,212-2 [μM]
D
IL-8
ng/mL
LPS
10
7.5
5
half max
2.5
0
IC50 = 3.69 μM
0 2 4 6 8 10 20
WIN55,212-2 [μM]
E
IL-6
ng/mL
6
4.5
3
1.5
0
**
- + + + + + + + + :FSL-1 (6h)
-2h -1h -0.5h 0 +0.5h +1h +2h
WIN55,212-2 [10 μM]
F
IL-8
ng/mL
12
9
6
3
0
**
- + + + + + + + + :FSL-1 (6h)
-2h -1h -0.5h 0 +0.5h +1h +2h
WIN55,212-2 [10 μM]

Figure 2.6. WIN55,212-2 inhibits the inflammatory activation of ECs when added prior to or after treatment with inflammatory agonists.

Levels of IL-6 (A, C and E) and IL-8 (B, D and F) were quantified in the supernatants of lung HMVECs that either were pre-treated for 1 hour with the indicated concentrations of WIN55,212-2, and then treated with either 10 μg/mL of FSL-1 (A and B) or LPS (C and D) for an additional 6 hours while in the continuous presence of WIN55,212-2 (n=4), or treated up to 2 hours prior to or 2 hours after the addition 10 μg/mL of FSL-1 (E and F). FSL-1 was added for exactly 6 hours, and once WIN55,212-2 was added it was continuously present until the supernatants were collected (n=4) (E and F). The IC_{50} value indicates the concentration of WIN55,212-2 required to reduce the maximum cytokine concentration induced by inflammatory agonist by half. $^{**}p < 0.01$, inflammatory agonist versus inflammatory agonist plus WIN55,212-2. All experiments were performed 2 times.

Figure 2.7

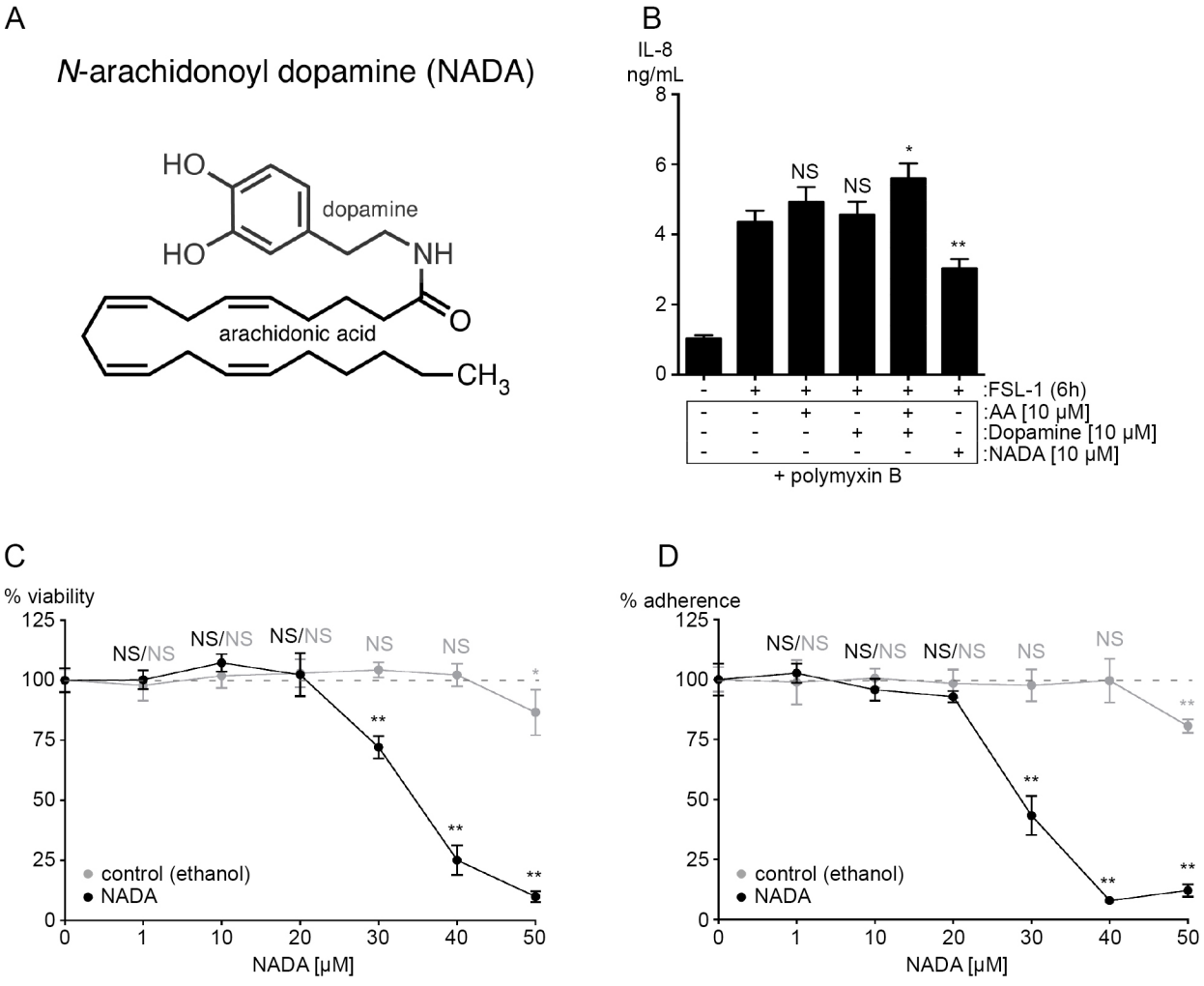
A
N-arachidonoyl dopamine (NADA)
HO
HO
dopamine
NH
O
arachidonic acid
CH3
B
IL-8
ng/mL
8
6
4
2
0
NS
NS
*
**
:FSL-1 (6h)
:AA [10 μM]
:Dopamine [10 μM]
:NADA [10 μM]
+ polymyxin B
C
% viability
125
100
75
50
25
0
NS/NS
NS/NS
NS/NS
NS
NS
*
**
**
**
control (ethanol)
NADA
0
1
10
20
30
40
50
NADA [μM]
D
% adherence
125
100
75
50
25
0
NS/NS
NS/NS
NS/NS
NS
NS
**
**
**
**
control (ethanol)
NADA
0
1
10
20
30
40
50
NADA [μM]

Figure 2.7. NADA, and not its chemical constituents AA and dopamine, reduces IL-8 secretion from lung HMVECs activated with FSL-1, and concentrations of NADA less than 20μM do not affect lung HMVEC viability.

(A) NADA is composed of AA and dopamine moieties covalently linked by an amide bond.

(B) Levels of IL-8 were quantified in the supernatants of lung HMVECs that were pretreated for 1 hour with either 10 μM of AA, 10 μM of dopamine, 10 μM of both AA and dopamine, or 10 μM NADA and then treated with 10 μg/mL FSL-1 for an additional 6 hours while in the continuous presence of AA, dopamine, or NADA (*n*=4). Polymyxin B at 50 μg/mL was added to each sample for the duration of the experiment. NS, not significant; *, $p < 0.05$; **, $p < 0.01$, FSL-1 versus FSL-1 plus AA, dopamine, or NADA

(C and D) An MTT (C, *n*=4) and crystal violet (D, *n*=4) assay was performed on lung HMVECs treated for 7 hours at the indicated concentrations of NADA. Control samples were incubated with a concentration of ethanol equivalent to that present in the NADA-treated samples. NS, not significant; **, $p < 0.01$; NADA versus ethanol control. The IL-8 ELISA was performed three times, and the MTT and crystal violet assays were performed two times.

Figure 2.8

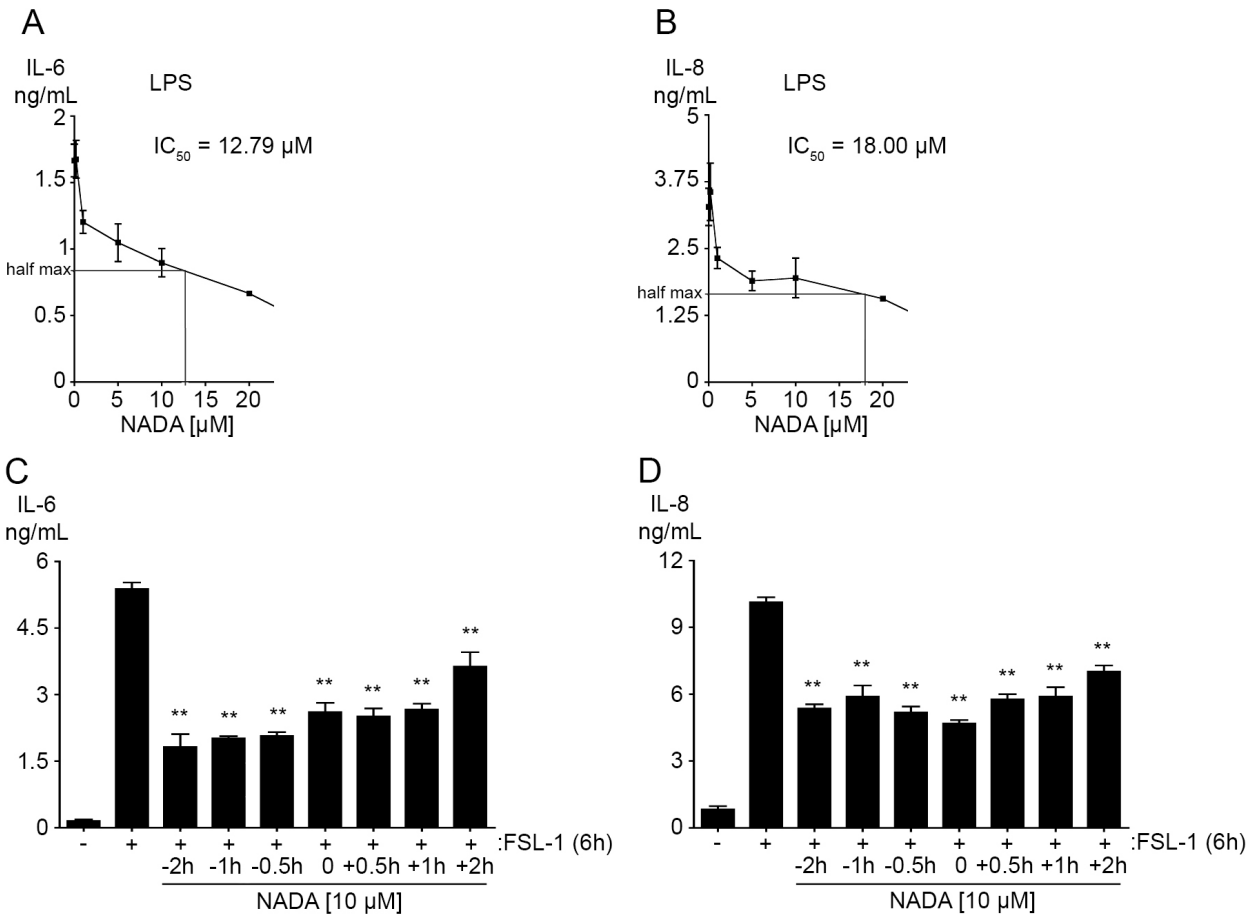
A
IL-6
ng/mL
LPS
IC50 = 12.79 μM
half max
NADA [μM]
B
IL-8
ng/mL
LPS
IC50 = 18.00 μM
half max
NADA [μM]
C
IL-6
ng/mL
:FSL-1 (6h)
-2h -1h -0.5h 0 +0.5h +1h +2h
NADA [10 μM]
D
IL-8
ng/mL
:FSL-1 (6h)
-2h -1h -0.5h 0 +0.5h +1h +2h
NADA [10 μM]

Figure 2.8. NADA inhibits the inflammatory activation of ECs when added prior to or after treatment with inflammatory agonists.

Levels of IL-6 (B and D) and IL-8 (A, C and E) were quantified in the supernatants of lung HMVECs that either were pre-treated for 1 hour with the indicated concentrations of NADA, and then treated with either 10 μg/mL of LPS (A-C) for an additional 6 hours while in the continuous presence of NADA (n=3-4), or treated up to 2 hours prior to or 2 hours after the addition 10 μg/mL of FSL-1 (D and E). FSL-1 was added for exactly 6 hours, and once NADA was added it was continuously present until the supernatants were collected (n=4) (D and E). Ethanol solutions of NADA purchased either from Sigma, Tocris or Cayman Chemical were used in the comparison assay in panel A, while NADA from sigma was used in panels B-E. The IC_{50} value indicates the concentration of NADA required to reduce the maximum cytokine concentration induced by LPS by half. $^{**}p < 0.01$, inflammatory agonist versus inflammatory agonist plus NADA. All experiments were performed two times.

Figure 2.9

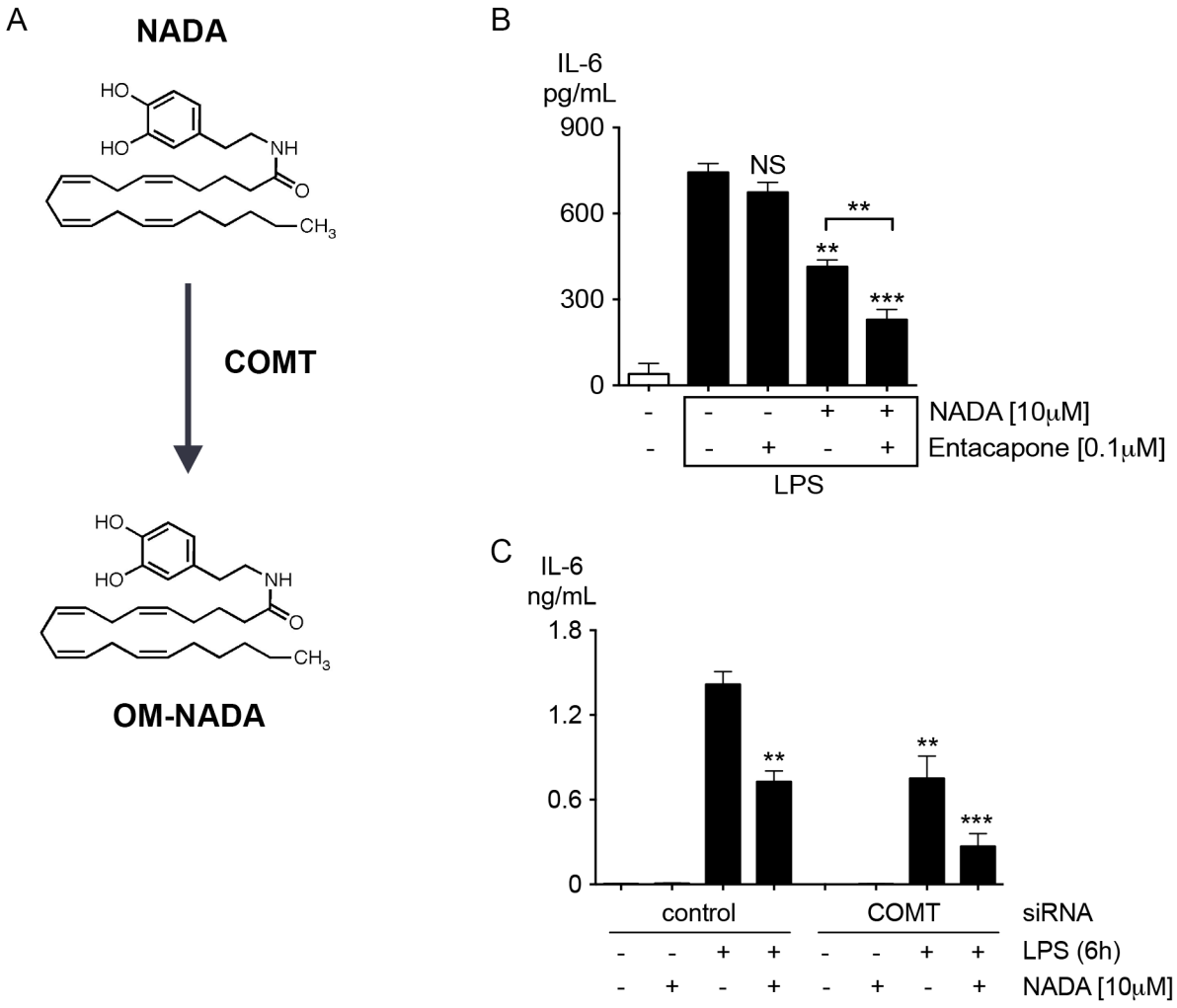
A
NADA
HO
HO
NH
O
CH3
COMT
HO
HO
NH
O
CH3
OM-NADA
B
IL-6
pg/mL
900
600
300
0
NS
**
**
***
- - - + + NADA [10μM]
- - + - + Entacapone [0.1μM]
LPS
C
IL-6
ng/mL
1.8
1.2
0.6
0
**
**
***
control
COMT
siRNA
- - + + - - + + LPS (6h)
- + - + - + - + NADA [10μM]

Figure 2.9. Inhibition or silencing of COMT expression enhances NADA activity in lung HMVECs.

(A) The dopamine moiety of NADA can be inactivated by COMT to generate *O*-methyl-NADA (OM-NADA).

(B) Levels of IL-6 were quantified in the supernatants of lung HMVECs that were pretreated for 1 hour with 10 μM NADA and 0.1 μM of the COMT inhibitor entacapone, and then treated with 10 μg/mL LPS for an additional 6 hours while in the continuous presence of NADA and the inhibitor (n=4). NS, not significant; **, $p < 0.01$; ***, $p < 0.001$ when comparing samples to LPS only treatment.

(C) Levels of IL-6 were quantified in the supernatants of lung HMVECs that had COMT silenced by siRNA. Cells were pretreated for 1 hour with 10 μM NADA and then treated with 10 μg/mL LPS for an additional 6 hours while in the continuous presence of NADA (n=4). **, $p < 0.01$; ***, $p < 0.001$ when comparing samples to LPS only treatment. All experiments were performed two times.

Figure 2.10

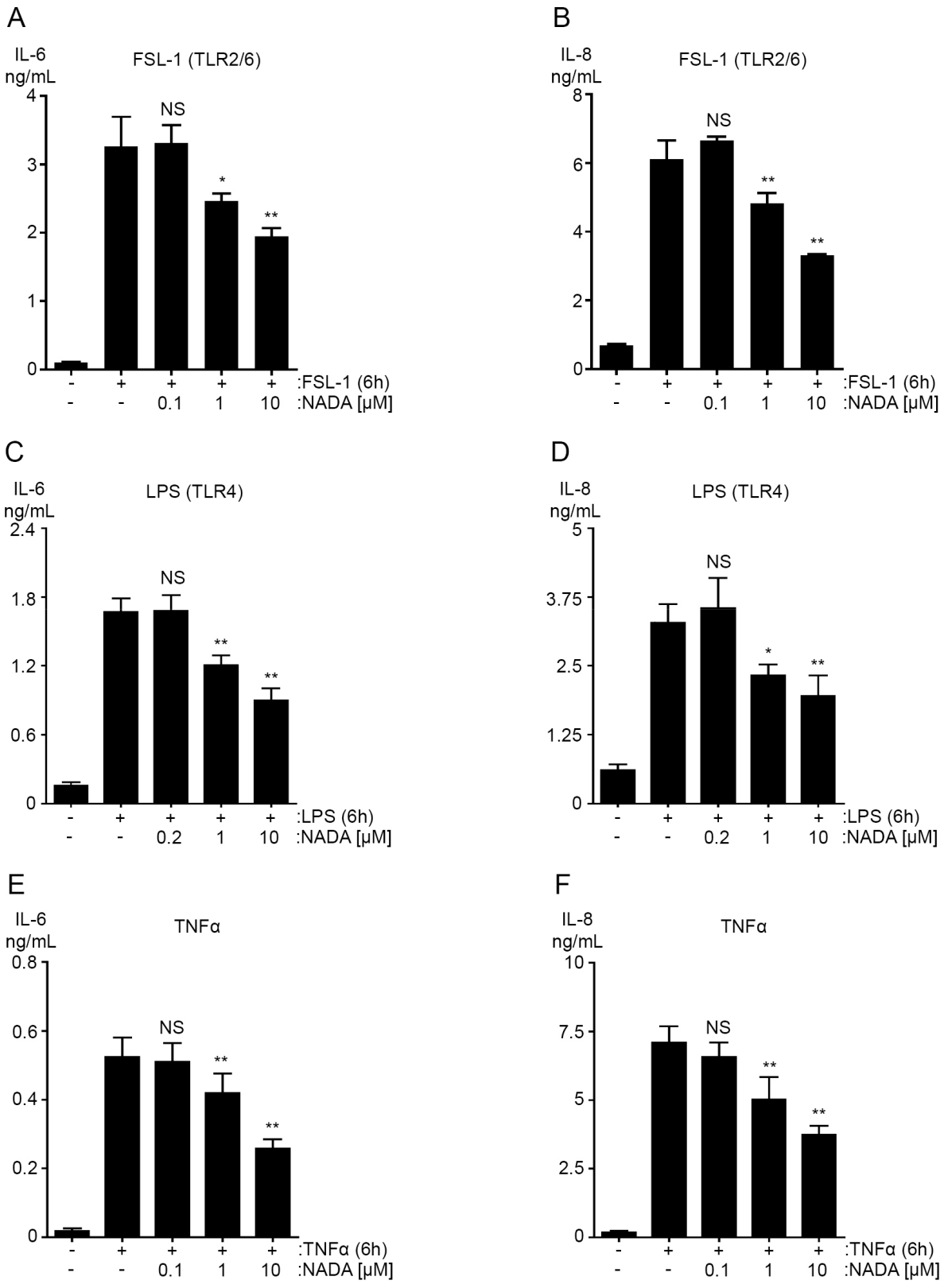
A
IL-6
ng/mL
FSL-1 (TLR2/6)
4
3
2
1
0
NS
*
**
- + + + + :FSL-1 (6h)
- - 0.1 1 10 :NADA [μM]
B
IL-8
ng/mL
FSL-1 (TLR2/6)
8
6
4
2
0
NS
**
**
- + + + + :FSL-1 (6h)
- - 0.1 1 10 :NADA [μM]
C
IL-6
ng/mL
LPS (TLR4)
2.4
1.8
1.2
0.6
0
NS
**
**
- + + + + :LPS (6h)
- - 0.2 1 10 :NADA [μM]
D
IL-8
ng/mL
LPS (TLR4)
5
3.75
2.5
1.25
0
NS
*
**
- + + + + :LPS (6h)
- - 0.2 1 10 :NADA [μM]
E
IL-6
ng/mL
TNFα
0.8
0.6
0.4
0.2
0
NS
**
**
- + + + + :TNFα (6h)
- - 0.1 1 10 :NADA [μM]
F
IL-8
ng/mL
TNFα
10
7.5
5
2.5
0
NS
**
**
- + + + + :TNFα (6h)
- - 0.1 1 10 :NADA [μM]

Figure 2.10. NADA reduces the secretion of IL-6 and IL-8 from lung HMVECs activated with inflammatory agonists.

Levels of IL-6 (A, C, and E) and IL-8 (B, D, and F) were quantified in the supernatants of lung HMVECs that were pretreated for 1 hour with the indicated concentrations of NADA and then treated with either 10 μg/mL FSL-1 (A and B) or LPS (C and D) or 100 ng/mL TNFα (E and F) for an additional 6 hours while in the continuous presence of NADA (*n*=4). NS, not significant; *, $p < 0.05$; **, $p < 0.01$; inflammatory agonist versus inflammatory agonist plus NADA. All experiments were performed four times.

Figure 2.11

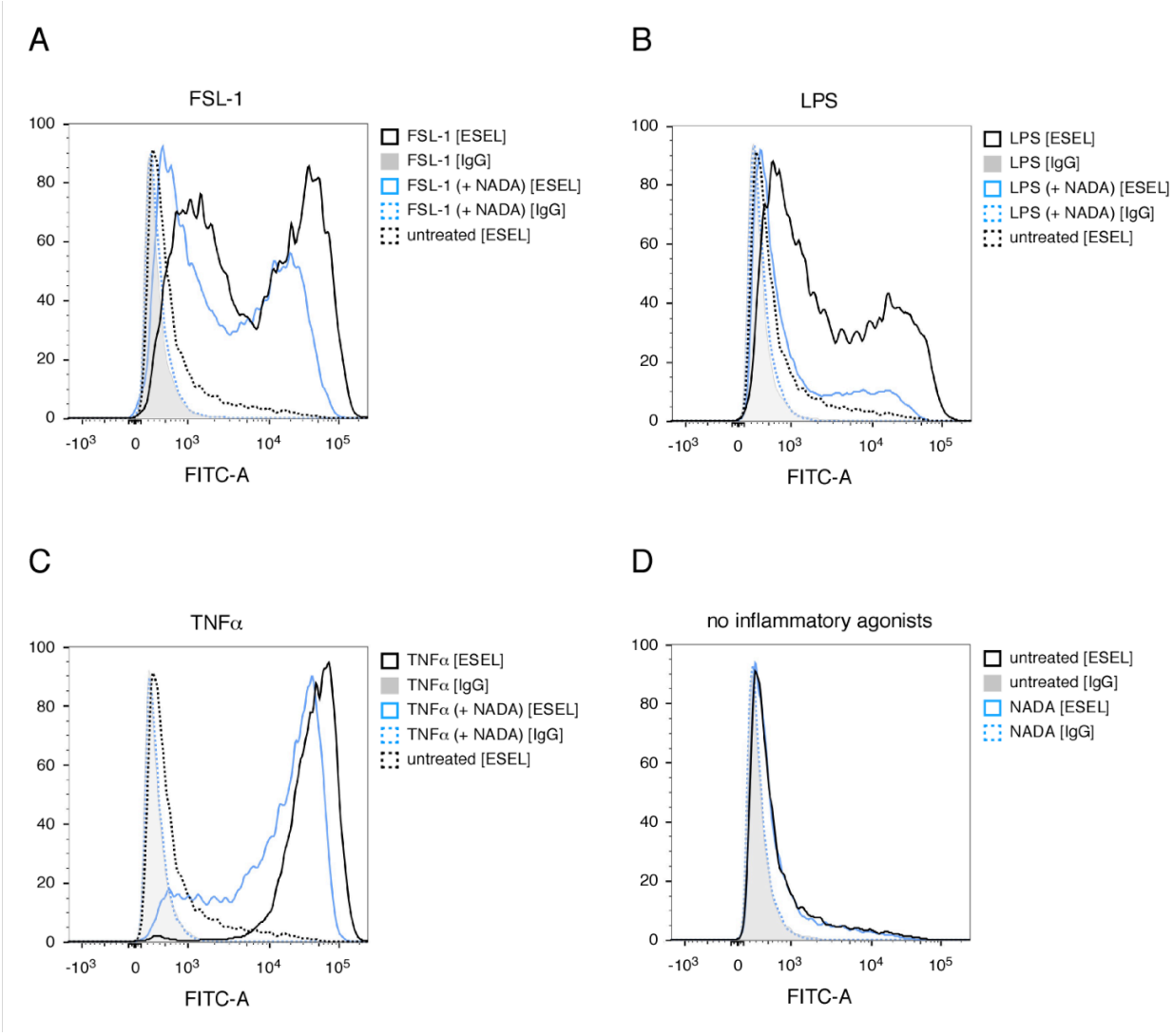
A
FSL-1
100
80
60
40
20
0
-10³
0
10³
10⁴
10⁵
FITC-A
FSL-1 [ESEL]
FSL-1 [IgG]
FSL-1 (+ NADA) [ESEL]
FSL-1 (+ NADA) [IgG]
untreated [ESEL]
B
LPS
LPS [ESEL]
LPS [IgG]
LPS (+ NADA) [ESEL]
LPS (+ NADA) [IgG]
untreated [ESEL]
C
TNFα
TNFα [ESEL]
TNFα [IgG]
TNFα (+ NADA) [ESEL]
TNFα (+ NADA) [IgG]
untreated [ESEL]
D
no inflammatory agonists
untreated [ESEL]
untreated [IgG]
NADA [ESEL]
NADA [IgG]

Figure 2.11. NADA reduces the surface expression of E-selectin on ECs activated by inflammatory agonists.

HUVECs were pretreated for 1 hour with 10 μM NADA and then treated with either 10 μg/mL FSL-1 (A) or LPS (B) or 100 ng/mL TNFα (C) for an additional 3 hours while in the continuous presence of NADA or treated with NADA only for 4 hours (D). FITC-labeled mouse IgG was used an antibody specificity control. Flow cytometry experiments were performed two times.

Figure 2.12

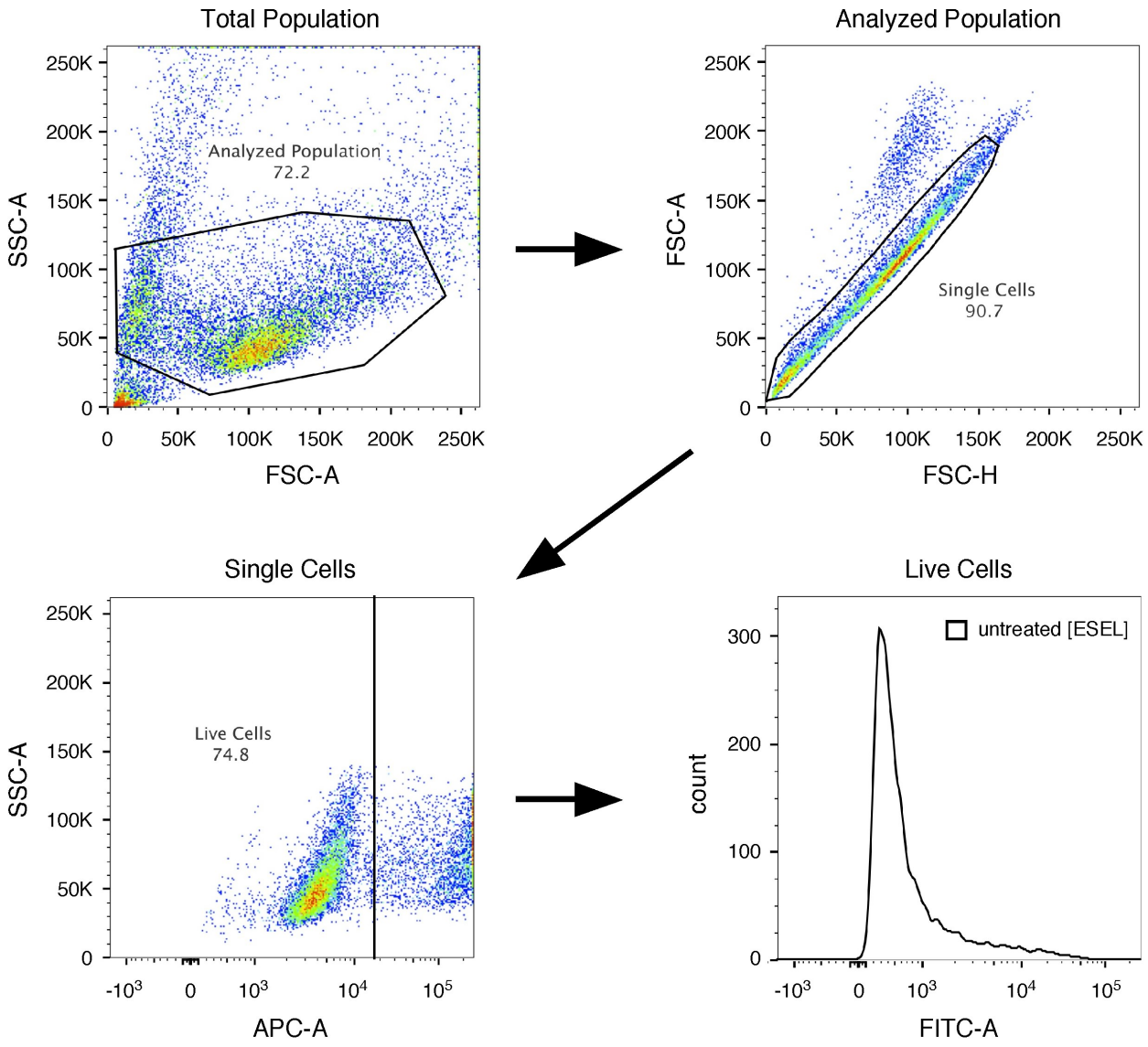
Total Population
Analyzed Population
72.2
SSC-A
FSC-A
250K
200K
150K
100K
50K
0
Analyzed Population
FSC-A
FSC-H
Single Cells
90.7
Single Cells
Live Cells
74.8
SSC-A
APC-A
Live Cells
untreated [ESEL]
count
FITC-A
300
200
100
-10^3
10^3
10^4
10^5

Figure 2.12. Gating strategy for the effects of NADA on the surface expression of E-selectin on activated ECs.

Flow cytometry was performed to assess surface expression of E-selectin on inflammatory agonist activated HUVECs in the presence and absence of NADA. An example schematic of the gating used to analyze E-selectin surface expression in Figure 2.11 is shown.

Figure 2.13

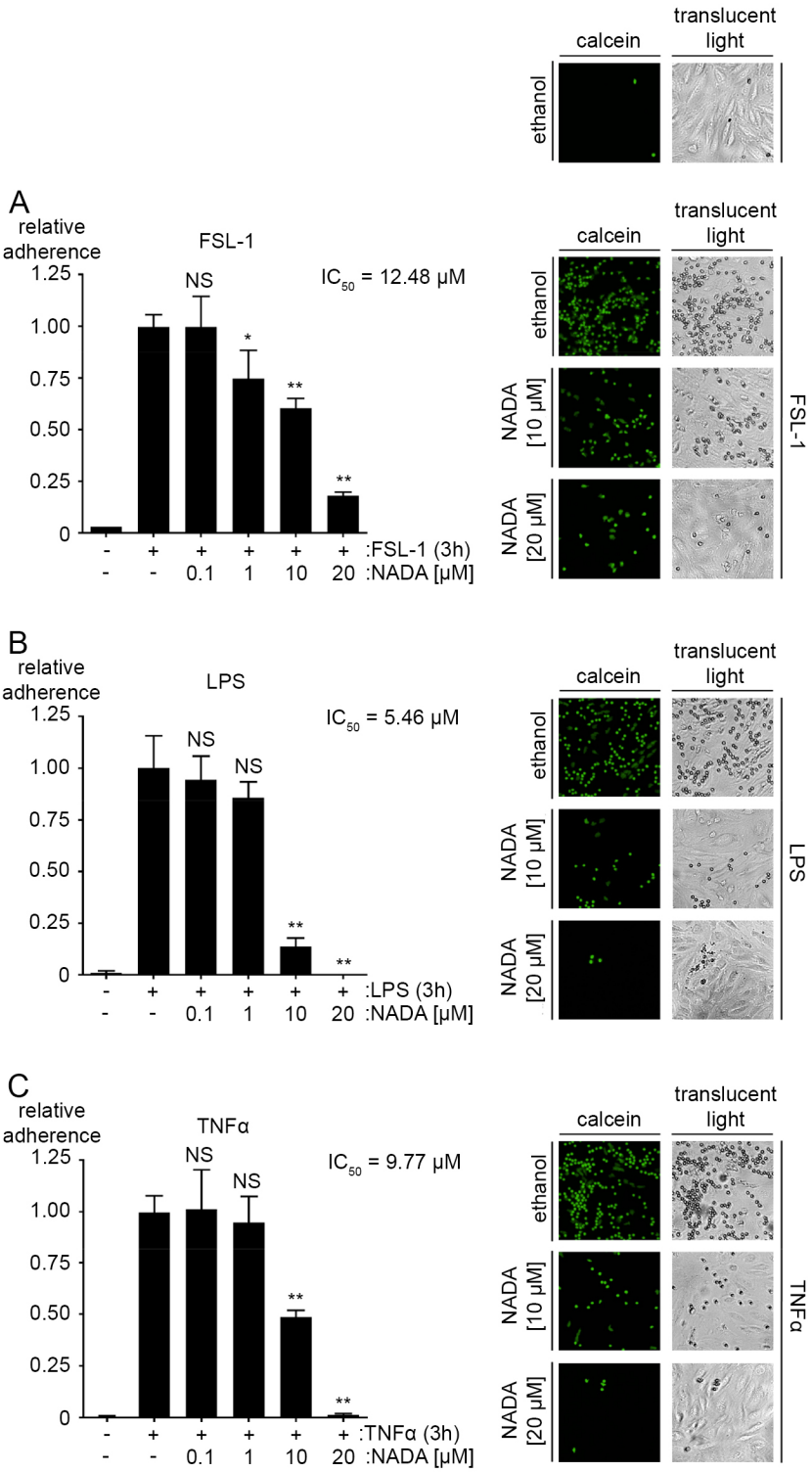
A
relative adherence
FSL-1
IC50 = 12.48 µM
NS
*
**
**
1.25
1.00
0.75
0.50
0.25
0
- + + + + + :FSL-1 (3h)
- - 0.1 1 10 20 :NADA [µM]
calcein
translucent light
ethanol
NADA [10 µM]
NADA [20 µM]
FSL-1
B
relative adherence
LPS
IC50 = 5.46 µM
NS
NS
**
**
1.25
1.00
0.75
0.50
0.25
0
- + + + + + :LPS (3h)
- - 0.1 1 10 20 :NADA [µM]
calcein
translucent light
ethanol
NADA [10 µM]
NADA [20 µM]
LPS
C
relative adherence
TNFα
IC50 = 9.77 µM
NS
NS
**
**
1.25
1.00
0.75
0.50
0.25
0
- + + + + + :TNFα (3h)
- - 0.1 1 10 20 :NADA [µM]
calcein
translucent light
ethanol
NADA [10 µM]
NADA [20 µM]
TNFα

Figure 2.13. NADA reduces the binding of neutrophils to activated ECs.

(A-C) Lung HMVECs were pretreated for 1 hour with the indicated concentrations of NADA and then treated with 10 μg/mL FSL-1 (A) or LPS (B) or 100 ng/mL TNFα (C) for an additional 3 hours while in the continuous presence of NADA. The lung HMVECs were then washed, and calcein AM-labeled primary human neutrophils were allowed to adhere for 20 minutes. Non-adherent neutrophils were subsequently removed, and the percentage of remaining adherent neutrophils was calculated (n=3). NS, not significant; *, $p < 0.05$; **, $p < 0.01$, inflammatory agonist versus inflammatory agonist plus NADA. Representative images of calcein-labeled neutrophils bound to lung HMVECs are shown to the right of the bar graphs. Fluorescence images taken with a fluorescein filter set are shown in the left-hand column, and translucent light microscopy images of the same field of reference are shown in the right-hand column. Images were taken at x10 magnification on an Olympus IX51 inverted microscope equipped with a Retiga 2000R camera (Q imaging). The neutrophil adhesion assays were performed two times.

Figure 2.14

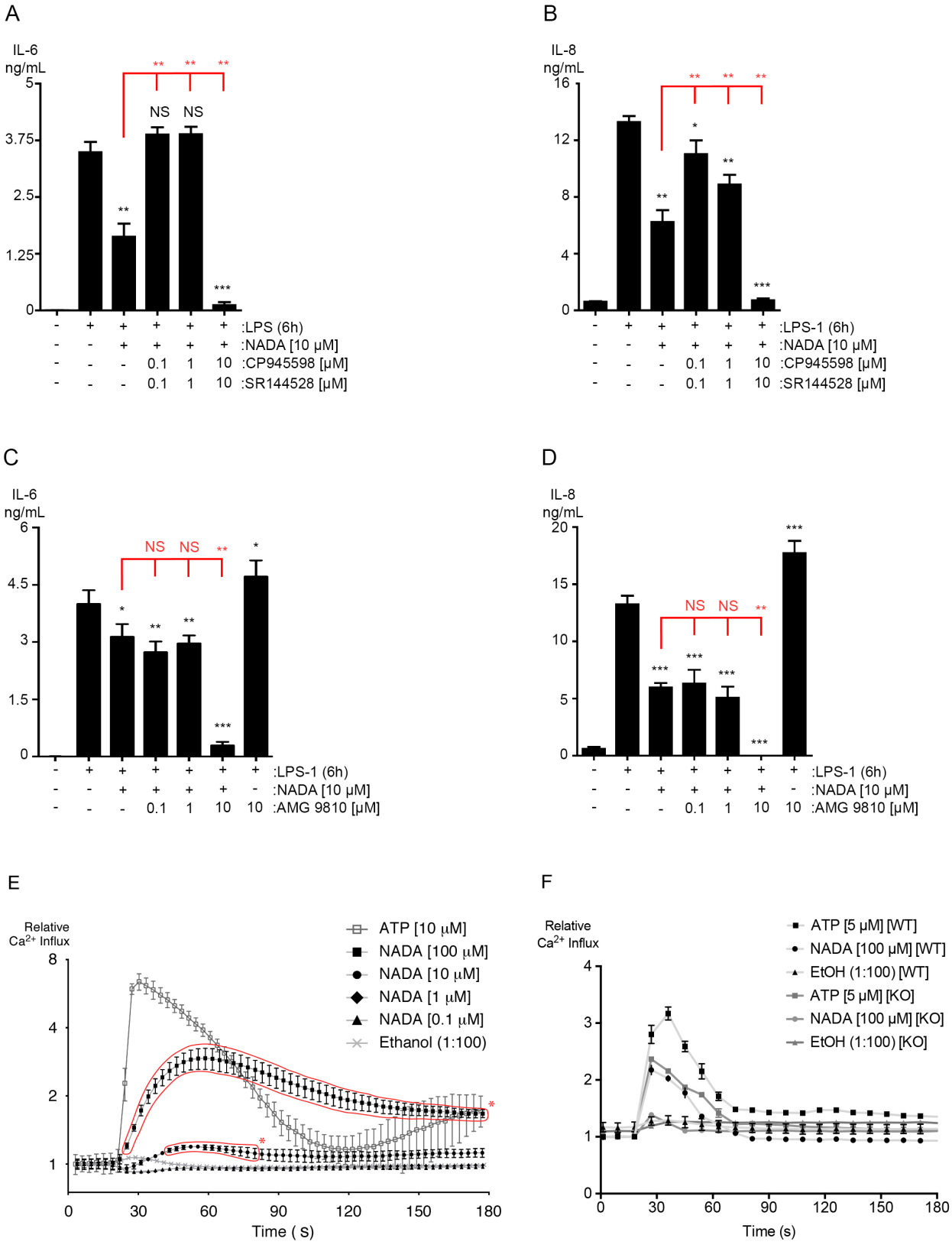
A
IL-6
ng/mL
5
3.75
2.5
1.25
0
NS NS
:LPS (6h)
:NADA [10 μM]
:CP945598 [μM]
:SR144528 [μM]
B
IL-8
ng/mL
16
12
8
4
0
:LPS-1 (6h)
:NADA [10 μM]
:CP945598 [μM]
:SR144528 [μM]
C
IL-6
ng/mL
6
4.5
3
1.5
0
NS NS
:LPS-1 (6h)
:NADA [10 μM]
:AMG 9810 [μM]
D
IL-8
ng/mL
20
15
10
5
0
NS NS
:LPS-1 (6h)
:NADA [10 μM]
:AMG 9810 [μM]
E
Relative
Ca2+ Influx
ATP [10 μM]
NADA [100 μM]
NADA [10 μM]
NADA [1 μM]
NADA [0.1 μM]
Ethanol (1:100)
Time (s)
F
Relative
Ca2+ Influx
ATP [5 μM] [WT]
NADA [100 μM] [WT]
EtOH (1:100) [WT]
ATP [5 μM] [KO]
NADA [100 μM] [KO]
EtOH (1:100) [KO]
Time (s)

Figure 2.14. CB_1R/CB_2R mediate the anti-inflammatory effects of NADA, whereas TRPV1 counters the anti-inflammatory properties of NADA in ECs.

(A and B) Levels of IL-6 (A) and IL-8 (B) were quantified in the supernatants of lung HMVECs that were pretreated for 30 minutes with either 0.1, 1, or 10 μM of CP945598/SR144528 and then incubated for another 30 minutes with 10 μM NADA in the presence of CP945598/SR144528. ECs were then treated with 10 μg/mL LPS for an additional 6 hours while in the continuous presence of CP945598/SR144528 and/or NADA (*n*=3). Crystal violet readings between samples were not significantly different.

(C and D) Cells were treated and analyzed similarly as A and B, except using the TRPV1 inhibitor AMG9810 (*n*=4). Crystal violet readings between samples were not significantly different.

A–D, *t* tests (black): NS, not significant; *, $p < 0.05$; **, $p < 0.01$; ***, $p < 0.001$; LPS versus LPS plus CP945598/SR144528 or AMG9810 and/or NADA. ANOVA (red): NS, not significant; **, $p < 0.01$, LPS plus NADA versus LPS plus NADA and CP945598/SR144528 or AMG9810.

(E) NADA induces Ca^{2+} influx into lung HMVECs. ECs were grown to confluency, and Ca^{2+} influx was measured as described in the Materials and Methods. Cells were treated with either ethanol, ATP (10 μM), or NADA at the indicated concentrations, and Ca^{2+} influx was measured for 3 minutes. The time points at which NADA induced significant influx are enclosed with a red border: *t* test, *, $p < 0.05$; NADA versus ethanol for each time point

(F) NADA induces Ca^{2+} influx into wild-type, but not *Trpv1*$^{-/-}$, primary murine lung endothelial cells. ECs were grown to confluency, and Ca^{2+} influx was measured as described in the Materials and Methods. Cells were treated with either ethanol, ATP (10 μM), or NADA at the indicated concentrations, and Ca^{2+} influx was measured for 3 minutes. WT, wild-type; KO, *Trpv1*$^{-/-}$.

Figure 2.15

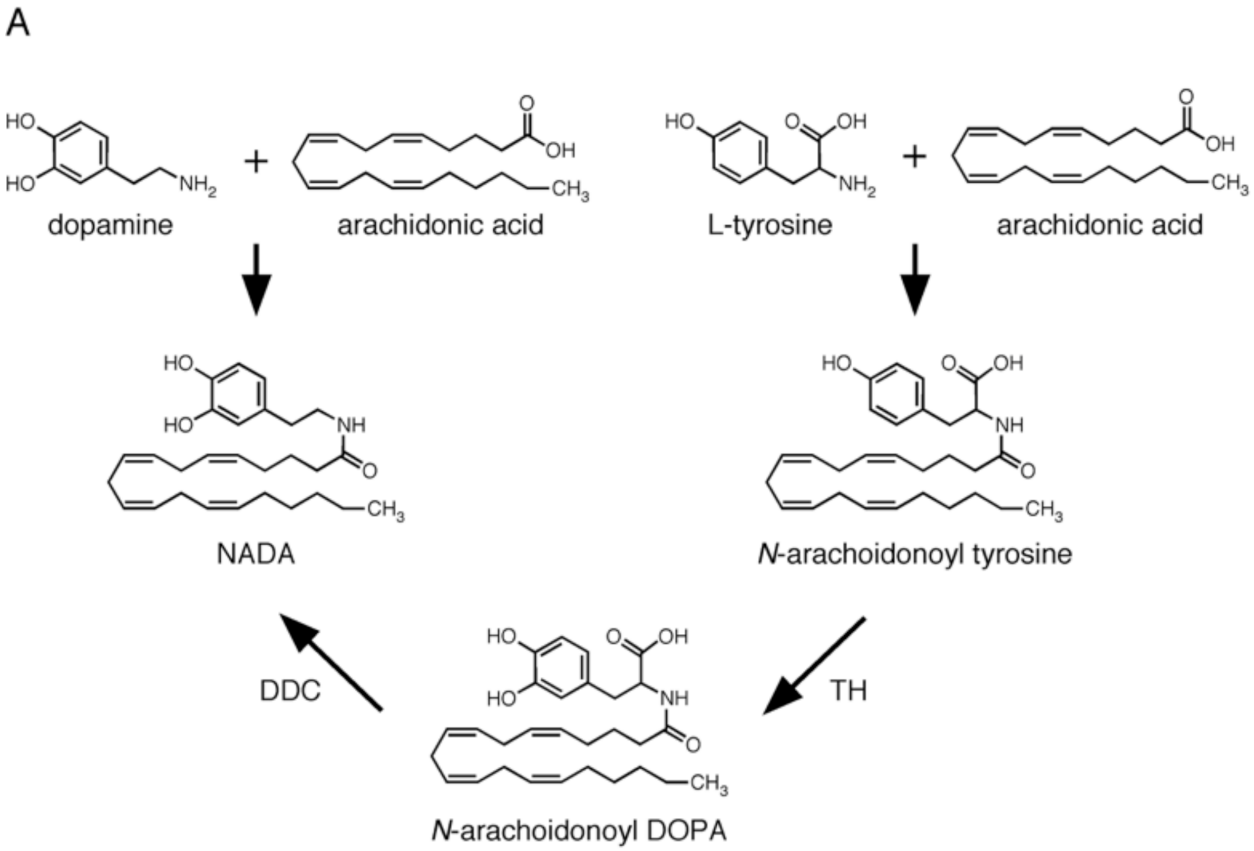
A
dopamine
arachidonic acid
L-tyrosine
arachidonic acid
NADA
N-arachoidonoyl tyrosine
DDC
TH
N-arachoidonoyl DOPA

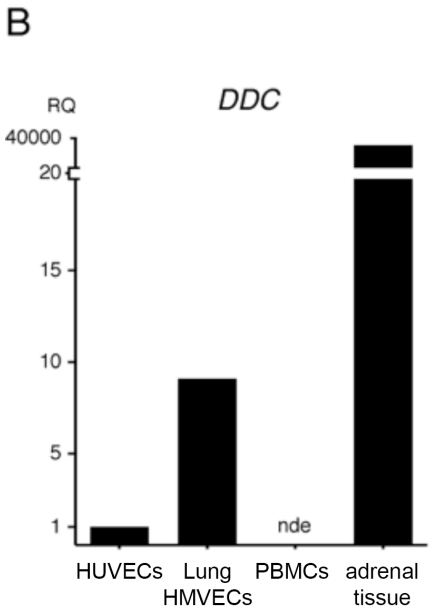
B
DDC
RQ
40000
20
15
10
5
1
nde
HUVECs
Lung HMVECs
PBMCs
adrenal tissue

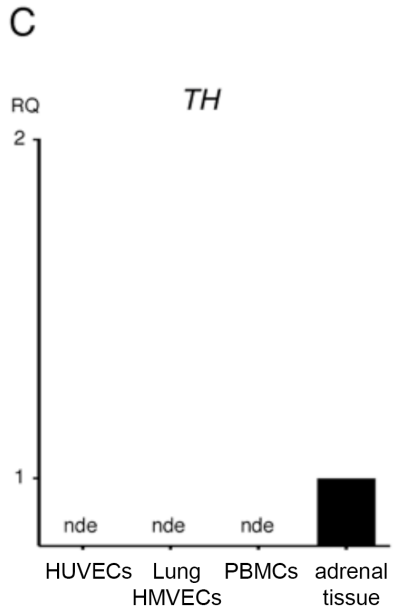
C
TH
RQ
2
1
nde
nde
nde
HUVECs
Lung HMVECs
PBMCs
adrenal tissue

Figure 2.15. The two proposed catabolic routes for NADA biosynthesis, and ECs express L-DOPA decarboxylase (DDC), but not tyrosine hydroxylase (TH).

(A) NADA can potentially be synthesized via two routes in cells. The first requires the direct ligation of AA to dopamine to generate NADA. The second requires the ligation of tyrosine to arachidonic acid to generate *N*-arachidonoyl tyosine, followed by the oxidation of the tyrosine moiety to L-DOPA by tyrosine hydroxylase (TH) to generate *N*-arachidonoyl DOPA. The L-DOPA moiety is then converted into dopamine by L-DOPA decarboxylase (DDC) to synthesize NADA.

(B and C) HUVECs (multiple donors), lung HMVECs (one donor), and PBMCs (one donor) were grown and lysed as described in Figure 2.1. Adrenal tissue cDNA was purchased from Zyagen (San Diego, CA). 80 ng, of cDNA was analyzed for each sample. The relative quantification (RQ) values shown in the graphs are relative to lowest detectable expressing cell type for each gene. When gene expression was not detected in more than half of the technical replicates, it was defined as not expressed (nde, not detectably expressed). Otherwise, the samples were analyzed as described in Figure 2.1 (see Table 2.2 for a more detailed description).

Figure 2.16

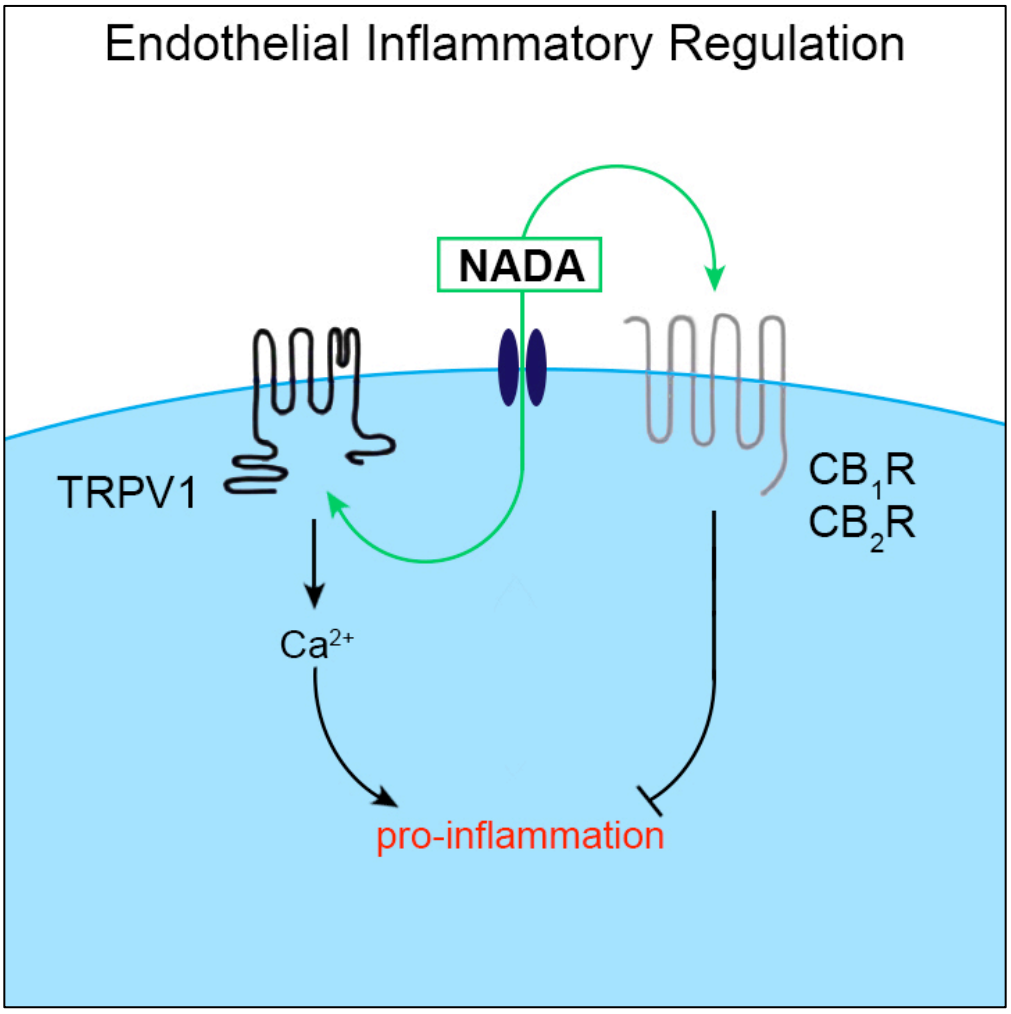
Endothelial Inflammatory Regulation
NADA
TRPV1
CB1R
CB2R
Ca2+
pro-inflammation

Figure 2.16. Proposed model depicting the role of CB_1R/CB_2R and TRPV1 in regulating endothelial inflammation by NADA.

NADA activates TRPV1 to induce Ca^{2+} influx and promote inflammatory pathways. In contrast, NADA can reduce inflammation via CB_1R/CB_2R, but the downstream pathways have not yet been fully delineated, nor has the existence of parallel anti-inflammatory pathways induced by NADA been determined in ECs. We hypothesize that NADA regulates endothelial inflammation through its contrasting actions at CB_1R/CB_2R and TRPV1. Furthermore, it is possible that the activity of NADA through CB_1R/CB_2R and TRPV1 is not parallel, but that these receptors dimerize or interact downstream to further regulate NADA signaling.

Table 2.1. Mean ΔC_t for cannabinoid receptor qPCR data.

	n	ng	*CNR1*	*CNR2* (assay 1)	*CNR2* (assay 2)	*GPR18*	*GPR55* (assay 1)	*GPR55* (assay 2)	*TRPV1*
HUVECs	m	5	nde	nde	nde	8.71	nde	8.28	4.94
		80	11.50	nde	12.22	10.88	nde	8.03	5.04
Brain HMVECs	2	5	nde	nde	nde	8.73	nde	nde	5.77
		80	10.74	nde	9.82	8.78	nde	10.42	5.84
Liver HMVECs	1	5	nde	nde	nde	8.28	nde	8.08	5.51
		80	12.09	nde	nde	8.44	nde	8.82	5.60
Lung HMVECs	1	5	nde	nde	nde	nde	nde	8.97	5.28
		80	10.50	nde	nde	11.23	nde	9.78	5.27
HCAECs	1	5	nde .	nde	nde	nde	nde	9.48	6.27
		80	11.78	nde	12.01	10.97	nde	9.14	6.23
PBMCs	3	5	5.57	2.41	nde	2.31	5.56	1.09	3.82
		80	5.64	1.98	9.50	2.15	5.30	0.83	3.95

n, number of donors; m, multiple donors (mixed batch); ng, nanograms of cDNA loaded per sample; nde, not detectably expressed
EC monolayers were grown in and PBMCs isolated into their respective growth media in the absence of inflammatory agonists prior to mRNA isolation from three independent biological replicates per donor (see Materials & Methods).
Genes that are “not detectably expressed” had undetectable gene expression in more than half of the technical replicates.

Three biological replicates, and two technical replicates per biological replicate, were analyzed for each donor. The mean C_t value of *HPRT1* and *GUSB* were used as the reference gene in calculating the ΔC_t values for each sample/biological replicate. Two input quantities, 5 ng and 80 ng, were analyzed for each sample. The average ΔC_t value is calculated by taking the mean of the individual ΔC_t values for each biological replicate of a group (ΔC_t = C_t of gene of interest (GOI) - the C_t of the *HPRT1* and *GUSB* mean (160, 161)). If more than one donor was utilized, than the mean ΔCt value represents the average ΔCt value for all donors. The ΔCt values shown are derived from the raw, uncorrected C_t values.

Table 2.2. Mean ΔC_t for metabolic enzymes qPCR data.

	n	ng	*ABHD4*	*ABHD6*	*ABHD12*	*DAGLa*	*FAAH*	*FAAH2*
HUVECs	m	5	2.69	3.06	0.76	2.55	9.06	8.14
		80	2.54	2.80	0.80	2.53	9.30	8.10
Lung HMVECs	1	5	1.23	1.91	0.67	2.17	9.03	8.53
		80	1.12	1.64	0.72	2.14	9.18	7.86
PBMCs	1	5	2.16	2.14	1.20	3.03	4.41	1.25
		80	1.97	1.11	1.27	2.88	4.25	1.04

	n	ng	*GDE1*	*MGLL*	*NAPEPLD*	*PTPN22*	*TH*	*DDC*
HUVECs	m	5	1.05	-1.02	3.60	5.15	nde	nde
		80	0.90	-1.21	3.53	5.01	nde	12.47
Lung HMVECs	1	5	0.45	-1.76	3.80	4.32	nde	nde
		80	0.39	-1.90	3.65	4.17	nde	9.29
PBMCs	1	5	0.58	2.11	2.27	-0.01	nde	nde
		80	0.31	1.91	2.15	-0.14	nde	nde
adrenal tissue	1	5	-	-	-	-	-4.00	-2.85
		80	-	-	-	-	-4.09	-2.44

n, number of donors; m, multiple donors (mixed batch); ng, nanograms of cDNA loaded per sample; nde, not detectably expressed; -, no data
EC monolayers were grown in and PBMCs isolated into their respective growth media in the absence of inflammatory agonists prior to mRNA isolation from three independent biological replicates per donor (see Materials & Methods). Human adrenal tissue cDNA was purchased from Zyagen (San Diego, CA)
Genes that are “not detectably expressed” had undetectable gene expression in more than half of the technical replicates.

Three biological replicates, and two technical replicates per biological replicate, were analyzed for each donor. The mean C_t value of *HPRT1* and *GUSB* were used as the reference gene in calculating the ΔC_t values for each sample/biological replicate. Two input quantities, 5 ng and 80 ng, were analyzed for each sample. The average ΔC_t value is calculated by taking the mean of the individual ΔC_t values for each biological replicate of a group (ΔC_t = C_t of gene of interest (GOI) - the C_t of the *HPRT1* and *GUSB* mean (160, 161)). The ΔC_t values shown are derived from the raw, uncorrected C_t values.

Table 2.3. Cannabinoid receptor agonists/antagonists used in experiments.

++, agonist activity < 100 nM; +, agonist activity 100 nM-10 mM; o, no effect; -, antagonist activity; =, inverse agonist; [in], indirect; (?), uncertain

Note: the discrepancies in binding specificities reported for individual compounds are due primarily to the different assays utilized in the studies (19).
2-AG, 2-arachidonoylglycerol; Abn-CBD, abnormal cannabidiol; ACEA, arachidonoyl-2'-chloroethylamide; AEA, *N*-arachidonoylethanolamine (anandamide); CBD, cannabidiol; CAP, capsaicin; NADA, *N*-arachidonoyl dopamine; NAGly, *N*-arachidonoylglycine; nd, no data (reported in good faith)

	cannabinoid receptor (CBR)					
	CB_1R	CB_2R	GPR18	GPR55	$TRPV_1$	reference
2-AG	++ / +	+	+	++ / o	+ / o	(162-168)
Abn-CBD	o	o	+	++ / + / o	o	(29, 162, 165, 166, 169)
ACEA	++	+	nd	nd	+	(71, 170, 171)
AEA[a]	++	+	+ / o	++ / + / o	+	(162, 165, 166, 172)
CBD[b]	- [in]	=	+ (?) / -	o / -	+ / o	(162, 166, 173-175)
CAP	nd	nd	nd	nd	++	(176)
HU-308	o	++	nd	nd	nd	(177)
NADA[c]	+	+ / o	nd	nd	++	(64, 65)
NAGly	o	o	++ / o	o	o	(163, 178-182)
WIN55[d]	++	++	o / -	o	o / - [in]	(162, 165, 166, 181, 183)

[a], inhibitor of TRPM8 (141)
[b], agonist for the $5\text{-}HT_{1A}$ (serotonin) receptor (184)
[c], no effect on dopamine receptor D_1 or D_2 (64); agonist of PPAR-γ (75); inhibitor of TRPM8 (141), calcineurin (78), FAAH (64), MAGL (113), anandamide membrane transporter (64, 82), arachidonate 5-lipoxygenase (139), pl12-LO (137), and T-type calcium channels (138)
[d], agonist of TRPA1 (84), calcineurin (83, 84), PPAR-γ (34), and PPAR-α (140)

Table 2.4. Mean inflammatory and viability indices, SEM, and significance for cannabinoid receptor agonist/antagonists

	IL-6 ELISA				IL-8 ELISA				MTT assay			
	mean	SEM	n	*p*	mean	SEM	n	*p*	mean	SEM	n	*p*
2-AG	1.00	0.05	5	0.9362	1.12	0.04	5	0.0421	0.98	0.09	2	0.8179
abn-CBD	1.11	0.11	4	0.4005	1.12	0.11	4	0.3569	0.95	0.10	5	0.6145
ACEA	0.85	0.11	5	0.2330	0.92	0.06	5	0.2687	0.98	0.00	3	0.0475
AEA	1.03	0.04	5	0.5242	1.09	0.06	5	0.2097	0.92	0.10	2	0.5807
CBD	0.18	0.15	4	0.0129	0.19	0.31	4	0.0130	0.64	0.07	5	0.0058
CAP	1.06	0.07	4	0.4712	1.06	0.05	3	0.3184	1.05	0.02	2	0.1907
HU-308	0.67	0.13	5	0.0647	0.73	0.12	5	0.0884	1.10	0.02	3	0.0252
NADA	0.64	0.10	5	0.0213	0.67	0.06	5	0.0062	0.99	0.05	5	0.8672
NAGly	1.21	0.05	4	0.0260	1.07	0.07	4	0.4042	0.97	0.01	2	0.3066
WIN55	0.02	0.02	5	0.0000	0.03	0.01	5	0.0000	0.98	0.02	6	0.3423

SEM, standard error of the mean; n, number of experiments.
$p < 0.05$ were considered significant and are highlighted in yellow.
2-AG, 2-arachidonoylglycerol; abn-CBD, abnormal cannabidiol; ACEA, arachidonoyl-2'-chloroethanolamine; AEA, *N*-arachidonoylethanolamine (anandamide); CBD, cannabidiol; CAP, capsaicin; NADA, *N*-arachidonoyl dopamine; NAGly, *N*-arachidonoylglycine.
Breakdown of IL-6/IL-8 *n* values (F, FSL-1; L, LPS; T, TNF): 2-AG (F-1, L-1, T-3); Abn-CBD (F-1, L-2, T-1); ACEA (F-2, L-2, T-1); AEA (F-2, L-2, T-1); CBD (F-1, L-2, T-1); CAP (F-1, L-2, T-1); HU-308 (F-2, L-2, T-1); NADA (F-2, L-2, T-1); NAGly (F-1, L-2, T-1); WIN55,212-2 (F-2, L-2, T-1).

For the IL-6 and IL-8 ELISAs, lung HMVEC monolayers were pretreated for 1 hour with 10 mM of the CBR agonist/antagonist, and then either 10 mg/mL of FSL-1 or LPS or 100 ng/mL of TNFa was added for an additional 6 hours in the continuous presence of 10 mM of the CBR agonist/antagonist. Subsequently, supernatants were collected and the concentrations of IL-6 and IL-8 were determined. For the MTT assay, 10 mM of the CBR agonist/antagonist was added to either HUVEC or lung HMVEC monolayers for 7 hours before solubilizing the cells with DMSO. To calculate the inflammatory indices, the relative inflammatory index in each independent experiment for each CBR agonist/antagonist was first calculated (i.e. the average cytokine concentration for the samples treated with both the inflammatory agonist (FSL-1, LPS or TNFα) and CBR

agonist/antagonist divided by the average cytokine concentration for the samples treated with inflammatory agonist alone; n=3 minimum). Then, the mean and SEM of these relative indices for each CBR agonist/antagonist were calculated (n=4-5). The MTT viability indices were calculated in the same manner. Student's unpaired, two-tail t-tests were performed on the indices of the samples treated with both the inflammatory agonist and CBR agonist/antagonist versus the indices of the samples treated with just the inflammatory agonists. $p < 0.05$ was considered significant. CBR agonists/antagonists of interest induced significant changes in both IL-6 and IL-8 secretion without significantly affecting viability (i.e. NADA and WIN55,212-2).

Materials and Methods

Cells

Human umbilical vein endothelial cells (HUVECs, passage 2-6, multiple donors) (Lonza, Walkersville, MD), human brain microvascular endothelial cells (brain HMVECs, passage 4-9, unknown donor gender) (Cell Sciences, Canton, MA), human liver sinusoidal microvascular endothelial cells (liver HMVECs, passage 4-9, unknown donor gender) (Cell Sciences), human lung microvascular endothelial cells (lung HMVECs, passage 4-9, female and male donors) (Lonza), and human coronary artery endothelial cells (HCAECs, passage 4-9, female donor) (Lonza) were incubated at 37°C under humidified 5% CO_2. HUVECs were grown in EGM-2, and brain, liver, and lung HMVECs and HCAECs were grown in microvascular EGM-2 (Lonza). Peripheral blood mononuclear cells (PBMCs) and neutrophils were isolated by gradient centrifugation using Lymphoprep and Polymorphprep (Axis-Shield, Oslo, Norway), respectively, from heparinized whole blood collected by venipuncture from healthy human volunteers. PBMCs were isolated according to the manufacturers supplied instructions and neutrophils as we have described previously (92).

Cannabinoid and inflammatory agonist treatments

ECs were grown to confluence before agonist treatment. Unless otherwise noted, in all experiments cells were pre-incubated with the cannabinoids or the TRPV1 agonist, capsaicin, at the indicated concentrations for 1 hour prior to and continuously during the inflammatory agonist treatment. In Figure 2.7B, samples were incubated continuously with polymyxin B (Invivogen, San Diego) at 50 μg/mL to minimize effects from contaminating LPS. Compounds used were 2-AG (Tocris, Ellisville, MO), abnormal

cannabidiol (Axon Medchem, Groningen, Netherlands), arachidonoyl-2'-chloroethylamide (Tocris), *N*-arachidonoylethanolamine (Sigma), AEA in Tocrisolve 100 (Tocris), CBD (Axon Medchem), capsaicin (Tocris), HU-308 (Tocris), *N*-arachidonoyl dopamine (NADA) (Sigma, Tocris, and Cayman Chemical), *N*-arachidonoyl glycine (Tocris), and WIN55,212-2 (Sigma). The inflammatory agonists used include FSL-1 (EMC Microcollections, Tubingen, Germany), LPS (List Laboratories, Los Gatos, CA), and recombinant human TNFα (PeproTech, Inc., Rocky Hill, NJ) at the indicated concentrations and times. Preparations of FSL-1, TNFα, capsaicin, and dopamine contained <0.1 EU/mL LPS based on the *Limulus* amoebocyte lysate chromogenic endotoxin quantitation assay (Thermo-Scientific). Because AA, 2-AG, AEA, *N*-arachidonoyl glycine, arachidonoyl-2'-chloroethylamide, HU-308, abnormal CBD, and NADA preparations caused the *Limulus* amoebocyte lysate substrate to become cloudy, the quantitative OD readings were unreliable; however, based on the observed color changes compared with the standards, the levels of LPS appeared qualitatively insignificant.

Immunoblots

Cells were lysed with RIPA-Lysis Buffer (4 mM sodium dihydrogen phosphate, pH 7.0; 6 mM disodium hydrogen phosphate, pH 7.0; 150 mM sodium chloride; 1% Nonidet P-40; 1% sodium deoxycholate; 0.1% SDS; 2 mM EDTA; 50 mM sodium fluoride; 0.1 mM sodium vanadate) plus protease inhibitor mixture (Sigma), and protein concentrations of the lysates were estimated using the RCDC protein assay kit (Bio-Rad). Total proteins were separated by SDS-PAGE (11%) and then transferred to PVDF membranes (Pall Corp, Ann Arbor, MI). Membranes were blocked in 3% BSA for 45 minutes at room

temperature (RT) and then incubated with primary antibody solution overnight at 4°C. Membranes were washed and then incubated with goat anti-rabbit peroxidase-conjugated secondary antibodies (111-035-045; Jackson ImmunoResearch, West Grove, PA). Immunoblots were developed using Super-Signal West Dura Extended Duration Substrate (34076; Thermo Scientific), and the signal was detected using a Gel Logic 2200 Imaging System (Eastman Kodak, Rochester, NY) run on Carestream imaging software (Carestream Health, Rochester, NY). The antibodies used were as follows: CB_1R (2 μg/mL, AP01265PU-N, Acris Antibodies, San Diego); CB_2R (1 μg/mL, ARP63486_P050, Aviva Systems Biology, San Diego); GPR18 (2 μg/mL, ab76258, Abcam, Cambridge, MA); GPR55 (0.8 μg/mL, orb101191, Biorbyt, Cambridge, UK); TRPV1 (1 μg/mL, ab111973, Abcam); and β-actin (0.1 μg/mL, A2066, Sigma).

ELISAs, MTT assay, and crystal violet assay

IL-6 and IL-8 levels were quantified in culture supernatants by ELISA (R&D Systems, Minneapolis, MN, and BD Biosciences, respectively) according to the manufacturer's instructions. For the MTT and crystal violet (CV) assays, the CBR agonist or antagonist was added at the indicated concentrations for 7 hours in the absence of inflammatory agonists. MTT Assays (Biotium, Hayward, CA) were performed in 96-well plates according to the manufacturer's instructions. Because NADA induces the formation of formazan crystal from tetrazolium salt in the absence of cells, in the MTT assay graph (Figure 2.7C), background ODs of NADA in the absence of cells were subtracted from ODs in the presence of cells at the same NADA concentration. For CV assays, after the indicated treatments, the cells in 48-well plates were washed twice with PBS and then stained with 0.5% CV in methanol for 10 minutes (100 μl). The plates were then

immersed several times in tap water to remove the excess CV solution, after which time the plates were gently tapped upside down on a paper towel to remove all traces of liquid. 1% SDS in water (300 μl) was then added to each well, and the remaining stained cells were allowed to solubilize for several hours. One well in the plate was left without cells to control for background staining. Absorbance was read at 570nm in a FLUOstar OPTIMA fluorescent plate reader (BMG Labtech, Cary, NC); the background staining was subsequently subtracted, and the percent adherence relative to the control was calculated.

siRNA transfection of lung HMVECs

COMT (L009520-00-0005) and control (L-005120-01-0005) siRNA ON-TARGET plus SMARTPools (ThermoScientific, Rockford, IL) were used in accordance with the manufacturer's suggested protocol for lung HMVEC transfections using Dharmafect 4 transfection reagent. Cells were treated with NADA and LPS as described above, and supernatants were collected after 7 hours for ELISAs.

Flow cytometry

HUVECs were detached using Accutase Cell Detachment Solution (Innovative Cell Technologies, San Diego). HUVECs were passed through a 70-μm filter, counted, and aliquoted at $5x10^5$ cells per sample. The cells were then washed using Flow Cytometry Staining Buffer (FCSB) (R&D Systems) and incubated with 10 μg/mL human IgG (R&D Systems) in FCSB for 15 minutes at 4°C. Next, the cells were incubated for 30 minutes at 4°C with either 0.25 μg/sample of FITC-mouse anti-human CD62E (E-selectin) (BBA21; R&D Systems) or FITC-mouse IgG1 (IC002F; R&D Systems). The samples

were washed once more with FCSB and then analyzed by flow cytometry (LSRII Flow Cytometer, BD Biosciences). A far-red fluorescent dye (L10119; Invitrogen) was used to assess cell viability. For primary murine lung endothelial cells, cells were stained with FITC-rat anti-mouse CD102, PE-rat anti-mouse CD31, FITC-rat anti-mouse IgG2a κ, and PE-rat anti-mouse IgG2a κ (BD Biosciences).

Quantitative real time PCR (qPCR)

Specific gene expression assays (*HPRT1* (Hs01003267_m1), *GUSB* (Hs99999908_m1), *CNR1* (Hs00275634_m1), *CNR2* (Hs00275635_m1; assay 1), *CNR2* (Hs00952005_m1; assay 2), *GPR18* (Hs00245542_m1), *GPR55* (Hs00995276_m1; assay 1), *GPR55* (Hs00271662_s1; assay 2), *TRPV1* (Hs00218912_m1), *ABHD4* (Hs01040459_m1), *ABHD6* (Hs00977889_m1), *ABHD12* (Hs01018047_m1), *DAGLA* (Hs00391374_m1), *FAAH1* (Hs01038660_m1), *FAAH2* (Hs00398732_m1), *GDE-1* (Hs00213347_m1), *MGLL* (Hs00200752_ m1), *NAPE-PLD* (Hs00419593_m1), *PTPN-22* (Hs01587518_m1), *DDC* (Hs01105048_m1), *TH* (Hs00165941_m1), and the manufacturer's suggested assay reagents were purchased from Applied Biosystems (Foster City, CA). HUVECs, HMVECs, HCAECs, and PBMCs were lysed, and mRNA was isolated using TRIzol according to the manufacturer's supplied protocol (Invitrogen). mRNA concentrations were determined with an ND-1000 (NanoDrop/Thermo Fisher Scientific), and mRNA was reverse-transcribed to cDNA using the High Capacity RNA-to-cDNA kit using 2 μg of mRNA per reaction (Invitrogen). Human adrenal tissue cDNA was purchased from Zyagen (San Diego). An input of either 5 or 80 ng of cDNA in 10 μl of total reaction volume per well containing TaqMan Fast Advanced Master Mix (Applied Biosystems) was used in all qPCR experiments,

and qPCR was performed using the StepOnePlus System (Applied Biosystems). For the run method, PCR activation at 95°C for 20s was followed by 40 cycles of 1s at 95°C and 20s at 60°C. The average C_t value of two technical replicates was used in all calculations. The average C_t value of the internal controls *HPRT1* and *GUSB* were used to calculate ΔC_t values. For single donor assays (liver HMVECs, lung HMVECs, and HCAECs (*n*=1)), data analysis was performed using the $2^{-\Delta\Delta Ct}$ method (160). For multiple donor assays (HUVECs (*n*=2 lots), brain HMVECs (*n*=2), and PBMCs (*n*=3)), the initial data analysis was performed using the $2^{-\Delta\Delta Ct}$ method, and the data were corrected using log transformation, mean centering, and auto scaling to ensure appropriate scaling between biological replicates (161). The methods of calculation utilized assume an amplification efficiency of 100% between successive cycles.

Neutrophil adhesion assay

The neutrophil adhesion assay was performed as described previously (92). Briefly, neutrophils were resuspended in RPMI 1640 medium at $2x10^6$ cells/mL and labeled with 3 μM calcein-AM (Invitrogen). Just prior to adding labeled neutrophils, 48-well plates containing lung HMVEC monolayers were washed three times with RPMI 1640 medium containing 3% BSA. Labeled neutrophils were then added at $6x10^5$ cells/300 μl/well and allowed to incubate for 20 minutes at 37°C in the dark before washing five times with PBS (with Ca^{2+} and Mg^{2+}) to remove nonadherent cells. Pre-washing and post-washing fluorescence was read at an excitation of 485nm and an emission of 520nm in a FLUOstar OPTIMA fluorescent plate reader. The relative adherence was calculated by first subtracting the background fluorescence of the ECs from the pre- and post-wash

readings and then dividing the post-wash reading by the pre-wash reading to quantitate the fluorescence decrease for each well. The ratio of adherence of each well is then divided by the average ratio of adherence for the positive control samples. Neutrophil adhesion was visualized using a Zeiss Axio Imager D1 microscope.

Electric cell-substrate impedance sensing (ECIS)

ECIS Z Theta system (Applied Biophysics, Troy, NY) was used to measure the transendothelial electrical resistance (TER), a measure of endothelial barrier integrity, of lung HMVEC monolayers, as described in detail by Giaever and Keese (185). Briefly, lung HMVECs ($1.4x10^5$ cells/cm^2) were seeded into wells containing 10 small gold electrodes and a larger counter electrode on a 96-well plate (Applied Biophysics) and were allowed to grow to confluence. Inflammatory agonists (FSL, LPS, and TNFα) and either NADA (2 or 10 μM) or WIN55,212-2 (1 or 2 μM) were then added to the wells. Resistance was measured repeatedly in each well for 8 hours. Data were normalized to the resistance mea- sured before the addition of inflammatory agonists and NADA.

Antagonist/inverse agonist and COMT inhibitor assays

Confluent monolayers of lung HMVECs were pretreated for 30 minutes with the TRPV1 antagonist AMG9810 (0.1, 1, or 10μM; Tocris), the COMT inhibitor entacapone (0.1μM; Tocris), or the combination of the CB_1R antagonist CP945598 (0.1, 1 or 10μM; Tocris) and the CB_2R inverse agonist SR144528 (0.1, 1, or 10μM; Cayman Chemical). Cells were then incubated for another 30 minutes with WIN55,212-2 (4 μM) or NADA (10 μM) in the continued presence of the inhibitor. ECs were then treated with LPS (10 μg/mL) for an additional 6 hours while in the continuous presence of the combination of the

inhibitor and cannabinoid. IL-6 and IL-8 were quantified in culture supernatants.

Calcium influx assay

Lung HMVECs or WT and *Trpv1*$^{-/-}$ murine endothelial cells were grown to confluency in 96-well black-walled TC plates. Endothelial Ca^{2+} influx was determined using the FLIPR Calcium 6 assay (Molecular Devices) according to the manufacturer's supplied instructions. Cells were treated with either ethanol, ATP (10 μM), or NADA at the indicated concentrations, and fluorescence output (*i.e.* Ca^{2+} influx) was measured for 3 minutes with a Flex Station fluorometer (Molecular Devices). The data were then normalized to the background readings before treatments for each condition.

Preparation of primary murine endothelial cells

Primary lung endothelial cells were prepared from 6-7 day old mouse pups immediately after decapitation as described (186). The purity of the cell populations was verified by flow cytometry as described above. WT and *Trpv1*$^{-/-}$ endothelial cell preparations were >94% pure.

LC-MS/MS to detect NADA in lung HMVECs

An analytical LC-MS/MS method to detect endocannabinoids in cell lysates was developed at Cayman Chemical Co. (Ann Arbor, MI). Confluent monolayers of lung HMVECs were grown in 15-cm tissue culture dishes and left untreated or treated either with FSL-1 (10 μg/mL), LPS (10 μg/mL), or TNFα (100 ng/mL) for 3 hours, and then lysed with 2.25 mL of RIPA lysis buffer (see above for formulation and procedures) per plate. For each sample, the lysate from 2x15-cm tissue culture dishes were combined (4.5 mL total). After an initial extraction with chloroform/ methanol (2:1), both 1 and 3 mL

of the lysate from each sample were concentrated and analyzed by LC-MS/MS. NADA standard was prepared at Cayman Chemical using RIPA buffer as the matrix.

Statistics

The data were analyzed using *t*-tests (unequal variance two-tail) or ANOVA using a Dunnett's post-test. GraphPad Prism or Excel 2008 was used for statistical analyses. $p < 0.05$ were considered significant for all data except crystal violet assays, where $p < 0.01$ were considered significant. Data were expressed as mean ± S.D., except for the data compiled in Figure 2.4, which are expressed as the mean ± S.E.

CHAPTER 3

N-arachidonoyl dopamine (NADA) modulates acute systemic inflammation via non-hematopoietic TRPV1

Abstract

N-arachidonoyl dopamine (NADA) is an endocannabinoid/endovanilloid with *in vitro* immunomodulatory activity. NADA is a potent agonist of the cation channel transient receptor potential vanilloid 1 (TRPV1), which mediates nociception and thermosensation via sensory neurons. Thus far, *in vivo* studies using NADA have focused on its neurological and behavioral roles. Here we show that NADA potently decreases *in vivo* systemic inflammatory responses and levels of the coagulation intermediary plasminogen activator inhibitor-1 in three mouse models of inflammation: lipopolysaccharide, bacterial lipopeptide, and polymicrobial intraabdominal sepsis. Additionally, NADA modulates blood levels of the neuropeptides calcitonin gene-related peptide (CGRP) and substance P in LPS-treated mice. We demonstrate that the immunomodulatory properties of NADA are mediated by TRPV1 expressed by non-hematopoietic cells, and provide data supporting a role for neuronal TRPV1 in NADA's immunomodulatory effects. These results suggest that NADA has novel TRPV1-dependent neuroimmunological properties, and furthermore, that the endovanilloid system might be targeted therapeutically in sepsis.

Introduction

N-arachidonoyl dopamine (NADA) is an endogenous lipid composed of an arachidonic acid backbone conjugated to a dopamine moiety (98). As an endocannabinoid, NADA possesses activity at the G protein-coupled cannabinoid receptors CB_1R and CB_2R (64, 81). NADA is also an endovanilloid, which are a group of endogenous activators of transient receptor potential vanilloid 1 (TRPV1), and include

the endocannabinoid anandamide and a variety of lipoxygenase products (176, 187, 188). TRPV1, a non-selective cation channel, is primarily known for its role in nociception and thermosensation. Of the known endovanilloids, NADA is the most potent TRPV1 agonist and is considered to be a principal endogenous TRPV1 ligand (65, 98, 188, 189). TRPV1 is activated by a variety of noxious insults, including heat greater than 42°C, low pH, and capsaicin, the active ingredient in chili peppers (188).

TRPV1 is highly expressed in the peripheral nervous system (PNS), including in a subset of small-diameter primary afferent neurons that detect noxious stimuli residing in Trigeminal and Dorsal Root Ganglion (TG and DRG respectively), and in the vagus nerve (190-194). Peripheral terminals derived of TRPV1-expressing nociceptors innervate most organs and tissues. TRPV1 expressed in the PNS functions to integrate multiple noxious stimuli, ultimately leading to the depolarization of primary afferent nociceptors and release of neuropeptides, such as calcitonin gene-related peptide (CGRP) and substance P, that elicit a pain and neurogenic inflammatory responses (195-199). TRPV1 is also expressed in the central nervous system (CNS), including the spinal cord, striatum, hippocampus, cerebellum, and amygdala, as well as the DRG (200-204). Finally, TRPV1 is expressed in non-neuronal cells, including leukocytes, smooth muscle cells, and endothelial cells, and T cell TRPV1 activation has been reported to modulate the T-cell function (191, 195, 205-209).

NADA has been detected in the striatum, cerebellum, hippocampus, thalamus, brainstem and DRG, and thus NADA and TRPV1 have overlapping distributions (65, 200-202, 210). The specific activation of TRPV1 by NADA has been previously documented. While NADA induces calcium influx into primary human and mouse

endothelial cells, it is unable to affect endothelial calcium levels after treatment with the TRPV1 antagonist capsazepine or in cells derived from *Trpv1*$^{-/-}$ mice (Chapter 2 and (209)). NADA also induces calcium influx in HEK293 cells overexpressing TRPV1, and this influx is abolished after treatment with the TRPV1 antagonist iodoresiniferatoxin (65). Furthermore, the ability of NADA to induce thermal hyperalgesia in mice is also dependent upon TRPV1, with both capsazepine and iodoresiniferatoxin inhibiting the actions of NADA *in vivo* (65). NADA has been proposed to dynamically modulate neuronal homeostasis by either reducing or inducing cation influx via activation of CB_1/CB_2 and TRPV1, respectively (98, 118). This dual modulatory effect may explain the observation that NADA displays both pro- and anti-nociceptive properties (70, 72). In addition to its neurological and behavioral effects, limited studies suggest that NADA can modulate inflammatory responses in non-neuronal cells, such as astrocytes, leukocytes and brain endothelial cells (17, 64, 76-78, 80, 209).

We previously found that treatment with NADA reduces the activation of cultured endothelial cells by bacterial lipopeptides (Toll-like receptor [TLR] 2 agonists), lipopolysaccharide (LPS, endotoxin, TLR4 agonist), and TNFα (209). Furthermore, our data using pharmacological inhibitors suggested that the activities of NADA may be mediated through cannabinoid receptors and TRP channels, and we proposed that NADA may fine-tune the inflammatory activation of endothelial cells through TRPs, similar to their function in neurons (209). These data led us to hypothesize that NADA may moderate sepsis-induced inflammation (64, 66, 67, 71, 72). While some studies suggest that TRPV1 modulates inflammation in models of sepsis, to our knowledge, there are no prior studies investigating the role of NADA or the NADA-TRPV1 axis in

sepsis (151, 195, 206, 211). We therefore tested the hypothesis that treatment with NADA would reduce acute systemic inflammation in sepsis via activation of TRPV1. We find that treatment with NADA reduces systemic inflammation in toxicity and infection models of sepsis, and that its anti-inflammatory effects depend upon non-hematopoietic TRPV1. We also find that the ability of NADA to regulate systemic inflammation does not require leukocyte or endothelial TRPV1, pointing to a potential role for neuronal TRPV1 expression in the anti-inflammatory effects of NADA.

Results

NADA reduces systemic pro-inflammatory cytokine production and plasminogen activator inhibitor (PAI-1) in mice challenged with LPS or Pam3Cys

To investigate the contribution of NADA to systemic inflammation and coagulopathy, we challenged mice with LPS (5 mg/kg, intravenously [i.v.]) immediately prior to treatment with NADA (1-10 mg/kg, i.v.). At 10 mg/kg, NADA significantly reduced plasma concentrations of IL-6 and CCL2 two hours after LPS challenge (Figure 3.1, A and B, $p < 0.01$). In comparison to vehicle-treated control mice, NADA also reduced the LPS-induced upregulation of PAI-1 (Figure 3.1C, $p < 0.01$). PAI-1 is an anti-fibrinolytic factor that is associated with an increased incidence of organ failure and death in sepsis (212). These results are consistent with data that we obtained using a 23-plex immunoassay, in which NADA decreased the production of the pro-inflammatory cytokines IL-1β, TNFα, CCL2-5, and IL-12p40, while significantly increasing the levels of the anti-inflammatory cytokine IL-10 induced by LPS challenge (data not shown).

While LPS is found exclusively on gram-negative bacteria, TLR2-activating lipoproteins are expressed by gram-positive and gram-negative bacteria (213). To test if NADA reduces TLR2-mediated inflammation, we challenged mice with the TLR2 ligand Pam3Cys (10 mg/kg, i.v.) immediately followed by NADA treatment (10 mg/kg, i.v.). Similar to LPS, treatment with NADA reduced Pam3Cys-induced IL-6, CCL2, and PAI-1, but increased IL-10 levels in plasma two hours after Pam3Cys challenge (Figure 3.2, A-D, $p < 0.01$). NADA alone did not affect baseline levels of inflammatory mediators or PAI-1 (data not shown).

Neither anandamide (AEA) nor 2-AG affect the induction of cytokines or PAI-1 in endotoxemic mice

We assessed the effects of two other endogenous cannabinoid receptor agonists, AEA and 2-AG (118). AEA also activates TRPV1, but less potently than NADA (65, 187, 214). Mice were challenged with LPS (5 mg/kg, i.v.) and then immediately treated with AEA or 2-AG (10 mg/kg, i.v.). In contrast to NADA, treatment with AEA or 2-AG did not abrogate the upregulation of IL-6, CCL2, CCL3, or PAI-1 levels two hours after LPS challenge (Figure 3.3, A-H), indicating that NADA's anti-inflammatory properties during systemic inflammation are not shared by all members of the endocannabinoid family.

NADA has a short half-life in the circulation

We measured plasma NADA levels at intervals through 60 minutes after treatment of mice with NADA (10 mg/kg, i.v.) using LC-MS/MS. NADA was rapidly

cleared from the circulation, and has a half-life of approximately 2.7 minutes (Figure 3.4). It is unclear if NADA is catabolized or distributed into tissues.

NADA modulates cytokines and PAI-1 in the cecal ligation and puncture (CLP) model of sepsis in mice

We assessed the effects of NADA in a CLP model of polymicrobial intraabdominal sepsis in order to determine its effects during active infection. We administered NADA immediately after and four hours after CLP surgery, and quantified plasma cytokines and PAI-1 at six hours. Mice that underwent sham surgery had background levels of cytokines in the presence or absence of NADA (Figure 3.5, A-D). NADA treatment reduced IL-6 ($p < 0.001$), CCL2 ($p < 0.0001$), and PAI-1 ($p < 0.0001$), and increased IL-10 levels ($p < 0.0001$) (Figure 3.5, A-D). Thus, NADA reduces the systemic pro-inflammatory response during an active infection.

NADA's anti-inflammatory activity *in vivo* requires TRPV1

To determine the role of TRPV1 expression in the anti-inflammatory effects of NADA, we challenged WT and *Trpv1*$^{-/-}$ mice with LPS (5 mg/kg, i.v.) or Pam3Cys (10 mg/kg, i.v.), treated them immediately after with NADA (10 mg/kg, i.v) or vehicle, and collected their plasma at two hours. NADA did not modulate plasma levels of IL-6, CCL2, IL-10, or PAI-1 in *Trpv1*$^{-/-}$ mice following challenge with LPS or Pam3Cys (Figure 3.6, A-D, and Figure 3.7). NADA alone did not affect baseline levels of inflammatory mediators or PAI-1 in WT or *Trpv1*$^{-/-}$ mice (data not shown). These data indicate that NADA's effect on cytokines and PAI-1 requires TRPV1.

NADA activates CB_1R and CB_2R in addition to TRPV1, and our prior study supported a dominant role for CB_1R and CB_2R in the anti-inflammatory effects of NADA in human endothelial cells (209). To determine whether or not TRPV1 activation in the absence of CB_1R or CB_2R activation might modulate systemic inflammation, we analyzed the effects of capsaicin, a TRPV1-specific agonist, in endotoxemic mice. We challenged WT mice with LPS or carrier and then immediately after administered capsaicin (0.2 mg/kg, i.v.) or vehicle. Treatment with capsaicin reduced IL-6, CCL2, and PAI-1, and increased IL-10 levels in endotoxemic mice (Figure 3.6, E-H, $p < 0.01$). Capsaicin on its own did not affect baseline expression of these mediators (Figure 3.6, E-H). These data suggest that TRPV1 activation has anti-inflammatory effects in sepsis.

NADA exerts its anti-inflammatory effects *in vivo* via non-hematopoietic TRPV1

TRPV1 is expressed in multiple cell lineages, including hematopoietic and non-hematopoietic cells. Therefore, we used bone marrow chimeras to determine the role of hematopoietic versus non-hematopoietic TRPV1 expression in NADA's anti-inflammatory properties. We transplanted WT or *Trpv1*$^{-/-}$ ($CD45.2^+$) bone marrow cells into irradiated WT mice ($CD45.1^+$) recipient mice to generate mice that do not express TRPV1 in hematopoietic cells. We verified bone marrow engraftment by flow cytometry, with >95% of leukocytes staining as donor $CD45.2^+$ cells (Figure 3.8, A and B). Eight to nine weeks after reconstitution, mice were challenged with LPS (5 mg/kg, i.v.) and then treated with NADA (10 mg/kg, i.v.). In contrast to our results in mice with global TRPV1 deletion, NADA reduced IL-6, CCL2, and PAI-1 levels, and increased IL-10 levels in mice with *Trpv1*$^{-/-}$ bone marrow cells (Figure 3.9, A-D, $p < 0.001$).

To confirm these results, we performed the reverse chimera, transplanting WT ($CD45.1^+$) or *Trpv1*$^{-/-}$ bone marrow into irradiated *Trpv1*$^{-/-}$ ($CD45.2^+$) recipients. These mice exclusively express TRPV1 in hematopoietic cells. As controls, WT ($CD45.1^+$) bone marrow was transplanted into irradiated WT ($CD45.2^+$) recipients. We verified bone marrow engraftment by flow cytometry, with >99% of leukocytes staining as donor cells (Figure 3.8, C and D). Consistently, NADA was unable to affect levels of IL-6, CCL-2, PAI-1, or IL-10 in mice lacking TRPV1 expression outside of the bone marrow (Figure 3.9, E-H). These data indicate that NADA does not require hematopoietic TRPV1 to exert its anti-inflammatory effects *in vivo* in endotoxemic mice.

NADA exerts its anti-inflammatory effects independently of TRPV1 in cultured primary murine hematopoietic cells and endothelial cells

Because our bone marrow chimera studies suggested that NADA mediates its anti-inflammatory effects via non-hematopoietic TRPV1, we performed *ex vivo* studies using cultured myeloid cells and endothelial cells prepared from WT and *Trpv1*$^{-/-}$ mice. For each of these studies, cells were pre-incubated with NADA, and then stimulated with LPS or Pam3Cys. NADA treatment reduced IL-6 production induced by LPS or Pam3Cys in both WT and *Trpv1*$^{-/-}$ bone marrow cells (Figure 3.10, A and B, $p < 0.05$). Similar results were obtained in peripheral blood mononuclear cells (PBMCs) and thioglycollate-elicited peritoneal macrophages from WT and *Trpv1*$^{-/-}$ mice (data not shown). Because irradiation may not fully deplete brain-resident microglia, we were concerned that the results of our bone marrow chimera studies could have been due to the residual TRPV1-expressing microglia in irradiated WT mice transplanted with

TRPV1 KO marrow (215). Similar to bone marrow cells, PMBCs, and macrophages, NADA treatment reduced the LPS-induced upregulation of IL-6 in microglia from both WT and *Trpv1*$^{-/-}$ mice (Figure 3.10, C and D). Finally, we tested the effects of NADA on LPS-induced activation of primary lung endothelial cells isolated from WT and *Trpv1*$^{-/-}$ mice. NADA induced a comparable decrease in LPS-induced IL-6 secretion by endothelial cells from *Trpv1*$^{-/-}$ and from WT mice (Figure 3.10, E and F). Consistent with these results, treatment of primary endothelial cells, bone marrow cells, or bone marrow-derived macrophages with capsaicin does not affect inflammatory cytokine production (data not shown). Collectively, these *ex vivo* data suggest that the effects of NADA on acute systemic inflammation are not mediated through TRPV1 expressed in endothelial cells or cells derived from the hematopoietic lineage, including microglia. Furthermore, they suggest that NADA reduces inflammatory activation of these cell populations through TRPV1-independent mechanisms, which is consistent with our prior work showing that CB_1R and CB_2R antagonists block the anti-inflammatory effects of NADA on human endothelial cells (209).

The anti-inflammatory activity of NADA systemically and in the hematopoietic compartment depends on CB_2R

Because NADA continued to possess anti-inflammatory activity in *Trpv1*$^{-/-}$ hematopoietic cells and endothelial cells, we hypothesized that NADA must activate an additional receptor in these cell types to regulate inflammation. Since CB_2R is expressed in hematopoietic cells, we tested the effects of NADA in WT and *Cnr2*$^{-/-}$ bone marrow cells (Figure 3.11, A and B) and endothelial cells (Figure 3.11, C and D) *ex vivo*.

For these studies, cells were pre-incubated with NADA, and then stimulated with LPS for 6 hours. NADA treatment reduced IL-6 production induced by LPS in WT, but not *Cnr2*$^{-/-}$, bone marrow cells and endothelial cells (Figure 3.11, A-D). These results indicate that the immunomodulatory activity of NADA depends upon CB_2R in endothelial cells and the hematopoietic compartment. To test the requirement of CB_2R on the effects of NADA systemically, we challenged WT and *Cnr2*$^{-/-}$ mice with i.v. LPS, treated them immediately after with i.v. NADA, and collected plasmas at two hours. In contrast to WT mice, NADA had no effect on IL-6, CCL2, IL-10, or PAI-1 levels in *Cnr2*$^{-/-}$ mice (Figure 3.11, E-H). Together, these results indicate that the anti-inflammatory activity of NADA is dependent upon both TRPV1 and CB_2R.

NADA modulates neuropeptide expression via TRPV1

We hypothesized that NADA may exert its anti-inflammatory effects via the release of the neuropeptides calcitonin gene-related peptide (CGRP) and substance P, both of which are released by TRPV1-expressing neurons in sensory ganglion. We quantified plasma levels of CGRP and substance P in mice treated with NADA and LPS (Figure 3.12). LPS alone has no effect on plasma levels of substance P in WT or *Trpv1*$^{-/-}$ mice (Figure 3.12A). NADA treatment augmented substance P levels in WT mice, but not in *Trpv1*$^{-/-}$ mice challenged with either LPS or carrier (Figure 3.12A, $p < 0.01$ and $p < 0.05$, respectively). In contrast, CGRP was induced in both WT and *Trpv1*$^{-/-}$ mice challenged with LPS, and treatment with NADA dramatically decreased CGRP levels in endotoxemic WT, but not *Trpv1*$^{-/-}$ mice (Figure 3.12B, $p < 0.01$ and $p < 0.05$, respectively). Capsaicin mimicked the effects of NADA on neuropeptide release (data

not shown).

Discussion

We have provided the first evidence that the endocannabinoid/endovanilloid NADA abates acute systemic inflammation *in vivo* in a TRPV1-dependent manner. Treatment with NADA reduces plasma levels of pro-inflammatory cytokines and PAI-1, and increases levels of the anti-inflammatory cytokine IL-10 in mice with intraabdominal sepsis induced by CLP, and following challenge with microbial TLR2 and TLR4 agonists. NADA also modulates circulating levels of neuropeptides in endotoxemic mice, reducing CGRP and increasing substance P. Our data in *Trpv1*$^{-/-}$ bone marrow chimeras suggest that TRPV1 expressed in non-hematopoietic cells mediates the effects of NADA on acute systemic inflammation. These data, in conjunction with our *ex vivo* data in microglia, PMBCs, and endothelial cells, raise the intriguing possibility that NADA exerts its anti-inflammatory effects via neuronal TRPV1. During septic shock, the excessive production of pro-inflammatory mediators and the failure to appropriately resolve inflammation, in conjunction with dysregulation of coagulation pathways, lead to organ failure, the most common cause of demise in this high mortality syndrome (2, 216, 217). We speculate that by reducing levels of pro-inflammatory cytokines and PAI-1, which is an inhibitor of fibrinolysis that facilitates clot persistence, the NADA-TRPV1 axis may protect against downstream pathologies such as multiple organ failure by abrogating the positive feedback loop that propagates pathological inflammation. Collectively, our results support the hypothesis that the endovanilloid system represents a novel potential therapeutic target for the treatment of disorders characterized by

dysregulated inflammation, such as sepsis.

Because NADA is considered to be the principal endogenous endovanilloid TRPV1 agonist we sought to determine the contribution of TRPV1 to the immunomodulatory activity of NADA *in vivo*. The effects of NADA on cytokine production, neuropeptide release, and PAI-1 induced by exposure TLR agonists were absent in *Trpv1*$^{-/-}$ mice, indicating that TRPV1 is required to elicit these early parameters of systemic and neuroinflammation. Functional TRPV1 expressed by a number of non-neuronal cells has been reported to regulate immune responses (151, 152, 205-209, 211). However, our data suggest that TRPV1 expressed in the hematopoietic compartment is not necessary for the effects of NADA on acute systemic inflammation. This is further supported by our *ex vivo* data that bone marrow, peritoneal cells, PBMCs, and microglia from *Trpv1*$^{-/-}$ mice all retain full responsiveness to the anti-inflammatory properties of NADA. Similarly, our *ex vivo* data using primary endothelial cells suggest that endothelial TRPV1 is not responsible for the NADA's *in vivo* anti-inflammatory properties in mice. We previously reported that cannabinoid receptors may mediate the anti-inflammatory effects of NADA in human endothelial cells, suggesting that CB_1R and/or CB_2R may be responsible for the anti-inflammatory effects of NADA on leukocyte and endothelial cell populations (209). We found that the activity of NADA in hematopoietic cells and endothelial cells *ex vivo* is dependent upon CB_2R, which is also able to mediate the systemic immunomodulatory effects of NADA. These results support the notion that CB_2R and non-hematopoietic TRPV1 primarily mediate the effects of NADA on inflammation in early sepsis. However, further studies are needed to determine if the anti-inflammatory effects of NADA may affect inflammation and other

outcomes, such as sepsis-induced organ failure, later in the course of sepsis.

Consistent with the cumulative evidence that points to a protective role for TRPV1 in murine sepsis models, we observe that TRPV1 activation displays a protective phenotype of reduced pro-inflammation, increased anti-inflammation and downregulation of PAI-1 in toxicity and infection models of sepsis (151, 195, 206, 211). However, in contrast to other reports on TRPV1 in sepsis, in the absence of NADA we did not detect differences in cytokine responses of *Trpv1*$^{-/-}$ versus WT mice treated with LPS or Pam3Cys. Because we used early time points (2-6 hours), our study does not define the role of TRPV1 at later stages of sepsis, which may account for such differences. Our study suggests that NADA may modulate sepsis-induced systemic inflammation through the activation of neuronal TRPV1. The nervous system is increasingly recognized as playing key roles in inflammation, and strong links have been established between the immune and nervous systems. Neurogenic inflammation is believed to be a critical component of inflammatory initiation, and the pain response (218, 219). There is also strong evidence that the links between the nervous and immune systems are bidirectional, with each able to modulate the activity of the other. In the area of sepsis, current evidence points to a neuroimmune response mediated through the vagus nerve and spleen (220, 221). Notably, TRPV1 is expressed in the vagus nerve, raising the possibility that it might be involved in the neuroimmune response (222).

Neurogenic inflammation is regulated by neuropeptides, such as CGRP and substance P, which are released from the peripheral terminals of sensory neurons (196). Neuropeptides act in an autocrine or paracrine manner on various target cells

such as vascular endothelial and smooth muscle cells to regulate vasodilation and capillary permeability, and on innate and adaptive immune cells to regulate chemotaxis and activation (196, 219). At present there is limited information regarding the importance of neuropeptides in sepsis. CGRP has been reported to mediate aspects of septic shock during in endotoxemic rats (223). Additionally, elevated plasma substance P and CGRP have been reported to be associated with worse outcomes in humans with sepsis (224, 225).

Activation of TRPV1 on nociceptors by a variety of stimuli promotes the secretion of CGRP and substance P, which induce pro-inflammatory responses and vasodilatation that facilitate the arrival leukocytes and inflammatory mediators in the circulation to sites of tissue distress (65, 193, 195, 226-231). Substance P has also been reported to induce an anti-inflammatory, wound-healing phenotype, by inducing IL-10 and a switch to M2 macrophages while inhibiting nitric oxide synthase and TNFα production (232-234). We observed that NADA enhances the release of substance P in a TRPV1-dependent manner, and abrogates the release of CGRP into the circulation in endotoxemic mice. We speculate that NADA-induced activation of TRPV1 may exert its anti-inflammatory effects by simultaneously decreasing CGRP and augmenting substance P in the systemic circulation. It is possible that NADA treatment reduced CGRP secretion via the acute desensitization of TRPV1, but this seems unlikely because NADA did upregulate substance P in the circulation (176). Additionally, the neuropeptides in the plasma may have been derived from non-neuronal cells, such as keratinocytes, which have been shown to express CGRP, or subsets of leukocytes that express substance P (234, 235). Finally, it is possible that the effects of NADA on

neuropeptide release and on acute systemic inflammation are independent of one another.

In conclusion, we have observed that treatment with NADA attenuates acute systemic inflammation and coagulopathy, and modulates neuropeptides in several models of sepsis in mice. These *in vivo* immunomodulatory effects of NADA appear to be dependent upon CB_2R, as well as TRPV1 expressed in non-hematopoietic cells. These results suggest that an endogenous NADA-TRPV1 neuronal axis dampens the pro-inflammatory response during the acute phase of sepsis through regulation of peripheral immune responses in sepsis and systemic inflammation. Further studies will be needed to thoroughly elucidate the mechanisms of by which NADA exerts its effects *in vivo*, and to determine the role of the NADA-TRPV1 axis in the later phases of sepsis and in sepsis-induced organ injury. Nonetheless, our observations may have important implications in sepsis and other acute inflammatory disorders, and suggest that the endovanilloid system may represents a unique, neuroimmunological therapeutic target for the treatment of inflammatory disorders.

Figure 3.1

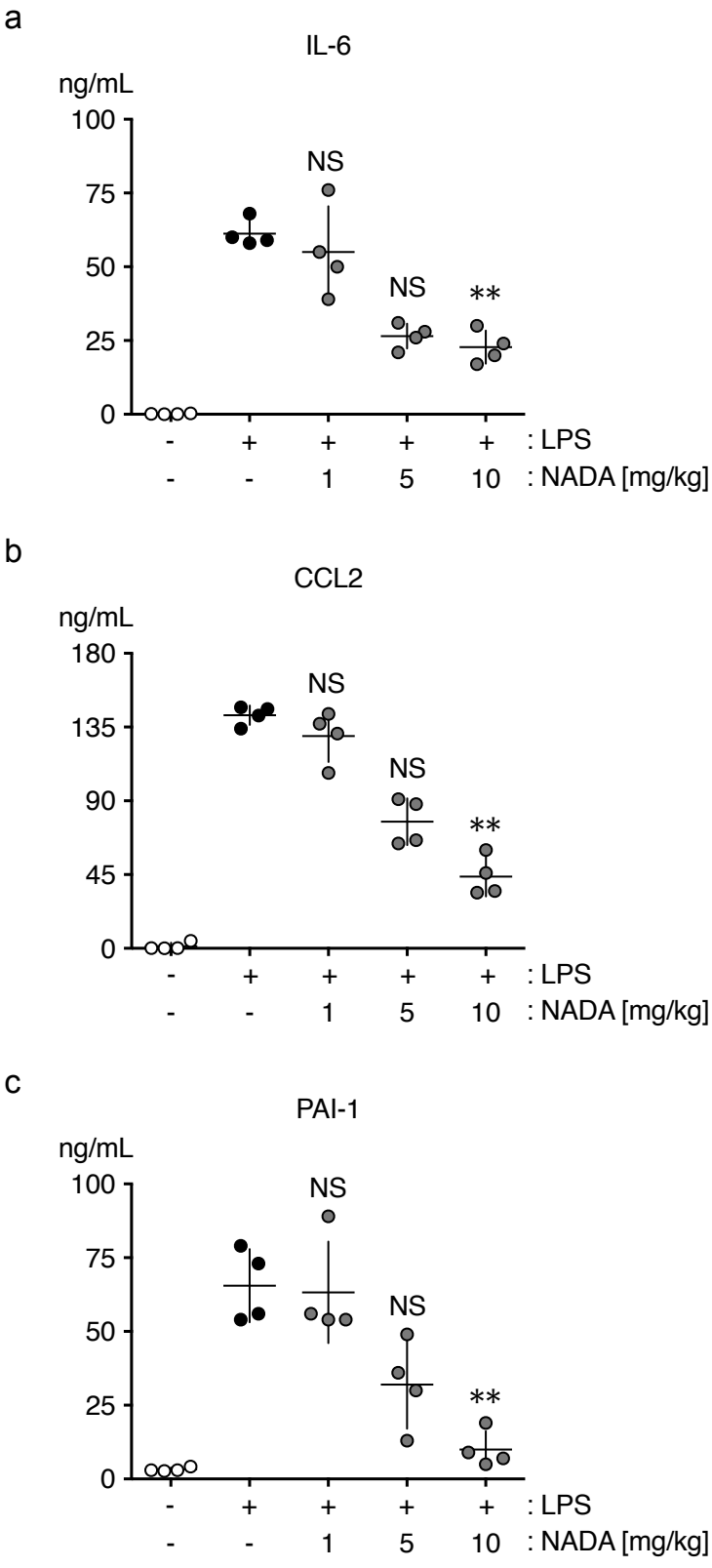
a
IL-6
ng/mL
100
75
50
25
0
NS
NS
**
- + + + + : LPS
- - 1 5 10 : NADA [mg/kg]
b
CCL2
ng/mL
180
135
90
45
0
NS
NS
**
- + + + + : LPS
- - 1 5 10 : NADA [mg/kg]
c
PAI-1
ng/mL
100
75
50
25
0
NS
NS
**
- + + + + : LPS
- - 1 5 10 : NADA [mg/kg]

Figure 3.1. NADA dose-dependently reduces circulating IL-6, CCL2, and PAI-1 levels in endotoxemic mice.

WT mice were challenged i.v. with LPS or carrier, and then immediate after were administered i.v. NADA (1-10 mg/kg) or vehicle. Levels of IL-6 (A) and CCL2 (B), and the activity of PAI-1 (C) were quantified in plasmas after 2 hours. NS, not significant. **, $p < 0.01$ when comparing LPS-treated mice in the presence or absence of NADA. Data are representative of two independent experiments (means ± SD of $n = 4$ mice per group).

Figure 3.2

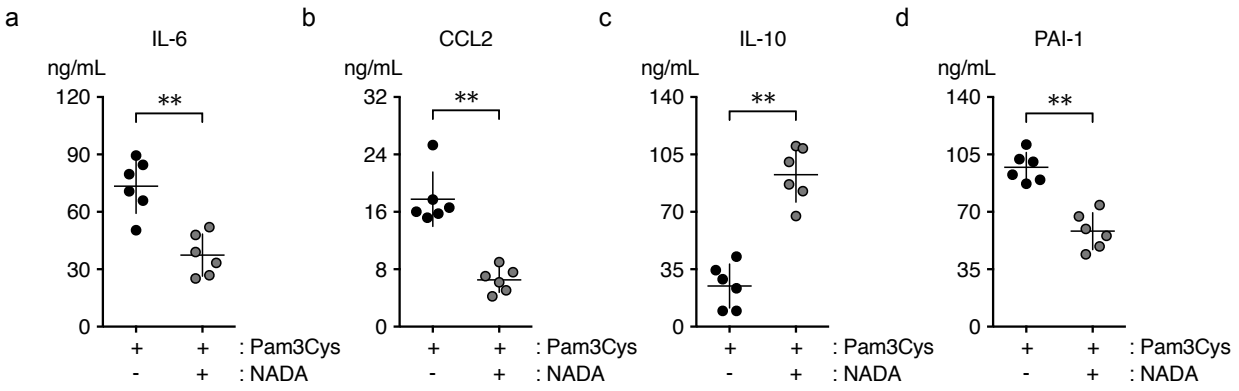
a
IL-6
ng/mL
120
90
60
30
0
**
+ + : Pam3Cys
- + : NADA
b
CCL2
ng/mL
32
24
16
8
0
**
+ + : Pam3Cys
- + : NADA
c
IL-10
ng/mL
140
105
70
35
0
**
+ + : Pam3Cys
- + : NADA
d
PAI-1
ng/mL
140
105
70
35
0
**
+ + : Pam3Cys
- + : NADA

Figure 3.2. NADA ameliorates the induction of pro-inflammatory cytokines and PAI-1 and enhances the induction of IL-10 in Pam3Cys-treated mice.

WT mice were challenged i.v. with Pam3Cys or carrier, immediately prior to i.v. administration of NADA (10 mg/kg) or vehicle. Plasma levels of IL-6 (A), CCL2 (B), IL-10 (C), and PAI-1 (D) were quantified 2 hours after Pam3Cys challenge. Vehicle-treated mice had background levels of all cytokines (data not shown). **, $p < 0.01$ when comparing Pam3Cys-treated mice in the presence or absence of NADA. Data are representative of three independent experiments (means ± SD of n = 4-6 mice per group).

Figure 3.3

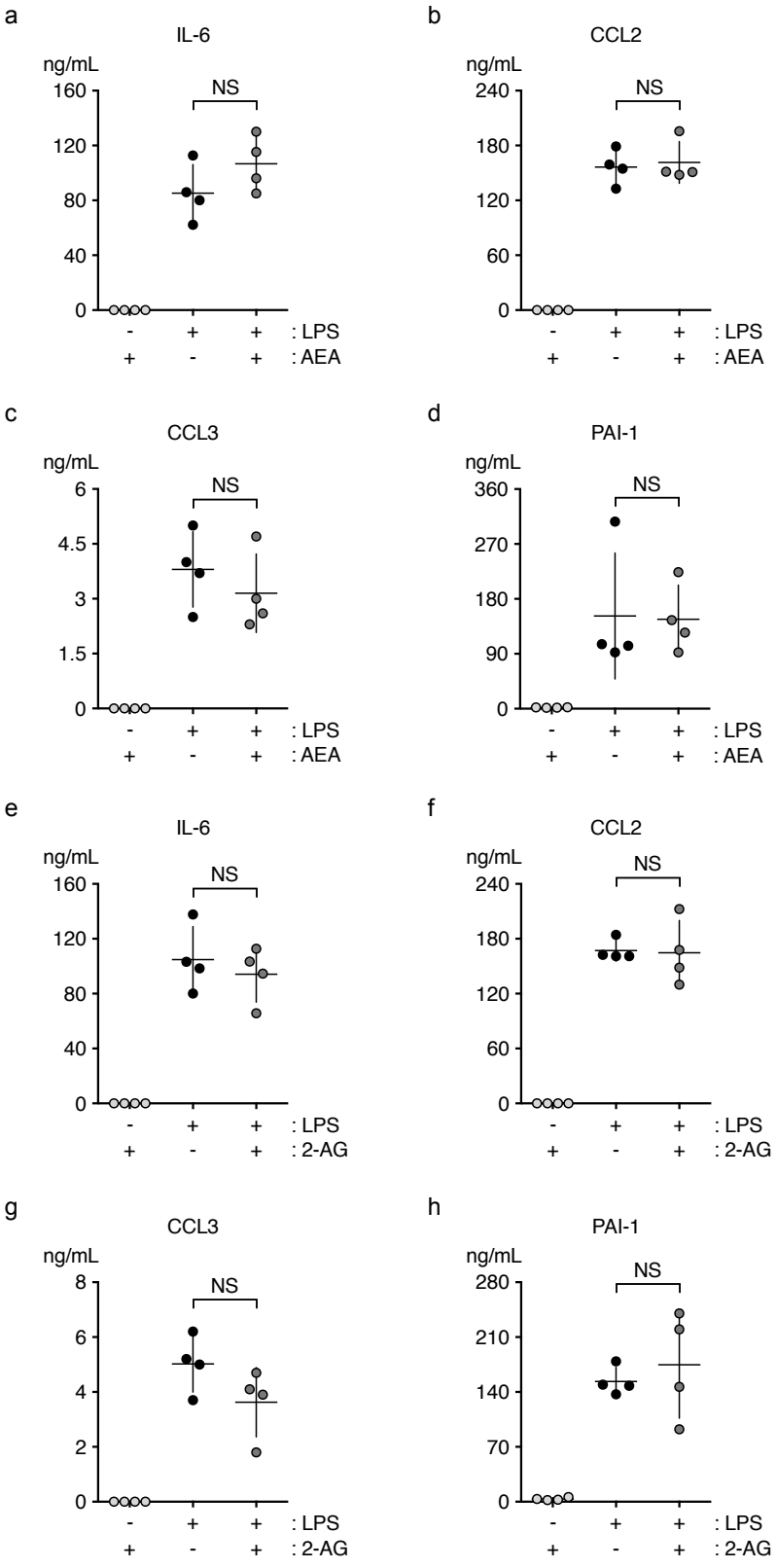
a
IL-6
ng/mL
160
120
80
40
0
NS
- + + : LPS
+ - + : AEA
b
CCL2
ng/mL
240
180
120
60
0
NS
- + + : LPS
+ - + : AEA
c
CCL3
ng/mL
6
4.5
3
1.5
0
NS
- + + : LPS
+ - + : AEA
d
PAI-1
ng/mL
360
270
180
90
0
NS
- + + : LPS
+ - + : AEA
e
IL-6
ng/mL
160
120
80
40
0
NS
- + + : LPS
+ - + : 2-AG
f
CCL2
ng/mL
240
180
120
60
0
NS
- + + : LPS
+ - + : 2-AG
g
CCL3
ng/mL
8
6
4
2
0
NS
- + + : LPS
+ - + : 2-AG
h
PAI-1
ng/mL
280
210
140
70
0
NS
- + + : LPS
+ - + : 2-AG

Figure 3.3. Neither anandamide (AEA) nor 2-AG affect the induction of cytokines or PAI-1 in endotoxemic mice.

WT mice were challenged i.v. with LPS or carrier, and immediately after were administered i.v. AEA or 2-AG (10 mg/kg) or vehicle. Levels of IL-6 (A and E), CCL2 (B and F), CCL3 (C and G), and the activity of PAI-1 (D and H) were quantified in plasmas at 2 hours. AEA or 2-AG alone did not affect baseline levels of inflammatory mediators or PAI-1 (data not shown). NS, not significant. Data are representative of two independent experiments (means ± SD of n = 4 mice per group).

Figure 3.4

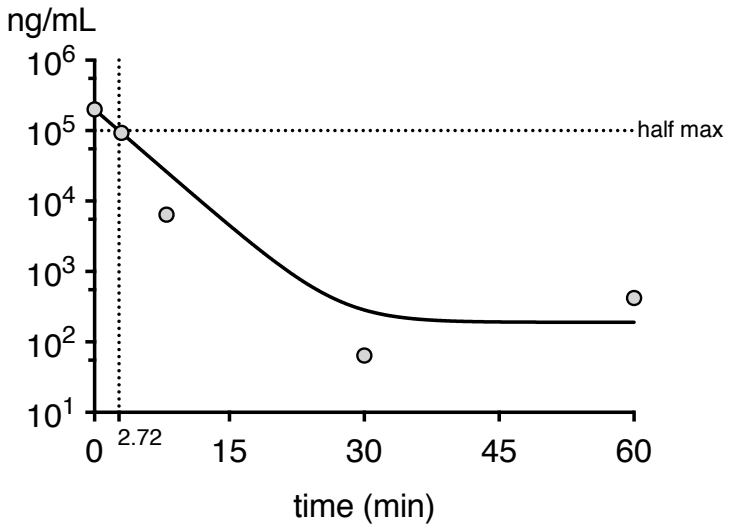

One phase decay	
Best-fit values	
Y0	200004
Plateau	190.1
K	0.2553
Half-life	2.715
Tau	3.917
Span	199814
Goodness of fit	
Robust sum of square	7.379
RSDR	570.1
Constraints	
K	K > 0.0
Number of points analyzed	
Analyzed	5

Figure 3.4. The half-life of NADA in plasma is in the order of minutes.

Plasma concentrations of NADA were quantified in the plasmas of WT mice by LC-MS/MS at intervals from t=0-60 minutes after i.v. administration of NADA (10 mg/kg).

Figure 3.5

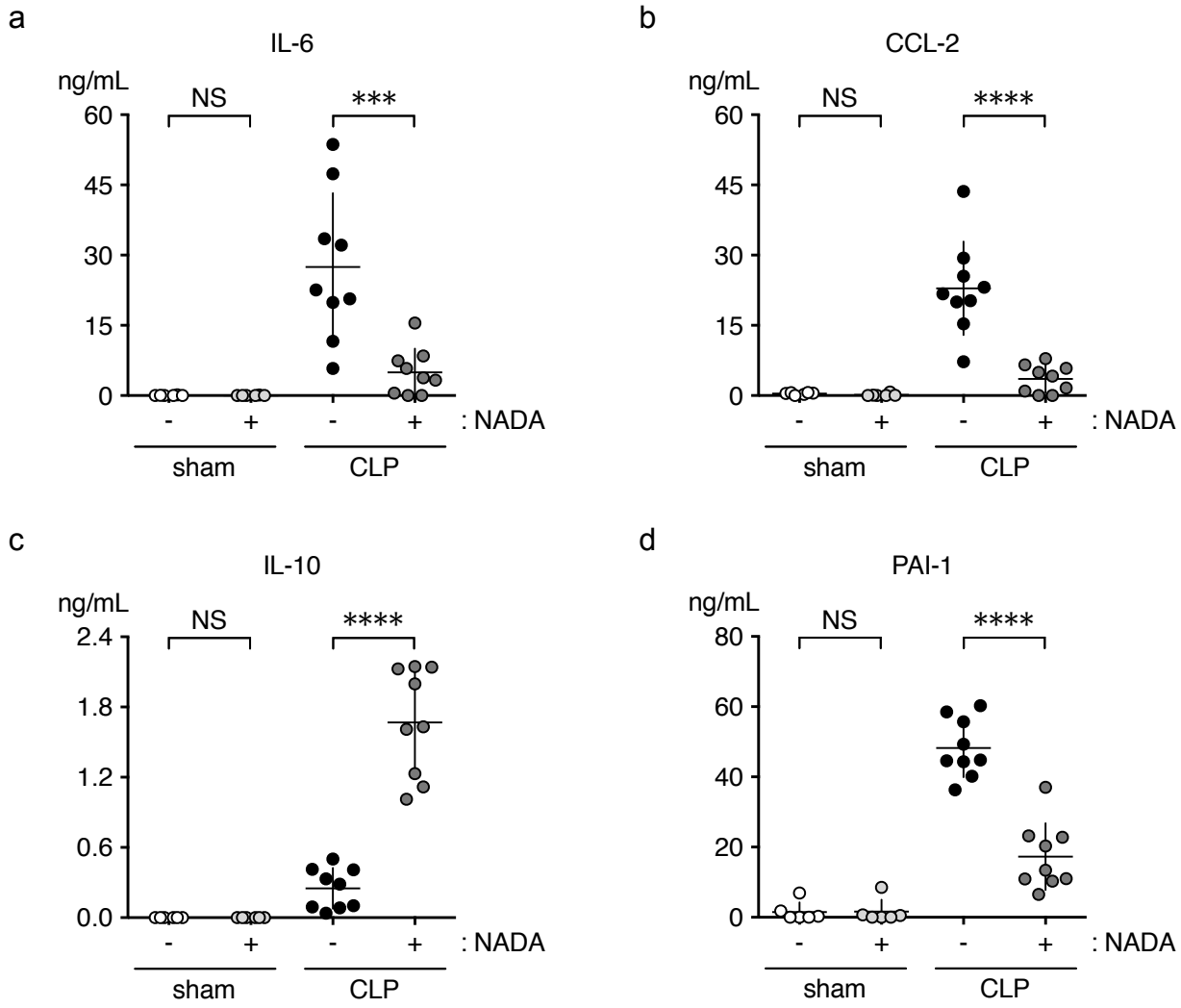
a
IL-6
ng/mL
NS
***
60
45
30
15
0
- + - + : NADA
sham
CLP
b
CCL-2
ng/mL
NS
****
60
45
30
15
0
- + - + : NADA
sham
CLP
c
IL-10
ng/mL
NS
****
2.4
1.8
1.2
0.6
0.0
- + - + : NADA
sham
CLP
d
PAI-1
ng/mL
NS
****
80
60
40
20
0
- + - + : NADA
sham
CLP

Figure 3.5. NADA modulates cytokines and PAI-1 in a CLP model of sepsis.

WT mice underwent CLP or sham surgeries and immediately after were administered i.v. NADA (10 mg/kg) or vehicle. Levels of IL-6 (A), CCL-2 (B), IL-10 (C), and PAI-1 (D) were quantified in plasmas 6 hours after surgery. ***, $p < 0.001$, ****, $p < 0.0001$, when comparing CLP mice in the presence or absence of NADA. Data are representative of three independent experiments (means ± SD of n = 4-10 mice per group).

Figure 3.6

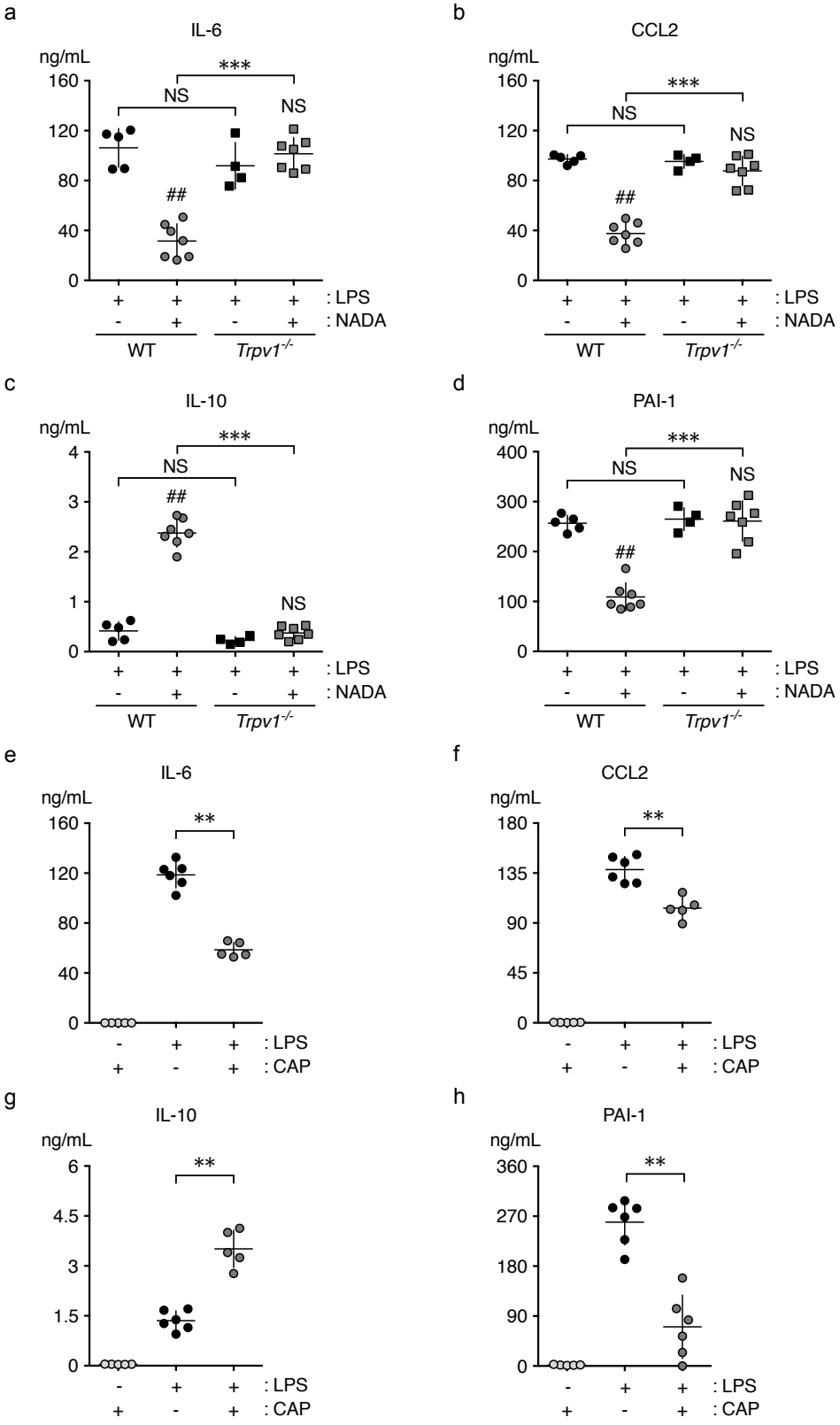
a
IL-6
ng/mL
160
120
80
40
0
***
NS
NS
##
+ + + + : LPS
- + - + : NADA
WT
Trpv1-/-
b
CCL2
ng/mL
160
120
80
40
0
***
NS
NS
##
+ + + + : LPS
- + - + : NADA
WT
Trpv1-/-
c
IL-10
ng/mL
4
3
2
1
0
***
NS
##
NS
+ + + + : LPS
- + - + : NADA
WT
Trpv1-/-
d
PAI-1
ng/mL
400
300
200
100
0
***
NS
NS
##
+ + + + : LPS
- + - + : NADA
WT
Trpv1-/-
e
IL-6
ng/mL
160
120
80
40
0
**
- + + : LPS
+ - + : CAP
f
CCL2
ng/mL
180
135
90
45
0
**
- + + : LPS
+ - + : CAP
g
IL-10
ng/mL
6
4.5
3
1.5
0
**
- + + : LPS
+ - + : CAP
h
PAI-1
ng/mL
360
270
180
90
0
**
- + + : LPS
+ - + : CAP

Figure 3.6. TRPV1 mediates NADA anti-inflammatory activity in endotoxemic mice.

WT and *Trpv1*$^{-/-}$ mice were challenged i.v. with LPS and immediately after were treated i.v. with NADA (10 mg/kg) or vehicle (A-D), capsaicin (0.2 mg/kg), or vehicle (E-H). Plasma concentrations of IL-6 (A and E) CCL2 (B and F), IL-10 (C and G), and PAI-1 (D and H) were quantified at 2 hours. Treatment with capsaicin alone did not affect baseline levels of inflammatory mediators or PAI-1 (data not shown). NS, not significant. ***, $p < 0.001$ when comparing LPS and NADA-treated WT versus *Trpv1*$^{-/-}$ mice; $^{\#\#}$, $p < 0.01$ when comparing LPS-treated WT mice in the presence or absence of NADA; **, $p < 0.01$ when comparing LPS-treated mice in the presence or absence of capsaicin. Data are representative of two independent experiments (means ± SD of $n = 4$ mice per group).

Figure 3.7

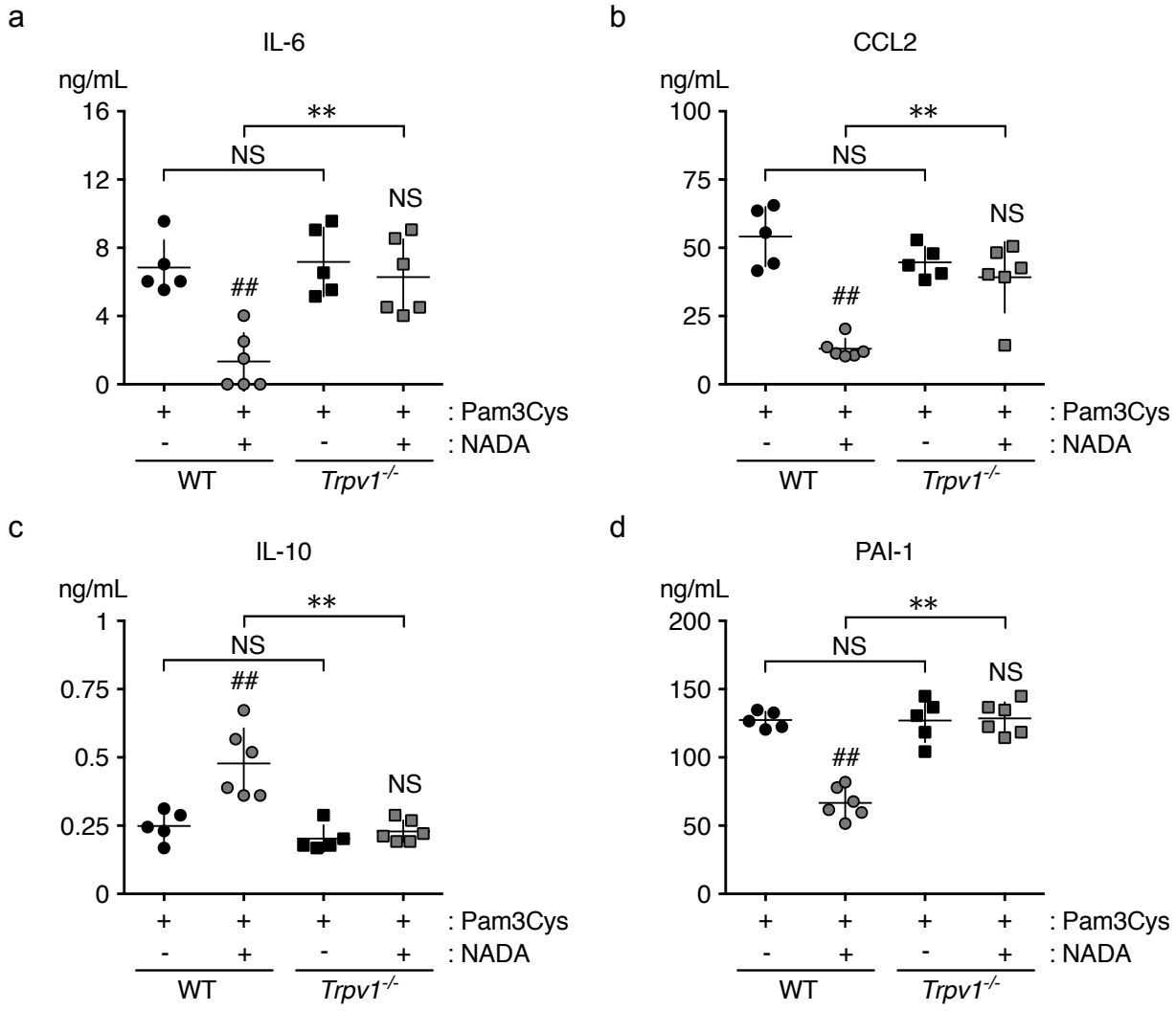
a
IL-6
ng/mL
16
12
8
4
0
**
NS
NS
##
+ + + + : Pam3Cys
- + - + : NADA
WT
Trpv1-/-
b
CCL2
ng/mL
100
75
50
25
0
**
NS
NS
##
+ + + + : Pam3Cys
- + - + : NADA
WT
Trpv1-/-
c
IL-10
ng/mL
1
0.75
0.5
0.25
0
**
NS
##
NS
+ + + + : Pam3Cys
- + - + : NADA
WT
Trpv1-/-
d
PAI-1
ng/mL
200
150
100
50
0
**
NS
NS
##
+ + + + : Pam3Cys
- + - + : NADA
WT
Trpv1-/-

Figure 3.7. TRPV1 mediates the effects of NADA on inflammatory cytokines and PAI-1 in Pam3Cys-treated mice.

WT and *Trpv1*$^{-/-}$ mice were challenged i.v. with Pam3Cys (10 mg/kg) immediately prior to i.v. administration of NADA (10 mg/kg) or vehicle (A-D). Plasma levels of IL-6 (A) CCL2 (B), IL-10 (C), and PAI-1 (D) were quantified 2 hours after Pam3Cys challenge. Mice that received saline instead of Pam3Cys had only background levels of cytokines regardless of NADA administration (data not shown). NS, not significant. **, $p < 0.01$ when comparing Pam3Cys+NADA-treated WT versus *Trpv1*$^{-/-}$ mice; $^{\#\#}$, $p < 0.01$ when comparing Pam3Cys-treated WT mice in the presence or absence of NADA. Data are representative of two independent experiments (means ± SD of n = 5-6 mice per group).

Figure 3.8

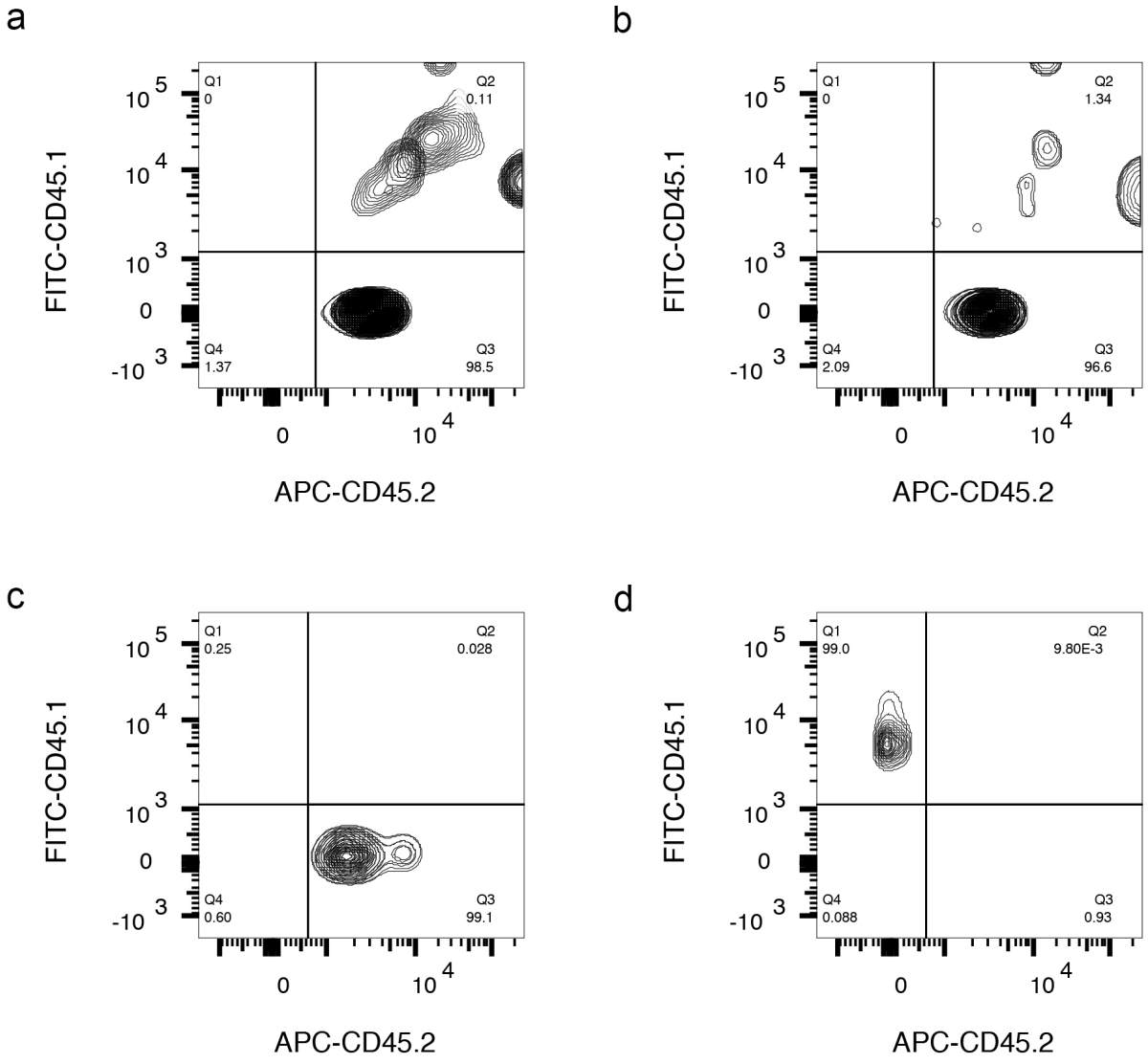
a
Q1
0
Q2
0.11
Q4
1.37
Q3
98.5
FITC-CD45.1
APC-CD45.2
b
Q1
0
Q2
1.34
Q4
2.09
Q3
96.6
FITC-CD45.1
APC-CD45.2
c
Q1
0.25
Q2
0.028
Q4
0.60
Q3
99.1
FITC-CD45.1
APC-CD45.2
d
Q1
99.0
Q2
9.80E-3
Q4
0.088
Q3
0.93
FITC-CD45.1
APC-CD45.2

Figure 3.8. Verification of bone marrow engraftment in chimera mice by flow cytometry.

Flow cytometry was performed to verify engraftment of donor bone marrow in recipient mice 8-9 weeks after irradiation. Whole blood was collected from recipient mice and stained for the expression of CD45.1 and CD45.2. Plots show data from the transfer of $CD45.2^+$ WT (A) or $CD45.2^+$ *Trpv1*$^{-/-}$ (B) bone marrow into $CD45.1^+$ WT recipient mice. Plots also show the reverse chimera in which $CD45.2^+$ *Trpv1*$^{-/-}$ (C) or $CD45.1^+$ WT (D) bone marrow was transferred into $CD45.2^+$ *Trpv1*$^{-/-}$ recipient mice. For both experiments >95% of the hematopoietic cells in the chimera mice were of donor origin.

Figure 3.9

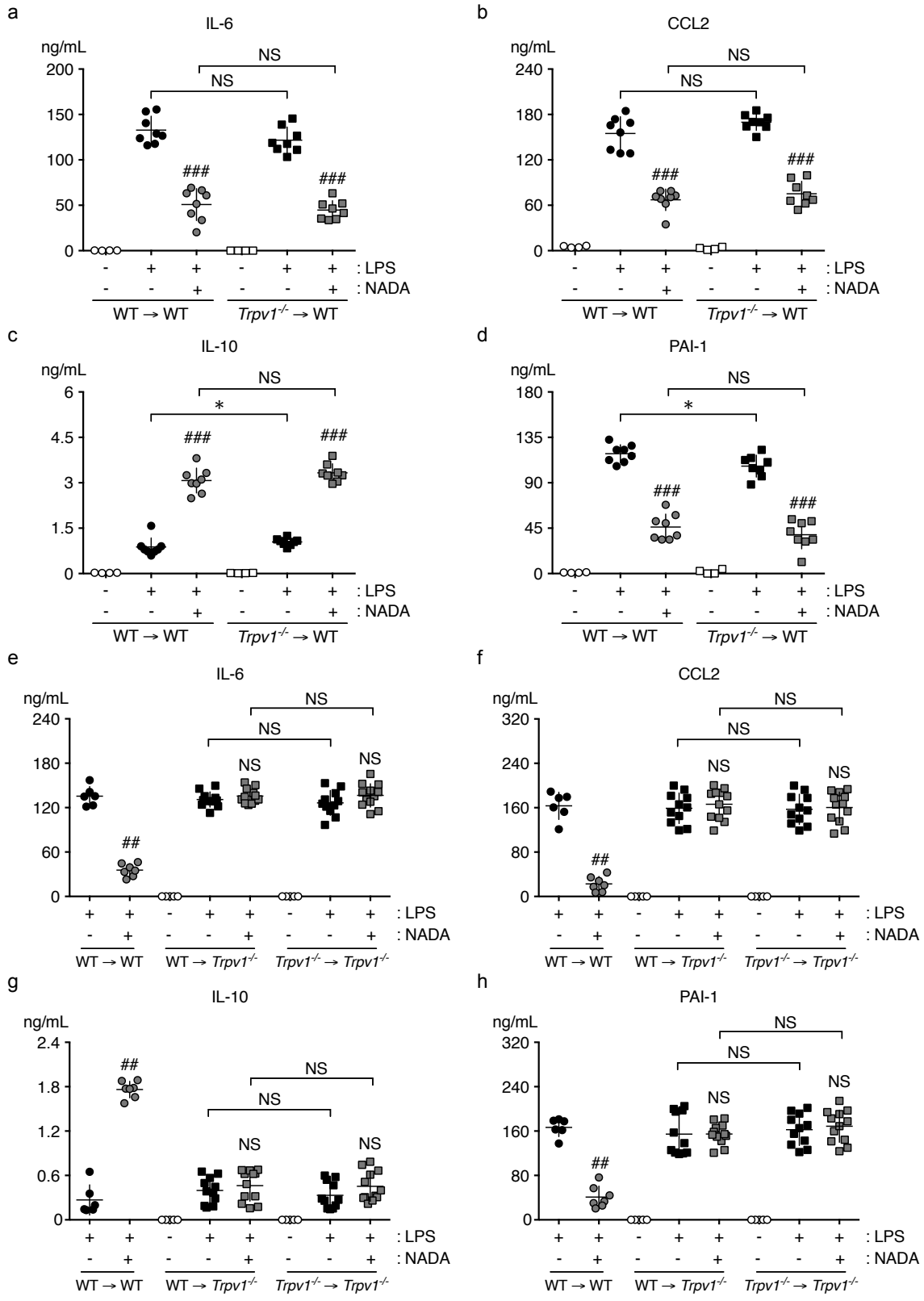
a
IL-6
ng/mL
200
150
100
50
0
NS
NS
###
###
- + + - + + : LPS
- - + - - + : NADA
WT → WT
Trpv1-/- → WT
b
CCL2
ng/mL
240
180
120
60
0
NS
NS
###
###
- + + - + + : LPS
- - + - - + : NADA
WT → WT
Trpv1-/- → WT
c
IL-10
ng/mL
6
4.5
3
1.5
0
NS
*
###
###
- + + - + + : LPS
- - + - - + : NADA
WT → WT
Trpv1-/- → WT
d
PAI-1
ng/mL
180
135
90
45
0
NS
*
###
###
- + + - + + : LPS
- - + - - + : NADA
WT → WT
Trpv1-/- → WT
e
IL-6
ng/mL
240
180
120
60
0
NS
NS
NS
NS
##
+ + - + + - + + : LPS
- + - - + - - + : NADA
WT → WT
WT → Trpv1-/-
Trpv1-/- → Trpv1-/-
f
CCL2
ng/mL
320
240
160
80
0
NS
NS
NS
NS
##
+ + - + + - + + : LPS
- + - - + - - + : NADA
WT → WT
WT → Trpv1-/-
Trpv1-/- → Trpv1-/-
g
IL-10
ng/mL
2.4
1.8
1.2
0.6
0
NS
NS
NS
NS
##
+ + - + + - + + : LPS
- + - - + - - + : NADA
WT → WT
WT → Trpv1-/-
Trpv1-/- → Trpv1-/-
h
PAI-1
ng/mL
320
240
160
80
0
NS
NS
NS
NS
##
+ + - + + - + + : LPS
- + - - + - - + : NADA
WT → WT
WT → Trpv1-/-
Trpv1-/- → Trpv1-/-

Figure 3.9. Non-hematopoietic TRPV1 mediates the anti-inflammatory activity of NADA in endotoxemic mice.

(A-D) Irradiated CD45.1^{+} recipient mice were reconstituted with WT or *Trpv1*$^{-/-}$ donor bone marrow. Following engraftment, bone marrow chimeras were challenged i.v. with LPS or vehicle and immediately after were treated i.v. with NADA (10 mg/kg) or vehicle. Plasma levels of IL-6 (A), CCL2 (B), IL-10 (C), and PAI-1 (D) were quantified at 2 hours. NADA on its own did not affect baseline levels of inflammatory mediators or PAI-1 (data not shown).

(E-H) Irradiated *Trpv1*$^{-/-}$ CD45.2^{+} recipient mice were reconstituted with CD45.1^{+} WT or *Trpv1*$^{-/-}$ donor bone marrow. As controls, WT CD45.2^{+} recipient mice were reconstituted with CD45.1^{+} WT donor bone marrow. Following engraftment, bone marrow chimeras were challenged i.v. with LPS or vehicle and immediately after were treated i.v. with NADA (10 mg/kg) or vehicle. Plasma levels of IL-6 (E), CCL2 (F), IL-10 (G), and PAI-1 (H) were quantified at 2 hours. NADA on its own did not affect baseline levels of inflammatory mediators or PAI-1 (data not shown).

NS, not significant. *, $p < 0.05$ when comparing LPS-treated recipient mice receiving WT versus *Trpv1*$^{-/-}$ bone marrow. $^{\#\#}$, $p < 0.01$; $^{\#\#\#}$, $p < 0.001$ when comparing LPS-treated mice in the presence or absence of NADA. Data are representative of two independent experiments (means ± SD of $n = 8$ mice per group).

Figure 3.10

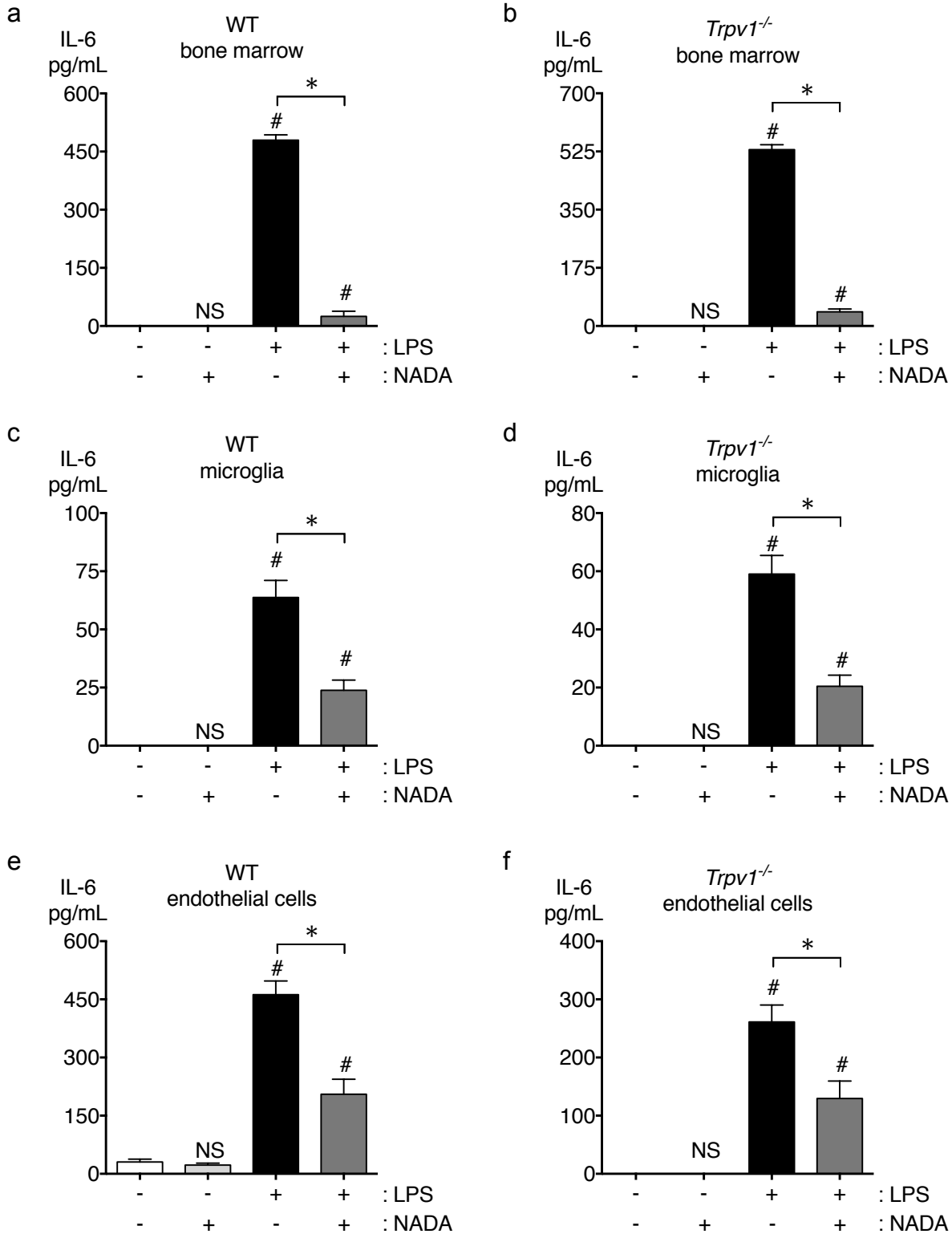
a
WT
bone marrow
IL-6
pg/mL
600
450
300
150
0
*
#
#
NS
- - + + : LPS
- + - + : NADA
b
Trpv1-/-
bone marrow
IL-6
pg/mL
700
525
350
175
0
*
#
#
NS
- - + + : LPS
- + - + : NADA
c
WT
microglia
IL-6
pg/mL
100
75
50
25
0
*
#
#
NS
- - + + : LPS
- + - + : NADA
d
Trpv1-/-
microglia
IL-6
pg/mL
80
60
40
20
0
*
#
#
NS
- - + + : LPS
- + - + : NADA
e
WT
endothelial cells
IL-6
pg/mL
600
450
300
150
0
*
#
#
NS
- - + + : LPS
- + - + : NADA
f
Trpv1-/-
endothelial cells
IL-6
pg/mL
400
300
200
100
0
*
#
#
NS
- - + + : LPS
- + - + : NADA

Figure 3.10. TRPV1 is not necessary for the anti-inflammatory activity of NADA in LPS-treated hematopoietic cells or endothelial cells *ex vivo*.

Cultured primary murine bone marrow (A and B), microglia (C and D), and lung endothelial cells (E and F) were pre-treated for 1 hour with NADA (1 μM), and then LPS (10 ng/mL) was added to wells for an additional 6 hours in the continued presence of NADA. IL-6 levels were quantified in culture supernatants. NS, not significant. *, $p < 0.05$ when comparing LPS-treated cells in the presence or absence of NADA. $^{\#}$, $p < 0.05$ when comparing cells to untreated controls. Data are representative of two independent experiments (means ± SD of $n = 4$ wells per group).

Figure 3.11

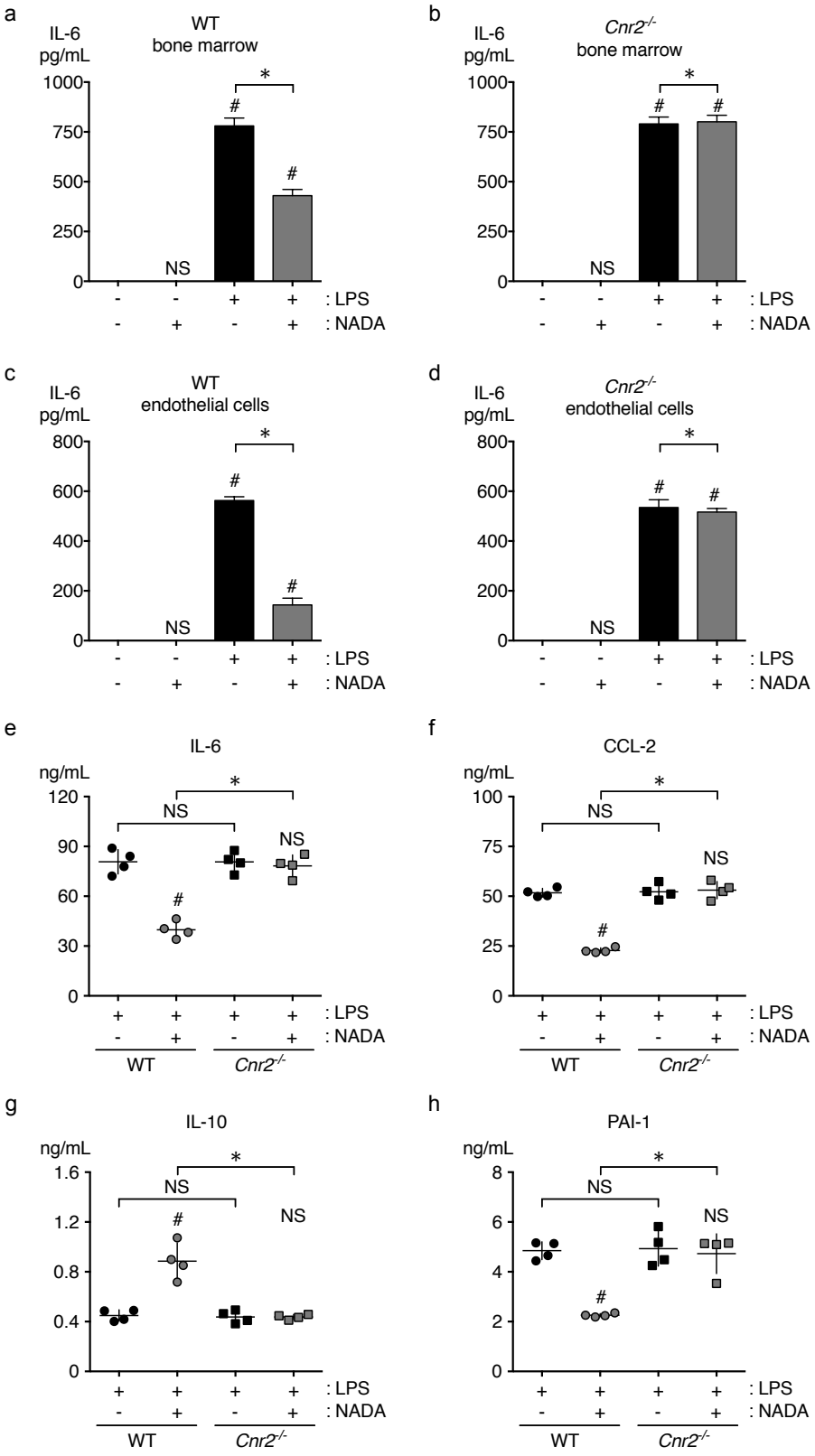
a
IL-6
pg/mL
WT
bone marrow
1000
750
500
250
0
*
#
#
NS
- - + + : LPS
- + - + : NADA
b
IL-6
pg/mL
Cnr2-/-
bone marrow
1000
750
500
250
0
*
#
#
NS
- - + + : LPS
- + - + : NADA
c
IL-6
pg/mL
WT
endothelial cells
800
600
400
200
0
*
#
#
NS
- - + + : LPS
- + - + : NADA
d
IL-6
pg/mL
Cnr2-/-
endothelial cells
800
600
400
200
0
*
#
#
NS
- - + + : LPS
- + - + : NADA
e
IL-6
ng/mL
120
90
60
30
0
*
NS
NS
#
+ + + + : LPS
- + - + : NADA
WT
Cnr2-/-
f
CCL-2
ng/mL
100
75
50
25
0
*
NS
NS
#
+ + + + : LPS
- + - + : NADA
WT
Cnr2-/-
g
IL-10
ng/mL
1.6
1.2
0.8
0.4
0
*
NS
NS
#
+ + + + : LPS
- + - + : NADA
WT
Cnr2-/-
h
PAI-1
ng/mL
8
6
4
2
0
*
NS
NS
#
+ + + + : LPS
- + - + : NADA
WT
Cnr2-/-

Figure 3.11. CB_2R mediates the anti-inflammatory activity of NADA systemically, and in LPS-treated hematopoietic cells and endothelial cells *ex vivo*.

(A-D) Cultured primary murine bone marrow (A and B) and endothelial cells (C and D) were pre-treated for 1 hour with NADA (1 μM), and then LPS (10 ng/mL) was added to wells for an additional 6 hours in the continued presence of NADA. IL-6 levels were quantified in culture supernatants. NS, not significant. *, $p < 0.05$ when comparing LPS-treated cells in the presence or absence of NADA. $^{\#}$, $p < 0.05$ when comparing cells to untreated controls. Data are representative of two independent experiments (means ± SD of $n = 4$ wells per group).

(E-H) WT and *Cnr2*$^{-/-}$ mice were challenged i.v. with LPS and immediately after were treated i.v. with NADA (10 mg/kg) or vehicle. Plasma concentrations of IL-6 (E) CCL2 (F), and IL-10 (G), and PAI-1 (H) were quantified at 2 hours. NS, not significant. *, $p < 0.05$ when comparing LPS and NADA-treated WT versus *Cnr2*$^{-/-}$ mice; $^{\#}$, $p < 0.05$ when comparing LPS-treated WT mice in the presence or absence of NADA. Data are representative of two independent experiments (means ± SD of $n = 4$ mice per group).

Figure 3.12

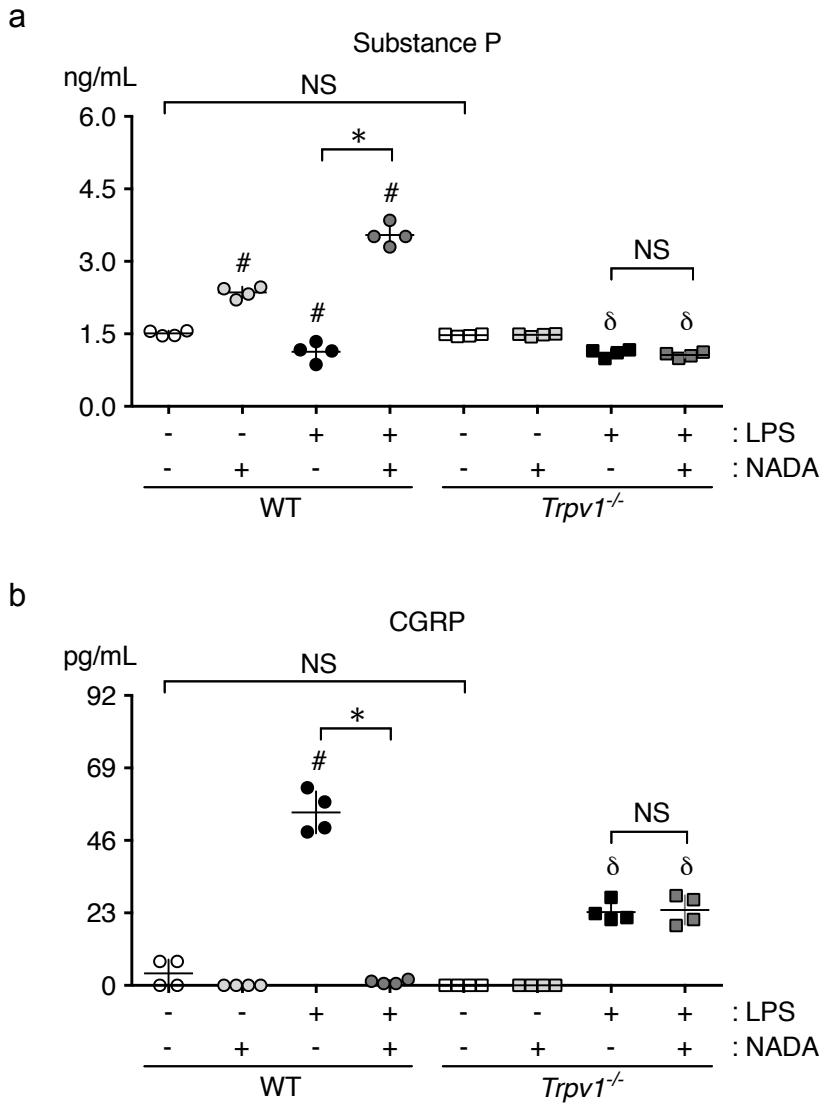
a
Substance P
ng/mL
NS
*
#
#
#
NS
δ
δ
6.0
4.5
3.0
1.5
0.0
- - + + - - + + : LPS
- + - + - + - + : NADA
WT
Trpv1-/-
b
CGRP
pg/mL
NS
*
#
NS
δ
δ
92
69
46
23
0
- - + + - - + + : LPS
- + - + - + - + : NADA
WT
Trpv1-/-

Figure 3.12. NADA regulates neuropeptide release via TRPV1 in endotoxemic mice.

WT and *Trpv1*$^{-/-}$ mice were challenged i.v. with LPS or carrier, and then immediately treated i.v. with NADA (10 mg/kg) or vehicle. Substance P (A) and CGRP (B) were quantified in plasmas at 2 hours. NS, not significant. *, $p < 0.05$ when comparing LPS-treated mice in the presence or absence of NADA; $^{\#,\delta}$, $p < 0.05$ when comparing WT ($^{\#}$) or *Trpv1*$^{-/-}$ ($^{\delta}$) mice to their respective vehicle controls. Data are representative of two independent experiments (means ± SD of n = 4-6 mice per group).

Materials and Methods

Mice

C57BL/6J wild-type (WT), B6.129X1-*Trpv1*^{tm1Jul}/J (*Trpv1*$^{-/-}$), congenic B6.SJL-*Ptprc*^{a} mice (CD45.1^{+}), and B6.129P2-*Cnr2*^{tm1Dgen}/J (*Cnr2*$^{-/-}$) mice were purchased (Jackson Laboratory, Bar Harbor, Maine). Experiments used 8-week-old male or female mice. The University of California San Francisco IACUC approved all animal studies, and experiments were performed in accordance with the PHS Policy on Humane Care and Use of Laboratory Animals. Unless otherwise noted, adult mice were euthanized using CO_2 asphyxiation followed by bilateral thoracotomies and exsanguination by direct cardiac puncture.

Treatment with LPS, Pam3Cys, NADA, AEA, 2-AG, and capsaicin

WT and *Trpv1*$^{-/-}$ mice were injected intravenously (i.v.) ("challenged") with either 0.9% saline, Pam3Cys (10 mg/kg; EMC Microcollections, Tubingen, Germany), LPS (5 mg/kg; Sigma-Aldrich, St. Louis, MO), or 0.9% saline (carrier for LPS and Pam3Cys) immediately prior to i.v. administration of NADA, AEA, 2-AG, or capsaicin (Tocris, Minneapolis, MN) dissolved in vehicle (5% tween-20 in PBS), or with vehicle alone. We used a capsaicin dose of 0.2 mg/kg based on pilot dose-response studies in which we found that capsaicin significantly reduced cytokine levels in endotoxemic mice at 0.2 mg/kg, but not at 0.01 or 0.05 mg/kg. Unless otherwise noted, whole blood was collected via cardiac puncture for cytokine analysis two hours post-injection using citrate as the anticoagulant. In each experiment, at least four mice were used per condition,

and experiments were performed at least twice on different weeks. The doses of Pam3Cys and LPS used were established in pilot dose-response studies.

Immunoassays and MTT assay

IL-6, CCL-2, IL-10, and PAI-1 levels were quantified in mouse plasmas by ELISA (R&D Systems, Minneapolis, MN and Innovative Research, Novi, MI, respectively). Substance P and CGRPα/β levels were quantified in mouse plasma samples by EIA (Enzo Life Sciences, Farmingdale, NY and Cayman Chemicals, Ann Arbor, MI, respectively), and absorbance read using a FLUOstar OPTIMA fluorescent plate reader (BMG Labtech, Cary, NC). Plasma samples were also analyzed for cytokines with the Bio-Plex Pro Mouse 23-Plex Group 1 magnetic bead-based multiplex assay (Bio-Rad, Hercules, CA) using the MAGPIX instrument and xPONENT analysis software (Luminex, Austin, TX) according to the manufacturer's specifications. The lower limit of detection and intra-assay % coefficient of variability (% CV) for this panel of analytes was: IL-1β = 47.68 pg/mL (4.8% CV); TNFα = 13.62 pg/mL (4.7% CV); IL-10 = 4.99 pg/mL (3.4% CV); CCL2 = 35.82 pg/mL (4.7% CV); CCL3 = 1.53 pg/mL (4.3% CV); CCL4 = 2.46 pg/mL (3.9% CV); CCL5 = 1.69 pg/mL (3.4% CV); IL-12p40 = 5.74 pg/mL (3.2% CV); and CXCL1 = 3.54 pg/mL (1.9% CV). MTT assays were performed to assess cell viability as described (209).

LC-MS/MS

An analytical LC-MS/MS method to detect endocannabinoids in plasma was developed at Cayman Chemical. Plasmas were collected at 0, 5, 10, 30, or 60 minutes after i.v.

administration of NADA to WT mice. Plasma samples were analyzed by LC-MS/MS using a NADA standard prepared at Cayman Chemical as described (209).

Cecal ligation and puncture (CLP)

CLP was performed on 8-week-old female WT mice as described (236). Briefly, mice were anesthetized with isoflurane and then were administered a 1mL bolus of saline subcutaneously (s.c.) to account for fluid loss. The abdominal cavity was opened, and the cecum was exteriorized and ligated midway between the tip and the ileocecal junction. The cecum was then punctured once using a 20-gauge needle, and light pressure was applied to extrude a small amount of stool from the puncture site. The cecum was replaced into the abdomen, the incision was closed using a silk suture, and the skin was closed using a clip stapler. For analgesia, bupivacaine was applied locally to the incision site during closure, and buprenorphine was administered s.c. immediately prior to incision and again at four hours. Sham mice underwent the identical procedure, but without the cecal ligation or puncture. NADA (10 mg/kg, i.v., Cayman Chemicals) or vehicle (5% tween-20 in PBS) was administered to mice immediately after surgery and again two hours post-operatively.

Preparation of primary murine cells

Peripheral blood mononuclear cells (PBMCs) were isolated from murine whole blood collected in citrate by gradient centrifugation using Lymphoprep^{TM} (Axis-Shield, Oslo, Norway) as per the manufacturer's instructions. Primary peritoneal cells were isolated from adult mice as described (237). Primary lung endothelial cells (mECs) and microglia

were prepared from 6-7 day old mouse pups immediately after decapitation as described (53, 186, 238). The purity of the cell populations was verified by flow cytometry as described below. WT and *Trpv1*$^{-/-}$ endothelial cells were 90.3% and 90.9% pure respectively.

Bone marrow chimera studies

Bone marrow was isolated from 8-week-old male WT and *Trpv1*$^{-/-}$ donor mice as described, and erythrocytes were lysed using RBC Lysis Buffer (Sigma-Aldrich) (239). For the generation of chimeric mice, bone marrow hematopoietic cells were suspended in PBS to a final concentration of 1x10^{7} cells/mL. Bone marrow chimeras were produced by lethally irradiating recipient CD45.1^{+} congenic mice with a split dose of 1,100 rad, followed by i.v. administration of 2x10^{6} WT or *Trpv1*$^{-/-}$ donor bone marrow cells. For the reverse bone marrow chimera, recipient CD45.2^{+} WT or *Trvp1*$^{-/-}$ mice were irradiated and administered WT CD45.1^{+} or *Trpv1*$^{-/-}$ bone marrow. To allow sufficient recovery time from the bone marrow transplantation, experiments were performed 8-9 weeks after irradiation. Recipient mice were fed antibiotic pellets containing Sulfamethoxadazole and Trimethoprim one week prior to and three weeks after irradiation. Bone marrow engraftment was verified by flow cytometry as described below. Chimeras were challenged with LPS and treated with NADA as described above.

***Ex vivo* NADA and inflammatory agonist treatments**

Endothelial cells were grown to confluence in 48-well plates before agonist treatment. Microglia were plated at 8x10^{4} cells/well in 48-well plates and used two days after

plating. In all experiments, cells were pre-incubated with NADA or vehicle (ethanol) at the indicated concentrations for one hour prior to and continuously during the inflammatory agonist treatment. The inflammatory agonists Pam3Cys (10 mg/mL) or LPS (10 ng/mL) were added for six hours. Preparations of Pam3Cys contained <0.002 EU/mL endotoxin based on the kinetic turbidimetric *Limulus* amoebocyte lysate assay.

Flow cytometry

Mice were euthanized and whole blood was collected by cardiac puncture, and erythrocytes were lysed using RBC Lysis Buffer. Cultured primary murine cells were detached with Accutase (Innovative Cell Technologies, San Diego, CA). Cells were passed through a 70 μM cell strainer, counted, and aliquoted at $1x10^6$ cells per sample. Cells were washed using PBS without Ca^{2+} and Mg^{2+} and incubated with LIVE/DEAD™ violet fluorescent reactive dye (Thermo Fisher Scientific, Waltham, MA) in PBS for 30 minutes at 4°C to assess cell viability. Cells were then washed using Flow Cytometry Staining Buffer (FCSB) (R&D Systems) and incubated with rat anti-mouse IgG (1 μg Thermo Fisher Scientific) in FCSB for 15 minutes at 4°C. Next, cells isolated from whole blood were incubated for 30 minutes at 4°C with specific antibody (1 μg) or isotype control (1 μg). Samples were washed twice with FCSB and then fixed using BD CytoFix (250μL, BD Bioscience, San Jose, CA) for 30 minutes at 4°C. The samples were washed once more with FCSB and then analyzed by flow cytometry (BD LSRII Flow Cytometer, BD Biosciences). Antibodies used were purchased from BD Biosciences unless otherwise noted: FITC-mouse anti-mouse CD45.1, APC-mouse anti-mouse CD45.2, FITC-mouse IgG2a κ, APC-mouse IgG2a κ, FITC-rat anti-mouse CD102, PE-

rat anti-mouse CD31, FITC-rat anti-mouse IgG2a κ, PE-rat anti-mouse IgG2a κ, and Alexa Fluor 750-rat anti-mouse αM/CD11b (R&D Systems).

Statistics

The data were analyzed using nonparametric-based biostatistics. Mann-Whitney tests were used to compare 2 groups; Kruskal-Wallis tests were used for multiple comparisons under a single, defined variable. $P < 0.05$ was considered to be statistically significant for all data. The data in graphs are presented as means ± SD. All experiments were repeated at least twice.

CHAPTER 4

N-arachidonoyl dopamine (NADA) affects inflammation by regulating endothelial and systemic prostanoid metabolism

Abstract

Bioactive lipids are a tightly regulated, complex network of mediators, and include the prostaglandins, thromboxane, leukotrienes, and endocannabinoids. Previous work in our lab has shown that the endocannabinoid *N*-arachidonoyl dopamine (NADA) is able to modulate inflammatory responses both *in vivo* and *in vitro* through cannabinoid receptors -1 and -2 (CB_1R and CB_2R) and transient receptor potential vanilloid 1 (TRPV1). Here we show that NADA induces the expression of cyclooxygenase (COX)-2 in primary human endothelial cells, and that the activation of CB_1R, CB_2R, and TRPV1 by NADA regulates this induction. Furthermore, we find that the anti-inflammatory activity of NADA in endothelial cells is dependent upon COX enzymes, and that treatment of endothelial cells with NADA during LPS challenge decreases prostanoid levels. Finally, we show that treatment with NADA generates the novel prostaglandin analog prostaglandin D_2-dopamine (PGD_2-DA), which possesses similar immunomodulatory activity to NADA *in vitro*. These results indicate that NADA has unique effects on prostanoid metabolism and raise the exciting possibility that the pathway of NADA may be targeted therapeutically for the regulation of acute inflammation in sepsis.

Introduction

The immune response is an intricate system of communication dependent upon cell-to-cell contact and soluble factors. A wide range of classes of molecules have pro-inflammatory effects that help initiate proper immune responses, including, but not limited to, amines (*e.g.* histamine, bradykinin), adhesion molecules, complement,

cytokines, chemokines, and nucleotides (240). Bioactive lipid mediators are increasingly recognized as playing key roles in the regulation of inflammation (241-243). Lipid mediators are a diverse group that includes ω-3, ω-6, and ω-9 polyunsaturated fatty acids. Unlike more classical inflammatory mediators, lipids cannot be stored in vesicles within cells prior to release, since they freely diffuse across membranes (244-246). As a result, lipids are synthesized on-demand from phospholipids in the plasma membrane (242, 244-246). Since lipid mediators have a short half-life (seconds to minutes), they are usually synthesized at their intended site of action, though their local signaling may have profound effects systemically (147, 247-249). After synthesis, lipids undergo both enzymatic and non-enzymatic degradation (242, 250-252). These unique characteristics allow for another layer of inflammatory regulation that can be rapidly induced and inactivated, independent of protein synthesis.

Arachidonic acid is a precursor for a number of bioactive lipids, termed eicosanoids (Figure 4.1). Both immune and non-immune cells produce eicosanoids, such as prostaglandins, leukotrienes, lipoxins, and endocannabinoids, in response to exogenous and endogenous stimuli (253-261). Eicosanoids regulate a vast array of cellular processes integral to the inflammatory response, including intercellular communication, cytokine production, leukocyte chemotaxis, vascular permeability, and coagulation (262, 263). Accordingly, drug classes including steroids and non-steroidal anti-inflammatory drugs (NSAIDs) affect inflammation by inhibiting eicosanoid production (243, 264-267). While the effects of some eicosanoids on inflammation have been studied extensively, the precise roles of others, including the endocannabinoids, are not as well understood. Our lab has recently shown that the endocannabinoid *N*-

arachidonoyl dopamine (NADA) uniquely reduces the secretion of the pro-inflammatory cytokines IL-6 and IL-8 by activated primary human endothelial cells (209). In addition, in endotoxemic and septic mice, we observe that NADA reduces plasma levels of IL-8, CCL2, and the anti-fibrinolytic factor plasminogen activator inhibitor-1 (PAI-1), while increasing levels of the anti-inflammatory cytokine IL-10 (Chapter 3). Neither of the thus far more extensively studied endocannabinoids, *N*-arachidonoylethanolamine (anandamide; AEA) or 2-arachidonoylglygerol (2-AG) affected endothelial or systemic cytokine production (Chapter 3 and (209)). NADA has also been reported to regulate smooth muscle contraction, vasorelaxation, and hyperalgesia (32, 64, 68, 69, 73, 75). Thus, similar to other eicosanoids, NADA is able to regulate diverse inflammatory and physiological responses. Furthermore, we have shown that the activity of NADA in endothelial cells is dependent upon the G-protein coupled receptors cannabinoid receptor-1 and -2 (CB_1R and CB_2R, respectively), as well as the non-specific cation channel transient receptor potential vanilloid 1 (TRPV1) (Chapter 3 and (65, 69-72, 209)). Together, these receptors fine-tune the human endothelial cell response to NADA.

NADA has also been reported to regulate the metabolism of other eicosanoids, which contributes to its immunomodulatory activity. For example, *N*-acyl-dopamines can act as substrates or inhibitors of the lipoxygenase pathway (139, 268, 269). In addition, NADA has been found to stabilize cyclooxygenase (COX)-2 mRNA in a murine brain endothelial cell line independently of the cannabinoid receptors and TRPV1, resulting in the accumulation of COX-2 protein (77). COX-2 is inducible and rapidly upregulated after an inflammatory insult to mediate the immune response (270-273). COX enzymes

catalyze the synthesis of the subclass of immunomodulatory eicosanoids, termed prostanoids (Figure 4.1). As a result, COX enzymes are the targets of numerous drugs, including, but not limited to, aspirin, ibuprofen, and naproxen (274, 275). In addition to upregulating COX-2, NADA has also been reported to specifically inhibit prostaglandin E_2 (PGE_2) and induce prostaglandin D_2 (PGD_2) in a murine brain endothelial cell line by differentially regulating their synthesis enzymes (77).

While endocannabinoids have been shown to regulate lipid biosynthesis, they have also been reported to serve as substrates themselves for lipid metabolism enzymes (276-279). Though COX-2 normally metabolizes arachidonic acid, it is also able to oxygenate the endocannabinoids AEA and 2-AG (276, 278, 280). This metabolism generates bioactive prostaglandin analogs, termed prostaglandin glycerol esters for 2-AG and prostaglandin ethanolamides (prostamides) for AEA (276-278, 280-283). These prostaglandin analogs have pharmacological properties that are distinct from their precursor endocannabinoids (253, 284). They can activate calcium signaling in macrophages, enhance postsynaptic currents in neurons, and regulate pain sensation, thus having critical functions in both the immune and nervous systems (285-288). Prostaglandin glycerol esters and prostamides are believed to bind to a specific receptor, or receptors, that are separate from the prostaglandin, cannabinoid, or TRP receptors (289-291). However, the wild-type prostaglandin receptor has also been hypothesized to heterodimerize with an alternative splicing variant to generate a binding site specific for the prostaglandin analog (292-294). Although a unique prostamide or prostaglandin glycerol ester receptor has not yet been identified, inhibitors and analogs

have been generated (284, 295-299). Overall, it is clear that endocannabinoids are critical components of the bioactive lipid metabolic network.

Our previous data showing the immunomodulatory effects of NADA in primary human endothelial cells, coupled with the reported effects of NADA on prostanoid metabolism, led us to hypothesize that NADA mediates its effects on endothelial inflammation by regulating lipid networks. Understanding the mechanisms of endothelial lipid signaling can provide essential insight into inflammatory regulation for disorders that are characterized by endothelial dysfunction, such as sepsis. Endothelial dysfunction can lead to coagulopathy with diffuse microvascular thrombosis, increased leukocyte activation within multiple organs, and capillary leak leading to intravascular hypovolemia and edema (16). Thus, the regulation of initial endothelial cell inflammatory responses can prevent more distal, excessive inflammation that harms the host. Consistent with previous reports, we find that NADA upregulates COX-2 expression in primary human endothelial cells. However, we show that this upregulation is dependent upon both cannabinoid receptors and TRPV1. We also report that the immunomodulatory activity of NADA is partially dependent upon COX enzyme activity. Furthermore, NADA inhibits LPS-induced PGE_2, TXA_2, and PGI_2. Finally, we are the first show that NADA, similar to the endocannabinoids AEA and 2-AG, is also metabolized by COX-2 to generate its own prostaglandin analog, prostaglandin D_2-dopamine (PGD_2-DA). Like NADA, PGD_2-DA reduces endothelial cytokine production induced by inflammatory agonists. Collectively, these data indicate that NADA is able to moderate endothelial inflammation through the regulation of endothelial lipid

metabolism, and suggests that this novel pathway may be targeted for the treatment of acute inflammatory disorders.

Results

The anti-inflammatory activity of NADA in endothelial cells depends upon its upregulation of COX-2

Since endocannabinoids have been shown to regulate lipid metabolism, we hypothesized that the mechanism of activity of NADA in endothelial cells may depend upon its regulation of eicosanoid metabolic enzymes. We tested the effects of NADA, AEA, and 2-AG on the expression of enzymes involved in lipid metabolism in primary human endothelial cells at baseline, as well as after treatment with the inflammatory agonists LPS and TNFα. Since we have previously shown that NADA, but neither AEA nor 2-AG, possesses anti-inflammatory activity in primary human endothelial cells, we were particularly interested in effects that were specific to NADA (209). We found that NADA, but neither of the other tested endocannabinoids, consistently induced the expression of COX-2 (prostaglandin G/H synthase 2; PTGS2) by qPCR (Table 4.1). This upregulation of COX-2 transcript was observed in endothelial cells treated with NADA alone, or in the presence of LPS or TNFα (Table 4.1). Of the panel of genes tested, NADA also reduced TNFα-induced transcript levels of prostaglandin E synthase (PTGES) (Table 4.1). In contrast, 2-AG further increased the levels of PTGES in the presence of TNFα (Table 4.1). The distinct effects of NADA on lipid metabolic enzyme expression suggest that the eicosanoid biosynthetic pathway may in part mediate the immunomodulatory properties of NADA in the endothelium.

We confirmed the upregulation of COX-2 by NADA at the protein level by immunoblot (Figure 4.2A). Primary human lung microvascular endothelial cells (lung HMVECs) were stimulated with AEA, 2-AG, NADA, or TNFα alone for 1, 6, or 20 hours. NADA and TNFα induced COX-2 protein levels to a similar extent by 20 hours, while neither AEA nor 2-AG affected COX-2 expression in comparison to ethanol treatment (Figure 4.2A). To determine if this upregulation of COX-2 by NADA contributes to its endothelial anti-inflammatory activity, we treated lung HMVECs with the COX inhibitor indomethacin for 1 hour, and then stimulated with NADA and LPS for an additional 20 hours while in the continuous presence of indomethacin. Indomethacin prevented the NADA-mediated reduction of both IL-6 and IL-8 in a dose-dependent manner (Figure 4.2, B and C). These data indicate that NADA not only upregulates COX-2 protein in endothelial cells, but also that NADA exerts its anti-inflammatory effects via COX activity.

The induction of COX-2 by NADA depends upon CB_1R/CB_2R and TRPV1

Previous work in our lab has shown that both the cannabinoid receptors and TRPV1 mediate the immunomodulatory activity of NADA in primary human and mouse endothelial cells (Chapter 3 and (209)). In order to determine if the upregulation of COX-2 by NADA depends upon any of these receptors, we incubated lung HMVECs with inhibitors of CB_1R and CB_2R (CP945598 and SR144528, respectively) or the TRPV1 inhibitor AMG9810 for 1 hour, and then stimulated with NADA for 20 hours. Lung HMVEC treatment with CB_1R/CB_2R inhibitors reduced the expression of COX-2,

whereas treatment with the TRPV1 inhibitor augmented COX-2 expression in comparison to NADA alone (Figure 4.3A).

To confirm these data, we isolated primary endothelial cells from WT, *Trpv1*$^{-/-}$, and *Cnr2*$^{-/-}$ mice and stimulated them with NADA or TNFα for 4 hours. After stimulation, mRNA transcript levels of COX-2 were measured by qPCR. In comparison to WT cells, *Cnr2*$^{-/-}$ endothelial cells had decreased COX-2 mRNA transcripts, while *Trpv1*$^{-/-}$ cells had augmented COX-2 mRNA levels (Figure 4.3B). To verify protein levels of COX-2, WT, *Trpv1*$^{-/-}$, and *Cnr2*$^{-/-}$ endothelial cells were isolated and stimulated with NADA or TNFα for 20 hours. Consistent with the results obtained using receptor inhibitors, *Cnr2*$^{-/-}$ murine endothelial cells had reduced COX-2 expression, while *Trpv1*$^{-/-}$ cells had augmented COX-2 protein levels (Figure 4.3C). These results confirm that the upregulation of COX-2 by NADA is promoted by its activation of CB_2R, and inhibited by its activation of TRPV1.

NADA inhibits LPS-induced PGI_2, TXA_2, and PGE_2 production, but promotes PGD_2 in endothelial cells

Since NADA modulates levels of both COX-2 and PTGES, we sought to determine if NADA affects the production of prostanoids, which are downstream of COX-2 activity. We treated lung HMVECs with NADA for 1 hour, and then stimulated with LPS for 20 hours, while in the continuous presence of NADA. NADA did not affect background levels of 6-keto-$PGF_{1\alpha}$ (used as a readout for PGI_2), TXB_2 (used as a readout for TXA_2), or PGE_2 in culture supernatants (Figure 4.4, A-C). However, NADA abated the LPS-induced levels of 6-keto-$PGF_{1\alpha}$, TXB_2, and PGE_2 (Figure 4.4, A-C). In

contrast, NADA upregulates PGD_2 in endothelial cells in the absence of LPS and augments LPS-induced PGD_2 production (Figure 4.4D). Consistent with results obtained using LPS, NADA also inhibits 6-keto-$PGF_{1\alpha}$, TXB_2, and PGE_2 production, and increases PGD_2 levels, after treatment with TNFα or IL-1β (data not shown). Thus, NADA is able to differentially regulate prostanoid metabolism.

AEA, 2-AG, and NADA have differential effects on endothelial prostanoid metabolism

We hypothesized that the effects of NADA on prostanoid metabolism contributes to its anti-inflammatory activity in endothelial cells. Since neither AEA nor 2-AG have immunomodulatory activity in the endothelium, we aimed to determine if they affected prostanoid production in a manner distinct from that of NADA. We treated lung HMVECs with AEA, 2-AG, or NADA for 1 hour, followed by LPS for 20 hours, while in the continuous presence of the endocannabinoid. In contrast to NADA, AEA and 2-AG augment LPS-induced 6-keto-$PGF_{1\alpha}$, TXB_2, and PGE_2 (Figure 4.5, A-C). Furthermore, while NADA augments baseline and LPS-induced PGD_2 levels, 2-AG reduces PGD_2 production in both conditions (Figure 4.5D). Similarly to NADA, AEA also increases LPS-induced PGD_2, but instead inhibits baseline PGD_2 production (Figure 4.5D). Taken together, these data illustrate that the different endocannabinoids distinctly regulate endothelial prostanoid metabolism, which we speculate may contribute to their unique effects on inflammatory outputs.

NADA reduces serum levels of PGI_2 *in vivo* during murine endotoxemia

We have previously shown that NADA has anti-inflammatory effects during murine endotoxemia (Chapter 3). In order to determine if NADA also regulates *in vivo* prostanoid metabolism in addition to endothelial prostanoid levels, we quantified serum levels of the prostanoids by mass spectrometry 2 hours after intravenous (i.v.) injection of NADA and LPS. Consistent with its results *in vitro*, NADA reduced levels of 6-keto-$PGF_{1\alpha}$ (Figure 4.6A). However, NADA did not affect serum levels of TXB_2, PGE_2, or PGD_2 (Figure 4.6, B-D).

R-profens inhibit the NADA-mediated induction of PGD_2

Since we found that NADA induced PGD_2 expression by EIA *in vitro* (Figure 4.4D), but did not observe the same results by mass spectrometry *in vivo* (Figure 4.6D), we hypothesized that NADA may be converted into a prostaglandin analog that cross-reacts with the PGD_2 EIA kit. Normally, arachidonic acid is oxygenated by COX-2 to generate PGD_2 (Figures 4.1 and 4.7A). However, it is possible that, similar to other endocannabinoids, NADA itself may be oxygenated by COX-2 to generate the prostaglandin analog, prostaglandin D_2-dopamine (PGD_2-DA), which could have its own immunological effects (Figure 4.7A).

To test this hypothesis, we utilized *R*-profens, which have been shown to inhibit the oxygenation of endocannabinoids without affecting the oxygenation of arachidonic acid by COX-2 (Figure 4.7A) (300). We treated lung HMVECs with the *R*-profen *R*-ibuprofen for 1 hour, and then stimulated with NADA and LPS for 20 hours while in the continuous presence of *R*-ibuprofen. *R*-ibuprofen significantly reduced PGD_2 levels after treatment with NADA and LPS, suggesting that the majority of the PGD_2 detected by the

EIA kit is the product of NADA oxygenation and likely a prostaglandin analog (Figure 4.7B). We requested the synthesis of PGD_2-DA by Cayman Chemical and confirmed its cross-reactivity with the PGD_2 EIA kit (data not shown).

To determine if the generation of a prostaglandin analog is required for the immunomodulatory functions of NADA in the endothelium, we also quantified supernatant levels of IL-8 and IL-6 after 20 hours (Figure 4.7, D and E). *R*-ibuprofen partially restored the production of both IL-8 and IL-6 in the presence of NADA and LPS (Figure 4.7, D and E). Consistently, the *R*-profen *R*-flurbiprofen also restored IL-8 and IL-6 levels after a 20 hours stimulation with NADA and LPS (Figure 4.8, A and B). As a control, we incubated lung HMVECs with *S*-ibuprofen, which inhibits oxygenation of both arachidonic acid and endocannabinoids (Figure 4.4A). In the presence of NADA and LPS, treatment with *S*-ibuprofen did not significantly alter levels of IL-6 or IL-8 in comparison to *R*-ibuprofen treatment, indicating that the modulation of cytokine production is due to the oxygenation of NADA and not arachidonic acid (Figure 4.7, D and E). Together, these results support the hypothesis that NADA induces the expression of the novel, bioactive prostaglandin analog, PGD_2-DA.

NADA induces the production of PGD_2-DA, a novel prostaglandin analog that has anti-inflammatory activity in the endothelium

Our results thus far supported the hypothesis that NADA induces the expression of a novel prostaglandin analog that cross-reacts with a PGD_2 EIA kit. To confirm the identity of this prostaglandin analog, we treated lung HMVECs with *R*-ibuprofen for 1 hour, and then with NADA for 20 hours and quantified PGD_2 and PGD_2-DA levels in cell

lysates by mass spectrometry. We found that NADA did not cause any significant changes in the levels of PGD_2 in the presence or absence of LPS (Figure 4.9A). However, we found that NADA did in fact induce the expression of PGD_2-DA in the absence of LPS (Figure 4.9B). While LPS itself did not induce PGD_2-DA, LPS did further augment PGD_2-DA levels in the presence of NADA (Figure 4.9B). *R*-ibuprofen significantly reduced levels of PGD_2-DA without affecting PGD_2 levels, consistent with its ability to inhibit oxygenation of NADA but not arachidonic acid (Figure 4.9, A and B). This is the first evidence of the production of PGD_2-DA by any cell type.

In order to determine if PGD_2-DA is responsible for the effects of NADA on endothelial activation, we incubated lung HMVECs with NADA or PGD_2-DA for 1 hour, and then stimulated cells with LPS for 6 hours. Similarly to NADA, PGD_2-DA dose-dependently reduced the production of IL-8 (Figure 4.9, C and D) and IL-6 (Figure 4.9, E and F). Together with the ability of *R*-profens to inhibit the anti-inflammatory activity of NADA (Figure 4.7, C and D, and Figure 4.8), these results indicate that PGD_2-DA is anti-inflammatory in endothelial cells and is likely part of the mechanism by which NADA modulates endothelial inflammation.

PGD_2-DA modulates inflammation via an unidentified receptor

In order to determine the receptor responsible for the immunomodulatory functions of PGD_2-DA, we submitted PGD_2-DA for massively-parallel physical screening of the entire druggable GPCR-ome (301). PGD_2-DA was tested for its binding affinity at all druggable GPCRs (Table 4.2) PGD_2-DA was found to bind dopamine receptor D_2 and D_3 (DRD2 and DRD3, respectively) (Table 4.2). To determine if either receptor is

required for the immunomodulatory activity of PGD_2-DA in endothelial cells, we incubated lung HMVECs with 0.01-10 μM of a selective DRD2 inhibitor (L-741,626) or DRD3 inhibitor (SB277011A) for 1 hour, followed by treatment with PGD_2-DA and LPS for 6 hours. None of the tested concentrations of DRD2 or DRD3 inhibitors were able to restore IL-8 or IL-6 production in cells treated with PGD_2-DA or LPS (Figure 4.10, A-D). Thus, the precise receptor required for endothelial PGD_2-DA activity remains unknown.

Discussion

We have shown that the endocannabinoid NADA upregulates COX-2 in primary endothelial cells via the cannabinoid receptors CB_1R/CB_2R and TRPV1, and that the anti-inflammatory activity of NADA in the endothelium is partially dependent upon COX activity. In addition to inducing COX-2, NADA uniquely modulates prostanoid production both in endothelial cells and systemically in mice. We have provided the first evidence that NADA induces the production of the novel bioactive prostaglandin analog, PGD_2-DA, which has immunomodulatory activity in the endothelium. Taken together, these data illustrate that NADA can regulate inflammatory outcomes by modulating eicosanoid metabolism. We speculate that the pathway of NADA may serve as a novel therapeutic target for the treatment of inflammatory disorders characterized by endothelial dysregulation, such as sepsis.

While COX-2 is usually associated with pro-inflammatory outcomes, we observe that the upregulation of COX-2 by NADA is required for its anti-inflammatory activity. COX-2 is induced in response to pathogens, host-derived damage-associated pro-inflammatory stimuli, cytokines, and mitogens (270, 302-305). This peak usually occurs

around 2 hours and is associated with maximal PGE_2 synthesis, an influx of polymorphonuclear leukocytes, and vasodilation (270, 302, 306-308). However, increasing evidence supports the idea that COX-2 may also possess anti-inflammatory activity over time. Approximately 48 hours after an inflammatory stimulus, there is a second, more dramatic peak in COX-2 levels (262, 306-311). This second peak in COX-2 is instead associated with minimal PGE_2 production, enhanced PGD_2 levels, and mononuclear leukocyte influx, suggesting that COX-2 is also involved in the resolution of inflammation (306, 309, 310). The dual nature of COX-2 in inflammation is also made evident by the fact that treatment with COX-2 inhibitors reduces inflammation at 2 hours, but exacerbates inflammation at 48 hours (306). Our results are consistent with this role for COX-2 in inflammatory resolution. Treatment with NADA induces a late peak (~20 hours) in COX-2 expression, and inhibition of COX activity restores LPS-induced IL-6 and IL-8 levels in NADA-treated samples. Accordingly, PGE_2 production is also minimized at this later time point. While further studies are needed to understand the precise role of COX-2 in regulating inflammation, our work supports COX-2 activity as a central mechanism by which NADA resolves endothelial inflammation.

We report that the upregulation of COX-2 protein by NADA is dependent upon the cannabinoid receptors CB_1R/CB_2R and the cation channel TRPV1. Treatment of lung HMVECs with CB_1R and CB_2R inhibitors caused a decrease in NADA-induced COX-2 protein, while treatment with a TRPV1 inhibitor augmented COX-2 levels. Consistent with these results, COX-2 mRNA transcript levels and protein levels were augmented in primary murine endothelial cells from *Trpv1*$^{-/-}$ mice, and reduced in cells isolated from *Cnr2*$^{-/-}$ mice. Though a genetic model of CB_1R disruption was unavailable,

these results support the fact that NADA modulates COX-2 expression via activity at the cannabinoid receptors and TRPV1, and are consistent with our earlier studies that show NADA modulates primary human endothelial cell activation via these receptors (209). Our previous results indicate that NADA promotes inflammatory cascades via activation of endothelial TRPV1, and instead promotes inflammatory resolution via the cannabinoid receptors (209). Our results indicating that COX-2 expression is promoted by the cannabinoid receptors and inhibited by TRPV1 provide further evidence that COX-2 activity in the endothelium is critical for the effects of NADA on immune regulation. Importantly, Navarrete *et al.* also reported that COX-2 protein was upregulated after a 20 hour NADA treatment in the murine brain endothelial cell line b.end5 (77). However, this upregulation was found to be independent of both CB_1R and TRPV1 (77). These seemingly contradictory results may provide key insights into NADA signaling in the endothelium. Conceivably, primary and immortalized endothelial cells, or endothelial cells derived from different tissues, express unique receptor isoforms that result in distinct signaling pathways. Alternatively, these cell types could have distinct levels of other accessory proteins or factors that could differentially sensitize receptors to NADA. Nevertheless, a deeper understanding of the characteristics of endothelial cells, as well as the precise downstream signaling mechanism of COX-2 upregulation by NADA will elucidate the vital functions of the endocannabinoid system in the endothelium.

In addition to inducing COX-2 expression, we demonstrate that NADA differentially regulates downstream prostanoid production compared to the endocannabinoids AEA and 2-AG. In direct contrast to AEA and 2-AG, and consistent

with its anti-inflammatory functions in the endothelium, NADA reduced the upregulation of PGE_2, PGI_2, and TXB_2 by LPS. PGE_2 is largely considered to be a pro-inflammatory prostanoid, as it promotes platelet aggregation, vascular permeability, and vasodilation (146, 147, 264, 288, 312, 313). TXA_2 similarly promotes platelet activation and aggregation, and also induces vasoconstriction (147, 264, 312). PGI_2 is the putative natural antagonist of TXA_2 and is thought to function alongside TXA_2 to maintain homeostatic balance (147, 264, 312, 314). PGI_2 inhibits platelet aggregation, angiogenesis, and pro-inflammatory cytokine production, and promotes vasodilation (147, 264, 312, 314). All three of these prostanoids are upregulated during sepsis, during which inflammatory pathways are globally activated (315-318). Our observations that NADA reduces levels of PGE_2, PGI_2, and TXB_2 while AEA and 2-AG increase their levels, further supports the role of NADA-induced COX-2 as a pro-resolving mediator during endothelial inflammation.

In addition to downregulating these prostanoids, we find that NADA induces PGD_2 production both in the absence and presence of LPS. PGD_2, which is mostly produced by mast cells, has been shown to inhibit platelet aggregation, promote vascular barrier function, and reduce pro-inflammatory cytokine production by endothelial cells (147, 264, 312, 319-321). While the upregulation of PGD_2 by NADA is consistent with previous reports, we were unable to validate these results by mass spectrometry (77). Instead, we have shown that NADA does not affect PGD_2 levels, but rather induces the production of PGD_2-DA, a novel, bioactive prostanoid. PGD_2-DA is able to replicate the effects of NADA on endothelial pro-inflammatory cytokine production, and inhibition of its generation by *R*-profen inhibitors prevents the anti-

inflammatory activity of NADA. This is the first report to our knowledge that suggests that NADA may be metabolized by COX-2 directly, and that in addition to prostaglandin glycerol esters and prostamides, there are also prostaglandin dopamine analogs. While we were unable to determine the precise receptor responsible for PGD_2-DA activity, we found that PGD_2-DA does not bind to any known druggable GPCR. Furthermore, PGD_2-DA does not function through the dopamine receptors, D_2 or D_3. This result indicates that PGD_2-DA activity is not due to its breakdown into PGD_2 and dopamine, and it is consistent with our previous findings that dopamine does not possess immunomodulatory activity in the endothelium (209). It is possible that, similar to prostamides, the wild-type PGD_2 receptor may heterodimerize with an alternative splice variant to generate a PGD_2-DA-specific binding site (292-294).

Our results provide critical insight into the ability of the endocannabinoid system to broadly regulate endothelial and systemic eicosanoid metabolism. While prostanoids are known to be upregulated during sepsis, the precise functions of endogenous NADA and PGD_2-DA in sepsis and other inflammatory disorders remain unknown. Further studies will be needed to determine the levels of NADA in different tissues at baseline, as well as during inflammation, to better understand its endogenous role in regulating immune responses. Furthermore, it remains unknown if PGD_2-DA is produced endogenously, or if it has the ability to regulate systemic inflammation as well. By understanding the functions of these anti-inflammatory lipids endogenously and their precise signaling mechanisms in different cell types, these pathways could be targeted and manipulated for the treatment of diseases characterized by excessive inflammation or endothelial dysfunction.

In conclusion, we have found that NADA regulates eicosanoid metabolism in primary endothelial cells via CB_1R/CB_2R and TRPV1 to modulate inflammatory responses. In addition, NADA induces the generation of the novel prostaglandin analog, PGD_2-DA, which is able to regulate inflammatory cytokine production by endothelial cells. These results suggest that the endocannabinoid NADA is able to modulate endothelial inflammatory outcomes by modifying the eicosanoid network. Further studies will be needed to delineate the mechanism of PGD_2-DA production and signaling, and to determine the effects of NADA's lipid regulation on outcomes in sepsis. Nonetheless, our observations have important implications for acute inflammatory disorders, and suggest that the NADA signaling pathway may represents an innovative, therapeutic target for the treatment of inflammatory disorders.

Figure 4.1

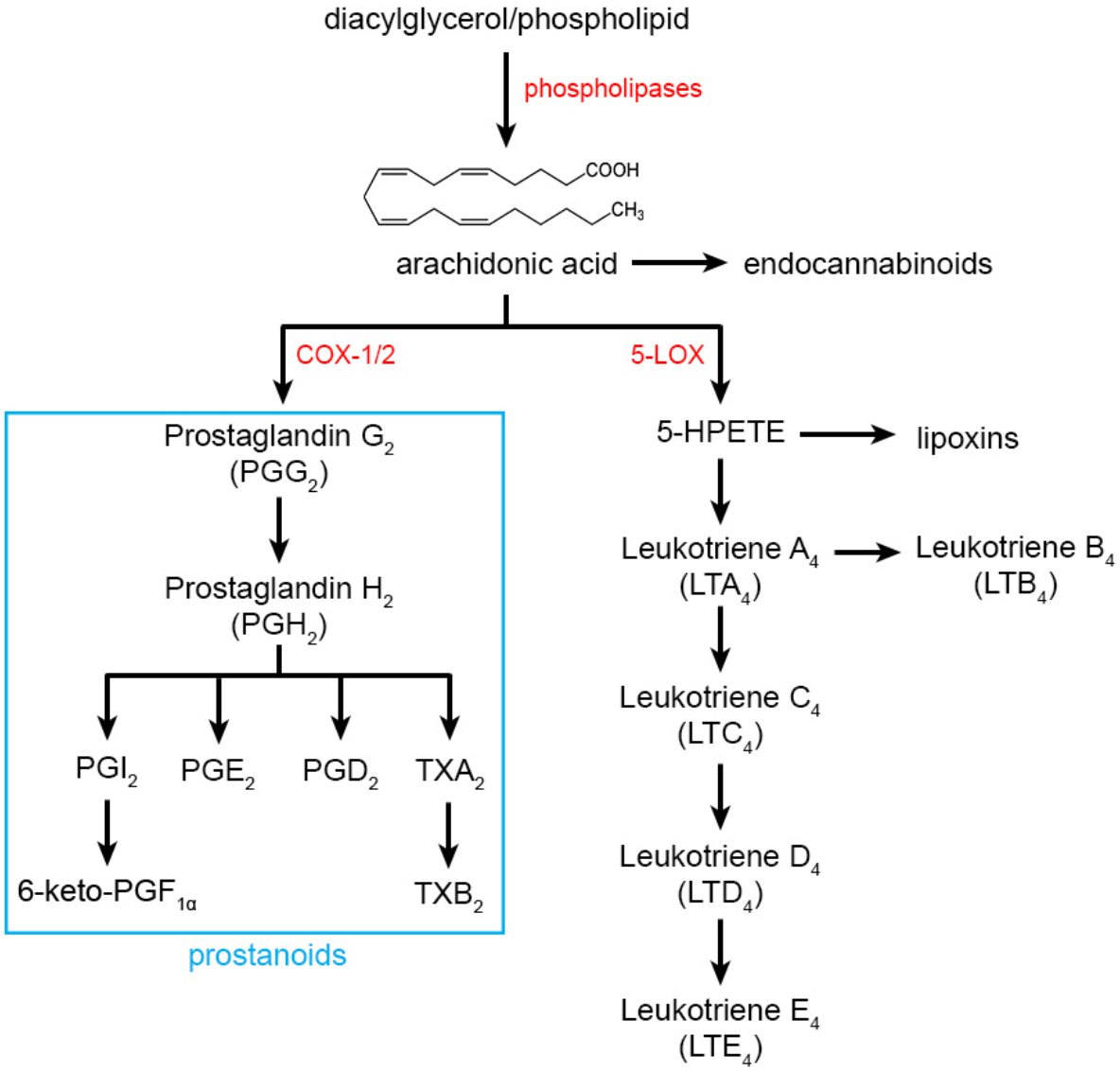
diacylglycerol/phospholipid
phospholipases
COOH
CH3
arachidonic acid
endocannabinoids
COX-1/2
5-LOX
Prostaglandin G2 (PGG2)
Prostaglandin H2 (PGH2)
PGI2
PGE2
PGD2
TXA2
6-keto-PGF1α
TXB2
prostanoids
5-HPETE
lipoxins
Leukotriene A4 (LTA4)
Leukotriene B4 (LTB4)
Leukotriene C4 (LTC4)
Leukotriene D4 (LTD4)
Leukotriene E4 (LTE4)

Figure 4.1. Overview of eicosanoid metabolism.

Arachidonic acid serves as the precursor to eicosanoid biosynthesis. Arachidonic acid can be converted to endocannabinoids, as well as hydroxyeicosatetraenoic acids (HETEs; not pictured). Alternatively, arachidonic acid can serve as a substrate for 5-lipoxygenase (5-LOX, ALOX-5) to generate leukotrienes and lipoxins, or as a substrate for cyclooxygenase-1 and -2 (COX-1/2) to generate prostanoids. Prostanoids include prostacyclin (PGI_2), prostaglandin E_2 (PGE_2), prostaglandin D_2 (PGD_2), and thromboxane A_2 (TXA_2). PGI_2 and TXA_2 are rapidly broken down into 6-keto-prostaglandin $F_{1\alpha}$ (6-keto-$PGF_{1\alpha}$) and thromboxane B_2 (TXB_2), respectively. Enzymes are colored red.

Figure 4.2

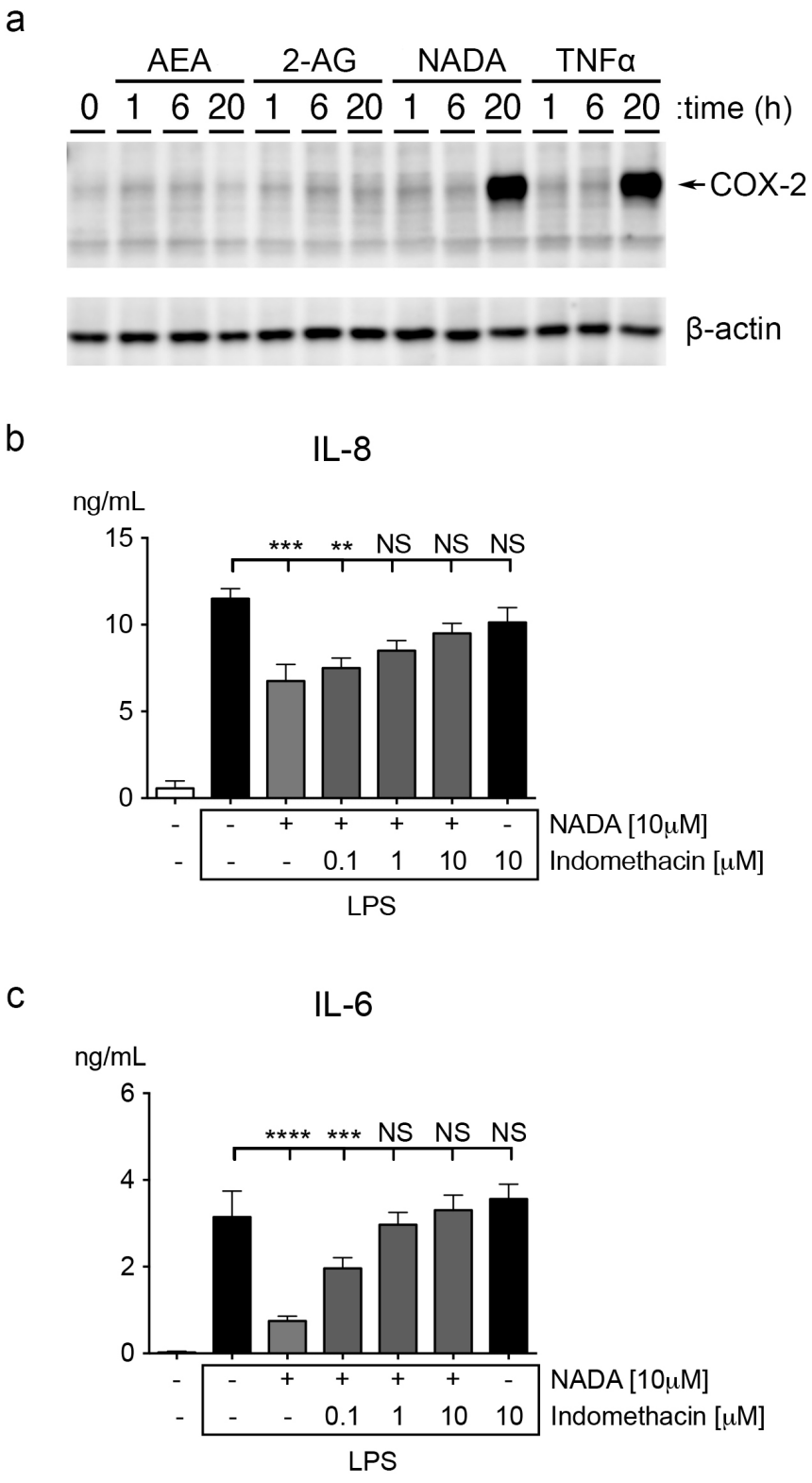
a
AEA
2-AG
NADA
TNFα
0 1 6 20 1 6 20 1 6 20 1 6 20 :time (h)
COX-2
β-actin
b
IL-8
ng/mL
15
10
5
0
*** ** NS NS NS
NADA [10μM]
Indomethacin [μM]
LPS
c
IL-6
ng/mL
6
4
2
0
**** *** NS NS NS
NADA [10μM]
Indomethacin [μM]
LPS

Figure 4.2. NADA induces the upregulation of COX-2, and the immunomodulatory activity of NADA in endothelial cells is dependent upon COX activity.

(A) NADA, but not the endocannabinoid AEA or 2-AG, upregulates COX-2 expression after 20 hours. We stimulated lung HMVECs with AEA, 2-AG, NADA, or TNFα for the indicated amount of time and assessed COX-2 protein levels by immunoblot (arrows indicate protein band). β-actin served as a loading control (bottom panel).

(B and C) The endothelial anti-inflammatory activity of NADA is dependent upon COX activity. Lung HMVECs were pretreated for 1 hour with the indicated dose of the COX inhibitor indomethacin, and then treated with NADA and LPS for an additional 20 hours while in the continuous presence of the inhibitor (n=4). Levels of IL-8 (B) and IL-6 (C) were quantified in supernatants. ANOVA: NS, not significant; **, $p < 0.01$; ***, $p < 0.001$, ****, $p < 0.0001$ when comparing samples to LPS only treatment.

Figure 4.3

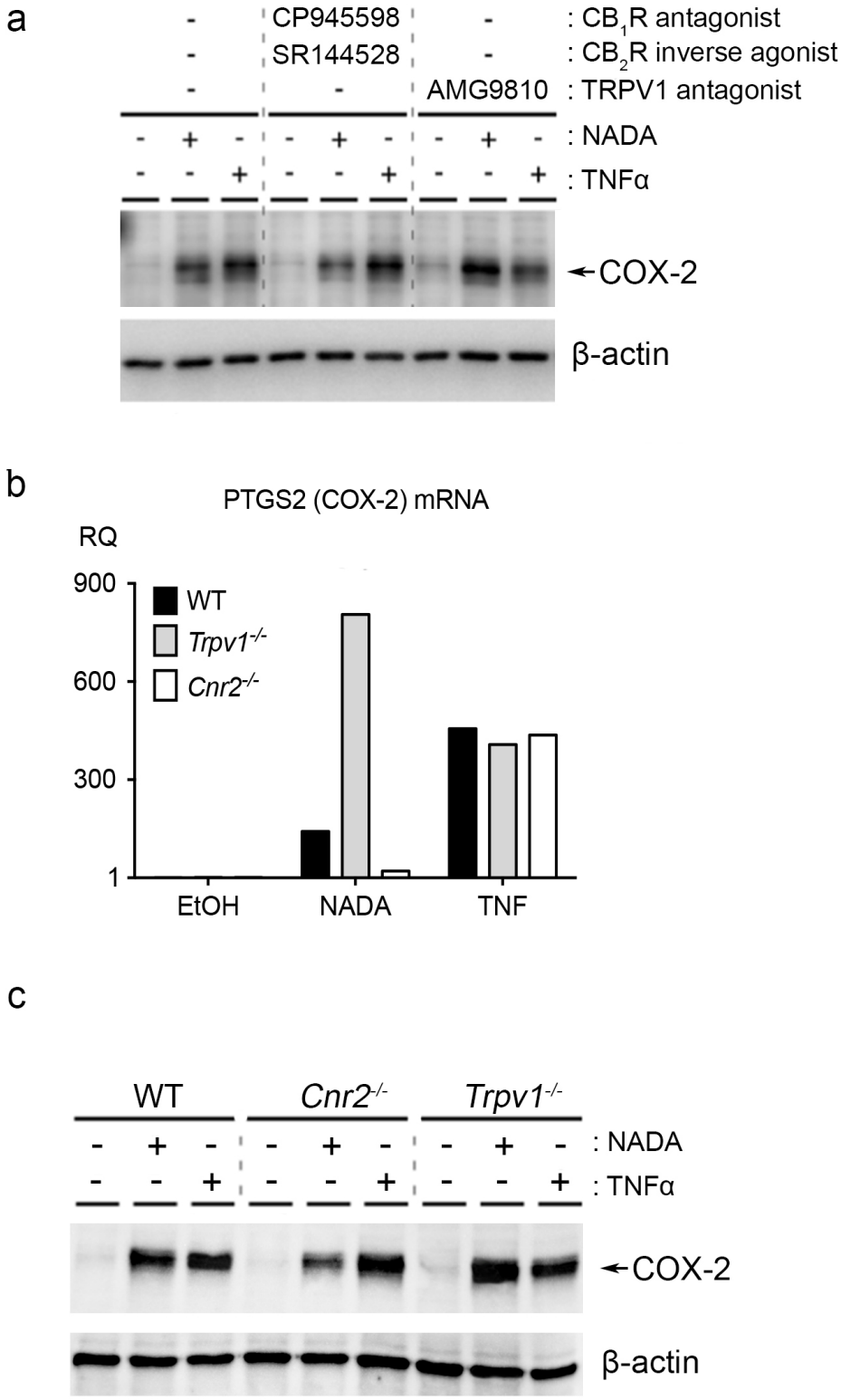
a
- CP945598 - : CB1R antagonist
- SR144528 - : CB2R inverse agonist
- - AMG9810 : TRPV1 antagonist
: NADA
: TNFα
←COX-2
β-actin
b
PTGS2 (COX-2) mRNA
RQ
900
600
300
1
WT
Trpv1-/-
Cnr2-/-
EtOH
NADA
TNF
c
WT
Cnr2-/-
Trpv1-/-
: NADA
: TNFα
←COX-2
β-actin

Figure 4.3. The upregulation of COX-2 by NADA is dependent upon CB_1R/CB_2R and TRPV1

(A) Lung HMVECs were treated with CB_1R and CB_2R inhibitors (CP945598 and SR144528) or the TRPV1 inhibitor AMG9810 for 1 hour, and then with NADA or TNFα for 20 hours. COX-2 protein levels were assessed by immunoblot (arrows indicate protein band), and β-actin served as a loading control (bottom panel).

(B) WT, *Trpv1*$^{-/-}$, or *Cnr2*$^{-/-}$ primary murine endothelial cells were grown to confluency and treated with ethanol (vehicle), NADA, or TNFα for 4 hours. Cells were then lysed with Trizol. The mean C_t value for GAPDH was used as the reference in calculating the ΔC_t values for each biological replicate, as described in the materials and methods. 10 ng of cDNA was analyzed for each sample. Relative quantification (RQ) values were calculated relative to the lowest detectable expressing gene. Data shown represents relative fold change in comparison to endothelial cells treated with ethanol alone.

(C) WT, *Trpv1*$^{-/-}$, or *Cnr2*$^{-/-}$ primary murine endothelial cells were stimulated for 20 hours with NADA or TNFα. COX-2 protein levels were assessed by immunoblot (arrows indicate protein band), and β-actin served as a loading control (bottom panel).

Figure 4.4

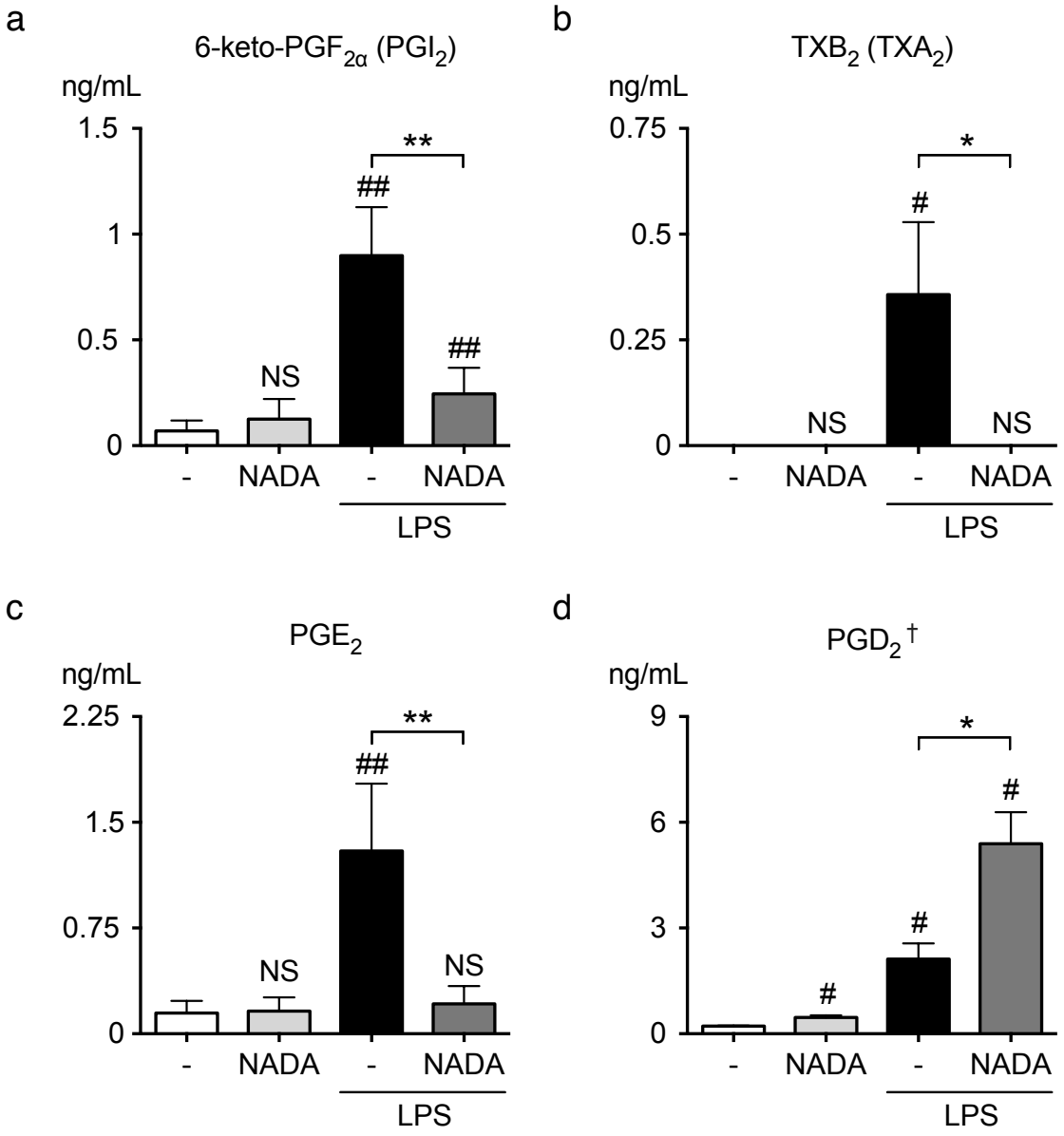
a
6-keto-PGF2α (PGI2)
ng/mL
1.5
1
0.5
0
**
##
##
NS
-
NADA
-
NADA
LPS
b
TXB2 (TXA2)
ng/mL
0.75
0.5
0.25
0
*
#
NS
NS
-
NADA
-
NADA
LPS
c
PGE2
ng/mL
2.25
1.5
0.75
0
**
##
NS
NS
-
NADA
-
NADA
LPS
d
PGD2 †
ng/mL
9
6
3
0
*
#
#
#
-
NADA
-
NADA
LPS

Figure 4.4. NADA inhibits LPS-induced PGI_2, TXA_2, and PGE_2 production, but induces PGD_2 in endothelial cells.

Lung HMVECs were treated with NADA for 1 hour, and then incubated with LPS for 20 hours while in the continuous presence of NADA. 6-keto-$PGF_{1\alpha}$ (A), TXB_2 (B), and PGE_2 (C) levels were quantified in culture supernatants. Cells were lysed in potassium phosphate buffer, and PGD_2 [†] levels were quantified in cleared cell lysates (D). NS, not significant; [#], $p < 0.05$; [##], $p < 0.01$ when comparing samples to vehicle only treatment. *, $p < 0.05$; **, $p < 0.01$ when comparing LPS-treated samples with versus without NADA.

[†], PGD_2 EIA kit has cross-reactivity with PGD_2-DA

Figure 4.5

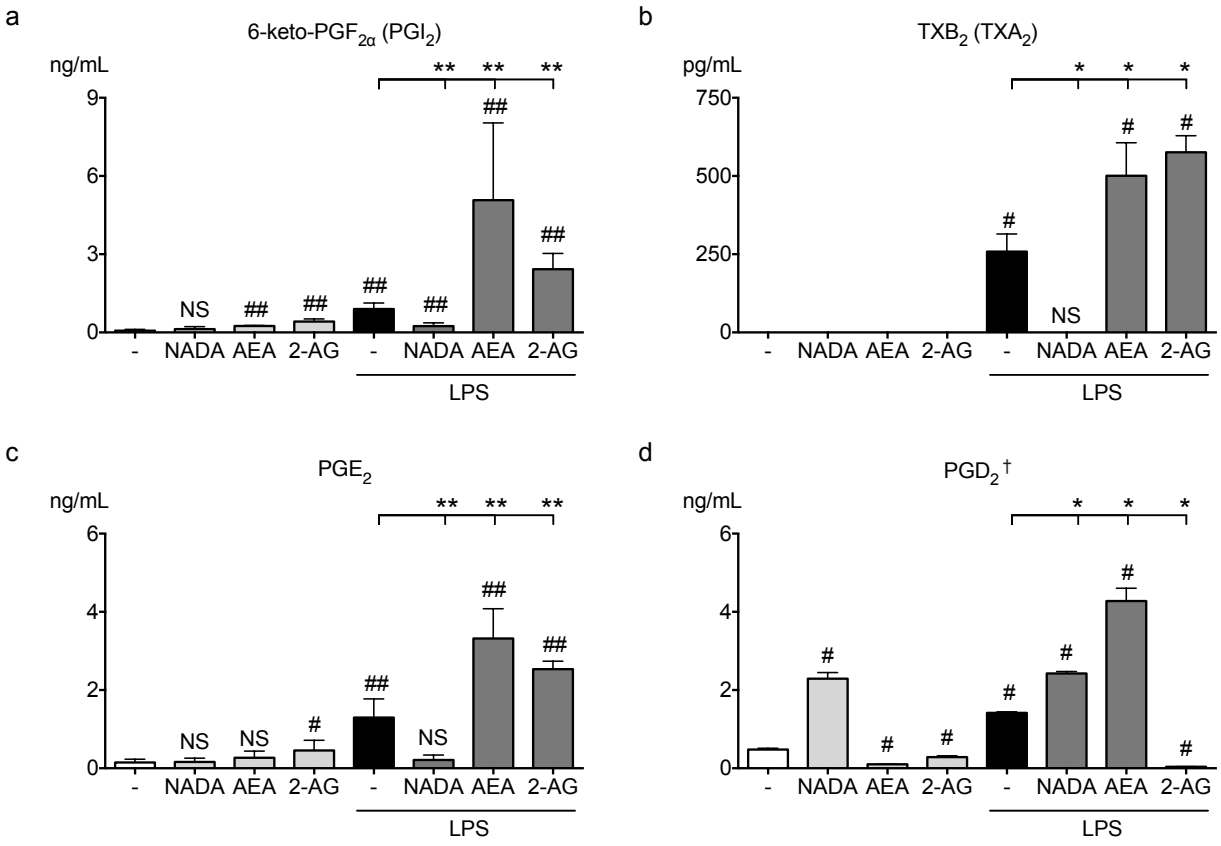
a
6-keto-PGF2α (PGI2)
ng/mL
9
6
3
0
** ** **
##
NS
- NADA AEA 2-AG - NADA AEA 2-AG
LPS
b
TXB2 (TXA2)
pg/mL
750
500
250
0
* * *
# # # #
NS
- NADA AEA 2-AG - NADA AEA 2-AG
LPS
c
PGE2
ng/mL
6
4
2
0
** ** **
##
NS NS NS
- NADA AEA 2-AG - NADA AEA 2-AG
LPS
d
PGD2 †
ng/mL
6
4
2
0
* * *
# # # # # # #
- NADA AEA 2-AG - NADA AEA 2-AG
LPS

Figure 4.5. Endocannabinoids have differential effects on endothelial prostanoid metabolism.

Lung HMVECs were treated with the indicated endocannabinoid for 1 hour, and then incubated with LPS for 20 hours while in the continuous presence of the endocannabinoid. $PGF_{1\alpha}$ (A), TXB_2 (B), and PGE_2 (C) levels were quantified in culture supernatants. Cells were lysed in potassium phosphate buffer and PGD_2 [†] levels were quantified in cleared cell lysates (D). NS, not significant; [#], $p < 0.05$; [##], $p < 0.01$ when comparing samples to vehicle only treatment. *, $p < 0.05$; **, $p < 0.01$ when comparing LPS-treated samples with versus without the indicated endocannabinoid.

[†], PGD_2 EIA kit has cross-reactivity with PGD_2-DA

Figure 4.6

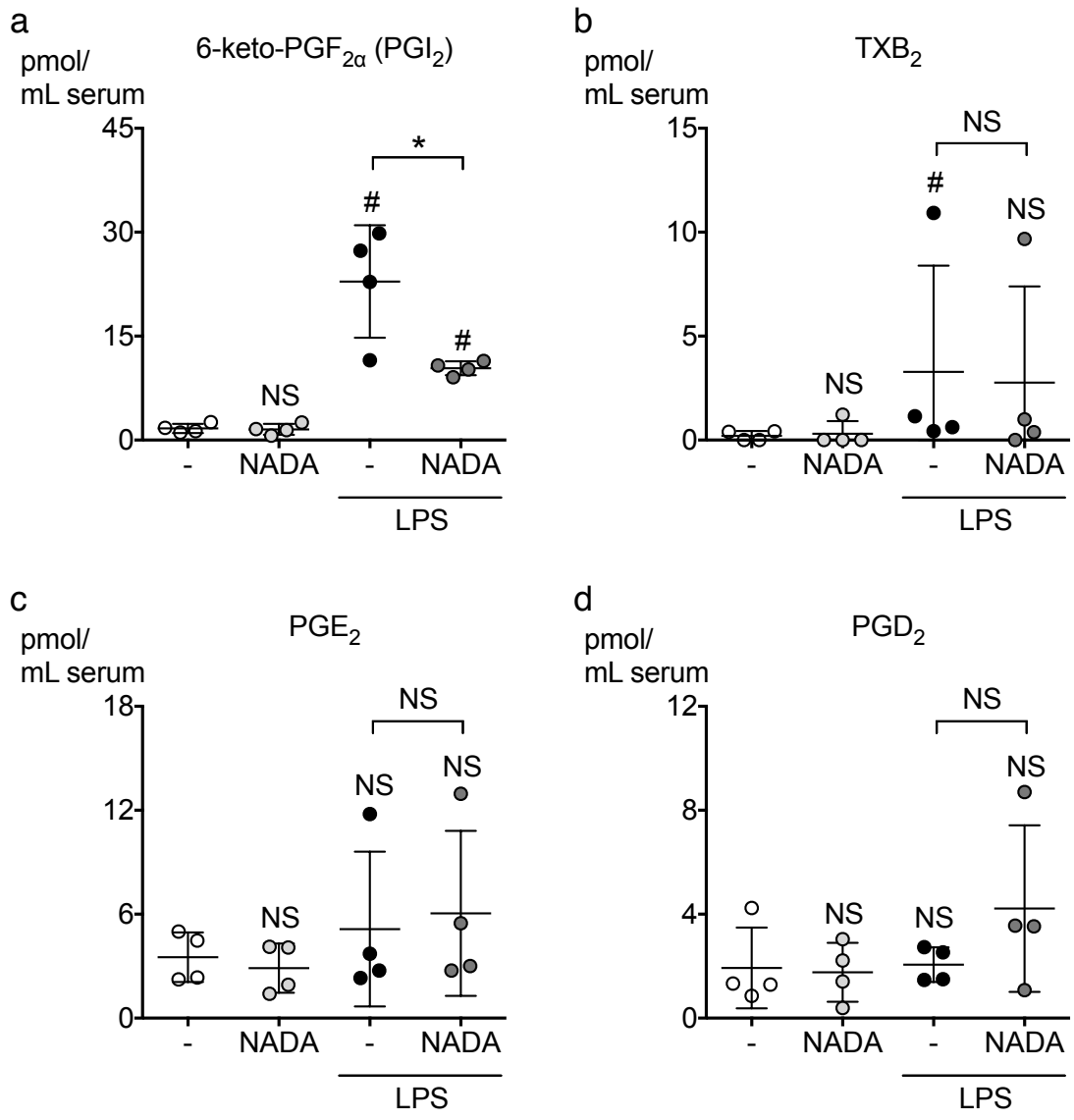
a
6-keto-PGF2α (PGI2)
pmol/
mL serum
45
30
15
0
*
#
#
NS
-
NADA
-
NADA
LPS
b
TXB2
pmol/
mL serum
15
10
5
0
NS
#
NS
NS
-
NADA
-
NADA
LPS
c
PGE2
pmol/
mL serum
18
12
6
0
NS
NS
NS
NS
-
NADA
-
NADA
LPS
d
PGD2
pmol/
mL serum
12
8
4
0
NS
NS
NS
NS
-
NADA
-
NADA
LPS

Figure 4.6. NADA reduces systemic levels of LPS-induced PGI_2, but does not affect TXA_2, PGE_2 or PGD_2 levels

Mice were injected intravenously (i.v.) with LPS, immediately followed by NADA. Serum levels of 6-keto-$PGF_{1\alpha}$ (A), TXB_2 (B), PGE_2 (C), and PGD_2 (D) levels were quantified by mass spectrometry after 2 hours. NS, not significant; $^{\#}$, $p < 0.05$ when comparing samples to vehicle only treatment. *, $p < 0.05$ when comparing LPS-treated samples with versus without NADA.

Figure 4.7

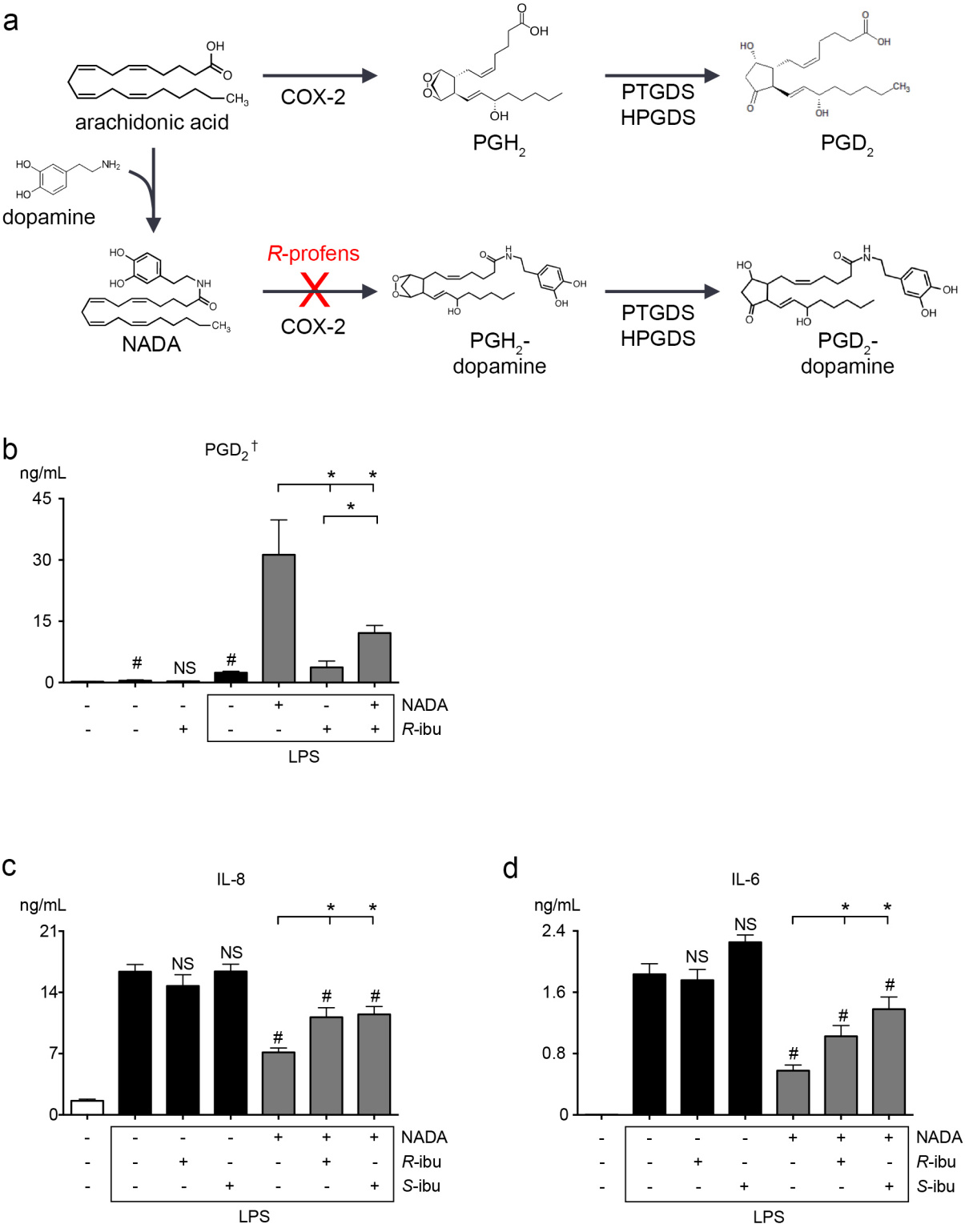
a
arachidonic acid
COX-2
PGH2
PTGDS
HPGDS
PGD2
dopamine
NADA
R-profens
COX-2
PGH2-
dopamine
PTGDS
HPGDS
PGD2-
dopamine
b
PGD2 †
ng/mL
45
30
15
0
NS
NADA
R-ibu
LPS
c
IL-8
ng/mL
21
14
7
0
NS
NS
NADA
R-ibu
S-ibu
LPS
d
IL-6
ng/mL
2.4
1.6
0.8
0
NS
NS
NADA
R-ibu
S-ibu
LPS

Figure 4.7. *R*-ibuprofen partially inhibits the effects of NADA on cytokine secretion and PGD_2 production.

(A) Schematic of the hypothesized metabolism of NADA into PGD_2-dopamine (PGD_2-DA). Normally, arachidonic acid is oxygenated by COX-2 into prostaglandin H_2 (PGH_2), which is converted into prostaglandin D_2 (PGD_2) by prostaglandin D_2 synthase (PGDS) or hematopoietic prostaglandin D_2 synthase (HPGDS). We hypothesize that, similar to other endocannabinoids, NADA itself can be oxygenated by COX-2 into prostaglandin H_2-dopamine (PGH_2-dopamine), which is converted by PGDS or HPGDS into PGD_2-DA. The oxygenation step of NADA by COX-2 can be inhibited by *R*-profens. In contrast, the oxygenation of both arachidonic acid and NADA by COX-2 is inhibited by *S*-profens.

(B-D) Lung HMVECs were pretreated for 1 hour with *R*- or *S*- ibuprofen, and then treated with NADA and/or LPS for an additional 20 hours while in the continuous presence of the inhibitor (n=4). $PGD_2^{\dagger}$ levels were quantified in cell lysates (B). Levels of IL-8 (B) and IL-6 (C) were quantified in supernatants. NS, not significant; $^{\#}$, $p < 0.05$ when comparing samples to LPS only treatment. *, $p < 0.05$ when comparing LPS and NADA-treated samples with versus without inhibitor.

†, PGD_2 EIA kit has cross-reactivity with PGD_2-DA

Figure 4.8

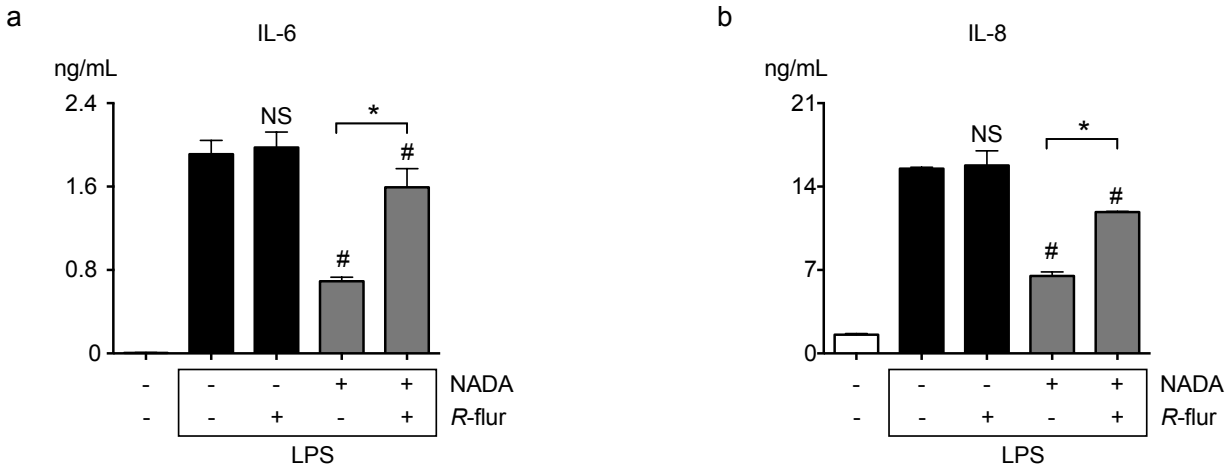
a
IL-6
ng/mL
2.4
1.6
0.8
0
NS
*
#
#
- - - + + NADA
- - + - + R-flur
LPS
b
IL-8
ng/mL
21
14
7
0
NS
*
#
#
- - - + + NADA
- - + - + R-flur
LPS

Figure 4.8. *R*-flurbiprofen partially inhibits the effects of NADA on cytokine secretion

Lung HMVECs were pretreated for 1 hour with NADA and/or *R*-flurbiprofen, and then treated with LPS for an additional 20 hours while in the continuous presence of NADA and the inhibitor (n=4). Levels of IL-8 (A) and IL-6 (B) were quantified in supernatants. NS, not significant; #, $p < 0.05$ when comparing samples to LPS only treatment. *, $p < 0.05$ when comparing LPS and NADA-treated samples with versus without *R*-flurbiprofen.

†, PGD_2 EIA kit has cross-reactivity with PGD_2-DA

Figure 4.9

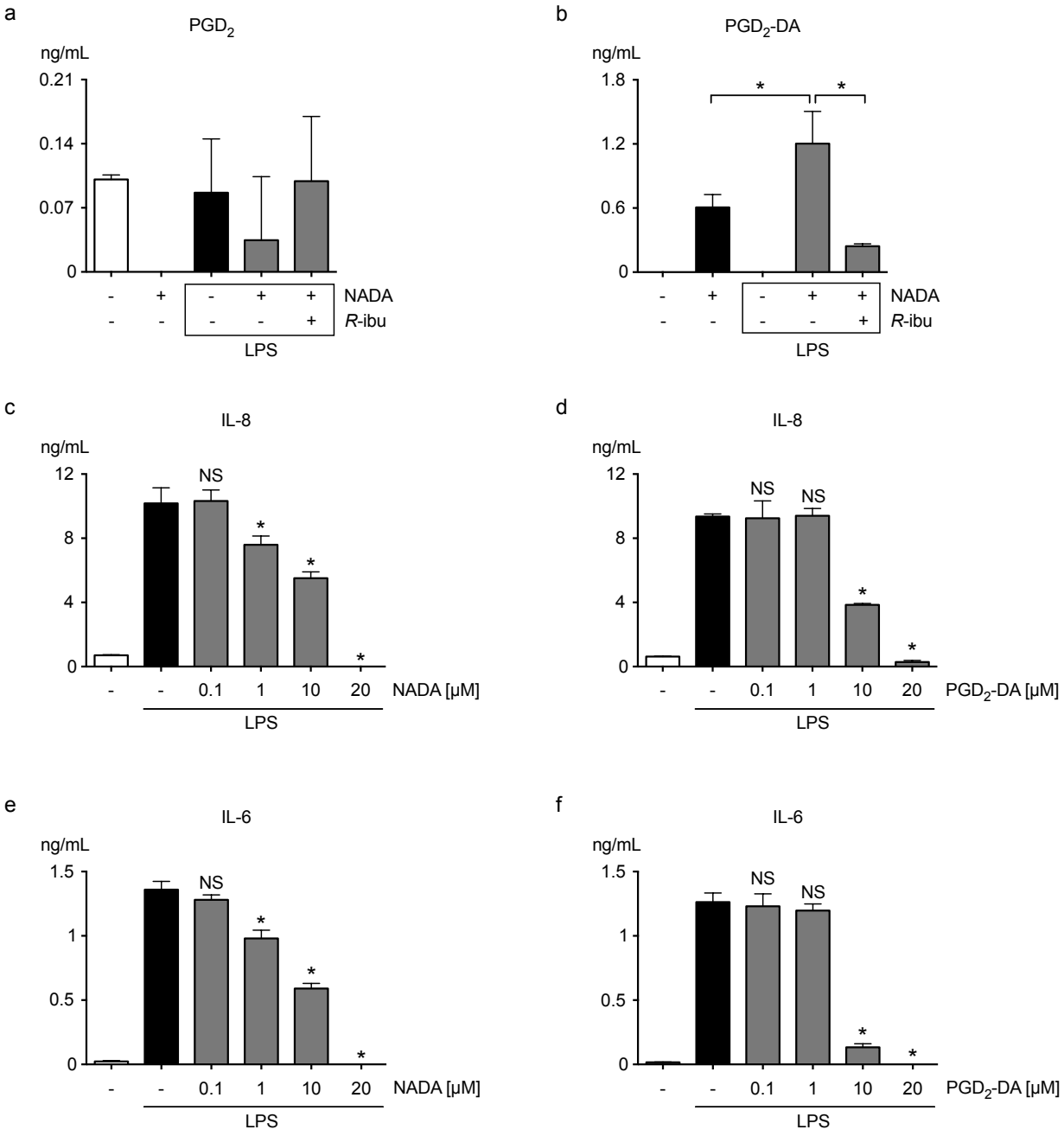
a
PGD2
ng/mL
0.21
0.14
0.07
0
- + - + + NADA
- - - - + R-ibu
LPS
b
PGD2-DA
ng/mL
1.8
1.2
0.6
0
* *
- + - + + NADA
- - - - + R-ibu
LPS
c
IL-8
ng/mL
12
8
4
0
NS
* * *
- - 0.1 1 10 20 NADA [μM]
LPS
d
IL-8
ng/mL
12
8
4
0
NS NS
* *
- - 0.1 1 10 20 PGD2-DA [μM]
LPS
e
IL-6
ng/mL
1.5
1
0.5
0
NS
* * *
- - 0.1 1 10 20 NADA [μM]
LPS
f
IL-6
ng/mL
1.5
1
0.5
0
NS NS
* *
- - 0.1 1 10 20 PGD2-DA [μM]
LPS

Figure 4.9. NADA induces PGD_2-DA production, which has anti-inflammatory activity in endothelial cells.

(A and B) Lung HMVECs were treated with NADA for 1 hour, and then incubated with LPS for 20 hours while in the continuous presence of NADA. Cells were lysed in potassium phosphate buffer, and PGD_2 (A) and PGD_2-DA (B) levels were quantified in cleared cell lysates by LC-MS/MS. *, $p < 0.05$ when comparing NADA-treated samples in the presence or absence of LPS or *R*-ibuprofen.

(C-F) Lung HMVECs were treated with NADA or PGD_2-DA for 1 hour, and then incubated with LPS for 6 hours while in the continuous presence of NADA or PGD_2-DA. IL-8 (C and D) and IL-6 (E and F) levels were quantified in supernatants. NS, not significant. *, $p < 0.05$ when comparing LPS-treated samples in the presence or absence of NADA or PGD_2-DA.

Figure 4.10

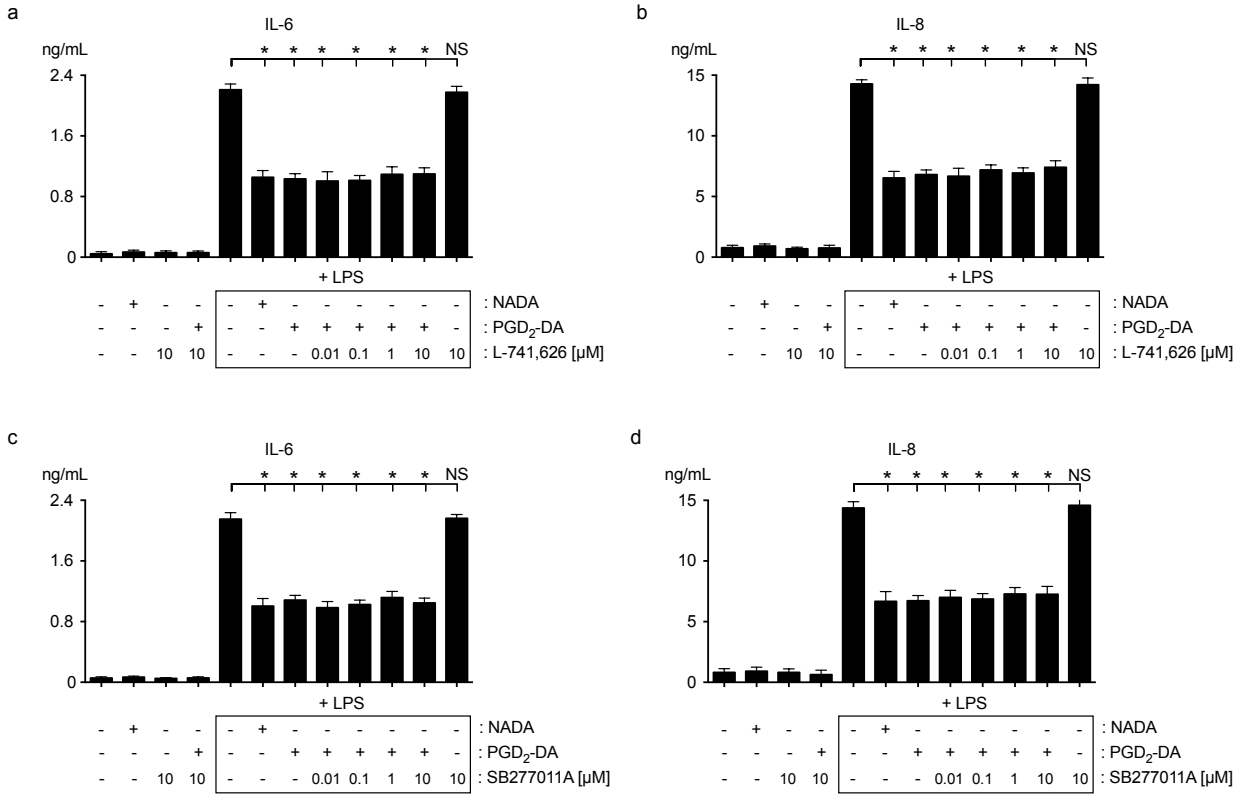
a
IL-6
ng/mL
2.4
1.6
0.8
0
* * * * * * NS
+ LPS
- + - - - + - - - - - - : NADA
- - - + - - + + + + + - : PGD2-DA
- - 10 10 - - - 0.01 0.1 1 10 10 : L-741,626 [μM]
b
IL-8
ng/mL
15
10
5
0
* * * * * * NS
+ LPS
- + - - - + - - - - - - : NADA
- - - + - - + + + + + - : PGD2-DA
- - 10 10 - - - 0.01 0.1 1 10 10 : L-741,626 [μM]
c
IL-6
ng/mL
2.4
1.6
0.8
0
* * * * * * NS
+ LPS
- + - - - + - - - - - - : NADA
- - - + - - + + + + + - : PGD2-DA
- - 10 10 - - - 0.01 0.1 1 10 10 : SB277011A [μM]
d
IL-8
ng/mL
15
10
5
0
* * * * * * NS
+ LPS
- + - - - + - - - - - - : NADA
- - - + - - + + + + + - : PGD2-DA
- - 10 10 - - - 0.01 0.1 1 10 10 : SB277011A [μM]

Figure 4.10. The immunomodulatory activity of PGD_2-DA in endothelial cells is independent of dopamine receptors D_2 and D_3

Lung HMVECs were treated with the DRD2 inhibitor L-741,626 (A and B) or the DRD3 inhibitor SB277011A (C and D) at the indicated concentrations for 1 hour, and then incubated with LPS and PGD_2-DA for 20 hours while in the continuous presence of the inhibitor. IL-6 (A and C) and IL-8 (B and D) levels were quantified in supernatants. NS, not significant. *, $p < 0.05$, when comparing LPS-treated samples in the presence or absence of the indicated inhibitor.

Table 4.1. The effects of endocannabinoids on arachidonic acid metabolic enzymes in endothelial cells

		-			LPS				TNF			
Enzyme	Gene	AEA	2AG	NADA	EtOH	AEA	2AG	NADA	EtOH	AEA	2AG	NADA
phospholipase A2, group 5	PLA2G5	-1.2	-1.3	-1.1	1.5	-1.1	-1.2	1.1	1.2	1.3	1.1	1.2
prostaglandin G/H synthase 1	PTGS1	-1.8	1.4	-1.1	-1.0	-2.1	-1.7	-1.1	-1.1	-1.7	-2.0	-2.2
prostaglandin G/H synthase 2	PTGS2	1.1	-1.2	15.8	3.3	2.0	2.0	14.6	3.2	4.0	3.6	13.1
prostacyclin synthase	PTGIS	-1.8	-1.2	-1.1	1.0	-2.1	-1.5	-1.2	-1.2	-2.0	-2.1	-1.2
prostaglandin D synthase	PTGDS	nd	-1.7	-1.1	1.2	-2.4	-1.9	-1.4	-1.3	-2.4	-1.6	-1.3
hematopoietic prostaglandin D synthase	HPGDS	-1.4	-2.8	-1.3	-1.0	-1.4	-1.7	-1.2	-1.5	-2.0	-2.5	-3.0
thromboxane A synthase 1	TBXAS1	-2.0	-2.9	1.1	-1.1	-1.9	-1.8	-1.0	-1.8	-2.0	-1.6	1.1
prostaglandin E synthase	PTGES	1.1	-2.1	-1.2	1.6	1.5	-1.2	2.0	23.8	24.4	42.5	18.3
prostaglandin E synthase 2	PTGES2	-2.0	-2.4	-1.7	-1.6	-3.5	-1.9	-1.7	-1.6	-1.9	-1.8	-3.3
prostaglandin E synthase 3	PTGES3	-1.9	-1.9	1.0	1.0	-1.9	-2.0	-1.0	-2.0	-1.9	-1.7	1.0
prostaglandin F(2-alpha) synthase	AKR1C3	-1.4	-1.1	-1.1	-1.0	-1.8	-1.4	-2.0	-2.0	-1.9	-1.8	-2.3
15-hydroxy prostaglandin dehydrogenase	HPGD	1.0	nd	-1.2	nd	-2.3	-2.5	nd	nd	-1.8	-1.9	-1.1
prostaglandin reductase 1	PTGR1	-2.0	-2.4	2.0	-1.1	-1.8	-1.9	-1.0	-1.9	-2.0	-1.9	1.0
prostaglandin reductase 2	PTGR2	-1.4	-1.0	1.1	1.0	-1.3	-1.8	-1.2	-1.2	-1.9	-1.8	-2.0
arachidonate 5-lipoxygenase	ALOX5	-1.7	-1.8	-2.0	-1.3	-2.6	-2.8	-1.2	-1.2	-2.0	-1.6	-1.5
5-lipoxygenase activating protein	ALOX5AP	-2.4	-2.1	-1.9	-1.6	-2.4	-2.0	-2.3	-1.6	-3.2	-3.1	-3.3
arachidonate 15-lipoxygenase	ALOX15	nd	nd	nd	nd	nd	nd	nd	nd	nd	nd	nd
arachidonate 15-lipoxygenase type II	ALOX15B	-1.9	nd	nd	nd	-3.4	nd	nd	-1.1	-3.0	-3.3	-2.1
leukotriene C4 synthase	LTC4S	-1.2	-1.7	-1.1	-1.1	-2.4	-1.5	-1.2	-1.2	-1.9	-2.1	-2.3
leukotriene A4 hydrolase	LTA4H	-1.6	-3.9	1.0	-1.0	-2.0	-1.9	-2.1	-2.0	-1.9	-1.9	-2.0
arachidonate 12-lipoxygenase	ALOX12	-1.0	-2.4	1.4	-1.2	-1.2	-2.2	1.1	-1.2	-1.2	-1.5	-1.2
epidermis-type lipoxygenase 3	ALOXE3	1.2	-3.3	1.6	-1.1	-2.0	-2.2	1.3	-1.4	-2.6	-1.4	1.6
leukotriene B4 omega hydroxylase	LTB4H	1.2	-1.7	-1.1	1.2	-1.9	-2.1	-2.1	-1.3	1.2	1.5	1.7
cytochrome P450, 2C8	CYP2C8	1.6	1.0	1.6	1.0	1.0	1.1	1.1	1.5	1.1	1.1	-1.0
cytochrome P450, 2J2	CYP2J2	1.1	1.1	1.6	1.2	-1.1	-1.0	1.2	1.0	-1.1	-1.1	1.3
epoxide hydrolase 2, cytoplasmic	EPHX2	1.2	1.0	-1.3	-1.0	1.0	1.1	-1.2	-1.1	1.1	1.2	-1.2
fatty acid amide hydrolase 1	FAAH	-1.2	-1.6	1.5	1.1	-1.4	-1.3	1.7	1.2	-1.3	-1.2	1.2
fatty acid amide hydrolase 2	FAAH2	-1.7	-2.6	1.1	-1.6	-3.0	-2.9	-1.5	-2.8	-3.8	-3.2	-1.7
monoacylglycerol lipase	MGLL	-1.3	-1.7	-1.0	-1.1	-2.4	-1.4	-1.2	1.9	1.7	1.9	-1.1
a/b hydrolase domain-containing protein 4	ABHD4	-1.8	-2.9	2.0	-1.1	-2.2	-2.1	-1.1	-2.2	-3.9	-4.2	-1.1
a/b hydrolase domain-containing protein 6	ABHD6	-1.1	-1.7	1.0	-1.2	-2.1	-1.9	-2.1	-3.7	-7.1	-7.4	-4.0
a/b hydrolase domain-containing protein 12	ABHD12	1.0	-1.8	-1.1	-1.2	-1.4	-1.2	-1.1	-1.1	-1.3	-1.3	-1.3
catechol-O-methyl transferase	COMT	-1.9	-3.0	-1.1	-1.1	-2.3	-1.8	-1.4	-1.3	-2.1	-1.9	-1.4

HUVECs (multiple donors) were grown to confluency and treated for 1 hour with AEA, 2AG, or NADA [10 μM], and then with LPS [10 μg/mL] or TNF [100 ng/mL] for 3 hours, in the continuous presence of AEA, 2-AG, or NADA. ECs were then lysed with Trizol. The mean C_t value for HPRT1 was used as the reference in calculating the ΔC_t values for each biological replicate, as described in the materials and methods. 30 ng of cDNA was analyzed for each sample. Relative quantification (RQ) values were calculated relative to the lowest detectable expressing gene. When gene expression was not detected in more than half of the technical replicates, it was defined as not expressed (nd, not detectable). Data shown represents relative fold change in comparison to ECs treated with ethanol (EtOH) alone. Light gray indicates upregulation and dark gray downregulation of greater than three fold.

Table 4.2. Binding affinity of PGD_2-DA to GPCRs

Receptor	Fold Binding	Receptor	Fold Binding	Receptor	Fold Binding	Receptor	Fold Binding	Receptor	Fold Binding
DRD2	61.9	GIPR	1.4	GRM1	1.2	CXCR2	1.2	P2RY1	1.1
DRD3	19.8	GLP1R	1.4	GABBR1	1.2	MRGPRX3	1.2	GPR83	1.1
DRD4	4.2	CYSLTR2	1.4	GPR39	1.2	DRD5	1.2	HRH1	1.1
DRD4	3.4	GPR156	1.4	HTR2A	1.2	GPR65	1.2	MC4R	1.1
GPRC5D	3.2	SSTR3	1.4	MAS1L	1.2	GPR12	1.2	CD97	1.1
ADRA1B	2.5	CALCRL	1.4	GPR34	1.2	HTR2C VNV	1.2	HCTR2	1.1
GRPR	2.0	GCGR	1.4	C5A	1.2	GPR78	1.1	GPR116	1.1
CXCR7	2.0	P2RY13	1.4	CYSLTR1	1.2	TACR2	1.1	GPR3	1.1
ADRA2C	1.9	CXCR1	1.4	PK1	1.2	OPRM1	1.1	HCA1	1.1
GPR32	1.9	CCR6	1.4	GPR153	1.2	GPR21	1.1	GPR84	1.1
PK2	1.8	GPR119	1.4	GPR87	1.2	NPS	1.1	GMR2	1.1
LHCGR	1.8	SSTR2	1.4	EDNRB	1.2	PTGER3	1.1	HCA2	1.1
HTR1A	1.7	GPR133	1.4	NTSR1	1.2	P2RY2	1.1	F2R-L1	1.1
AGTR1	1.7	SSTR4	1.4	CHRM3	1.2	GPR22	1.1	DRD1	1.1
TAAR5	1.7	ADRA2A	1.4	GPR110	1.2	ADORA1	1.1	GPR171	1.1
GPR142	1.7	MRGPRX4	1.3	SCTR	1.2	GAL3	1.1	CXCR4	1.1
PTGDR	1.6	BB3	1.3	MRGPRF	1.2	CCKAR	1.1	TACR1	1.1
ADRA2B	1.6	NMUR2	1.3	S1PR1	1.2	LPAR6	1.1	GPR113	1.1
CCRL2	1.6	HTR1F	1.3	HTR2C VGV	1.2	MC1R	1.1	FFA3	1.1
MRGPRX1	1.6	PTGER2	1.3	S1PR5	1.2	HTR1E	1.1	P2RY10	1.1
MRGPRG	1.6	CHRM2	1.3	GPR162	1.2	GHSR	1.1	GPR151	1.0
GPR25	1.6	HTR6	1.3	GPR97	1.2	MTNR1B	1.1	ELTD1	1.0
GPR44	1.5	P2RY11	1.3	CHRM1	1.2	GPR144	1.1	MCHR2R	1.0
P2RY12	1.5	GPR82	1.3	CXCR6	1.2	GPR126	1.1	LPA4	1.0
P2RY8	1.5	P2RY14	1.3	CXCR2	1.2	P2RY4	1.1	VIPR1	1.0
GPR135	1.5	OXTR	1.3	MRGPRX3	1.2	LPAR5	1.1	MRGPRD	1.0
CRHR1	1.5	GPR55	1.3	DRD5	1.2	CASR	1.1	S1PR3	1.0
BDKBR2	1.5	GAL1	1.3	GPR65	1.2	PTGFR	1.1	GRM7	1.0
GPBA	1.5	GPR183	1.3	GPR12	1.2	FFA1	1.1	C3AR1	1.0
GPR52	1.5	HRH3	1.3	HTR2C VNV	1.2	ADORA3	1.1	AVPR2	1.0
RXFP3	1.5	CCR5	1.3	S1PR5	1.2	PTH1R	1.1	GNRHR	1.0
SSTR1	1.5	HTR2C VSV	1.2	GPR162	1.2	S1PR4	1.1	GPR150	1.0
TACR3	1.4	HRH4	1.2	GPR97	1.2	ADRA1D	1.1	MLNR	1.0
SSTR5	1.4	HTR1B	1.2	CHRM1	1.2	CRHR2	1.1	BDKBR1	1.0
ADRB1	1.4	CHRM4	1.2	CXCR6	1.2	OPRD1	1.1	GPR158	1.0

Receptor	Fold Binding	Receptor	Fold Binding	Receptor	Fold Binding	Receptor	Fold Binding	Receptor	Fold Binding
GPR4	1.0	CCR10	0.9	OXER1	0.9	GPR37	0.8	GPR64	0.7
GPRC5A	1.0	FPR1	0.9	PRRP	0.9	GPR68	0.8	GAL2	0.6
CCR8	1.0	VIPR2	0.9	CX3CR1	0.8	LTB4R	0.8	RXFP4	0.6
AGTR2	1.0	F2RL2	0.9	FPR3	0.8	QRFP	0.8	EDNRA	0.6
OPRL1	1.0	CXCR5	0.9	GPR146	0.8	GPR101	0.7	S1PR2	0.6
CXCR3	1.0	MAS1	0.9	GPR161	0.8	ADCYAP1R1	0.7	TAAR6	0.6
HTR4	1.0	GPR18	0.9	GPR149	0.8	NPY1R	0.7	GPR62	0.6
GPR141	1.0	NPBW1	0.9	Buffer	0.8	GPR174	0.7	GPR63	0.6
HTR7	1.0	APJ	0.9	MC2R	0.8	TSHR	0.7	GPR77	0.6
MCHR1R	1.0	GPRC5B	0.9	HTR2C INI	0.8	TAAR2	0.7	GPR45	0.6
GPRC5C	1.0	SUCNR1	0.9	FFA2	0.8	CCR2	0.7	HCTR1	0.6
OPRK1	1.0	GPR125	0.9	CALCRb	0.8	MC5R	0.7	CNR1	0.6
GPR123	1.0	LTB4R2B	0.9	GPR157	0.8	GPR152	0.7	GPR20	0.6
MTNR1A	1.0	AVPR1A	0.9	PTGER4	0.8	PTGER1	0.7	GPR173	0.6
CCR4	1.0	GPR85	0.9	NPFF1	0.8	NPY2R	0.7	RXFP1	0.6
ADORA2B	1.0	GPR88	0.9	ADRA1A	0.8	GPR17	0.7	GPR50	0.6
F2RL3	1.0	LPAR2	0.9	HCA3	0.8	GPR160	0.7	OXGR1	0.6
GPR35	1.0	OPN3	0.9	GRM5	0.8	LPAR1	0.7	RXFP2	0.6
GPER	1.0	HTR5	0.9	HTR1D	0.8	ADRB2	0.7	CMKLR1	0.6
NMBR	1.0	GPR182	0.9	GPR143	0.8	CCR7	0.7	ADORA2A	0.5
CCR3	1.0	GLP2R	0.9	TAAR8	0.8	GPR31	0.7	GPR1	0.5
PTAFR	1.0	HTR2B	0.9	GPR15	0.8	GPR61	0.7	GPR114	0.5
NPY5R	1.0	NPY4R	0.9	GPR111	0.8	TBXA2R	0.7	GPRC6A	0.5
FPR2	1.0	GPR132	0.9	TA1	0.8	MRGPRX2	0.7	GPR120	0.5
CHRM5	1.0	CCKBR	0.9	PTH2R	0.8	F2R	0.7	CNR2	0.5
P2RY6	1.0	GPR26	0.9	GPR37L1	0.8	FSHR	0.7	KISSPEPTIN	0.4
MRGPRE	1.0	GPR27	0.9	Buffer	0.8	GPR6	0.7	NTSR2	0.4
AVPR1B	1.0	MC3Rb	0.9	UTS2R	0.8	NPBW2	0.7	HRH2	0.3
GPR56	0.9	GPR19	0.9	GPR148	0.8	GPR124	0.7		
GPR115	0.9	GRM4	0.9	PTGIR	0.8	NMUR1	0.7		
GPR75	0.9	ADRB3	0.9	NPFF2	0.8	TAAR9	0.7		
GRM8	0.9	OPN5	0.9	GRM6	0.8	GHRHR	0.7		

1 μM PGD_2-DA was added to cells expressing the listed GPCR for 20 hours. Binding values are the fold change in binding compared to the fold of the average basal

response. Samples were run in quadruplicate, with four sample wells and four basal wells. 100 nM quinpirole was incubated with cells expressing DRD2 on each assay plate as a control.

Table 4.3. List of qPCR primers used

Gene	Catalog #	Gene	Catalog #
18S	Hs99999901_s1	*ALOX15*	Hs00993765_g1
HPRT	Hs01003267_m1	*ALOX15B*	Hs00153988_m1
PLA2G5	Hs00173472_m1	*LTC4S*	Hs00168529_m1
PTGS1	Hs00377726_m1	*LTA4H*	Hs01075871_m1
PTGS2	Hs00153133_m1	*ALOX12*	Hs00167524_m1
PTGIS	Hs00919949_m1	*ALOXE3*	Hs00222134_m1
PTGDS	Hs00168748_m1	*LTB4H*	Hs01587865_g1
HPGDS	Hs01023933_m1	*CYP2C8*	Hs00426387_m1
TBXAS1	Hs01022706_m1	*CYP2J2*	Hs00951113_m1
PTGES	Hs01115610_m1	*EPHX2*	Hs00157403_m1
PTGES2	Hs00228159_m1	*FAAH*	Hs01038660_m1
PTGES3	Hs00832847_gH	*FAAH2*	Hs00398732_m1
AKR1C3	Hs00366267_m1	*MGLL*	Hs00200752_m1
HPGD	Hs00960586_g1	*ABHD4*	Hs01040459_m1
PTGR1	Hs00400932_m1	*ABHD6*	Hs00977889_m1
PTGR2	Hs01584044_m1	*ABHD12*	Hs01018047_m1
ALOX5	Hs01095330_m1	*COMT*	Hs00241349_m1
ALOX5AP	Hs00233463_m1	*mPTGS2*	Mm01307329_m1
GAPDH	Mm99999915_g1*		

Materials and Methods

Cells

Human umbilical vein endothelial cells (HUVECs, passage 2-6, multiple donors) (Promocell, Heidelberg, Germany) and human lung microvascular endothelial cells (lung HMVECs, passage 4-9, female and male donors) (Promocell) were incubated at 37°C under humidified 5% CO_2. HUVECs were grown in EGM-2 and lung HMVECs were grown in microvascular EGM-2 (Lonza, Walkersville, MD).

Preparation of primary murine endothelial cells

Primary lung endothelial cells were prepared from 6-7 day old mouse pups immediately after decapitation as described (186). The purity of the cell populations was verified by flow cytometry as described above. WT, *Trpv1*$^{-/-}$, and *Cnr2*$^{-/-}$ endothelial cell preparations were >96% pure.

Endocannabinoid, PGD_2-DA, inhibitor, and inflammatory agonist treatments

ECs were grown to confluence before agonist treatment. Unless otherwise noted, in all experiments cells were pre-incubated with the endocannabinoids or prostaglandin D_2-dopamine (PGD_2-DA) at 10 μM for 1 hour prior to and continuously during inflammatory agonist treatment. For experiments involving an inhibitor, the inhibitor was also added 1 hour prior and continuously during inflammatory agonist treatment. Endocannabinoids used were 2-AG (Tocris, Ellisville, MO), *N*-arachidonoylethanolamine (AEA) (Sigma, St. Louis, MO), and *N*-arachidonoyl dopamine (NADA) (Cayman Chemical, Ann Arbor, MI). PGD_2-DA was synthesized by Cayman Chemical. Unless specified, endocannabinoids and PGD_2-DA were used at a concentration of 10μM. Unless otherwise noted, inhibitors

were purchased from Cayman Chemical: TRPV1 antagonist AMG9810 (Tocris; 10 μM), CB_1R antagonist CP945598 (10 μM; Tocris), CB_2R inverse agonist SR144528 (10 μM), indomethacin (0.1-10 μM), *R*-ibuprofen (2μM), *S*-ibuprofen (2 μM), and *R*-flurbiprofen (1 μM). For inflammatory agonist challenge, cells were incubated with 10 ng/mL LPS (List Laboratories, Los Gatos, CA) or 100 ng/mL recombinant human TNFα (PeproTech, Inc., Rocky Hill, NJ) for the specified time, unless otherwise indicated.

Immunoblots

Cells were incubated with the specified inhibitor, endocannabinoid, and/or TNFα for the indicated amount of time. Cells were then lysed with RIPA-Lysis Buffer (4 mM sodium dihydrogen phosphate, pH 7.0; 6 mM disodium hydrogen phosphate, pH 7.0; 150 mM sodium chloride; 1% Nonidet P-40; 1% sodium deoxycholate; 0.1% SDS; 2 mM EDTA; 50 mM sodium fluoride; 0.1 mM sodium vanadate) plus protease inhibitor mixture (Sigma), and protein concentrations of the lysates were estimated using the RCDC protein assay kit (Bio-Rad). Total proteins were separated by SDS-PAGE (11%) and then transferred to PVDF membranes (Pall Corp, Ann Arbor, MI). Membranes were blocked in 3% BSA for 45 minutes at room temperature (RT) and then incubated with primary antibody solution overnight at 4°C. Membranes were washed and then incubated with goat anti-rabbit (111-035-045; Jackson ImmunoResearch, West Grove, PA) or rabbit anti-goat (31403; ThermoFisher Scientific, Waltham, MA) peroxidase-conjugated secondary antibodies. Immunoblots were developed using Super-Signal West Dura Extended Duration Substrate (34076; Thermo Scientific), and the signal was detected using a Gel Logic 2200 Imaging System (Eastman Kodak, Rochester, NY) run on Carestream imaging software (Carestream Health, Rochester, NY). The antibodies

used were as follows: COX-2 (0.1 μg/mL, 100034, Cayman Chemical) and β-actin (0.1 μg/mL, A2066, Sigma).

ELISAs and EIAs

IL-6, (R&D Systems, Minneapolis, MN), IL-8 (BD Biosciences), 6-keto-$PGF_{1\alpha}$ (Cayman Chemical), TXB_2 (Cayman Chemical), and PGE_2 (R&D Systems) levels were quantified in culture supernatants by ELISA (cytokines) or EIA (prostanoids) according to the manufacturer's instructions. For quantification of PGD_2, cells were lysed in 0.1M potassium phosphate buffer, pH 7.4 and sonicated. Cleared cell lysates were used in the PGD_2 EIA (Cayman Chemical), following the manufacturer's instructions.

MTT assay, and crystal violet assay

For MTT and crystal violet (CV) assays, NADA or PGD_2-DA (0.1-20μM) was added for 7 hours in the absence of inflammatory agonists. MTT Assays (Biotium, Hayward, CA) were performed in 96-well plates according to the manufacturer's instructions. For CV assays, after the indicated treatments, the cells in 48-well plates were washed twice with PBS and then stained with 0.5% CV in methanol for 10 minutes (100 μl). The plates were then immersed several times in tap water to remove the excess CV solution, after which time the plates were gently tapped upside down on a paper towel to remove all traces of liquid. 1% SDS in water (300 μl) was then added to each well, and the remaining stained cells were allowed to solubilize for several hours. One well in the plate was left without cells to control for background staining. Absorbance was read at 570nm in a FLUOstar OPTIMA fluorescent plate reader (BMG Labtech, Cary, NC); the background staining was subsequently subtracted, and the

percent adherence relative to the control was calculated.

Flow cytometry

Primary murine endothelial cells were detached using Accutase Cell Detachment Solution (Innovative Cell Technologies, San Diego). Cells were passed through a 70-μm filter, counted, and aliquoted at $5x10^5$ cells per sample. The cells were then washed using Flow Cytometry Staining Buffer (FCSB) (R&D Systems) and incubated with 10 μg/mL mouse IgG (R&D Systems) in FCSB for 15 minutes at 4°C. Next, the cells were incubated for 30 minutes at 4°C with either 0.25 μg/sample of FITC-rat anti-mouse CD102, PE-rat anti-mouse CD31, FITC-rat anti-mouse IgG2a κ, and PE-rat anti-mouse IgG2a κ (BD Biosciences). The samples were washed once more with FCSB and then analyzed by flow cytometry (LSRII Flow Cytometer, BD Biosciences). A far-red fluorescent dye (L10119; Invitrogen) was used to assess cell viability.

Quantitative real time PCR (qPCR)

Specific gene expression assays were ordered from Applied Biosystems (Foster City, CA). See Table 4.3 for a list of assay numbers. The manufacturer's suggested assay reagents were purchased from Applied Biosystems. HUVECs or primary murine endothelial cells were stimulated for 1 hour with the endocannabinoid, then 3 hours with LPS or TNFα. Cells were then lysed, and mRNA was isolated using TRIzol according to the manufacturer's supplied protocol (Invitrogen). mRNA concentrations were determined with an ND-1000 (NanoDrop/Thermo Fisher Scientific), and mRNA was reverse-transcribed to cDNA using the High Capacity RNA-to-cDNA kit using 2 μg of mRNA per reaction (Invitrogen). An input of either 5, 10, or 30 ng of cDNA in 10 μl of

total reaction volume per well containing TaqMan Fast Advanced Master Mix (Applied Biosystems) was used in all qPCR experiments, and qPCR was performed using the StepOnePlus System (Applied Biosystems). For the run method, PCR activation at 95°C for 20s was followed by 40 cycles of 1s at 95°C and 20s at 60°C. The average C_t value of two technical replicates was used in all calculations. The average C_t value of the internal control *HPRT1* (human) or *GAPDH* (mouse) was used to calculate ΔC_t values. Initial data analysis was performed using the $2^{-_{\Delta\Delta}Ct}$ method, and the data were corrected using log transformation, mean centering, and auto scaling to ensure appropriate scaling between biological replicates (161). The methods of calculation utilized assume an amplification efficiency of 100% between successive cycles.

LC-MS/MS

Confluent monolayers of lung HMVECs were grown in 6-well tissue culture plates. Cells were incubated with ethanol (control) or NADA (10 μM) for 1 hour, then treated with LPS (10 μg/mL) for 20 hours. Cells were lysed with 1 mL of potassium phosphate buffer, pH 7.4 per well. For each sample, the lysate from 3 tissue culture wells were combined. Samples were analyzed by LC-MS/MS. NADA, PGD_2, and PGD_2-DA standards were prepared at Cayman Chemical. For *in vivo* prostanoid analysis, 8-week-old C57BL/6J WT mice were injected with 10 mg/kg NADA i.v., followed immediately by 5 mg/kg LPS i.v. Plasma was collected 2 hours after challenge and submitted to the University of California San Diego Lipidomics Core for analysis.

Statistics

Mann-Whitney tests were used to compare 2 groups; Kruskal-Wallis tests were used for

multiple comparisons under a single, defined variable. $p < 0.05$ was considered to be statistically significant for all data. The data in graphs are presented as means ± SD. Experiments were repeated at least twice.

CHAPTER 5

Conclusions

Conclusions

We have shown that the endocannabinoid/endovanilloid NADA has immunomodulatory activity in the endothelium, as well as systemically. NADA modulates endothelial inflammation via the cannabinoid receptors CB_1R/CB_2R and the cation channel TRPV1. Through these receptors, NADA reduces pro-inflammatory cytokine expression and leukocyte adhesion. NADA also regulates the expression of COX-2 and thus differentially affects the expression of downstream prostanoids. We provide the first evidence of the existence of a bioactive prostaglandin analog PGD_2-DA, and demonstrate the immunomodulatory functions of this prostanoid in the endothelium. In addition to its effects *in vitro*, NADA reduces systemic inflammation in murine models of endotoxemia via non-hematopoietic TRPV1. We believe the systemic immunomodulatory effects of NADA via TRPV1 are due to the contributions of neuronal TRPV1, supporting an essential role of a neuroinflammatory arc in endocannabinoid signaling. Furthermore, we show that NADA also regulates systemic inflammation via hematopoietic and endothelial CB_2R, indicating that NADA functions distinctly through multiple receptors in different tissues to carefully control inflammatory outcomes. A working model based on our observations with NADA is presented in Figure 5.1, and a summation can be found in the figure legend.

These results illustrate the complexity of the endocannabinoid system. However, the ability of NADA to signal through a variety of mechanisms and tissues makes it a strong, reasonable target for therapeutic interventions. NADA signaling could be replicated with receptor agonists or antagonists specifically in the nervous system, endothelium, or hematopoietic cells. Furthermore, sepsis involves the multifaceted

activation of numerous inflammatory cascades, and thus, more effective therapies may be distal and regulate a variety of general outputs, including coagulation, permeability, and inflammation (16). Our results support the growing body of research that illustrates the essential importance of lipid signaling in inflammation and immune regulation, and specifically showcase the immunomodulatory activity of lipids in endothelial cells. The elucidation of the precise signaling mechanisms of the endocannabinoid system basally and during inflammation may finally lead to effective therapies for the treatment of sepsis and other acute inflammatory disorders may finally be generated.

Figure 5.1

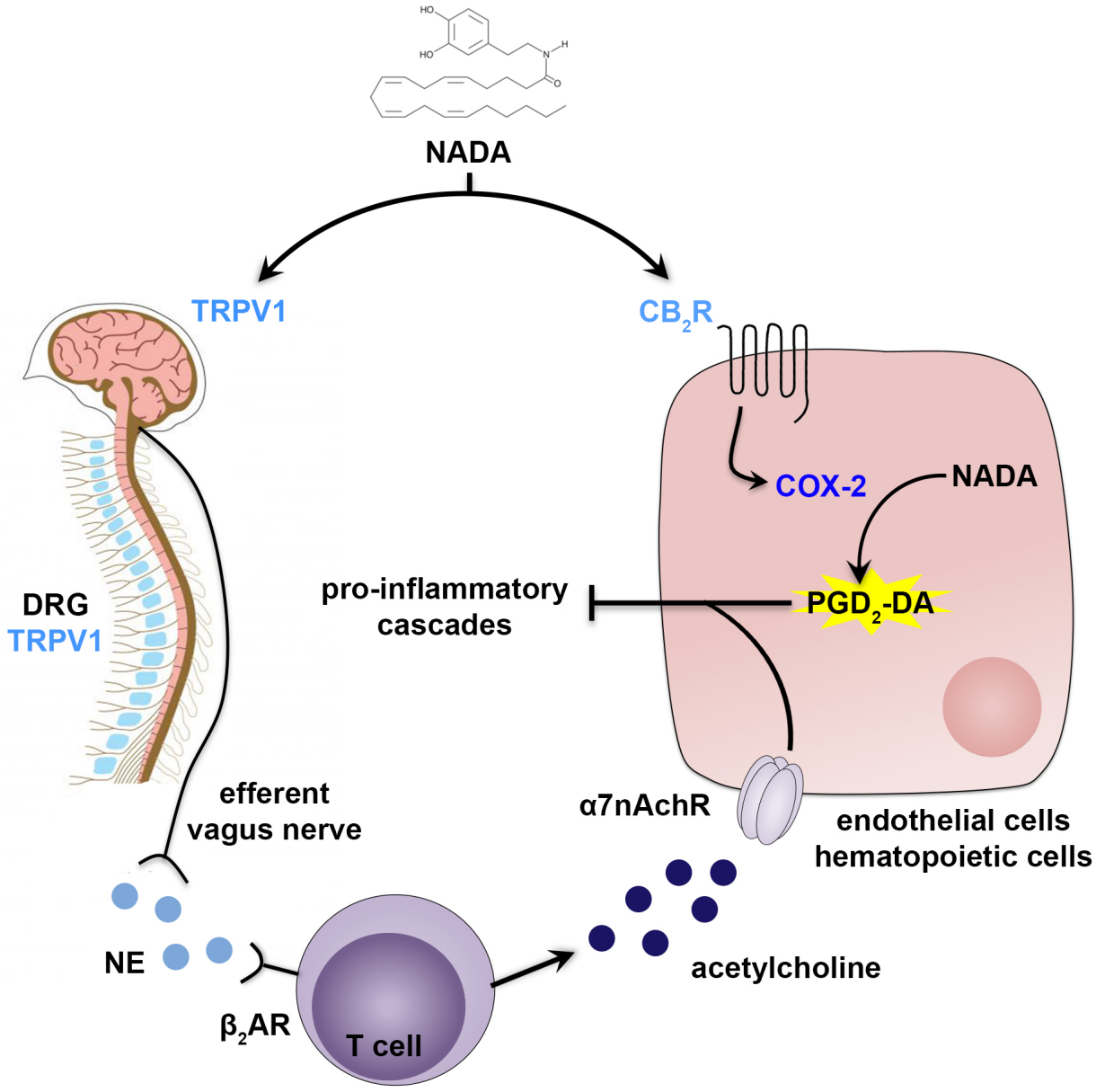
NADA
TRPV1
CB2R
COX-2
NADA
DRG
TRPV1
pro-inflammatory
cascades
PGD2-DA
efferent
vagus nerve
α7nAchR
endothelial cells
hematopoietic cells
NE
β2AR
T cell
acetylcholine

Figure 5.1. Proposed model.

NADA activates CB_2R expressed on endothelial cells and hematopoietic cells, and future experiments will determine if NADA also activates CB_2R on non-hematopoietic cell types, including neurons. CB_2R activation results in the upregulation of COX-2 protein. COX-2 helps catalyze NADA into the novel prostaglandin analog, prostaglandin D_2-dopamine (PGD_2-DA), which in turn decreases pro-inflammatory outputs. In addition, NADA activates TRPV1 expressed on non-hematopoietic cells, which likely includes neurons. These neurons may be peripheral or central, and may be localized in areas such as the dorsal root ganglion (DRG), which has high expression of TRPV1. Preliminary results suggest that NADA-induced stimulation of the efferent vagus nerve activates the cholinergic anti-inflammatory pathway, resulting in the release of norepinephrine (NE) from sympathetic postganglionic nerve fibers. NE activates the β_2 adrenergic receptor (β_2AR) on lymphocytes and macrophages, inducing the release of acetylcholine. Acetylcholine binds to the α7 nicotinic acetylcholine receptor (α7nAchR), which inhibits pro-inflammatory cascades.

REFERENCES

1. Angus, D. C. (2011) The Search for Effective Therapy for Sepsis: Back to the Drawing Board? *JAMA* **306**, 2614–2615

2. Rittirsch, D., Flierl, M. A., and Ward, P. A. (2008) Harmful molecular mechanisms in sepsis. *Nat. Rev. Immunol.* **8**, 776–787

3. Kumar, P., Shen, Q., Pivetti, C. D., Lee, E. S., Wu, M. H., and Yuan, S. Y. (2009) Molecular mechanisms of endothelial hyperpermeability: implications in inflammation. *Expert Rev. Mol. Med.* **11**, e19

4. Dellinger, R. P., Levy, M. M., Rhodes, A., Annane, D., Gerlach, H., Opal, S. M., Sevransky, J. E., Sprung, C. L., Douglas, I. S., Jaeschke, R., Osborn, T. M., Nunnally, M. E., Townsend, S. R., Reinhart, K., Kleinpell, R. M., Angus, D. C., Deutschman, C. S., Machado, F. R., Rubenfeld, G. D., Webb, S. A., Beale, R. J., Vincent, J.-L., Moreno, R., and Subgroup, S. S. C. G. C. I. T. P. (2013) Surviving sepsis campaign: international guidelines for management of severe sepsis and septic shock: 2012. *Crit. Care Med.* **41**, 580–637

5. Sprung, C. L., Annane, D., Keh, D., Moreno, R., Singer, M., Freivogel, K., Weiss, Y. G., Benbenishty, J., Kalenka, A., Forst, H., Laterre, P.-F., Reinhart, K., Cuthbertson, B. H., Payen, D., Briegel, J., CORTICUS Study Group. (2008) Hydrocortisone therapy for patients with septic shock. *N. Engl. J. Med.* **358**, 111–124

6. Ranieri, V. M., Thompson, B. T., Barie, P. S., Dhainaut, J.-F., Douglas, I. S., Finfer, S., Gårdlund, B., Marshall, J. C., Rhodes, A., Artigas, A., Payen, D., Tenhunen, J., Al-Khalidi, H. R., Thompson, V., Janes, J., Macias, W. L., Vangerow, B., Williams, M. D., PROWESS-SHOCK Study Group. (2012) Drotrecogin alfa (activated) in adults with septic shock. *N. Engl. J. Med.* **366**, 2055–2064

7. Opal, S. M., Laterre, P.-F., Francois, B., LaRosa, S. P., Angus, D. C., Mira, J.-P., Wittebole, X., Dugernier, T., Perrotin, D., Tidswell, M., Jauregui, L., Krell, K., Pachl, J., Takahashi, T., Peckelsen, C., Cordasco, E., Chang, C.-S., Oeyen, S., Aikawa, N., Maruyama, T., Schein, R., Kalil, A. C., Van Nuffelen, M., Lynn, M., Rossignol, D. P., Gogate, J., Roberts, M. B., Wheeler, J. L., Vincent, J.-L., ACCESS Study Group. (2013) Effect of eritoran, an antagonist of MD2-TLR4, on mortality in patients with severe sepsis: the ACCESS randomized trial. *JAMA* **309**, 1154–1162

8. Ley, K., Laudanna, C., Cybulsky, M. I., and Nourshargh, S. (2007) Getting to the site of inflammation: the leukocyte adhesion cascade updated. *Nat. Rev. Immunol.* **7**, 678–689

9. Hickey, M. J. and Kubes, P. (2009) Intravascular immunity: the host-pathogen encounter in blood vessels. *Nat. Rev. Immunol.* **9**, 364–375

10. Aird, W. C. (2005) Spatial and temporal dynamics of the endothelium. *J. Thromb. Haemost.* **3**, 1392–1406

11. Bianconi, E., Piovesan, A., Facchin, F., Beraudi, A., Casadei, R., Frabetti, F., Vitale, L., Pelleri, M. C., Tassani, S., Piva, F., Perez-Amodio, S., Strippoli, P., and Canaider, S. (2013) An estimation of the number of cells in the human body. *Ann. Hum. Biol.* **40**, 463–471

12. Robbins, C. S. and Swirski, F. K. (2010) The multiple roles of monocyte subsets in steady state and inflammation. *Cell. Mol. Life Sci.* **67**, 2685–2693

13. Pegu, A., Qin, S., Fallert Junecko, B. A., Nisato, R. E., Pepper, M. S., and Reinhart, T. A. (2008) Human lymphatic endothelial cells express multiple functional TLRs. *J. Immunol.* **180**, 3399–3405

14. Pryshchep, O., Ma-Krupa, W., Younge, B. R., Goronzy, J. J., and Weyand, C. M. (2008) Vessel-specific Toll-like receptor profiles in human medium and large arteries. *Circulation* **118**, 1276–1284

15. Nagyőszi, P., Wilhelm, I., Farkas, A. E., and Fazakas, C. (2010) Expression and regulation of toll-like receptors in cerebral endothelial cells. *Neurochemistry* **57**, 556–564

16. Khakpour, S., Wilhelmsen, K., and Hellman, J. (2015) Vascular endothelial cell Toll-like receptor pathways in sepsis. *Innate Immun.* **21**, 827–846

17. Peters, K., Unger, R. E., Brunner, J., and Kirkpatrick, C. J. (2003) Molecular basis of endothelial dysfunction in sepsis. *Cardiovasc. Research* **60**, 49–57

18. Lee, W. L. and Liles, W. C. (2011) Endothelial activation, dysfunction and permeability during severe infections. *Curr. Opin. Hematol.* **18**, 191–196

19. Pertwee, R. G., Howlett, A. C., Abood, M. E., Alexander, S. P. H., Di Marzo, V., Elphick, M. R., Greasley, P. J., Hansen, H. S., Kunos, G., Mackie, K., Mechoulam, R., and Ross, R. A. (2010) International Union of Basic and Clinical Pharmacology. LXXIX. Cannabinoid receptors and their ligands: beyond CB_1 and CB_2. *Pharmacol. Rev.* **62**, 588–631

20. De Petrocellis, L. and Di Marzo, V. (2009) An introduction to the endocannabinoid system: from the early to latest concepts. *Best Pract. Res. Clin. Endocrinol. & Metab.* **23**, 1–15

21. Rom, S. and Persidsky, Y. (2013) Cannabinoid receptor 2: potential role in immunomodulation and neuroinflammation. *J. Neuroimmune Pharmacol.* **8**, 608–

620

22. Scheen, A. J. (2007) Cannabinoid-1 receptor antagonists in type-2 diabetes. *Best Pract. Res. Clin. Endocrinol. & Metab.* **21**, 535–553

23. Croxford, J. L. and Yamamura, T. (2005) Cannabinoids and the immune system: Potential for the treatment of inflammatory diseases? *J. Neuroimmunol.* **166**, 3–18

24. Nagarkatti, P., Pandey, R., Rieder, S. A., Hegde, V. L., and Nagarkatti, M. (2009) Cannabinoids as novel anti-inflammatory drugs. *Future Med. Chem.* **1**, 1333–1349

25. Reis, F., Cunha, P., Mascarenhas-Melo, F., Romão, A., and Teixeira, H. (2011) Endocannabinoid system in cardiovascular disorders - new pharmacotherapeutic opportunities. *J. Pharm. Bioall. Sci.* **3**, 350

26. Perkins, J. M. and Davis, S. N. (2008) Endocannabinoid system overactivity and the metabolic syndrome: prospects for treatment. *Curr. Diab. Rep.* **8**, 12–19

27. Rosenson, R. S. (2009) Role of the Endocannabinoid System in Abdominal Obesity and the Implications for Cardiovascular Risk. *Cardiology* **114**, 212–225

28. Kunos, G., Osei-Hyiaman, D., Bátkai, S., Sharkey, K. A., and Makriyannis, A. (2009) Should peripheral CB1 cannabinoid receptors be selectively targeted for therapeutic gain? *Trends Pharmacol. Sci.* **30**, 1–7

29. Járai, Z., Wagner, J. A., Varga, K., Lake, K. D., Compton, D. R., Martin, B. R., Zimmer, A. M., Bonner, T. I., Buckley, N. E., and Mezey, E. (1999) Cannabinoid-induced mesenteric vasodilation through an endothelial site distinct from CB1 or CB2 receptors. *Proc. Natl. Acad. Sci. U.S.A.* **96**, 14136–14141

30. Harris, D., McCulloch, A. I., Kendall, D. A., and Randall, M. D. (2002) Characterization of vasorelaxant responses to anandamide in the rat mesenteric arterial bed. *J. Physiol.* **539**, 893–902

31. Stanley, C. and O'Sullivan, S. E. (2013) Vascular targets for cannabinoids: animal and human studies. *Br. J. Pharmacol.* **171**, 1361-1378

32. O'Sullivan, S. E., Kendall, D. A., and Randall, M. D. (2004) Characterisation of the vasorelaxant properties of the novel endocannabinoid *N*-arachidonoyl-dopamine (NADA). *Br. J. Pharmacol.* **141**, 803–812

33. Kozłowska, H., Baranowska, M., Schlicker, E., Kozłowski, M., Laudañski, J., and Malinowska, B. (2009) Virodhamine relaxes the human pulmonary artery through the endothelial cannabinoid receptor and indirectly through a COX product. *Br. J.*

Pharmacol. **155**, 1034–1042

34. Mestre, L., Docagne, F., Correa, F., Loría, F., Hernangómez, M., Borrell, J., and Guaza, C. (2009) A cannabinoid agonist interferes with the progression of a chronic model of multiple sclerosis by downregulating adhesion molecules. *Molec. Cell. Neurosci.* **40**, 258–266

35. Mestre, L., Iñigo, P. M., Mecha, M., Correa, F. G., Hernangómez-Herrero, M., Loría, F., Docagne, F., Borrell, J., and Guaza, C. (2011) Anandamide inhibits Theiler's virus induced VCAM-1 in brain endothelial cells and reduces leukocyte transmigration in a model of blood brain barrier by activation of CB(1) receptors. *Journal of Neuroinflammation* **8**, 102

36. Opitz, C. A., Rimmerman, N., Zhang, Y., Mead, L. E., Yoder, M. C., Ingram, D. A., Walker, J. M., and Rehman, J. (2007) Production of the endocannabinoids anandamide and 2-arachidonoylglycerol by endothelial progenitor cells. *FEBS Lett.* **581**, 4927–4931

37. Varga, K., Lake, K., Martin, B. R., and Kunos, G. (1995) Novel antagonist implicates the CB< sub> 1</sub> cannabinoid receptor in the hypotensive action of anandamide. *Eur. J. Pharmac.*

38. Wang, Y. and Wang, D. H. (2013) TRPV1 Ablation Aggravates Inflammatory Responses and Organ Damage during Endotoxic Shock. *Clinical and Vaccine Immunology* **20**, 1008–1015

39. Pertwee, R. G. (2006) Cannabinoid pharmacology: the first 66 years. *Br. J. Pharmacol.* **147**, S163–S171

40. Ueda, N., Tsuboi, K., and Uyama, T. (2013) Metabolism of endocannabinoids and related *N*-acylethanolamines: canonical and alternative pathways. *FEBS J.* **280**, 1874–1894

41. Castillo, P. E., Younts, T. J., Chávez, A. E., and Hashimotodani, Y. (2012) Endocannabinoid signaling and synaptic function. *Neuron* **76**, 70–81

42. Elphick, M. R. (2012) The evolution and comparative neurobiology of endocannabinoid signalling. *Philos. Trans. R. Soc. Lond. B Biol. Sci,* **367**, 3201–3215

43. Luchicchi, A. and Pistis, M. (2012) Anandamide and 2-arachidonoylglycerol: pharmacological properties, functional features, and emerging specificities of the two major endocannabinoids. *Mol. Neurobiol.* **46**, 374–392

44. Piomelli, D. (2014) More surprises lying ahead. The endocannabinoids keep us guessing. *Neuropharmacology* **76**, 228–234

45. Galiègue, S., Mary, S., Marchand, J., Dussossoy, D., Carrière, D., Carayon, P., Bouaboula, M., Shire, D., Le Fur, G., and Casellas, P. (1995) Expression of central and peripheral cannabinoid receptors in human immune tissues and leukocyte subpopulations. *Eur. J. Biochem.* **232**, 54–61

46. Graham, E. S., Angel, C. E., Schwarcz, L. E., Dunbar, P. R., and Glass, M. (2010) Detailed characterisation of CB2 receptor protein expression in peripheral blood immune cells from healthy human volunteers using flow cytometry. *Int. J. Immunopathol. Pharmacol.* **23**, 25–34

47. Lee, S. F., Newton, C., Widen, R., Friedman, H., and Klein, T. W. (2001) Differential expression of cannabinoid CB_2 receptor mRNA in mouse immune cell subpopulations and following B cell stimulation. *Eur. J. Pharmac.* **423**, 235–241

48. Tschöp, J., Kasten, K. R., Nogueiras, R., Goetzman, H. S., Cave, C. M., England, L. G., Dattilo, J., Lentsch, A. B., Tschop, M. H., and Caldwell, C. C. (2009) The cannabinoid receptor 2 is critical for the host response to sepsis. *J. Immunol.* **183**, 499–505

49. Kasten, K. R., Tschöp, J., Hans Tschöp, M., and Caldwell, C. C. (2010) The cannabinoid 2 receptor as a potential therapeutic target for sepsis. *Endocr. Metab. Immune Disord. Drug Targets* **10**, 224–234

50. Gui, H., Sun, Y., Luo, Z.-M., Su, D.-F., Dai, S.-M., and Liu, X. (2013) Cannabinoid receptor 2 protects against acute experimental sepsis in mice. *Mediators Inflamm.* **2013**

51. Klein, T. W., Newton, C., Larsen, K., Lu, L., Perkins, I., Nong, L., and Friedman, H. (2003) The cannabinoid system and immune modulation. *J. Leukocyte Biol.* **74**, 486–496

52. Kozela, E., Pietr, M., Juknat, A., Rimmerman, N., Levy, R., and Vogel, Z. (2010) Cannabinoids Δ^9-tetrahydrocannabinol and cannabidiol differentially inhibit the lipopolysaccharide-activated NF-κB and interferon-β/STAT proinflammatory pathways in BV-2 microglial cells. *J. Biol. Chem.* **285**, 1616–1626

53. Shin, H. S., Xu, F., Bagchi, A., Herrup, E., Prakash, A., Valentine, C., Kulkarni, H., Wilhelmsen, K., Warren, S., and Hellman, J. (2011) Bacterial lipoprotein TLR2 agonists broadly modulate endothelial function and coagulation pathways *in vitro* and *in vivo*. *J. Immunol.* **186**, 1119–1130

54. Wilhelmsen, K., Mesa, K. R., Lucero, J., Xu, F., and Hellman, J. (2012) ERK5 protein promotes, whereas MEK1 protein differentially regulates, the Toll-like receptor 2 protein-dependent activation of human endothelial cells and monocytes. *J. Biol. Chem.* **287**, 26478–26494

55. Wilhelmsen, K., Mesa, K. R., Prakash, A., Xu, F., and Hellman, J. (2012) Activation of endothelial TLR2 by bacterial lipoprotein upregulates proteins specific for the neutrophil response. *Innate Immun* **18**, 602–616

56. Aird, W. C. (2003) The role of the endothelium in severe sepsis and multiple organ dysfunction syndrome. *Blood* **101**, 3765–3777

57. Makó, V., Czúcz, J., Weiszhár, Z., Herczenik, E., Matkó, J., Prohászka, Z., and Cervenak, L. (2010) Proinflammatory activation pattern of human umbilical vein endothelial cells induced by IL-1β, TNF-α, and LPS. *Cytometry* **77A**, 962–970

58. Facchinetti, F., Del Giudice, E., Furegato, S., Passarotto, M., and Leon, A. (2003) Cannabinoids ablate release of TNFα in rat microglial cells stimulated with lypopolysaccharide. *Glia* **41**, 161–168

59. Hao, M.-X., Jiang, L.-S., Fang, N.-Y., Pu, J., Hu, L.-H., Shen, L.-H., Song, W., and He, B. (2010) The cannabinoid WIN55,212-2 protects against oxidized LDL-induced inflammatory response in murine macrophages. *J. Lipid Res.* **51**, 2181–2190

60. Li, Y. Y., Yuece, B., Cao, H. M., Lin, H. X., Lv, S., Chen, J. C., Ochs, S., Sibaev, A., Deindl, E., Schaefer, C., and Storr, M. (2013) Inhibition of p38/Mk2 signaling pathway improves the anti-inflammatory effect of WIN55 on mouse experimental colitis. *Lab. Invest.* **93**, 322–333

61. Sheng, W. S., Hu, S., Min, X., Cabral, G. A., Lokensgard, J. R., and Peterson, P. K. (2005) Synthetic cannabinoid WIN55,212-2 inhibits generation of inflammatory mediators by IL-1β-stimulated human astrocytes. *Glia* **49**, 211–219

62. Mormina, M. E., Thakur, S., Molleman, A., Whelan, C. J., and Baydoun, A. R. (2006) Cannabinoid signalling in TNF-α induced IL-8 release. *Eur. J. Pharmac.* **540**, 183–190

63. Croxford, J. L., Wang, K., Miller, S. D., Engman, D. M., and Tyler, K. M. (2005) Effects of cannabinoid treatment on Chagas disease pathogenesis: balancing inhibition of parasite invasion and immunosuppression. *Cell. Microbiol.* **7**, 1592–1602

64. Bisogno, T., Melck, D., Bobrov MYu, Gretskaya, N. M., Bezuglov, V. V., De Petrocellis, L., and Di Marzo, V. (2000) *N*-acyl-dopamines: novel synthetic CB_1 cannabinoid-receptor ligands and inhibitors of anandamide inactivation with cannabimimetic activity *in vitro* and *in vivo*. *Biochem. J.* **351**, 817–824

65. Huang, S. M., Bisogno, T., Trevisani, M., Al-Hayani, A., De Petrocellis, L., Fezza, F., Tognetto, M., Petros, T. J., Krey, J. F., Chu, C. J., Miller, J. D., Davies, S. N.,

Geppetti, P., Walker, J. M., and Di Marzo, V. (2002) An endogenous capsaicin-like substance with high potency at recombinant and native vanilloid VR1 receptors. *Proc. Natl. Acad. Sci. U.S.A.* **99**, 8400–8405

66. Bezuglov, V., Bobrov, M., Gretskaya, N., Gonchar, A., Zinchenko, G., Melck, D., Bisogno, T., Di Marzo, V., Kuklev, D., Rossi, J. C., Vidal, J. P., and Durand, T. (2001) Synthesis and biological evaluation of novel amides of polyunsaturated fatty acids with dopamine. *Bioorg. Med. Chem. Lett.* **11**, 447–449

67. Little, P. J., Compton, D. R., Johnson, M. R., Melvin, L. S., and Martin, B. R. (1988) Pharmacology and stereoselectivity of structurally novel cannabinoids in mice. *J. Pharmacol. and Exp. Ther.* **247**, 1046–1051

68. Martin, B. R., Compton, D. R., Thomas, B. F., Prescott, W. R., Little, P. J., Razdan, R. K., Johnson, M. R., Melvin, L. S., Mechoulam, R., and Ward, S. J. (1991) Behavioral, biochemical, and molecular modeling evaluations of cannabinoid analogs. *Pharmacol. Biochem. Behav.* **40**, 471–478

69. Huang, S. M. and Walker, J. M. (2006) Enhancement of spontaneous and heat-evoked activity in spinal nociceptive neurons by the endovanilloid/endocannabinoid *N*-arachidonoyldopamine (NADA). *J. Neurophysiol.* **95**, 1207–1212

70. Marinelli, S., Di Marzo, V., Florenzano, F., Fezza, F., Viscomi, M. T., van der Stelt, M., Bernardi, G., Molinari, M., Maccarrone, M., and Mercuri, N. B. (2006) *N*-arachidonoyl-dopamine tunes synaptic transmission onto dopaminergic neurons by activating both cannabinoid and vanilloid receptors. *Neuropsychopharmacology* **32**, 298–308

71. Price, T. J., Patwardhan, A., Akopian, A. N., Hargreaves, K. M., and Flores, C. M. (2004) Modulation of trigeminal sensory neuron activity by the dual cannabinoid-vanilloid agonists anandamide, *N*-arachidonoyl-dopamine and arachidonyl-2-chloroethylamide. *Br. J. Pharmacol.* **141**, 1118–1130

72. Sagar, D. R., Smith, P. A., Millns, P. J., Smart, D., Kendall, D. A., and Chapman, V. (2004) TRPV1 and CB_1 receptor-mediated effects of the endovanilloid/endocannabinoid *N*-arachidonoyl-dopamine on primary afferent fibre and spinal cord neuronal responses in the rat. *Eur. J. Neurosci.* **20**, 175–184

73. Bobrov, M. Y., Lizhin, A. A., Andrianova, E. L., Gretskaya, N. M., Frumkina, L. E., Khaspekov, L. G., and Bezuglov, V. V. (2008) Antioxidant and neuroprotective properties of *N*-arachidonoyldopamine. *Neurosci. Lett.* **431**, 6–11

74. Harrison, S., De Petrocellis, L., Trevisani, M., Benvenuti, F., Bifulco, M., Geppetti, P., and Di Marzo, V. (2003) Capsaicin-like effects of *N*-arachidonoyl-dopamine in

the isolated guinea pig bronchi and urinary bladder. *Eur. J. Pharmac.* **475**, 107–114

75. O'Sullivan, S. E., Kendall, D. A., and Randall, M. D. (2009) Time-dependent vascular effects of endocannabinoids mediated by peroxisome proliferator-activated receptor gamma (PPARγ). *PPAR Res.* **2009**, 425289

76. Navarrete, C. M., Fiebich, B. L., de Vinuesa, A. G., Hess, S., de Oliveira, A. C. P., Candelario-Jalil, E., Caballero, F. J., Calzado, M. A., and Muñoz, E. (2009) Opposite effects of anandamide and *N*-arachidonoyl dopamine in the regulation of prostaglandin E_2 and 8-iso-$PGF_{2\alpha}$ formation in primary glial cells. *J. Neurochem.* **109**, 452–464

77. Navarrete, C. M., Pérez, M., de Vinuesa, A. G., Collado, J. A., Fiebich, B. L., Calzado, M. A., and Muñoz, E. (2010) Endogenous *N*-acyl-dopamines induce COX-2 expression in brain endothelial cells by stabilizing mRNA through a p38 dependent pathway. *Biochem. Pharmacol.* **79**, 1805–1814

78. Sancho, R., Macho, A., La Vega, de, L., Calzado, M. A., Fiebich, B. L., Appendino, G., and Muñoz, E. (2004) Immunosuppressive activity of endovanilloids: *N*-arachidonoyl-dopamine inhibits activation of the NF-κB, NFAT, and activator protein 1 signaling pathways. *J. Immunol.* **172**, 2341–2351

79. Sancho, R., La Vega, de, L., Macho, A., Appendino, G., Di Marzo, V., and Muñoz, E. (2005) Mechanisms of HIV-1 inhibition by the lipid mediator *N*-arachidonoyldopamine. *J. Immunol.* **175**, 3990–3999

80. Yoo, J.-M., Park, E. S., Kim, M. R., and Sok, D.-E. (2013) Inhibitory effect of *N*-acyl dopamines on IgE-mediated allergic response in RBL-2H3 cells. *Lipids* **48**, 383–393

81. Felder, C. C., Joyce, K. E., Briley, E. M., Mansouri, J., Mackie, K., Blond, O., Lai, Y., Ma, A. L., and Mitchell, R. L. (1995) Comparison of the pharmacology and signal transduction of the human cannabinoid CB1 and CB2 receptors. *Mol. Pharmacol.* **48**, 443–450

82. De Petrocellis, L., Bisogno, T., Davis, J. B., Pertwee, R. G., and Di Marzo, V. (2000) Overlap between the ligand recognition properties of the anandamide transporter and the VR1 vanilloid receptor: inhibitors of anandamide uptake with negligible capsaicin-like activity. *FEBS Lett.* **483**, 52–56

83. Patwardhan, A. M., Jeske, N. A., Price, T. J., Gamper, N., Akopian, A. N., and Hargreaves, K. M. (2006) The cannabinoid WIN 55,212-2 inhibits transient receptor potential vanilloid 1 (TRPV1) and evokes peripheral antihyperalgesia via calcineurin. *Proc. Natl. Acad. Sci. U.S.A.* **103**, 11393–11398

84. Jeske, N. A., Patwardhan, A. M., Gamper, N., Price, T. J., Akopian, A. N., and Hargreaves, K. M. (2006) Cannabinoid WIN 55,212-2 Regulates TRPV1 Phosphorylation in Sensory Neurons. *J. Biol. Chem.* **281**, 32879–32890

85. Zavala, K., Lee, J., Chong, J., Sharma, M., Eilers, H., and Schumacher, M. A. (2014) The anticancer antibiotic mithramycin-A inhibits TRPV1 expression in dorsal root ganglion neurons. *Neurosci. Lett.* **578**, 211–216

86. Eilers, H., Lee, S.-Y., Hau, C. W., Logvinova, A., and Schumacher, M. A. (2007) The rat vanilloid receptor splice variant VR.5'sv blocks TRPV1 activation. *Neuroreport* **18**, 969–973

87. Szallasi, A., Cortright, D. N., Blum, C. A., and Eid, S. R. (2007) The vanilloid receptor TRPV1: 10 years from channel cloning to antagonist proof-of-concept. *Nat. Rev. Drug. Discov.* **6**, 357–372

88. Gavva, N. R., Tamir, R., Qu, Y., Kilonsky, L., Zhang, T. J., Immke, D., Wang, J., Zhu, D., Vanderah, T. W., Porreca, F., Doherty, E. M., Norman, M. H., Wild, K. D., Bannon, A. W., Louis, J.-C., and Treanor, J. J. S. (2004) AMG 9810 [(E)-3-(4-t-Butylphenyl)-N-(2,3-dihydrobenzo[b][1,4] dioxin-6-yl)acrylamide], a Novel Vanilloid Receptor 1 (TRPV1) Antagonist with Antihyperalgesic Properties. *J. Pharmacol. and Exp. Ther.* **313**, 474–484

89. Holladay, C. S., Wright, R. M., and Spangelo, B. L. (1993) Arachidonic acid stimulates interleukin-6 release from rat peritoneal macrophages in vitro: evidence for a prostacyclin-dependent mechanism. *Prostaglandins Leukot. and Essent. Fatty Acids* **49**, 915–922

90. Cristino, L., Starowicz, K., De Petrocellis, L., Morishita, J., Ueda, N., Guglielmotti, V., and Di Marzo, V. (2008) Immunohistochemical localization of anabolic and catabolic enzymes for anandamide and other putative endovanilloids in the hippocampus and cerebellar cortex of the mouse brain. *Neuroscience* **151**, 955–968

91. Wojtalla, A., Herweck, F., Granzow, M., Klein, S., Trebicka, J., Huss, S., Lerner, R., Lutz, B., Schildberg, F. A., Knolle, P. A., Sauerbruch, T., Singer, M. V., Zimmer, A., and Siegmund, S. V. (2012) The endocannabinoid *N*-arachidonoyl dopamine (NADA) selectively induces oxidative stress-mediated cell death in hepatic stellate cells but not in hepatocytes. *Am. J. Physiol. Gastrointest. Liver Physiol.* **302**, G873–G887

92. Wilhelmsen, K., Farrar, K., and Hellman, J. (2013) Quantitative *in vitro* assay to measure neutrophil adhesion to activated primary human microvascular endothelial cells under static conditions. *J. Vis. Exp.* e50677–e50677

93. Griffith, D. A., Hadcock, J. R., Black, S. C., Iredale, P. A., Carpino, P. A.,

DaSilva-Jardine, P., Day, R., DiBrino, J., Dow, R. L., Landis, M. S., O'Connor, R. E., and Scott, D. O. (2009) Discovery of 1-[9-(4-chlorophenyl)-8-(2-chlorophenyl)-9H-purin-6-yl]-4-ethylaminopiperidine-4-carboxylic acid amide hydrochloride (CP-945,598), a novel, potent, and selective cannabinoid type 1 receptor antagonist. *J. Med. Chem.* **52**, 234–237

94. Portier, M., Rinaldi-Carmona, M., Pecceu, F., Combes, T., Poinot-Chazel, C., Calandra, B., Barth, F., Le Fur, G., and Casellas, P. (1999) SR 144528, an antagonist for the peripheral cannabinoid receptor that behaves as an inverse agonist. *J. Pharmacol. Exp. Ther.* **288**, 582–589

95. Rinaldi-Carmona, M., Barth, F., Millan, J., Derocq, J. M., Casellas, P., Congy, C., Oustric, D., Sarran, M., Bouaboula, M., Calandra, B., Portier, M., Shire, D., Brelière, J. C., and Le Fur, G. L. (1998) SR 144528, the first potent and selective antagonist of the CB2 cannabinoid receptor. *J. Pharmacol. Exp. Ther.* **284**, 644–650

96. Billstrom, M. A., Johnson, G. L., Avdi, N. J., and Worthen, G. S. (1998) Intracellular signaling by the chemokine receptor US28 during human cytomegalovirus infection. *J. Virol.* **72**, 5535–5544

97. Akimov, M. G., Gretskaia, N. M., Shevchenko, K. V., Shevchenko, V. P., Miasoedov, N. F., Bobrov, M., and Bezuglov, V. V. (2007) New aspects of biosynthesis and metabolism of *N*-acyldopamines in rat tissues. *Bioorg. Khim.* **33**, 648–652

98. Hu, S. S.-J., Bradshaw, H. B., Benton, V. M., Chen, J. S.-C., Huang, S. M., Minassi, A., Bisogno, T., Masuda, K., Tan, B., Roskoski, R., Cravatt, B. F., Di Marzo, V., and Walker, J. M. (2009) The biosynthesis of *N*-arachidonoyl dopamine (NADA), a putative endocannabinoid and endovanilloid, via conjugation of arachidonic acid with dopamine. *Prostaglandins Leukot. and Essent. Fatty Acids* **81**, 291–301

99. Huang, N.-L., Juang, J.-M., Wang, Y.-H., Hsueh, C.-H., Liang, Y.-J., Lin, J.-L., Tsai, C.-T., and Lai, L.-P. (2010) Rimonabant inhibits TNF-α-induced endothelial IL-6 secretion via CB1 receptor and cAMP-dependent protein kinase pathway. *Acta Pharmacol. Sin.* **31**, 1447–1453

100. Liu, J., Gao, B., Mirshahi, F., Sanyal, A. J., Khanolkar, A. D., Makriyannis, A., and Kunos, G. (2000) Functional CB1 cannabinoid receptors in human vascular endothelial cells. *Biochem. J.* **346**, 835–840

101. Rajesh, M., Mukhopadhyay, P., Bátkai, S., Haskó, G., Liaudet, L., Huffman, J. W., Csiszár, A., Ungvári, Z., Mackie, K., Chatterjee, S., and Pacher, P. (2007) CB2-receptor stimulation attenuates TNF-α-induced human endothelial cell activation, transendothelial migration of monocytes, and monocyte-endothelial

adhesion. *Am. J. Physiol. Heart Circ. Physiol.* **293**, H2210–H2218

102. Rajesh, M., Mukhopadhyay, P., Haskó, G., Liaudet, L., Mackie, K., and Pacher, P. (2010) Cannabinoid-1 receptor activation induces reactive oxygen species-dependent and -independent mitogen-activated protein kinase activation and cell death in human coronary artery endothelial cells. *Br. J. Pharmacol.* **160**, 688–700

103. Sugiura, T., Kodaka, T., Nakane, S., Kishimoto, S., Kondo, S., and Waku, K. (1998) Detection of an endogenous cannabimimetic molecule, 2-arachidonoylglycerol, and cannabinoid CB1 receptor mRNA in human vascular cells: is 2-arachidonoylglycerol a possible vasomodulator? *Biochem. Biophys. Res. Commun.* **243**, 838–843

104. Waldeck-Weiermair, M., Zoratti, C., Osibow, K., Balenga, N., Goessnitzer, E., Waldhoer, M., Malli, R., and Graier, W. F. (2008) Integrin clustering enables anandamide-induced Ca^{2+} signaling in endothelial cells via GPR55 by protection against CB1-receptor-triggered repression. *J. Cell. Sci.* **121**, 1704–1717

105. Ramirez, S. H., Hasko, J., Skuba, A., Fan, S., Dykstra, H., McCormick, R., Reichenbach, N., Krizbai, I., Mahadevan, A., Zhang, M., Tuma, R., Son, Y. J., and Persidsky, Y. (2012) Activation of cannabinoid receptor 2 attenuates leukocyte-endothelial cell interactions and blood-brain barrier dysfunction under inflammatory conditions. *J. Neurosci.* **32**, 4004–4016

106. Golech, S. A., McCarron, R. M., Chen, Y., Bembry, J., Lenz, F., Mechoulam, R., Shohami, E., and Spatz, M. (2004) Human brain endothelium: coexpression and function of vanilloid and endocannabinoid receptors. *Brain Res. Mol. Brain Res.* **132**, 87–92

107. Lu, T.-S., Avraham, H. K., Seng, S., Tachado, S. D., Koziel, H., Makriyannis, A., and Avraham, S. (2008) Cannabinoids inhibit HIV-1 Gp120-mediated insults in brain microvascular endothelial cells. *J. Immunol.* **181**, 6406–6416

108. Alhouayek, M., Masquelier, J., and Muccioli, G. G. (2014) Controlling 2-arachidonoylglycerol metabolism as an anti-inflammatory strategy. *Drug Discov. Today* **19**, 295–304

109. Bátkai, S., Rajesh, M., Mukhopadhyay, P., Haskó, G., Liaudet, L., Cravatt, B. F., Csiszár, A., Ungvári, Z., and Pacher, P. (2007) Decreased age-related cardiac dysfunction, myocardial nitrative stress, inflammatory gene expression, and apoptosis in mice lacking fatty acid amide hydrolase. *Am. J. Physiol. Heart Circ. Physiol.* **293**, H909–H918

110. Chang, Y. H., Lee, S. T., and Lin, W. W. (2001) Effects of cannabinoids on LPS-stimulated inflammatory mediator release from macrophages: involvement of eicosanoids. *J. Cell. Biochem.* **81**, 715–723

111. Gallily, R., Breuer, A., and Mechoulam, R. (2000) 2-Arachidonylglycerol, an endogenous cannabinoid, inhibits tumor necrosis factor-α production in murine macrophages, and in mice. *Eur. J. Pharmac.* **406**, R5–R7

112. Ouyang, Y., Hwang, S. G., Han, S. H., and Kaminski, N. E. (1998) Suppression of interleukin-2 by the putative endogenous cannabinoid 2-arachidonyl-glycerol is mediated through down-regulation of the nuclear factor of activated T cells. *Mol. Pharmacol.* **53**, 676–683

113. Björklund, E., Norén, E., Nilsson, J., and Fowler, C. J. (2010) Inhibition of monoacylglycerol lipase by troglitazone, *N*-arachidonoyl dopamine and the irreversible inhibitor JZL184: comparison of two different assays. *Br. J. Pharmacol.* **161**, 1512–1526

114. Gokoh, M., Kishimoto, S., Oka, S., Metani, Y., and Sugiura, T. (2005) 2-Arachidonoylglycerol, an endogenous cannabinoid receptor ligand, enhances the adhesion of HL-60 cells differentiated into macrophage-like cells and human peripheral blood monocytes. *FEBS Lett.* **579**, 6473–6478

115. Sugiura, T. (2009) Physiological roles of 2-arachidonoylglycerol, an endogenous cannabinoid receptor ligand. *Biofactors* **35**, 88–97

116. Sugiura, T., Oka, S., Gokoh, M., Kishimoto, S., and Waku, K. (2004) New perspectives in the studies on endocannabinoid and cannabis: 2-arachidonoylglycerol as a possible novel mediator of inflammation. *J. Pharmacol. Sci.* **96**, 367–375

117. De Petrocellis, L., Bisogno, T., Maccarrone, M., Davis, J. B., Finazzi-Agro, A., and Di Marzo, V. (2001) The activity of anandamide at vanilloid VR1 receptors requires facilitated transport across the cell membrane and is limited by intracellular metabolism. *J. Biol. Chem.* **276**, 12856–12863

118. De Petrocellis, L. and Di Marzo, V. (2009) Role of endocannabinoids and endovanilloids in Ca^{2+} signalling. *Cell Calcium* **45**, 611–624

119. Jordt, S. E. and Julius, D. (2002) Molecular basis for species-specific sensitivity to “hot” chili peppers. *Cell* **108**, 421–430

120. Chu, C. J., Huang, S. M., De Petrocellis, L., Bisogno, T., Ewing, S. A., Miller, J. D., Zipkin, R. E., Daddario, N., Appendino, G., Di Marzo, V., and Walker, J. M. (2003) *N*-Oleoyldopamine, a novel endogenous capsaicin-like lipid that produces hyperalgesia. *J. Biol. Chem.* **278**, 13633–13639

121. Millns, P. J., Chimenti, M., Ali, N., Ryland, E., De Lago, E., Fernandez Ruiz, J., Chapman, V., and Kendall, D. A. (2006) Effects of inhibition of fatty acid amide

hydrolase vs. the anandamide membrane transporter on TRPV1-mediated calcium responses in adult DRG neurons; the role of CB_1 receptors. *Eur. J. Neurosci.* **24**, 3489–3495

122. Price, T. J., Patwardhan, A. M., Flores, C. M., and Hargreaves, K. M. (2005) A role for the anandamide membrane transporter in TRPV1-mediated neurosecretion from trigeminal sensory neurons. *Neuropharmacology* **49**, 25–39

123. Premkumar, L. S., Qi, Z.-H., Van Buren, J., and Raisinghani, M. (2004) Enhancement of Potency and Efficacy of NADA by PKC-Mediated Phosphorylation of Vanilloid Receptor. *J. Neurophysiol.* **91**, 1442–1449

124. Vellani, V., Mapplebeck, S., Moriondo, A., Davis, J. B., and McNaughton, P. A. (2001) Protein kinase C activation potentiates gating of the vanilloid receptor VR1 by capsaicin, protons, heat and anandamide. *J. Physiol.* **534**, 813–825

125. Olah, Z., Karai, L., and Iadarola, M. J. (2001) Anandamide activates vanilloid receptor 1 (VR1) at acidic pH in dorsal root ganglia neurons and cells ectopically expressing VR1. *J. Biol. Chem.* **276**, 31163–31170

126. Kwak, J., Wang, M. H., Hwang, S. W., Kim, T. Y., Lee, S. Y., and Oh, U. (2000) Intracellular ATP increases capsaicin-activated channel activity by interacting with nucleotide-binding domains. *J. Neurosci.* **20**, 8298–8304

127. Tiruppathi, C., Ahmmed, G. U., Vogel, S. M., and Malik, A. B. (2006) Ca^{2+} signaling, TRP channels, and endothelial permeability. *Microcirculation* **13**, 693–708

128. Talreja, J., Kabir, M. H., B Filla, M., Stechschulte, D. J., and Dileepan, K. N. (2004) Histamine induces Toll-like receptor 2 and 4 expression in endothelial cells and enhances sensitivity to Gram-positive and Gram-negative bacterial cell wall components. *Immunology* **113**, 224–233

129. Andriopoulou, P., Navarro, P., Zanetti, A., Lampugnani, M. G., and Dejana, E. (1999) Histamine induces tyrosine phosphorylation of endothelial cell-to-cell adherens junctions. *Arterioscler. Thromb. Vasc. Biol.* **19**, 2286–2297

130. Schaefer, U., Schneider, A., Rixen, D., and Neugebauer, E. (1998) Neutrophil adhesion to histamine stimulated cultured endothelial cells is primarily mediated via activation of phospholipase C and nitric oxide synthase isozymes. *Inflamm. Res.* **47**, 256–264

131. Jeannin, P., Delneste, Y., Gosset, P., Molet, S., Lassalle, P., Hamid, Q., Tsicopoulos, A., and Tonnel, A. B. (1994) Histamine induces interleukin-8 secretion by endothelial cells. *Blood* **84**, 2229–2233

132. Pertwee, R. G. (2010) Receptors and channels targeted by synthetic cannabinoid receptor agonists and antagonists. *Curr. Med. Chem.* **17**, 1360–1381

133. Chang, W.-C. (2006) Store-operated calcium channels and pro-inflammatory signals. *Acta Pharmacol. Sin.* **27**, 813–820

134. Li, S. W., Westwick, J., and Poll, C. T. (2002) Receptor-operated Ca^{2+} influx channels in leukocytes: a therapeutic target? *Trends Pharmacol. Sci.* **23**, 63–70

135. Liu, W. and Matsumori, A. (2011) Calcium channel blockers and modulation of innate immunity. *Curr. Opin. Infect. Dis.* **24**, 254–258

136. Southall, M. D., Li, T., Gharibova, L. S., Pei, Y., Nicol, G. D., and Travers, J. B. (2003) Activation of epidermal vanilloid receptor-1 induces release of proinflammatory mediators in human keratinocytes. *J. Pharmacol. Exp. Ther.* **304**, 217–222

137. Prusakiewicz, J. J., Turman, M. V., Vila, A., Ball, H. L., Al-Mestarihi, A. H., Di Marzo, V., and Marnett, L. J. (2007) Oxidative metabolism of lipoamino acids and vanilloids by lipoxygenases and cyclooxygenases. *Arch. Biochem. Biophys.* **464**, 260–268

138. Ross, H. R., Gilmore, A. J., and Connor, M. (2009) Inhibition of human recombinant T-type calcium channels by the endocannabinoid *N*-arachidonoyl dopamine. *Br. J. Pharmacol.* **156**, 740–750

139. Tseng, C. F., Iwakami, S., Mikajiri, A., Shibuya, M., Hanaoka, F., Ebizuka, Y., Padmawinata, K., and Sankawa, U. (1992) Inhibition of *in vitro* prostaglandin and leukotriene biosyntheses by cinnamoyl-*β*-phenethylamine and *N*-acyldopamine derivatives. *Chem. Pharm. Bull.* **40**, 396–400

140. Sun, Y., Alexander, S. P. H., Kendall, D. A., and Bennett, A. J. (2006) Cannabinoids and PPARα signalling. *Biochem. Soc. Trans.* **34**, 1095–1097

141. De Petrocellis, L., Starowicz, K., Moriello, A. S., Vivese, M., Orlando, P., and Di Marzo, V. (2007) Regulation of transient receptor potential channels of melastatin type 8 (TRPM8): Effect of cAMP, cannabinoid CB_1 receptors and endovanilloids. *Exp. Cell Res.* **313**, 1911–1920

142. Salas, M. M., Hargreaves, K. M., and Akopian, A. N. (2009) TRPA1-mediated responses in trigeminal sensory neurons: interaction between TRPA1 and TRPV1. *Eur. J. Neurosci.* **29**, 1568–1578

143. Reddy, A. T., Lakshmi, S. P., Kleinhenz, J. M., Sutliff, R. L., Hart, C. M., and Reddy, R. C. (2012) Endothelial cell peroxisome proliferator-activated receptor γ reduces endotoxemic pulmonary inflammation and injury. *J. Immunol.* **189**, 5411–5420

144. Sasaki, M., Jordan, P., Welbourne, T., Minagar, A., Joh, T., Itoh, M., Elrod, J. W., and Alexander, J. S. (2005) Troglitazone, a PPARγ activator prevents endothelial cell adhesion molecule expression and lymphocyte adhesion mediated by TNF-α. *BMC Physiol.* **5**, 3

145. Zandbergen, F. and Plutzky, J. (2007) PPARα in atherosclerosis and inflammation. *Biochim. Biophys. Acta* **1771**, 972–982

146. Agro, A., Langdon, C., Smith, F., and Richards, C. D. (1996) Prostaglandin E2 enhances interleukin 8 (IL-8) and IL-6 but inhibits GMCSF production by IL-1 stimulated human synovial fibroblasts *in vitro*. *J. Rheumatol.* **23**, 862–868

147. Ricciotti, E. and FitzGerald, G. A. (2011) Prostaglandins and Inflammation. *Arterioscler. Thromb. Vasc. Biol.* **31**, 986–1000

148. Turu, G. and Hunyady, L. (2010) Signal transduction of the CB_1 cannabinoid receptor. *J. Mol. Endocrinol.* **44**, 75–85

149. Bhave, G., Zhu, W., Wang, H., Brasier, D. J., Oxford, G. S., and Gereau, R. W. (2002) cAMP-dependent protein kinase regulates desensitization of the capsaicin receptor (VR1) by direct phosphorylation. *Neuron* **35**, 721–731

150. Alawi, K. and Keeble, J. (2010) The paradoxical role of the transient receptor potential vanilloid 1 receptor in inflammation. *Pharmacol. Ther.* **125**, 181–195

151. Clark, N., Keeble, J., Fernandes, E. S., Starr, A., Liang, L., Sugden, D., de Winter, P., and Brain, S. D. (2007) The transient receptor potential vanilloid 1 (TRPV1) receptor protects against the onset of sepsis after endotoxin. *FASEB J.* **21**, 3747–3755

152. Fernandes, E. S., Liang, L., Smillie, S. J., Kaiser, F., Purcell, R., Rivett, D. W., Alam, S., Howat, S., Collins, H., Thompson, S. J., Keeble, J. E., Riffo-Vasquez, Y., Bruce, K. D., and Brain, S. D. (2012) TRPV1 deletion enhances local inflammation and accelerates the onset of systemic inflammatory response syndrome. *J. Immunol.* **188**, 5741–5751

153. Wang, H., Yu, M., Ochani, M., Amella, C. A., Tanovic, M., Susarla, S., Li, J. H., Wang, H., Yang, H., Ulloa, L., Al-Abed, Y., Czura, C. J., and Tracey, K. J. (2003) Nicotinic acetylcholine receptor α7 subunit is an essential regulator of inflammation. *Nature* **421**, 384–388

154. Rosas-Ballina, M., Olofsson, P. S., Ochani, M., Valdes-Ferrer, S. I., Levine, Y. A., Reardon, C., Tusche, M. W., Pavlov, V. A., Andersson, U., Chavan, S., Mak, T. W., and Tracey, K. J. (2011) Acetylcholine-synthesizing T cells relay neural signals in a vagus nerve circuit. *Science* **334**, 98–101

155. Tracey, K. J. (2009) Reflex control of immunity. *Nat. Rev. Immunol.* **9**, 418–428

156. Bradshaw, H. B., Rimmerman, N., Krey, J. F., and Walker, J. M. (2006) Sex and hormonal cycle differences in rat brain levels of pain-related cannabimimetic lipid mediators. *Am. J. Physiol. Regul. Integr. Comp. Physiol.* **291**, R349–R358

157. Hamel, E. (2006) Perivascular nerves and the regulation of cerebrovascular tone. *J. Appl. Physiol.* **100**, 1059–1064

158. Girouard, H. and Iadecola, C. (2006) Neurovascular coupling in the normal brain and in hypertension, stroke, and Alzheimer disease. *J. Appl. Physiol.* **100**, 328–335

159. Goyal, R. K. and Chaudhury, A. (2013) Structure activity relationship of synaptic and junctional neurotransmission. *Auton. Neurosci.* **176**, 11–31

160. Livak, K. J. and Schmittgen, T. D. (2001) Analysis of relative gene expression data using real-time quantitative PCR and the $2^{-\Delta\Delta C(T)}$ method. *Methods* **25**, 402–408

161. Willems, E., Leyns, L., and Vandesompele, J. (2008) Standardization of real-time PCR gene expression data from independent biological replicates. *Anal. Biochem.* **379**, 127–129

162. De Petrocellis, L. and Di Marzo, V. (2010) Non-CB_1, non-CB_2 receptors for endocannabinoids, plant cannabinoids, and synthetic cannabimimetics: focus on G-protein-coupled receptors and transient receptor potential channels. *J. Neuroimmune Pharmacol.* **5**, 103–121

163. McHugh, D., Hu, S. S., Rimmerman, N., Juknat, A., Vogel, Z., Walker, J. M., and Bradshaw, H. B. (2010) *N*-arachidonoyl glycine, an abundant endogenous lipid, potently drives directed cellular migration through GPR18, the putative abnormal cannabidiol receptor. *BMC Neurosci.* **11**, 44

164. Mechoulam, R., Ben-Shabat, S., Hanus, L., Ligumsky, M., Kaminski, N. E., Shatz, A. R., Gopher, A., Almog, S., Martin, B. R., and Compton, D. R. Identification of an endogenous 2-monoglyceride, present in canine gut, that binds to cannabinoid receptors. *Biochem. Pharmacol.* **50**, 83–90

165. Okuno, T. and Yokomizo, T. (2011) What is the natural ligand of GPR55? *J. Biochem.* **149**, 495–497

166. Ryberg, E., Larsson, N., Sjögren, S., Hjorth, S., Hermansson, N.-O., Leonova, J., Elebring, T., Nilsson, K., Drmota, T., and Greasley, P. J. (2007) The orphan receptor GPR55 is a novel cannabinoid receptor. *Br. J. Pharmacol.* **152**, 1092–

1101

167. Sugiura, T., Kodaka, T., Nakane, S., Miyashita, T., Kondo, S., Suhara, Y., Takayama, H., Waku, K., Seki, C., Baba, N., and Ishima, Y. (1999) Evidence that the cannabinoid CB1 receptor is a 2-arachidonoylglycerol receptor: Structure-activity relationship of 2-arachidonoylglycerol, ether-linked analogues, and related compounds. *J. Biol. Chem.* **274**, 2794–2801

168. Sugiura, T., Kondo, S., Kishimoto, S., Miyashita, T., Nakane, S., Kodaka, T., Suhara, Y., Takayama, H., and Waku, K. (2000) Evidence that 2-arachidonoylglycerol but not *N*-palmitoylethanolamine or anandamide is the physiological ligand for the cannabinoid CB2 receptor: Comparison of the agonistic activities of various cannabinoid receptor ligands in HL-60 cells. *J. Biol. Chem.* **275**, 605–612

169. Johns, D. G., Behm, D. J., Walker, D. J., Ao, Z., Shapland, E. M., Daniels, D. A., Riddick, M., Dowell, S., Staton, P. C., Green, P., Shabon, U., Bao, W., Aiyar, N., Yue, T.-L., Brown, A. J., Morrison, A. D., and Douglas, S. A. (2007) The novel endocannabinoid receptor GPR55 is activated by atypical cannabinoids but does not mediate their vasodilator effects. *Br. J. Pharmacol.* **152**, 825–831

170. Hillard, C. J., Manna, S., Greenberg, M. J., DiCamelli, R., Ross, R. A., Stevenson, L. A., Murphy, V., Pertwee, R. G., and Campbell, W. B. (1999) Synthesis and characterization of potent and selective agonists of the neuronal cannabinoid receptor (CB1). *J. Pharmacol. Exp. Ther.* **289**, 1427–1433

171. Pertwee, R. G. (1999) Pharmacology of cannabinoid receptor ligands. *Curr. Med. Chem.* **6**, 635–664

172. Hillard, C. J. (2000) Biochemistry and pharmacology of the endocannabinoids arachidonylethanolamide and 2-arachidonylglycerol. *Prostaglandins Other Lipid Mediat.* **61**, 3–18

173. Costa, B., Giagnoni, G., Franke, C., Trovato, A. E., and Colleoni, M. (2004) Vanilloid TRPV1 receptor mediates the antihyperalgesic effect of the nonpsychoactive cannabinoid, cannabidiol, in a rat model of acute inflammation. *Br. J. Pharmacol.* **143**, 247–250

174. Petitet, F., Jeantaud, B., Reibaud, M., Imperato, A., and Dubroeucq, M. C. (1998) Complex pharmacology of natural cannabinoids: evidence for partial agonist activity of Δ^9-tetrahydrocannabinol and antagonist activity of cannabidiol on rat brain cannabinoid receptors. *Life Sci.* **63**, PL1–PL6

175. Thomas, A., Baillie, G. L., Phillips, A. M., Razdan, R. K., Ross, R. A., and Pertwee, R. G. (2007) Cannabidiol displays unexpectedly high potency as an antagonist of CB_1 and CB_2 receptor agonists *in vitro*. *Br. J. Pharmacol.* **150**, 613–

623

176. Caterina, M. J., Schumacher, M. A., Tominaga, M., Rosen, T. A., Levine, J. D., and Julius, D. (1997) The capsaicin receptor: a heat-activated ion channel in the pain pathway. *Nature* **389**, 816–824

177. Hanus, L., Breuer, A., Tchilibon, S., Shiloah, S., Goldenberg, D., Horowitz, M., Pertwee, R. G., Ross, R. A., Mechoulam, R., and Fride, E. (1999) HU-308: a specific agonist for CB_2, a peripheral cannabinoid receptor. *Proc. Natl. Acad. Sci. U.S.A.* **96**, 14228–14233

178. Caldwell, M. D., Hu, S. S.-J., Viswanathan, S., Bradshaw, H., Kelly, M. E. M., and Straiker, A. (2013) A GPR18-based signalling system regulates IOP in murine eye. *Br. J. Pharmacol.* **169**, 834–843

179. Kohno, M., Hasegawa, H., Inoue, A., Muraoka, M., Miyazaki, T., Oka, K., and M, Y. (2006) Identification of *N*-arachidonoylglycine as the endogenous ligand for orphan G-protein-coupled receptor GPR18. *Biochem. Biophys. Res. Commun.* **347**, 827–832

180. Lu, V. B., Puhl, H. L., and Ikeda, S. R. (2013) *N*-Arachidonyl glycine does not activate G protein-coupled receptor 18 signaling via canonical pathways. *Mol. Pharmacol.* **83**, 267–282

181. McHugh, D., Page, J., Dunn, E., and Bradshaw, H. B. (2012) Δ^9 - tetrahydrocannabinol and *N*-arachidonyl glycine are full agonists at GPR18 receptors and induce migration in human endometrial HEC-1B cells. *Br. J. Pharmacol.* **165**, 2414–2424

182. Sheskin, T., Hanus, L., Slager, J., Vogel, Z., and Mechoulam, R. (1997) Structural requirements for binding of anandamide-type compounds to the brain cannabinoid receptor. *J. Med. Chem.* **40**, 659–667

183. D'Ambra, T. E., Estep, K. G., Bell, M. R., Eissenstat, M. A., Josef, K. A., Ward, S. J., Haycock, D. A., Baizman, E. R., Casiano, F. M., and Beglin, N. C. (1992) Conformationally restrained analogues of pravadoline: nanomolar potent, enantioselective, (aminoalkyl)indole agonists of the cannabinoid receptor. *J. Med. Chem.* **35**, 124–135

184. Russo, E. B., Burnett, A., Hall, B., and Parker, K. K. (2005) Agonistic properties of cannabidiol at 5-HT1a receptors. *Neurochem. Res.* **30**, 1037–1043

185. Giaever, I. and Keese, C. R. (1991) Micromotion of mammalian cells measured electrically. *Proc. Natl. Acad. Sci. U.S.A.* **88**, 7896–7900

186. Lim, Y.-C. and Luscinskas, F. W. (2006) Isolation and culture of murine heart and

lung endothelial cells for in vitro model systems. *Methods Mol. Biol.* **341**, 141–154

187. Tóth, A., Blumberg, P. M., and Boczán, J. (2009) Anandamide and the vanilloid receptor (TRPV1). *Vitam. Horm.* **81**, 389–419

188. van der Stelt, M. and Di Marzo, V. (2004) Endovanilloids. Putative endogenous ligands of transient receptor potential vanilloid 1 channels. *Eur. J. Biochem.* **271**, 1827–1834

189. Mogg, A. J., Mill, C., Folly, E. A., Beattie, R. E., Blanco, M. J., Beck, J. P., and Broad, L. M. (2013) Altered pharmacology of native rodent spinal cord TRPV1 after phosphorylation. *Br. J. Pharmacol.* **168**, 1015–1029

190. Cavanaugh, D. J., Chesler, A. T., Bráz, J. M., Shah, N. M., Julius, D., and Basbaum, A. I. (2011) Restriction of transient receptor potential vanilloid-1 to the peptidergic subset of primary afferent neurons follows its developmental downregulation in nonpeptidergic neurons. *J. Neurosci.* **31**, 10119–10127

191. Cavanaugh, D. J., Chesler, A. T., Jackson, A. C., Sigal, Y. M., Yamanaka, H., Grant, R., O'Donnell, D., Nicoll, R. A., Shah, N. M., Julius, D., and Basbaum, A. I. (2011) *Trpv1* reporter mice reveal highly restricted brain distribution and functional expression in arteriolar smooth muscle cells. *J. Neurosci.* **31**, 5067–5077

192. Helliwell, R. J., McLatchie, L. M., Clarke, M., Winter, J., Bevan, S., and McIntyre, P. (1998) Capsaicin sensitivity is associated with the expression of the vanilloid (capsaicin) receptor (VR1) mRNA in adult rat sensory ganglia. *Neurosci. Lett.* **250**, 177–180

193. Piomelli, D. and Sasso, O. (2014) Peripheral gating of pain signals by endogenous lipid mediators. *Nat. Neurosci.* **17**, 164–174

194. Tominaga, M., Caterina, M. J., Malmberg, A. B., Rosen, T. A., Gilbert, H., Skinner, K., Raumann, B. E., Basbaum, A. I., and Julius, D. (1998) The cloned capsaicin receptor integrates multiple pain-producing stimuli. *Neuron* **21**, 531–543

195. Devesa, I., Planells-Cases, R., Fernández-Ballester, G., Gonzalez-Ros, Ferrer-Montiel, A., and Fernández-Carvajal, A. (2011) Role of the transient receptor potential vanilloid 1 in inflammation and sepsis. *J. Inflamm. Res.* 67–81

196. Holzer, P. (1988) Local effector functions of capsaicin-sensitive sensory nerve endings: involvement of tachykinins, calcitonin gene-related peptide and other neuropeptides. *Neuroscience* **24**, 739–768

197. Laird, J. M., Olivar, T., Roza, C., De Felipe, C., Hunt, S. P., and Cervero, F. (2000) Deficits in visceral pain and hyperalgesia of mice with a disruption of the tachykinin NK1 receptor gene. *Neuroscience* **98**, 345–352

198. Schumacher, M. A. (2010) Transient receptor potential channels in pain and inflammation: therapeutic opportunities. *Pain Pract.* **10**, 185–200

199. Thán, M., Németh, J., Szilvássy, Z., Pintér, E., Helyes, Z., and Szolcsányi, J. (2000) Systemic anti-inflammatory effect of somatostatin released from capsaicin-sensitive vagal and sciatic sensory fibres of the rat and guinea-pig. *Eur. J. Pharmac.* **399**, 251–258

200. Cristino, L., De Petrocellis, L., Pryce, G., and Baker, D. (2006) Immunohistochemical localization of cannabinoid type 1 and vanilloid transient receptor potential vanilloid type 1 receptors in the mouse brain. *Neuroscience* **139**, 1405–1415

201. Mezey, E., Tóth, Z. E., Cortright, D. N., Arzubi, M. K., Krause, J. E., Elde, R., Guo, A., Blumberg, P. M., and Szallasi, A. (2000) Distribution of mRNA for vanilloid receptor subtype 1 (VR1), and VR1-like immunoreactivity, in the central nervous system of the rat and human. *Proc. Natl. Acad. Sci. U.S.A.* **97**, 3655–3660

202. Roberts, J. C., Davis, J. B., and Benham, C. D. (2004) [3H]Resiniferatoxin autoradiography in the CNS of wild-type and TRPV1 null mice defines TRPV1 (VR-1) protein distribution. *Brain Res.* **995**, 176–183

203. Steenland, H. W., Ko, S. W., Wu, L.-J., and Zhuo, M. (2006) Hot receptors in the brain. *Mol. Pain* **2**, 34

204. Szolcsányi, J., Joó, F., and Jancsó-Gábor, A. (1971) Mitochondrial changes in preoptic neurones after capsaicin desensitization of the hypothalamic thermodetectors in rats. *Nature* **229**, 116–117

205. Bertin, S., Aoki-Nonaka, Y., de Jong, P. R., Nohara, L. L., Xu, H., Stanwood, S. R., Srikanth, S., Lee, J., To, K., Abramson, L., Yu, T., Han, T., Touma, R., Li, X., González-Navajas, J. M., Herdman, S., Corr, M., Fu, G., Dong, H., Gwack, Y., Franco, A., Jefferies, W. A., and Raz, E. (2014) The ion channel TRPV1 regulates the activation and proinflammatory properties of $CD4^+$ T cells. *Nat. Immunol.* **15**, 1055–1063

206. Fernandes, E. S., Fernandes, M. A., and Keeble, J. E. (2012) The functions of TRPA1 and TRPV1: moving away from sensory nerves. *Br. J. Pharmacol.* **166**, 510–521

207. Himi, N., Hamaguchi, A., Hashimoto, K., Koga, T., Narita, K., and Miyamoto, O.

(2012) Calcium influx through the TRPV1 channel of endothelial cells (ECs) correlates with a stronger adhesion between monocytes and ECs. *Adv. in Med. Sci.* **57**, 224–229

208. Spinsanti, G., Zannolli, R., Panti, C., Ceccarelli, I., Marsili, L., Bachiocco, V., Frati, F., and Aloisi, A. M. (2008) Quantitative Real-Time PCR detection of TRPV1-4 gene expression in human leukocytes from healthy and hyposensitive subjects. *Mol. Pain* **4**, 51

209. Wilhelmsen, K., Khakpour, S., Tran, A., Sheehan, K., Schumacher, M., Xu, F., and Hellman, J. (2014) The endocannabinoid/endovanilloid N-arachidonoyl dopamine (NADA) and synthetic cannabinoid WIN55,212-2 abate the inflammatory activation of human endothelial cells. *J. Biol. Chem.* **289**, 13079–13100

210. Ji, D., Jang, C.-G., and Lee, S. (2014) A sensitive and accurate quantitative method to determine *N*-arachidonoyldopamine and *N*-oleoyldopamine in the mouse striatum using column-switching LC-MS-MS: use of a surrogate matrix to quantify endogenous compounds. *Anal. Bioanal. Chem.* **406**, 4491–4499

211. Guptill, V., Cui, X., Khaibullina, A., Keller, J. M., Spornick, N., Mannes, A., Iadorola, M., and Quezado, Z. M. N. (2011) Disruption of the rransient Receptor potential vanilloid 1 can affect survival, bacterial clearance, and cytokine gene expression during murine sepsis. *Anesthesiology* **114**, 1190–1199

212. Mesters, R. M., Flörke, N., Ostermann, H., and Kienast, J. (1996) Increase of plasminogen activator inhibitor levels predicts outcome of leukocytopenic patients with sepsis. *Thromb. Haemost.* **75**, 902–907

213. Kawai, T. and Akira, S. (2010) The role of pattern-recognition receptors in innate immunity: update on Toll-like receptors. *Nat. Immunol.* **11**, 373–384

214. Starowicz, K., Nigam, S., and Di Marzo, V. (2007) Biochemistry and pharmacology of endovanilloids. *Pharmacol. Ther.* **114**, 13–33

215. Ajami, B., Bennett, J. L., Krieger, C., Tetzlaff, W., and Rossi, F. M. V. (2007) Local self-renewal can sustain CNS microglia maintenance and function throughout adult life. *Nat. Neurosci.* **10**, 1538–1543

216. Evans, T. W. and Fink, M. P. (2002) Mechanisms of organ dysfunction in critical illness. vol. 38,

217. Schouten, M., Wiersinga, W. J., Levi, M., and van der Poll, T. (2008) Inflammation, endothelium, and coagulation in sepsis. *J. Leukocyte Biol.* **83**, 536–545

218. Cao, Y. Q., Mantyh, P. W., Carlson, E. J., Gillespie, A. M., Epstein, C. J., and Basbaum, A. I. (1998) Primary afferent tachykinins are required to experience moderate to intense pain. *Nature* **392**, 390–394

219. Chiu, I. M., Hehn, von, C. A., and Woolf, C. J. (2012) Neurogenic inflammation and the peripheral nervous system in host defense and immunopathology. *Nat. Neurosci.* **15**, 1063–1067

220. Borovikova, L. V., Ivanova, S., Zhang, M., and Yang, H. (2000) Vagus nerve stimulation attenuates the systemic inflammatory response to endotoxin. *Nature* **405**, 458–462

221. Rosas-Ballina, M. and Tracey, K. J. (2009) The neurology of the immune system: neural reflexes regulate immunity. *Neuron* **64**, 28–32

222. Ni, D., Gu, Q., Hu, H.-Z., Gao, N., Zhu, M. X., and Lee, L.-Y. (2006) Thermal sensitivity of isolated vagal pulmonary sensory neurons: role of transient receptor potential vanilloid receptors. *Am. J. Physiol. Regul. Integr. Comp. Physiol.* **291**, R541–R550

223. Hüttemeier, P. C., Ritter, E. F., and Benveniste, H. (1993) Calcitonin gene-related peptide mediates hypotension and tachycardia in endotoxic rats. *Am. J. Physiol.* **265**, H767–H769

224. Beer, S., Weighardt, H., Emmanuilidis, K., Harzenetter, M. D., Matevossian, E., Heidecke, C.-D., Bartels, H., Siewert, J.-R., and Holzmann, B. (2002) Systemic neuropeptide levels as predictive indicators for lethal outcome in patients with postoperative sepsis. *Crit. Care Med.* **30**, 1794–1798

225. Joyce, C. D., Fiscus, R. R., Wang, X., Dries, D. J., and Morris, R. C. (1990) Calcitonin gene-related peptide levels are elevated in patients with sepsis. *Surgery* **108**, 1097–1101

226. Cuesta, M. C., Quintero, L., Pons, H., and Suarez-Roca, H. (2002) Substance P and calcitonin gene-related peptide increase IL-1 beta, IL-6 and TNF alpha secretion from human peripheral blood mononuclear cells. *Neurochem. Int.* **40**, 301–306

227. Kawasaki, H., Takasaki, K., Saito, A., and Goto, K. (1988) Calcitonin gene-related peptide acts as a novel vasodilator neurotransmitter in mesenteric resistance vessels of the rat. *Nature* **335**, 164–167

228. Murata, Y. and Masuko, S. (2006) Peripheral and central distribution of TRPV1, substance P and CGRP of rat corneal neurons. *Brain Res.* **1085**, 87–94

229. Tang, Y., Feng, Y., and Wang, X. (1998) Calcitonin gene-related peptide

potentiates LPS-induced IL-6 release from mouse peritoneal macrophages. *J. Neuroimmunol.* **84**, 207–212

230. Yaraee, R., Ebtekar, M., Ahmadiani, A., and Sabahi, F. (2003) Neuropeptides (SP and CGRP) augment pro-inflammatory cytokine production in HSV-infected macrophages. *Int. J. Immunopharmac.* **3**, 1883–1887

231. Zygmunt, P. M., Petersson, J., Andersson, D. A., Chuang, H.-H., Sørgård, M., Di Marzo, V., Julius, D., and Högestätt, E. D. (1999) Vanilloid receptors on sensory nerves mediate the vasodilator action of anandamide. *Nature* **400**, 452–457

232. Ho, W. Z., Kaufman, D., Uvaydova, M., and Douglas, S. D. (1996) Substance P augments interleukin-10 and tumor necrosis factor-alpha release by human cord blood monocytes and macrophages. *J. Neuroimmunol.* **71**, 73–80

233. Jiang, M. H., Chung, E., Chi, G. F., Ahn, W., Lim, J. E., Hong, H. S., Kim, D. W., Choi, H., Kim, J., and Son, Y. (2012) Substance P induces M2-type macrophages after spinal cord injury. *Neuroreport* **23**, 786–792

234. Weinstock, J. V. (2015) Substance P and the regulation of inflammation in infections and inflammatory bowel disease. *Acta Physiol.* **213**, 453–461

235. Hou, Q., Barr, T., Gee, L., Vickers, J., Wymer, J., Borsani, E., Rodella, L., Getsios, S., Burdo, T., Eisenberg, E., Guha, U., Lavker, R., Kessler, J., Chittur, S., Fiorino, D., Rice, F., and Albrecht, P. (2011) Keratinocyte expression of calcitonin gene-related peptide β: implications for neuropathic and inflammatory pain mechanisms. *Pain* **152**, 2036–2051

236. Toscano, M. G., Ganea, D., and Gamero, A. M. (2011) Cecal Ligation Puncture Procedure. *J. Vis. Exp.* 1–5

237. Zhang, X., Goncalves, R., and Mosser, D. M. (2008) The isolation and characterization of murine macrophages. *Curr. Protoc. Immunol.* **Chapter 14**, 14.1–14.1.14

238. Harms, A. S. and Tansey, M. G. (2013) Isolation of murine postnatal brain microglia for phenotypic characterization using magnetic cell separation technology. *Microglia* **1041**, 33–39

239. Swamydas, M. and Lionakis, M. S. (2013) Isolation, purification and labeling of mouse bone marrow neutrophils for functional studies and adoptive transfer experiments. *J. Vis. Exp.* 1–7

240. Cabral, G. A. (2005) Lipids as bioeffectors in the immune system. *Life Sci.* **77**, 1699–1710

241. Shimizu, T. and Wolfe, L. S. (1990) Arachidonic acid cascade and signal transduction. *J. Neurochem.* **55**, 1–15

242. Shimizu, T. (2009) Lipid mediators in health and disease: enzymes and receptors as therapeutic targets for the regulation of immunity and inflammation. *Annu. Rev. Pharmacol. Toxicol.* **49**, 123–150

243. Funk, C. D. (2001) Prostaglandins and leukotrienes: advances in eicosanoid biology. *Science* **294**, 1871–1875

244. Leung, D., Saghatelian, A., Simon, G. M., and Cravatt, B. F. (2006) Inactivation of N-acyl phosphatidylethanolamine phospholipase D reveals multiple mechanisms for the biosynthesis of endocannabinoids. *Biochem.* **45**, 4720–4726

245. Marnett, L. J. (1992) Aspirin and the potential role of prostaglandins in colon cancer. *Cancer Res.* **52**, 5575–5589

246. Whelton, A. and Hamilton, C. W. (1991) Nonsteroidal anti-inflammatory drugs: effects on kidney function. *J. Clin. Pharmacol.* **31**, 588–598

247. Lawrence, T., Willoughby, D. A., and Gilroy, D. W. (2002) Anti-inflammatory lipid mediators and insights into the resolution of inflammation. *Nat. Rev. Immunol.* **2**, 787–795

248. Stone, K. D., Prussin, C., and Metcalfe, D. D. (2010) IgE, mast cells, basophils, and eosinophils. *J. Allergy Clin. Immunol.* **125**, S73–S80

249. Bouchard, J.-F., Lépicier, P., and Lamontagne, D. (2003) Contribution of endocannabinoids in the endothelial protection afforded by ischemic preconditioning in the isolated rat heart. *Life Sci.* **72**, 1859–1870

250. Baracos, V., Rodemann, H. P., Dinarello, C. A., and Goldberg, A. L. (1983) Stimulation of muscle protein degradation and prostaglandin E_2 release by leukocytic pyrogen (interleukin-1). *N. Engl. J. Med.* **308**, 553–558

251. Smith, G. S., Warhurst, G., and Turnberg, L. A. (1982) Synthesis and degradation of prostaglandin E_2 in the epithelial and sub-epithelial layers of the rat intestine. *Biochim. Biophys. Acta* **713**, 684–687

252. Grimminger, F., Kreusler, B., Schneider, U., Becker, G., and Seeger, W. (1990) Influence of miscrovascular adherence on neutrophil leukotriene generation. Evidence for cooperative eicosanoid synthesis. *J. Immunol.* **144**, 1866–1872

253. Di Marzo, V. (2008) Targeting the endocannabinoid system: to enhance or reduce? *Nat. Rev. Drug. Discov.* **7**, 438–455

254. Caraceni, P., Viola, A., Piscitelli, F., Giannone, F., Berzigotti, A., Cescon, M., Domenicali, M., Petrosino, S., Giampalma, E., Riili, A., Grazi, G., Golfieri, R., Zoli, M., Bernardi, M., and Di Marzo, V. (2010) Circulating and hepatic endocannabinoids and endocannabinoid‐related molecules in patients with cirrhosis. *Liver Int.* **30**, 816–825

255. Williams, A. E., van Dam, A. M., Man-A-Hing, W. K., Berkenbosch, F., Eikelenboom, P., and Fraser, H. (1994) Cytokines, prostaglandins and lipocortin-1 are present in the brains of scrapie-infected mice. *Brain Res.* **654**, 200–206

256. Reiss, C. S. (2010) Cannabinoids and viral infections. *Pharmaceuticals (Basel)* **3**, 1873–1886

257. Genis, P., Jett, M., Bernton, E. W., Boyle, T., Gelbard, H. A., Dzenko, K., Keane, R. W., Resnick, L., Mizrachi, Y., and Volsky, D. J. (1992) Cytokines and arachidonic metabolites produced during human immunodeficiency virus (HIV)-infected macrophage-astroglia interactions: implications for the neuropathogenesis of HIV disease. *J. Exp. Med.* **176**, 1703–1718

258. Svensson, C. I., Zattoni, M., and Serhan, C. N. (2007) Lipoxins and aspirin-triggered lipoxin inhibit inflammatory pain processing. *J. Exp. Med.* **204**, 245–252

259. Pavlov, V. A. and Tracey, K. J. (2004) Neural regulators of innate immune responses and inflammation. *Cell. Mol. Life Sci.* **61**, 2322–2331

260. Henderson, W. R. (1994) The role of leukotrienes in inflammation. *Ann. of Intern. Med.*

261. Murakami, M. (2011) Lipid mediators in life science. *Exp. Anim.* **60**, 7–20

262. Serhan, C. N., Chiang, N., and Van Dyke, T. E. (2008) Resolving inflammation: dual anti-inflammatory and pro-resolution lipid mediators. *Nat. Rev. Immunol.*

263. Robinson, D. R. (1989) Eicosanoids, inflammation, and anti-inflammatory drugs. *Clin. Exp. Rheumatol.* **7 Suppl 3**, S155–S161

264. Marcus, A. J. (1984) The eicosanoids in biology and medicine. *J. Lipid Res.* **25**, 1511–1516

265. Famaey, J. P. (1982) Phospholipases, eicosanoid production and inflammation. *Clin. Rheumatol.* **1**, 84–94

266. Vane, J. R. and Botting, R. M. (1995) New insights into the mode of action of anti-inflammatory drugs. *Inflamm. Res.* **44**, 1–10

267. Curtis-Prior, P. (2004) The Eicosanoids. (Curtis-Prior, P., ed) John Wiley & Sons,

Chichester, UK

268. Bezuglov, V. V., Manevich, E. M., Archakov, A. V., Bobrov, M., Kuklev, D. V., Petrukhina, G. N., Makarov, V. A., and Buznikov, G. A. (1997) Artificially functionalized polyenoic fatty acids--a new lipid bioregulators. *Bioorg. Khim.* **23**, 211–220

269. Kozak, K. R., Gupta, R. A., Moody, J. S., Ji, C., Boeglin, W. E., DuBois, R. N., Brash, A. R., and Marnett, L. J. (2002) 15-Lipoxygenase metabolism of 2-arachidonylglycerol. Generation of a peroxisome proliferator-activated receptor alpha agonist. *J. Biol. Chem.* **277**, 23278–23286

270. Seibert, K. and Masferrer, J. L. (1993) Role of inducible cyclooxygenase (COX-2) in inflammation. *Receptor*

271. Kuwano, T., Nakao, S., and Ishibashi, T. (2004) Cyclooxygenase 2 is a key enzyme for inflammatory cytokine induced angiogenesis. *Invest. Opthamol. Vis. Sci.*

272. Samad, T. A., Moore, K. A., Sapirstein, A., and Billet, S. (2001) Interleukin-1β-mediated induction of Cox-2 in the CNS contributes to inflammatory pain hypersensitivity. *Nature* **410**, 471–475

273. Vane, J. R., Bakhle, Y. S., and Botting, R. M. (1998) Cyclooxygenases 1 and 2. *Annu. Rev. Pharmacol. Toxicol.* **38**, 97–120

274. Harris, R. E., Beebe-Donk, J., Doss, H., and Burr Doss, D. (2005) Aspirin, ibuprofen, and other non-steroidal anti-inflammatory drugs in cancer prevention: a critical review of non-selective COX-2 blockade (review). *Oncol. Rep.* **13**, 559–583

275. Van Hecken, A., Schwartz, J. I., Depré, M., De Lepeleire, I., Dallob, A., Tanaka, W., Wynants, K., Buntinx, A., Arnout, J., Wong, P. H., Ebel, D. L., Gertz, B. J., and De Schepper, P. J. (2000) Comparative inhibitory activity of rofecoxib, meloxicam, diclofenac, ibuprofen, and naproxen on COX-2 versus COX-1 in healthy volunteers. *J. Clin. Pharmacol.* **40**, 1109–1120

276. Urquhart, P., Nicolaou, A., and Woodward, D. F. (2015) Endocannabinoids and their oxygenation by cyclo-oxygenases, lipoxygenases and other oxygenases. *Biochim. Biophys. Acta* **1851**, 366–376

277. Ueda, N., Yamamoto, K., Yamamoto, S., Tokunaga, T., Shirakawa, E., Shinkai, H., Ogawa, M., Sato, T., Kudo, I., and Inoue, K. (1995) Lipoxygenase-catalyzed oxygenation of arachidonylethanolamide, a cannabinoid receptor agonist. *Biochim. Biophys. Acta* **1254**, 127–134

278. Kozak, K. R., Rowlinson, S. W., and Marnett, L. J. (2000) Oxygenation of the endocannabinoid, 2-arachidonylglycerol, to glyceryl prostaglandins by cyclooxygenase-2. *J. Biol. Chem.* **275**, 33744–33749

279. Kozak, K. R., Crews, B. C., Morrow, J. D., Wang, L.-H., Ma, Y. H., Weinander, R., Jakobsson, P.-J., and Marnett, L. J. (2002) Metabolism of the endocannabinoids, 2-arachidonylglycerol and anandamide, into prostaglandin, thromboxane, and prostacyclin glycerol esters and ethanolamides. *J. Biol. Chem.* **277**, 44877–44885

280. Yu, M., Ives, D., and Ramesha, C. S. (1997) Synthesis of prostaglandin E2 ethanolamide from anandamide by cyclooxygenase-2. *J. Biol. Chem.* **272**, 21181–21186

281. Kozak, K. R., Prusakiewicz, J. J., Rowlinson, S. W., Schneider, C., and Marnett, L. J. (2001) Amino acid determinants in cyclooxygenase-2 oxygenation of the endocannabinoid 2-arachidonylglycerol. *J. Biol. Chem.* **276**, 30072–30077

282. Snider, N. T., Walker, V. J., and Hollenberg, P. F. (2010) Oxidation of the endogenous cannabinoid arachidonoyl ethanolamide by the cytochrome P450 monooxygenases: physiological and pharmacological implications. *Pharmacol. Rev.* **62**, 136–154

283. Chen, J.-K., Chen, J., Imig, J. D., Wei, S., Hachey, D. L., Guthi, J. S., Falck, J. R., Capdevila, J. H., and Harris, R. C. (2008) Identification of novel endogenous cytochrome p450 arachidonate metabolites with high affinity for cannabinoid receptors. *J. Biol. Chem.* **283**, 24514–24524

284. Woodward, D. F., Liang, Y., and Krauss, A. H.-P. (2008) Prostamides (prostaglandin-ethanolamides) and their pharmacology. *Br. J. Pharmacol.* **153**, 410–419

285. Nirodi, C. S., Crews, B. C., Kozak, K. R., Morrow, J. D., and Marnett, L. J. (2004) The glyceryl ester of prostaglandin E2 mobilizes calcium and activates signal transduction in RAW264.7 cells. *Proc. Natl. Acad. Sci. U.S.A.* **101**, 1840–1845

286. Sang, N., Zhang, J., and Chen, C. (2006) PGE2 glycerol ester, a COX-2 oxidative metabolite of 2-arachidonoyl glycerol, modulates inhibitory synaptic transmission in mouse hippocampal neurons. *J. Physiol.* **572**, 735–745

287. Sang, N., Zhang, J., and Chen, C. (2007) COX-2 oxidative metabolite of endocannabinoid 2-AG enhances excitatory glutamatergic synaptic transmission and induces neurotoxicity. *J. Neurochem.* **102**, 1966–1977

288. Hu, S. S.-J., Bradshaw, H. B., Chen, J. S.-C., Tan, B., and Walker, J. M. (2008) Prostaglandin E2 glycerol ester, an endogenous COX-2 metabolite of 2-

arachidonoylglycerol, induces hyperalgesia and modulates NFkappaB activity. *Br. J. Pharmacol.* **153**, 1538–1549

289. Jordan, W. K. and Merritt, H. H. (1950) Neurology. *N. Engl. J. Med.* **243**, 408–418

290. Berglund, B. A., Boring, D. L., and Howlett, A. C. (1999) Investigation of structural analogs of prostaglandin amides for binding to and activation of CB1 and CB2 cannabinoid receptors in rat brain and human tonsils. *Adv. Exp. Med. Biol.* **469**, 527–533

291. Griffin, B. W., Klimko, P., Crider, J. Y., and Sharif, N. A. (1999) AL-8810: a novel prostaglandin $F_{2\alpha}$ analog with selective antagonist effects at the prostaglandin $F_{2\alpha}$ (FP) receptor. *J. Pharmacol. Exp. Ther.* **290**, 1278–1284

292. Silvestri, C., Martella, A., Poloso, N. J., Piscitelli, F., Capasso, R., Izzo, A., Woodward, D. F., and Di Marzo, V. (2013) Anandamide-derived prostamide F2α negatively regulates adipogenesis. *J. Biol. Chem.* **288**, 23307–23321

293. Liang, Y., Woodward, D. F., Guzman, V. M., Li, C., Scott, D. F., Wang, J. W., Wheeler, L. A., Garst, M. E., Landsverk, K., Sachs, G., Krauss, A. H.-P., Cornell, C., Martos, J., Pettit, S., and Fliri, H. (2008) Identification and pharmacological characterization of the prostaglandin FP receptor and FP receptor variant complexes. *Br. J. Pharmacol.* **154**, 1079–1093

294. Ligresti, A., Martos, J., Wang, J., Guida, F., Allarà, M., Palmieri, V., Luongo, L., Woodward, D., and Di Marzo, V. (2014) Prostamide F(2) α receptor antagonism combined with inhibition of FAAH may block the pro-inflammatory mediators formed following selective FAAH inhibition. *Br. J. Pharmacol.* **171**, 1408–1419

295. Spada, C. S., Krauss, A. H.-P., Woodward, D. F., Chen, J., Protzman, C. E., Nieves, A. L., Wheeler, L. A., Scott, D. F., and Sachs, G. (2005) Bimatoprost and prostaglandin $F_{2\alpha}$ selectively stimulate intracellular calcium signaling in different cat iris sphincter cells. *Exp. Eye Res.* **80**, 135–145

296. Liang, Y., Li, C., Guzman, V. M., Evinger, A. J., Protzman, C. E., Krauss, A. H.-P., and Woodward, D. F. (2003) Comparison of prostaglandin F2alpha, bimatoprost (prostamide), and butaprost (EP2 agonist) on Cyr61 and connective tissue growth factor gene expression. *J. Biol. Chem.* **278**, 27267–27277

297. Woodward, D. F., Krauss, A. H.-P., Chen, J., Liang, Y., Li, C., Protzman, C. E., Bogardus, A., Chen, R., Kedzie, K. M., Krauss, H. A., Gil, D. W., Kharlamb, A., Wheeler, L. A., Babusis, D., Welty, D., Tang-Liu, D. D.-S., Cherukury, M., Andrews, S. W., Burk, R. M., and Garst, M. E. (2003) Pharmacological characterization of a novel antiglaucoma agent, bimatoprost (AGN 192024). *J. Pharmacol. Exp. Ther.* **305**, 772–785

298. Woodward, D. F., Carling, R. W. C., Cornell, C. L., Fliri, H. G., Martos, J. L., Pettit, S. N., Liang, Y., and Wang, J. W. (2008) The pharmacology and therapeutic relevance of endocannabinoid derived cyclo-oxygenase (COX)-2 products. *Pharmacol. Ther.* **120**, 71–80

299. Woodward, D. F., Krauss, A. H., Wang, J. W., Protzman, C. E., Nieves, A. L., Liang, Y., Donde, Y., Burk, R. M., Landsverk, K., and Struble, C. (2007) Identification of an antagonist that selectively blocks the activity of prostamides (prostaglandin-ethanolamides) in the feline iris. *Br. J. Pharmacol.* **150**, 342–352

300. Duggan, K. C., Hermanson, D. J., Musee, J., Prusakiewicz, J. J., Scheib, J. L., Carter, B. D., Banerjee, S., Oates, J. A., and Marnett, L. J. (2011) (R)-Profens are substrate-selective inhibitors of endocannabinoid oxygenation by COX-2. *Nat Chem Biol* **7**, 803–809

301. Kroeze, W. K., Sassano, M. F., Huang, X. P., and Lansu, K. (2015) PRESTO-Tango as an open-source resource for interrogation of the druggable human GPCRome. *Nat. Struct. Mol. Biol.*

302. Maloney, C. G., Kutchera, W. A., Albertine, K. H., McIntyre, T. M., Prescott, S. M., and Zimmerman, G. A. (1998) Inflammatory agonists induce cyclooxygenase type 2 expression by human neutrophils. *J. Immunol.* **160**, 1402–1410

303. Jones, D. A., Carlton, D. P., McIntyre, T. M., Zimmerman, G. A., and Prescott, S. M. (1993) Molecular cloning of human prostaglandin endoperoxide synthase type II and demonstration of expression in response to cytokines. *J. Biol. Chem.* **268**, 9049–9054

304. Hla, T. and Neilson, K. (1992) Human cyclooxygenase-2 cDNA. *Proc. Natl. Acad. Sci. U.S.A.* **89**, 7384–7388

305. Minghetti, L. (2007) Role of COX-2 in inflammatory and degenerative brain diseases. *Subcell. Biochem.* **42**, 127–141

306. Gilroy, D. W., Colville-Nash, P. R., Willis, D., Chivers, J., Paul-Clark, M. J., and Willoughby, D. A. (1999) Inducible cyclooxygenase may have anti-inflammatory properties. *Nat. Med.* **5**, 698–701

307. Serhan, C. N., Yacoubian, S., and Yang, R. (2008) Anti-inflammatory and proresolving lipid mediators. *Annu. Rev. Pathol.* **3**, 279–312

308. Gilroy, D. W. and Colville-Nash, P. R. (2000) New insights into the role of COX 2 in inflammation. *J. Mol. Med.* **78**, 121–129

309. Robertson, J. A., Sauer, D., Gold, J. A., and Nonas, S. A. (2012) The role of

cyclooxygenase-2 in mechanical ventilation-induced lung injury. *Am. J. Respir. Cell Mol. Biol.* **47**, 387–394

310. Fukunaga, K., Kohli, P., Bonnans, C., Fredenburgh, L. E., and Levy, B. D. (2005) Cyclooxygenase 2 plays a pivotal role in the resolution of acute lung injury. *J. Immunol.* **174**, 5033–5039

311. Rajakariar, R., Yaqoob, M. M., and Gilroy, D. W. (2006) COX-2 in inflammation and resolution. *Mol. Interv.* **6**, 199–207

312. Smith, J. B. (1981) Prostaglandins and platelet aggregation. *Acta Med. Scand. Suppl.* **651**, 91–99

313. Downey, G. P., Gumbay, R. S., Doherty, D. E., LaBrecque, J. F., Henson, J. E., Henson, P. M., and Worthen, G. S. (1988) Enhancement of pulmonary inflammation by PGE_2: evidence for a vasodilator effect. *J. Appl. Physiol.* **64**, 728–741

314. Hwa, J. (2011) Prostacyclin: an inflammatory paradox. 1–8

315. Aronoff, D. M. (2012) Cyclooxygenase inhibition in sepsis: is there life after death? *Mediators Inflamm.* **2012**, 1–7

316. Fullerton, J. N., O'Brien, A. J., and Gilroy, D. W. (2014) Lipid mediators in immune dysfunction after severe inflammation. *Trends in Immunol.* **35**, 12–21

317. Noursadeghi, M. and Cohen, J. (2000) Immunopathogenesis of severe sepsis. *J. R. Coll. Physicians Lon.* **34**, 432

318. Bernard, G. R., Reines, H. D., and Halushka, P. V. (1991) Prostacyclin and thromboxane A2 formation is increased in human sepsis syndrome: Effects of cyclooxygenase inhibition. *Am. Rev. Resp. Dis.* **144**, 1095–1101

319. Herlong, J. L. and Scott, T. R. (2006) Positioning prostanoids of the D and J series in the immunopathogenic scheme. *Immunology Letters* **102**, 121–131

320. Buckley, C. D., Gilroy, D. W., and Serhan, C. N. (2014) Proresolving lipid mediators and mechanisms in the resolution of acute inflammation. *Immunity* **40**, 315–327

321. Serhan, C. N. and Savill, J. (2005) Resolution of inflammation: the beginning programs the end. *Nat. Immunol.* **6**, 1191–1197

Publishing Agreement

It is the policy of the University to encourage the distribution of all theses, dissertations, and manuscripts. Copies of all UCSF theses, dissertations, and manuscripts will be routed to the library via the Graduate Division. The library will make all theses, dissertations, and manuscripts accessible to the public and will preserve these to the best of their abilities, in perpetuity.

Please sign the following statement:

I hereby grant permission to the Graduate Division of the University of California, San Francisco to release copies of my thesis, dissertation, or manuscript to the Campus Library to provide access and preservation, in whole or in part, in perpetuity.

Author Signature

6/7/17
Date